New aspects of septin assembly and cell cycle control in multinucleated *A. gossypii*

Inauguraldissertation

zur

Erlangung der Würde eines Doktors der Philosophie

vorgelegt der

Philosophisch-Naturwissenschaftlichen Fakultät

der Universität Basel

von

Hanspeter Helfer

aus Selzach, SO

Basel, 2007

Genehmigt von der Philosophisch-Naturwissenschaftlichen Fakultät

auf Antrag von

Prof. Dr. Peter Philippsen, Prof. Dr. Anne Spang und Prof. Dr. Jean Pieters

Basel, 6. Juni 2006

Prof. Dr. Hans-Jakob Wirz

Dekan

Table of Contents

Summary

Chapter I
Nuclei in the filamentous ascomycete *Ashbya gossypii* divide asynchronously and most nuclei have the potential to divide (Alberti-Segui *et al.*, 2001; Gladfelter *et al.*, 2006). Although cytoplasmic extension is restricted to growing tips and emerging branches, the distances between nuclei are uniform along the entire hyphal length. This implies active control of nuclear distribution and division to maintain an ideal nuclear to cytoplasmic ratio, potentially depending on environmental conditions. The question of nuclear distribution has already been addressed earlier (Alberti-Segui *et al.*, 2001). We have investigated how the rate of mitosis is regulated in response to intra- and extracellular signals. Here we show that homologues of *S. cerevisiae* morphogenesis checkpoint components are involved in starvation response in *A. gossypii:* Phosphorylation of the cyclin dependent kinase AgCdc28p at tyrosine 18 by the protein kinase AgSwe1p is used to delay mitosis under low-nutrient conditions, leading to an increase in the average distance between nuclei. This effect is markedly reduced in Ag*swe1*Δ or Agcdc28Y18F mutants where the CDK cannot be phosphorylated. Overexpression of Ag*SWE1* leads to decreased nuclear density even under non-starving conditions. Addition of rapamycin mimics starvation response, suggesting that AgSwe1p may be under control of AgTor1/2p.

In unperturbed budding yeast cells, ScSwe1p is recruited to the septin ring at the mother-bud neck where it is phosphorylated and subsequently degraded. We have speculated that the septins in *A. gossypii* could serve as spatial markers to locally inactivate AgSwe1p and increase nuclear division rate in areas of growth. Time-lapse analysis has revealed that mitoses in wild type are most common near branching points. Interestingly, AgSep7p-GFP localizes to branching points and septin deletion mutants show random distribution of mitoses. We propose a model in which AgSwe1p may regulate mitosis in response to cell intrinsic morphogenesis cues and external nutrient availability in multinucleated cells.

Chapter II
Septins are evolutionary conserved proteins with essential functions in cytokinesis, and more subtle roles throughout the cell cycle. Much of our knowledge about septins originates from studies with *S. cerevisiae,* where they form a ring-like protein scaffold at the mother-bud neck. We have asked what functions the septins may hold in an organism that does not complete cytokinesis prior to sporulation. Interestingly, all budding yeast septins are conserved in *A. gossypii* and one is even duplicated (S. Brachat, personal communication; Dietrich *et al.*, 2004). *In vivo* studies of AgSep7p-GFP have revealed that septins assemble into discontinuous hyphal rings close to growing tips and sites of branch formation and into asymmetric structures at the base of branching points. Rings are made of filaments which are long and diffuse close to growing tips and short and compact further away from the tip. During septum formation, the septin ring splits into two to form a double ring.

Ag*cdc3*Δ, Ag*cdc10*Δ, and Ag*cdc12*Δ mutants display aberrant morphology and are defective for actin-ring formation, chitin-ring formation, and sporulation. Due to the lack of septa, septin deletion mutants are highly sensitive, and lesion of a single hypha can have catastrophic consequences for a young mycelium. Strains lacking Ag*CDC11A* show morphological defects comparable with other septin deletion mutants, but actin- and chitin-ring formation are not disabled. Deletion of Ag*CDC11B* results in no detectable phenotype under standard laboratory conditions.

General Introduction

Filamentous fungi differ in many striking ways from common single-celled eukaryotes. The mycelium formed by hyphal growth is a dense, complex network of branched filaments, whose size is only limited by external conditions such as availability of resources, environmental stresses, and competing organisms. Mitosis are either synchronized (all nuclei divide simultaneously), or they occur in an asynchronous manner (Nygaard *et al.*, 1960; Clutterbuck, 1970). In either way, nuclear division is not followed by cytokinesis, leading to multinucleated hyphae which share one common cytoplasm. Thus, although by appearance such mycelia certainly do not correspond to the common perception of a cell, a mycelium formed by true hyphal growth has to be considered as one single, multinucleated cell. Filamentous growth enables these organisms to rapidly cover and exploit solid surfaces, and the polarized force generated by apical extension allows them to penetrate tissue which would otherwise not be accessible. However, this growth mode also bears new challenges: How can one single cell have the flexibility to react to conditions, which may greatly differ from one part of the mycelium to the other? How can it prevent local damage from spreading through the entire mycelium? How are hyphal extension and branching regulated to ensure optimized growth and resource exploitation? How does such a cell maintain an optimal protein per cytoplasm ratio, although the cytoplasmic volume may increase with various speed in different places of the mycelium?

We sought to study some of these questions in the filamentous *Ascomycete Ashbya gossypii*, a pathogen of cotton and citrus fruits and phylogenetically a close relative of *S. cerevisiae* (Ashby and Nowell, 1926; Prillinger *et al.*, 1997; Wendland *et al.*, 1999; Dietrich *et al.*, 2004). *A. gossypii* is exclusively found in a filamentous, multinucleated hyphal form. It has a very small haploid genome (9.2 Mb) encoding 4718 genes, which shows a high degree of synteny (conservation of gene order between different species) and homology with the *S. cerevisiae* genome. Combined with highly efficient homologous recombination allowing PCR-based gene targeting, these features make *A. gossypii* an attractive system to perform studies of regulation of filamentous growth based on genetic functional analysis (Steiner *et al.*, 1995; Altmann-Johl and Philippsen, 1996; Mohr, PhD Thesis, 1997; Wendland *et al.*, 2000; Wendland and Philippsen, 2000; Dietrich *et al.*, 2004).

The *A. gossypii* life cycle starts with the only known phase of isotropic growth in wild type: germination of the haploid spore to form a germ bubble. This is followed by apical growth, extending two germ tubes in succession on opposing sites of the germ bubble. More axes of polarity are established with lateral branch formation in young mycelium. Maturation is characterized by apical branching and a dramatic increase of growth speed (up to 200 μm/h at 30°C, (Knechtle *et al.*, 2003)), which enables it to cover an 8 cm-Petri-dish of full medium in about 7 days. Sporulation is thought to be induced by nutrient deprivation, leading to contraction at the septa, cytokinesis and subsequent abscission of sporangia which contain up to 8 haploid spores (Figure Intro.1, adopted from Brachat, PhD thesis, 2003) (Ayad-Durieux *et al.*, 2000; Brachat, PhD thesis, 2003; Knechtle *et al.*, 2003). Hyphae are compartmentalized by septa, which in young parts appear as rings that allow transfer of nuclei (Alberti-Segui *et al.*, 2001) and in older parts may appear as closed discs. Compartments typically contain around eight nuclei. Nuclear pedigree analyses carried out by Peter Philippsen and Amy Gladfelter have shown that neighboring nuclei are in different division cycle stages. Most nuclei have the potential to divide, with the time between two divisions varying greatly from 46 – 250 min (Gladfelter *et al.*, 2006). Despite limitation of growth to tips and branching sites, distances between the nuclei are largely uniform along the entire hyphal length, with an average distance of 4 – 5 μm. This is surprising as one might expect cytoplasmic expansion to cause a decrease of nuclear density in areas of growth. The fact that this is not the case indicates active maintenance of nuclear to cytoplasmic ratio along the hyphae. How may such a regulation be achieved? C. Alberti-Segui has shown that deletion of the microtubule-based dynein motor AgDhc1p leads to clustering of nuclei at the hyphal tips of *A. gossypii.* Thus, long range nuclear migration has been identified as the key element in regulating nuclear distribution (Alberti-Segui *et al.*, 2001). Besides nuclear distribution, also the division rate of nuclei needs to be controlled in order to

maintain an ideal nuclear to cytoplasmic ratio. This ratio may vary depending on environmental conditions. Mutants where such regulatory mechanisms are affected should display altered nuclear densities under standard growth conditions. Deletion of the kinesin motor AgCin8p leads to a dramatic increase of the distance between two nuclei to about 11 μm (Alberti-Segui, PhD thesis, 2001). However, AgCin8p generates the pushing force of the nuclear spindle and therefore has to be regarded as a requirement for efficient mitosis rather than a regulator. What do we know about regulation of nuclear division in other organisms?

The molecular machinery of eukaryotic cell cycle control is most fully worked out for budding yeast *Saccharomyces cerevisiae*. Under conditions of limited nutrients, budding yeast cells arrest as small, unbudded cells in early G1 phase ("Gap-1"). Addition of nutrients allows them to begin growing. If they achieve a critical size and no mating pheromone is present, the cells commit to a complete cell cycle. This execution point at late G1 is called START (Pringle and Hartwell, 1981; Tyers *et al.*, 1992). Bud emergence corresponds to the initiation of S phase (Synthesis), during which DNA replication, spindle pole body (SPB, fungal equivalent of the centrosome) separation and nuclear positioning occur. In G2 phase (Gap-2), apical growth of the bud is replaced by isotropic growth, and the SPBs migrate to opposite sides of the nucleus forming a short metaphase spindle which is oriented in parallel to the mother-bud axis (Byers and Goetsch, 1975; Jacobs *et al.*, 1988; Donaldson and Kilmartin, 1996; Carminati and Stearns, 1997; Shaw *et al.*, 1997). During M phase (Mitosis), the spindle extends at least 5-fold, separating the sister chromatids to opposite poles, thus leading to nuclear division (Winey and Byers, 1993; Snyder, 1994). With mitotic exit the anaphase spindle disassembles, and the cell cycle is concluded by cytokinesis and cell separation (abscission) (Kilmartin and Adams, 1984; Epp and Chant, 1997; Bi *et al.*, 1998; Lippincott and Li, 1998b, 1998a; Vallen *et al.*, 2000).

Lee Hartwell spearheaded cell cycle research in *S. cerevisiae* with his screen for conditional cell division cycle (cdc) mutants in the 1960s and 1970s (Hartwell, 1971a). Under restrictive conditions, cdc mutants arrest with characteristic cell division morphologies, called terminal phenotypes. His detailed examination of these mutants revealed interdependence of many cell-cycle events but also demonstrated that at least three independent cycles can be distinguished in budding yeast: the cytoplasmic cycle (bud formation), the chromosome cycle (replication) and the centrosome cycle (SPB cycle). Each of these cycles depends on START for initiation and each must be completed for cells to undergo the metaphase to anaphase transition. *cdc28* mutants have a terminal phenotype at this principal restriction point of the yeast cell division cycle. This lead to the discovery of cyclin dependant kinases (CDKs), whose changes in activity are responsible for driving key cell cycle transitions (Hartwell *et al.*, 1974; Nasmyth and Reed, 1980). *S. cerevisiae* possesses at least five CDKs, with Cdc28p being the principal regulator of the cell cycle. Cdc28p activity is regulated by nine cyclins that accumulate, for the most part, at START and at G2/M that are regulated transcriptionally and proteolytically, several protein kinases (e.g. Sic1p, Swe1p) and phosphoprotein phosphatases (e.g. Mih1p), and at least four other binding proteins. Cdc28p cyclins have been classified into two groups: the three G1 cyclins Cln1p, Cln2p, and Cln3p, and the six B-type (mitotic) cyclins Clb1p to Clb6p (Richardson *et al.*, 1989; Surana *et al.*, 1991; Fitch *et al.*, 1992; Richardson *et al.*, 1992; Schwob and Nasmyth, 1993). Regulation of cyclin associated Cdc28p activity is mainly achieved by successive waves of cyclins, provided by a mechanism of transient expression and subsequent degradation. Each wave stimulates degradation of the preceding cyclins and expression of the following cyclins. This allows the Cyclin-CDK complex to drive the cell through the different stages of the cell cycle.

Although bud formation, DNA replication and the centrosome cycle can proceed independently from each other once START has been passed, other events require tight coordination. Surveillance mechanisms termed checkpoints are set at various stages of the cell cycle and allow delayed processes to catch up and re-coordiante upon perturbation (Hartwell and Weinert, 1989). START itself can be regarded as checkpoint, preventing initiation of a cell division cycle under bad nutritional conditions or in the presence of mating partners (Gallego *et al.*, 1997). TOR (target of rapamycin) signaling plays a central role in adjusting cell growth to the nutritional environment (Barbet *et al.*, 1996; Helliwell *et al.*, 1998; Harris and Lawrence, 2003; Jacinto and Hall, 2003; Wullschleger *et al.*, 2006). To prevent the cells from disastrous segregation of incompletely replicated or damaged DNA, the "DNA damage and replication checkpoint" can delay the cell cycle in G1 and prior to anaphase in multiple ways. The "morphogenesis checkpoint" prevents formation of binucleate cells by delaying nuclear division until a bud has been formed (Lew and Reed,

1995; Sia *et al.*, 1996; McMillan *et al.*, 1998). Normally, the kinase Swe1p is recruited to the mother-bud neck in G2 by the concerted action of Hsl7p, Hsl1p and the septins. At the neck, it is phosphorylated by the polo-like kinase Cdc5p, leading to SCF-mediated ubiquitination and subsequent degradation (Sakchaisri *et al.*, 2004). Inhibitory Y19 phosphorylation of Cdc28p is reversed by the phosphatase Mih1p (Sia *et al.*, 1996; McMillan *et al.*, 1999b). Perturbations of the actin cytoskeleton delay bud formation and therefore recruitment of neck proteins. Swe1p remains stable and inhibits Cdc28p by Y19 phosphorylation. The morphogenesis checkpoint is described in detail in Chapter I: Introduction. Bipolar attachment of all the chromosomes to the mitotic spindle is monitored by the "spindle assembly checkpoint" prior to anaphase. This checkpoint is important for equal distribution of chromosomes to the mother and daughter cell (Hoyt *et al.*, 1991; Li and Murray, 1991; Weiss and Winey, 1996; Amon, 1999). The "nuclear migration checkpoint" (also known as cytokinesis or spindle position checkpoint) couples exit from mitosis to the correct migration of one nucleus into the bud (Bardin *et al.*, 2000; Bloecher *et al.*, 2000; Pereira *et al.*, 2000).

Could such a surveillance mechanism have adapted to regulate the rate of mitosis in *A. gossypii*? One could say that the morphogenesis checkpoint in *S. cerevisiae* regulates "nuclear density" by preventing formation of multinucleated cells. It has been argued that not only formation of a proper neck but also cytoplasmic extension of the bud could be a requirement before the cells are released into mitosis (Harvey and Kellogg, 2003). Recent analyses have demonstrated that ScSwe1p is also used to delay mitosis in response to environmental signals such as high osmolarity (Clotet *et al.*, 2006). We sought to investigate whether *A. gossypii* homologues of morphogenesis checkpoint components (AgSwe1p, AgMih1p, AgHsl1p, AgHsl7p, septins) have evolved to control nuclear division rate in response to hyphal extension and extracellular stimuli such as stress and availability of nutrients (Chapter I). The septins are crucial for the recruitment and inactivation of ScSwe1p in budding yeast. Thus, we further investigated the possibility of morphogenesis checkpoint proteins providing spatial control of mitosis, with the septins functioning as cortical markers to locally trigger mitosis in areas of growth.

The functions of *S. cerevisiae* septins are far from being restricted to the recruitment of morphogenesis checkpoint components. This conserved family of GTP-binding proteins was discovered through Lee Hartwell's genetic screening for *S. cerevisiae* mutants defective in cell-cycle progression (Hartwell, 1971b). The original temperature sensitive septin mutants (*cdc3, cdc10, cdc11* and *cdc12*) form multinucleated cellular clusters with elongated buds and thus were assigned essential functions in cytokinesis (Cooper and Kiehart, 1996; Longtine *et al.*, 1996; Field and Kellogg, 1999). Together with a fifth septin, ScSep7p (ScShs1p), the septins form a ring encircling the mother-bud neck, but they also occur at the presumptive bud site, at the bud scar after cytokinesis and at the tip of the shmoo in presence of mating pheromones (Longtine *et al.*, 1996; Mino *et al.*, 1998; Gladfelter *et al.*, 2001b). The septin ring serves several functions (Kinoshita, 2003): Firstly, it is a spatial landmark for bud site selection (Chant *et al.*, 1995; Sanders and Herskowitz, 1996). Further, the septins form a cortical barrier that prevents membrane-associated molecules from diffusing from the bud cortex into the mother cortex (Barral *et al.*, 2000; Takizawa *et al.*, 2000; Faty *et al.*, 2002). They form a scaffold to recruit molecules for the cytokinesis apparatus, cell-wall synthesis, and for positioning of the mitotic spindle (DeMarini *et al.*, 1997; Kusch *et al.*, 2002). Finally, they recruit the protein kinases ScGin4p, ScKcc4p and ScHsl1p, which belongs to the morphogenesis checkpoint, and one component of the mitosis exit network, ScTem1p (Carroll *et al.*, 1998; Jimenez *et al.*, 1998; Longtine *et al.*, 1998; Barral *et al.*, 1999; Lippincott *et al.*, 2001).

Despite profound morphological differences between budding yeast and *A. gossypii,* homologues to all five mitotic *S. cerevisiae* septins have been identified in *A. gossypii*, with *CDC11* being duplicated (S. Brachat, personal communication; Dietrich *et al.*, 2004). What function do the septins have in an organism that does not undergo complete cytokinesis unless for sporulation? Where do they localize in the absence of a bud neck or a division plane? The aim of Chapter II is to shed light on these questions by studying localization of AgSep7p-GFP and by functional analyses of deletion mutants.

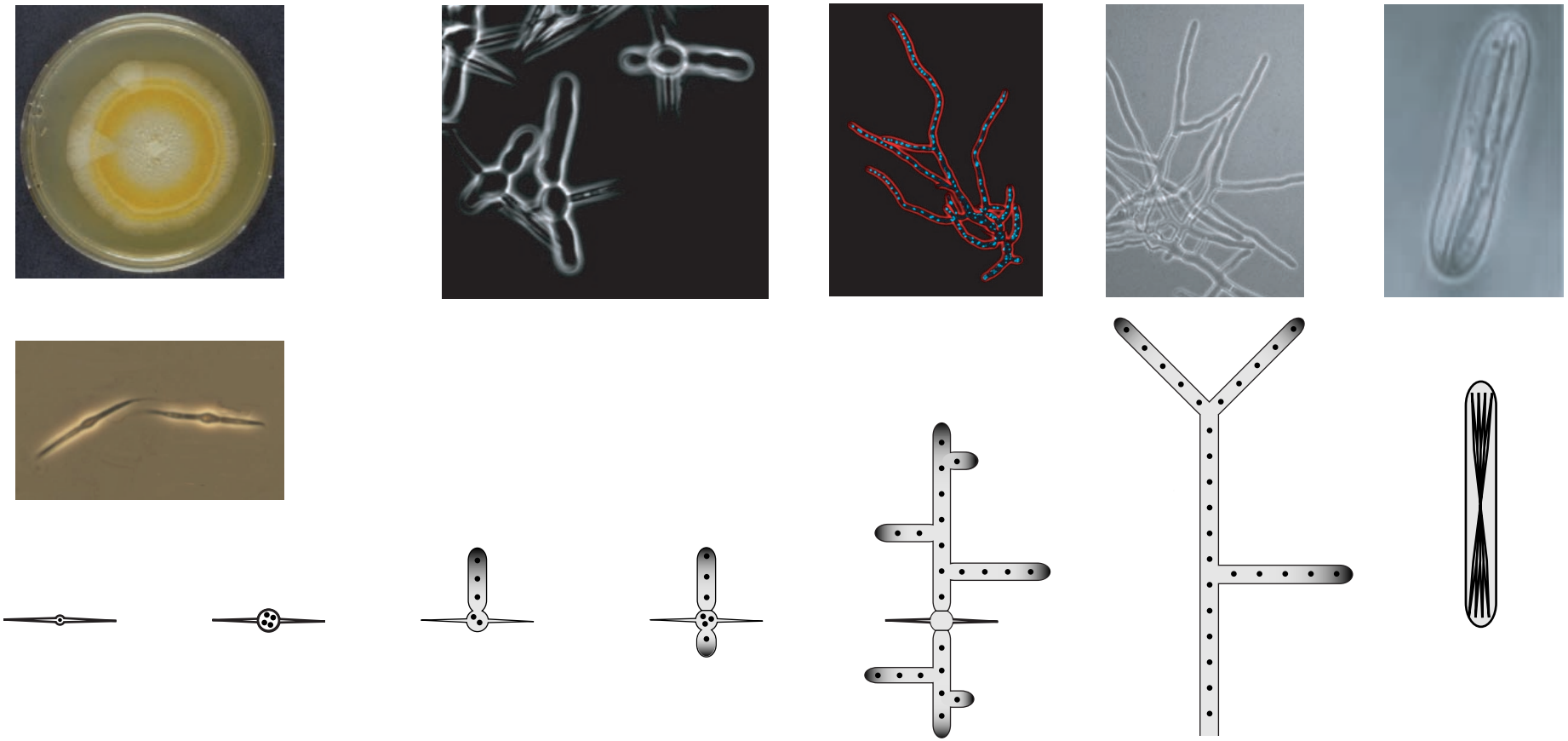

Figure Intro.1. *A. gossypii* life cycle (adopted from S. Brachat, Thesis, 2003). *A. gossypii* mycelium grown on solid medium gives rise to needle-shaped spores, recognizable as white fluff in the middle of the colony. Isotropic growth during germination leads to the formation of a germ bubble in the center of the spore. After a permanent switch to polarized, apical growth, two germ-tubes emerge successively on opposing sites of the germ bubble. Nuclear division occurs without subsequent cytokinesis, leading to multinucleated hyphae. New axis of polarity are established by lateral branching in young mycelium. During maturation of the mycelium, the tip extension rate is markedly increased and apical branching (tip splitting) now is the predominant form of branching. Upon growth for an extended time, the sporulation program is initiated, leading to the formation of sporangia and concluding the cycle.

Chapter I

A conserved cell cycle control module leading to CDK tyrosine phosphorylation functions in the *A. gossypii* starvation response

Introduction

Multinucleated cells are common throughout the biosphere. Filamentous, pathogenic fungi, metastasizing tumor cells and the cells of the musculoskeletal and blood systems of mammals are examples of the diverse types of cells which contain many nuclei in one cytoplasm (Mills and Frausto, 1997; Woodhouse *et al.*, 1997; Su *et al.*, 1998; Wakefield *et al.*, 2000; Winding *et al.*, 2000; Atkins *et al.*, 2001). In some cases these cells are produced from specialized cell cycles in which nuclear division occurs without cell division leading to large syncytia. For fungi, multinucleated cells may extend over hundreds of meters so that different regions of a single cell experience dramatically different microenvironments.

Mitosis in multinucleated cells can occur either in a coordinated, synchronous manner where all nuclei divide simultaneously or asynchronously where individual nuclei divide independently in time and space. Both synchronous and asynchronous patterns of mitosis are observed in syncytial cells and the different modes of nuclear division bring different potential advantages to cells (Nygaard *et al.*, 1960; Clutterbuck, 1970; Gladfelter *et al.*, 2006). In synchronous division, nuclei in distant regions of the cell can be coordinated and a cell can globally respond to a signal or stimulus with a limited spatial distribution. In asynchronous division, the cell can restrict mitosis to particular nuclei providing a more local and spatially controlled response to a signal.

Asynchronous or local control of mitosis, which is observed in several filamentous fungi including *Neurospora crassa* and *Ashbya gossypii*, may enable “cells” or mycelia to target both growth and nuclear division into nutrient rich regions while arresting these processes in areas of the mycelium lacking sufficient resources (Minke *et al.*, 1999; Freitag *et al.*, 2004; Gladfelter *et al.*, 2006). Additionally, asynchronous control of mitosis may allow mycelia to link morphogenesis programs, such as branching patterns and septal positioning, to nuclear division. Thus external triggers such as nutrients and/or internal signals involving shape of the mycelium could spatially direct asynchronous mitosis in multinucleated hyphae.

To prevent the formation of aberrant binucleate cells in *Saccharomyces cerevisae*, it is crucial not to start nuclear division before a proper bud has been formed. Therefore, mitotic entry is tightly coordinated with bud formation by the morphogenesis checkpoint (Figure I.1). Mitosis is promoted by a complex of mitotic cyclin with the cyclin dependant kinase (ScCdc28p). When bud formation is delayed due to defects in the actin cytoskeleton or if the septin scaffold (see Chapter II) is perturbed then the intrinsically unstable Swe1p kinase (Wee1 homologue) is stabilized and translocates to the nucleus where it can inhibit Cdc28/Clb2p, through phosphorylation of the tyrosine 19 residue on Cdc28p (Sia *et al.*, 1996; McMillan *et al.*, 1998; Sia *et al.*, 1998; McMillan *et al.*, 1999a; McMillan *et al.*, 1999b). This provides a G2-delay for cells to recover proper morphogenesis prior to mitosis ensuring aberrant binucleate cells do not form in the absence of budding. The G2-delay is determined by the ratio of active ScSwe1p to the phosphatase ScMih1p (Cdc25 homologue), which can reverse phosphorylation of the CDK (Ciliberto *et al.*, 2003). If proper morphogenesis is not recovered after several hours, ScMih1p activity leads to adaptation and the unbudded cells undergo mitosis and become binucleate (Sia *et al.*, 1996). During unperturbed cell growth, ScSwe1p is targeted for ubiquitin mediated degradation in the proteasome by phosphorylation (Sia *et al.*, 1998). ScSwe1p is sequentially phosphorylated at multiple sites by at least three protein kinases (Sakchaisri *et al.*, 2004; Lee *et al.*, 2005). If proper morphogenesis is underway, ScCla4p (PAK) localizes to the septin cortex at the neck and phosphorylates ScSwe1p during S-Phase, which is only found at low levels during this stage (Mitchell and Sprague, 2001; Sakchaisri *et al.*, 2004). In G2, ScSwe1p becomes abundant and potently inhibits Clb-ScCdc28p. Before the onset of M-phase, a raise in levels of mitotic Clb leads to Clb-CDK dependent phosphorylation of ScSwe1p (Sia *et al.*, 1998; McMillan *et al.*, 2002; Asano *et al.*, 2005). This promotes interaction of

ScSwe1p with the Polo-like kinase ScCdc5p, phosphorylation and subsequent degradation of ScSwe1p (Bartholomew *et al.*, 2001; Park *et al.*, 2003; Sakchaisri *et al.*, 2004; Asano *et al.*, 2005). In addition, data from frog egg extracts raise the possibility of a positive feedback loop, where Clb-CDK could phosphorylate and activate ScMih1p and by that further antagonize ScSwe1p activity (Izumi *et al.*, 1992; Ciliberto *et al.*, 2003). Efficient translocation of ScCdc5p to the neck and tethering of ScSwe1p to the septin filaments both require interaction with ScHsl1p and ScHsl7p, which are recruited by the septins (Barral *et al.*, 1999; Shulewitz *et al.*, 1999; Longtine *et al.*, 2000; McMillan *et al.*, 2002; Sakchaisri *et al.*, 2004; Asano *et al.*, 2005). Thus, in *S. cerevisiae,* the septin scaffold functions to coordinate bud morphogenesis and nuclear progression by regulating the abundance of ScSwe1p. Additionally, defects in the actin cytoskeleton are thought to trigger a second signaling pathway, operating through a MAPK (Mpk1), which leads to inhibition of ScMih1p (Harrison *et al.*, 2001).

Interestingly, similar cell cycle modules in other model organisms are used by the DNA damage/replication checkpoint (*S. pombe, X. laevis*) and by the stress response pathway (*S. pombe*) (Rhind *et al.*, 1997; Rhind and Russell, 1998; Yamada *et al.*, 2004; Petersen and Hagan, 2005). The homologues of all morphogenesis checkpoint factors in *S. cerevisiae* are present with varying degrees of homology in the genome of the multinucleated, filamentous fungus *A. gossypii*, which never reproduces by budding and rather is exclusively found in a filamentous, multinucleated hyphal form (Dietrich *et al.*, 2004). Given the absence of budding yet the conservation of all factors involved in the morphogenesis checkpoint, we speculated that this cell cycle module may have co-opted for control of nuclear density in *A. gossypii* and sought to identify triggers that would lead to a delay in nuclear division. We show here that AgSwe1p regulates nuclear progression in response to external nutrient status through inhibitory phosphorylation of the CDK. In addition, the septin proteins may use this module to link morphogenesis to nuclear cycle in this filamentous fungus by directing where mitosis takes place in the mycelium. We propose that this dual role for Swe1p may be used to facilitate a spatially controlled reaction to limited nutrient availability in the natural world.

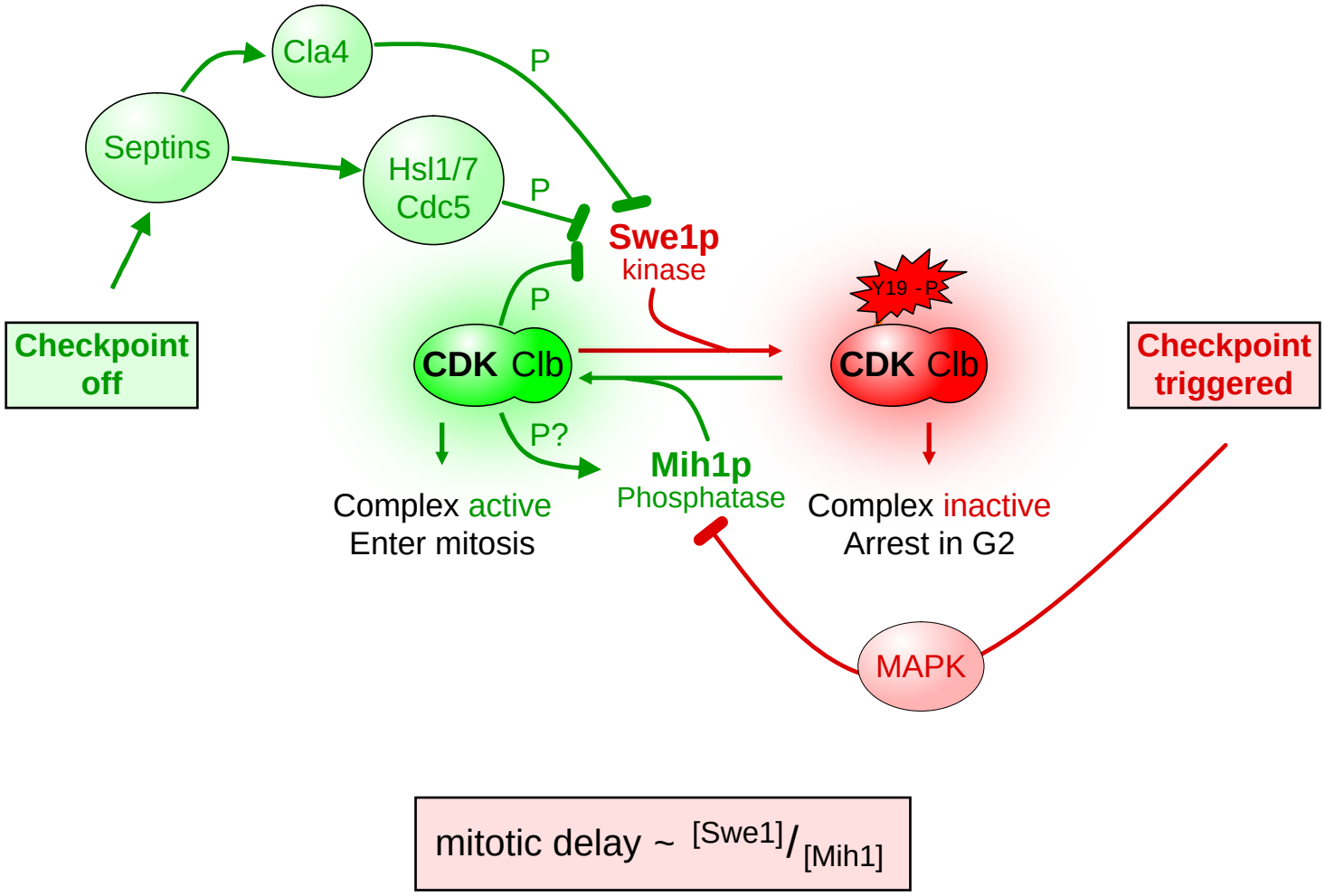

Figure I.1. Morphogenesis checkpoint in *S. cerevisiae.* The G2-delay is determined by the ratio of active ScSwe1p to the phosphatase ScMih1p. This ratio is regulated at multiple steps to link proper control of mitotic entry with morphogenetic events. See Chapter I, Introduction for detailed information.

Results

Phosphorylation of Cdc28-Y18 is a candidate for regulation of the nuclear cycle

Phosphorylation of a conserved tyrosine residue of the CDK is a widespread way to delay the cell- or nuclear cycle in response to a variety of intra- or extracellular signals, which differ between different organisms (Rhind *et al.*, 1997; Rhind and Russell, 1998; Yamada *et al.*, 2004; Petersen and Hagan, 2005; Nakashima *et al.*, unpublished). Alignment of the respective sequence among a selection of eukaryotes revealed Tyr18 to be a likely candidate of regulatory phosphorylation of the *A. gossypii* CDK, AgCdc28p (Figure I.2A). Effectively delaying the nuclear cycle via inhibitory phosphorylation of AgCdc28p would only possible, if AgCdc28p represented the key regulator of the nuclear cycle. To test the essential function of the *A. gossypii* CDK, Ag*cdc28*Δ deletion mutants were created. Heterokaryotic mycelia were able to grow at normal rates under selective conditions, indicating that transformed nuclei were still able to divide. This was in contrast to homokaryotic mycelium grown from spores: growth stopped at the stage of bipolar germlings, with rare attempts of branch formation. Hoechst staining revealed up to 4 nuclei per germling (Figure I.2B top right), dominated by nuclear debris which may be the result of nuclear breakdown (Fig I.2B large picture). Although up to two mitoses could still occur in the deletion mutants, AgCdc28p must play an essential role already early in the development of mycelium.

Minimal AgCdc28-Y18 phosphorylation under ideal growth conditions

We asked which conditions may cause *A. gossypii* to phosphorylate its CDK and potentially delay the nuclear cycle by using a phospho-specific anti-cdc2 antibody on mycelia and total proteins. Even under ideal growth conditions, phosphorylation of the CDK may be an integral part of nuclear cycle regulation, for instance to maintain asynchrony of mitoses. To test this, phosphorylated CDK was assayed for in mycelia by immunofluorescence to see if a subset of nuclei may be enriched for modified AgCdc28p (Figure I.3A). No phosphorylated protein was detected by this method but potentially this could be due to technical problems resolving the protein with this antibody by immunofluorescence. Thus, whole cell extracts from mycelia were also generated to evaluate if the antibody could recognize the *A. gossypii* CDK by western blot. Only minimal phosphorylation on AgCdc28p (compared to inducing conditions in later experiments) was apparent in either asynchronously growing mycelia or mycelia that had been artificially synchronized (approximately 70% synchrony) in G2/M with nocodazole and released for progression through mitosis (Figure I.3B). Hence, it can be assumed that CDK phosphorylation only plays a marginal role during normal growth conditions.

AgCdc28p is phosphorylated on tyrosine 18 when hyphae are starved for nutrients

Given the common role of CDK phosphorylation in different checkpoint responses across eukaryotes, we evaluated if AgCdc28p was phosphorylated when mycelia were exposed to potential checkpoint triggers and environmental stresses including Hydroxyurea (to impair DNA replication), nocodazole (to impede spindle assembly), starvation, osmotic shock, and high temperature (42 °C). Latrunculin A could not be used at the required concentration for large volume cultures and therefore was not assayed. No or limited phosphorylation was detected using the anti-phosphoTyr15-cdc2 antibody on whole cell extracts from cultures treated with Hydroxyurea or nocodazole (Figure I.3C). High temperature stress and osmotic shock resulted in moderate phosphorylation on a protein of the predicted size of AgCdc28p. Surprisingly, starvation that was induced by high-density growth (evaluation described in materials and methods) resulted in a level of phosphorylation that was markedly stronger than in any other condition tested (Figure I.3C). This phosphorylated form of AgCdc28p was visible both in whole cell extracts from high-density cultures and in the nuclei of starving intact mycelia visualized by immunofluorescence (Figure I.4A). The high-density/ nutrient deprivation-induced phosphorylation was reversed, along with the phenotype associated with starvation (prominent vacuoles) but relatively slowly upon feeding the mycelia with fresh media (Figure I.4B). The phosphorylation was reduced after 3 hours in fresh media and at the minimal levels found in low-density cultures after 5 hours. The response was independent of the type of nutrient that was restricted and was observed when either carbon (AFM with 0.1% glucose), nitrogen (ASD-Asn) or amino acids (ASD with one quarter amino acid concentration) was the limiting resource even when the cultures were grown to low density (Figure I.4C).

To confirm that the phosphorylation observed was as predicted on the tyrosine 18 residue of AgCdc28p, this residue was mutated to phenylalanine which cannot be phosphorylated. The phosphorylated AgCdc28p found in high-

density cultures of the reference strain is not present in lysates generated from Ag*cdc28*Y18F mycelia grown to similar high-density (Figure I.4D). This indicates that the anti-phospho-cdc2 antibody is recognizing the conserved tyrosine phosphorylation on the *A. gossypii* CDK.

This phosphorylated AgCdc28p observed in densely grown cultures could be formed in response to nutrient deprivation or could be a density-dependent reaction to a quorum-sensing molecule that accumulates at high density. Several approaches were taken to attempt to distinguish between these possibilities. First, it was examined whether cultures grown on plates could release factors that would inhibit growth of new cultures on the same plates. For that, AFM plates were inoculated with *A. gossypii* wt and grown for ten days. The mycelium was scraped off, leaving behind a mixture of spores and small pieces of mycelium. Half of the plates were soaked with 5 ml dH_2O to replace the liquid lost by evaporation. To replace the consumed nutrients, 5 ml of 6xAFM were added to the other half of the plates. If the plates contained quorum from the previous cultures, no growth should be observed on any of the plates. However, two days later, dense growth was observed on the plates treated with 6xAFM, but not on the watered plates. This implies that growth on used plates is not inhibited by quorum factors, but by nutrient deprivation.

In the next approach, cultures were treated with rapamycin which likely inhibits the kinase AgTor1/2p, which has a conserved role in nutrient sensing in a variety of eukaryotes. Inhibition of Tor kinase mimics starvation in many cells and in yeast simulates nitrogen starvation (Martin and Hall, 2005). In *A. gossypii* mycelium grown at low density in rich nutrient conditions, AgCdc28Y18 phosphorylation clearly accumulated with time in the presence of rapamycin (Figure I.4E). Thus, the appearance of the phosphorylated form does not depend upon high density here but does appear during this mock starvation. Furthermore, when mycelia grown at low density are transferred to MOPS/ KCl buffer (osmotically stable but without nutriaents) to induce rapid low-density starvation, CDK phosphorylation appears within 30 minutes and accumulates to levels comparable to high-density starvation by 105 minutes (Figure I.4E). Thus, AgCdc28Y18 phosphorylation appears in response to nutrient deprivation rather than other possible signals that may accumulate at high-density growth.

The nuclear cycle is delayed in specific stages of division during starvation

If phosphorylation of the CDK was inhibitory, as would be predicted, then we would expect a delay or inhibition of the nuclear cycle that leads to a change in nuclear density when hyphae are limited for nutrients. In fact the nuclear to cytoplasmic ratio was significantly different between high and low density grown cultures. Nuclei from mycelia grown to low density which presumably were not yet limited for nutrients were an average of 4.6 μm apart whereas in nutrient limited conditions this distance expanded to 10.2 μm (N>500 nuclei) (Figure I.5A). This can only be explained by polarized hyphal growth continuing (presumably until internal energy supplies such as lipid droplets are depleted) while the nuclear cycle is delayed or blocked under starvation. Ag*cdc28*Y18F mycelia which were resistant to CDK phosphorylation showed an intermediate nuclear density in low nutrients of 7.9 μm (N>300 nuclei) suggesting that some but not all of the delay in nuclear division was due tyrosine phosphorylation based inhibition of AgCdc28p (Figure I.5B).

If such a delay was stochastic such that limited nutrients can block nuclei in any stage of the nuclear cycle then high density cultures would be expected to have similar proportions of nuclei in each nuclear cycle stage as found in low-density cultures. If, however, the delay was regulated such that it occurs in a specific window of time, the proportions of nuclei in each stage of nuclear division should vary between the different growth conditions. Under high-density growth conditions, more nuclei accumulated in hyphae with duplicated SPBs (41%) and metaphase spindles (16%) compared to low density cultures (28% duplicated SPBs, 4% metaphase, N>400 nuclei). Thus the deprivation of nutrients leads to accumulation of nuclei in specific stages of division, both just prior to and during metaphase (Figure I.5C).

Homologues of the yeast morphogenesis checkpoint components in *A. gossypii*

In *S. cerevisiae,* inhibitory phosphorylation of ScCdc28p at Tyr19 by the kinase ScSwe1p is the principle response to a delay in bud formation (absence of proper septin collar leads to stabilization of ScSwe1p) or perturbation of the actin cytoskeleton. Despite dramatic morphogenetic differences between *A. gossypii* and budding yeast, homologues of the entire *S. cerevisiae* morphogenesis checkpoint are present in *A. gossypii.* Whereas the CDK, the polo kinase Cdc5p and the septins are highly conserved between the two organisms, considerable diversity was observed between the homologues

of the Swe1 regulators Hsl1p and Hsl7p and the phosphatase Mih1p (Table 1). Given that AgCdc28p is strongly phosphorylated in starving mycelium which results in a nuclear cycle delay, we asked whether the components of this cell cycle control module have evolved in *A. gossypii* to link CDK activity to availability of nutrients.

AgSwe1p is responsible for AgCdc28Y18 phosphorylation

We generated deletion mutants of the kinase AgSwe1p, its putative inhibitors AgHsl1p, AgHsl7p, the septins, and the phosphatase AgMih1p to investigate their role in AgCdc28Y18 phosphorylation. As in Ag*cdc28*Y18F mutants, *Agswe1*Δ mutants failed to accumulate phosphorylated AgCdc28p in high-density conditions in contrast to reference mycelia (Figure I.7A). Additionally, low-density grown Ag*swe1*Δ mycelia that were incubated with rapamycin also did not have detectable AgCdc28p phosphorylation showing that both, the rapamycin and starvation induced modification involved AgSwe1p (Figure I.7A). Ag*mih1*Δ mutants had comparable levels of phosphorylation to reference mycelia (Figure I.7A) suggesting that under these conditions AgMih1p may be down regulated in wild type. Growing Ag*cdc12*Δ and Ag*hsl1*Δ mutants to high density was only partially possible due to the growth defects of these mutants. As a result, only moderate phosphorylation was observed. Interestingly, when AgMih1p was deleted in addition to Ag*cdc12*Δ or Ag*hsl1*Δ, the CDK phosphorylation was markedly increased although these double mutants were afflicted by the same culturing problems as the single mutants (Figure I.7B). This implies that AgMih1p may at least be one phosphatase of the CDK that keeps AgSwe1p dependent phosphorylation in check. This would entail reduced reversibility of AgCdc28p phosphorylation in Ag*mih1*Δ mutants. Experiments were undertaken to see whether Ag*mih1*Δ single mutants or combination mutants with Ag*hsl1*Δ and Ag*hsl7*Δ displayed impaired capability to recover after starvation, upon feeding the mycelia with fresh full medium. No conclusive results were obtained because it was not possible to grow all the strains to the same density and therefore they were starved to a different degree when the recovery experiment was started (data not shown). In none of the cases, however, did the mutant strains display reduced recovery capacity compared to the reference strain. This indicates the existence of additional, AgMih1p independent mechanisms by which the CDK phosphorylation can be reverted.

Only minimal role of morphogenesis checkpoint homologues in regulating nuclear density under non-starving conditions

We wanted to know whether the changes in AgCdc28Y18 phosphorylation caused by some of the mutants were also reflected in the average distances between nuclei and the lengths of nuclear cycle stages. Single and combination mutants were evaluated for growth and nuclear density. Under normal growth conditions in rich media all mutant mycelia, with the exception of septin mutants, grew with wild-type like radial growth rates (Figure I.6A). Nuclear density was comparable to the reference (4.6 µm between nuclei) in Ag*hsl1*Δ (3.8 µm), Ags*we1*Δ (3.8 µm), Ag*mih1*Δ (3.8 µm) and Ag*cdc12*Δ (4.7 µm) mutants (N> 300 nuclei scored for each strain, (Figure I.6B). The nuclear cycle phase proportions were similar to the reference for the different mutant strains (Figure I.6C, nuclear cycle stage scoring based on spindle appearance by anti-tubulin immunofluorescence) however, there was a moderate increase in the percentage of metaphase and anaphase nuclei in Ag*hsl1*Δ (12% vs 7% in wt) and Ag*cdc12*Δ (14%) mutants suggesting there may be some delay late in the nuclear division cycle due to the absence of these proteins.

Based on homologues in other systems, Ag*hsl1*Δ*mih1*Δ double mutants or double deletion strains of Ag*MIH1* and any of the crucial septins would be predicted to have a synthetic interaction due to the release of inhibition of AgSwe1p in the absence of the phosphatase, AgMih1p, which likely opposes AgSwe1p. In yeast the analogous mutations lead to inviable cells which are blocked at the G2-M transition (McMillan *et al.*, 1999a). Amazingly, there was no additive effect in terms of growth in Ag*hsl1*Δ*mih1*Δ, Ag*cdc3*Δ*mih1*Δ, Ag*cdc10*Δ*mih1*Δ or Ag*cdc12*Δ*mih1*Δ double mutant strains in *A. gossypii*. Even analyzing nuclear density or nuclear division cycle stages did not reveal any synthetic effect in Ag*hsl1*Δ*mih1*Δ or Ag*cdc12*Δ–*mih1*Δ (Figure I.6A-C). These data combined suggest that despite the conservation of this cell cycle control module in the genome there is only a minimal “global” role for the septins/AgHsl1p/AgSwe1p, and AgMih1p in *A. gossypii* for regulating the frequency of nuclear division under standard laboratory (low-density / rich nutrient) growth conditions.

Starvation induced nuclear cycle delay depends on AgSwe1p

Strong AgCdc28-Y18 phosphorylation was only observed under starving conditions, except in Ag*cdc18*Y18F and *Agswe1*Δ mutants. Thus, even if components of this cell cycle control

module have no clear effect on the nuclear cycle under standard laboratory conditions, they may still be involved in regulation of the nuclear cycle delay we had observed under starving conditions. To investigate this possibility, we evaluated average distances of nuclei in deletion mutants grown to high density (starvation). Ag*cdc12Δ* (13.3 µm), Ag*hsl1*Δ*mih1*Δ (14.7 µm) and Ag*cdc12*Δ*mih1*Δ (15.5 µm) mutants all had in average higher nuclear densities than the reference (10.2 µm) (Figure I.8C). One caveat to these experiments however is that the slower growth rate of septin mutants necessitates a longer period of overall growth to achieve high density and thus the growth time is not identical between septin mutant strains and other strains. Ag*swe1*Δ mycelia grown to high density failed to respond as strongly to these conditions as the reference (10.2 µm), but still showed some increase in average nuclear distance (8.0 µm) compared to non-starving conditions (3.8 µm). This was comparable to the 7.9 µm measured in starving Ag*cdc28*Y18F hyphae (Figure I.7C). *Agswe1*Δ mutant mycelia had fewer nuclei with duplicated SPBs than reference hyphae at high density but retained a similar proportion of mitotic nuclei (Figure I.8A). These results suggest that AgSwe1p induced AgCdc28Y18 phosphorylation is responsible for a delay in nuclear division in G2 and that some other factors are responsible for the increased proportion of metaphase nuclei in high-density growth.

To determine if Swe1p activity was sufficient for AgCdc28p phosphorylation and altered nuclear division even in the absence of high-density starvation, AgSwe1p was overexpressed in mycelium grown in low-density conditions. For this experiment the AgSwe1p promoter was replaced with the *S. cerevisiae HIS3* promoter which leads to high, constitutive expression of proteins in *A. gossypii* (Dominic Hœpfner, personal communication). Protein levels were assayed by western blot against a 6HA-epitope tag fused to the C-terminus of AgSwe1p to confirm that the *HIS3* promoter leads to overexpression of the AgSwe1p protein (Figure I.8B). Additionally, Ag*SWE1* expression under its own promoter was evaluated for regulation and to confirm that the HA fusion protein was functional during high and low-density growth. Under control of the native promoter, AgSwe1p-6HA was barely detected in low-density cultures and appeared to migrate slower compared to in high-density growth, where it was more abundant and the bulk of the protein appeared in a faster migrating form that also predominated in the hyphae with AgSwe1p overexpressed. Unlike in reference mycelia, phosphorylated AgCdc28p was readily detected in low-density conditions when AgSwe1p was overexpressed from the *ScHIS3* promoter (lanes 2 and 4 compared to 6, (Figure I.8B).

To determine if this Y18 phosphorylation of AgCdc28p could alter nuclear cycle progression even in low-density cultures, nuclear density was evaluated in these hyphae overexpressing AgSwe1p. The overexpressed AgSwe1p and presumably the subsequent AgCdc28p phosphorylation led to a 50% decrease in nuclear density with an average distance between nuclei of 8.4 µm compared to 4.6 µm in the reference at low density (Figure I.7C). Additionally, the overexpressed AgSwe1p led to a dramatic delay in the nuclear cycle leading to a population in which almost 60% of nuclei had duplicated SPBs compared to only 28% in reference low density cultures further suggesting that AgSwe1p-induced AgCdc28p phosphorylation acts prior to metaphase (Figure I.8A).

Mitosis are concentrated at sites of branch formation

So far, we have not succeeded to clearly show involvement of the septins or AgHsl1p and AgHsl7p in regulating AgSwe1p activity, mainly due to technical difficulties. Nevertheless, they are the key regulators of ScSwe1p in budding yeast. Are the *A. gossypii* homologues of these proteins involved in a way of AgSwe1p regulation which is far more subtle than starvation response? One way how the septins could regulate AgSwe1p is by locally inactivating this kinase to provide an increase in the rate of mitosis in regions of growth. To see whether the septins are in the right place for such a regulation, we localized septin proteins in *A. gossypii* using a GFP-tagged septin, AgSep7p-GFP, and by immunofluorescence using an antibody generated against ScCdc11p. Detailed information on septin localization is found in chapter II (Figure II.2). Anticipatory, septins did actually localize to regions of growth: bar like rings were found near growing tips and close to sites of branch formation, asymmetric structures were found at the bases of branches. In order to have a mitosis promoting effect, the septins would have to bring together AgSwe1p and its inhibitors in these regions. We attempted to evaluate this by localizing AgSwe1p and one of its possible inhibitors, AgHsl7p. AgSwe1p was not visible when tagged either with GFP or epitopes in normally growing mycelia but AgHsl7p was visible in *A. gossypii* hyphae. AgHsl7-GFP expressed from the endogenous promoter was concentrated in discontinuous rings reminiscent of septin rings (Figure I.9A-D). Co-localization by immunostaining against GFP

and Cdc11p showed that in fact AgHsl7p co-localized with some but not all septin rings and in no case was AgHsl7p observed in the absence of a septin ring (Amy Galdfelter, personal communication). AgHsl7p was not observed in cortical rings in either Ag*cdc12*Δ or Ag*hsl1*Δ mutants suggesting that this likely Swe1p regulator is concentrated in specific regions of the mycelium by septins (Figure I.9E, F).

To investigate whether the rate of nuclear division is increased in these regions, we measured the mitotic index in tips, branch points and regions between these growth areas as illustrated in Figure I.10A, using several methods. First we observed mycelia growing on agar expressing GFP-labeled Histone H4 as nuclear marker (AgH4-GFP) using time-lapse microscopy to follow nuclear dynamics and morphogenesis over multiple hours *in vivo* (Movie 1). Mitoses were frequently observed near newly emerging branches at the junction between the new branch and the "mother" hypha. Example frames from the movie are shown in Figure I.10B, where mitosis occurred at the branching site at 171', 183', 201', and 213'. Mitoses are labeled with a box just prior to division and new daughter nuclei are then outlined with circles. In 84 total mitoses captured by time-lapse, 10 (12%) were at hyphal tips (11% of hyphal length), 43 (51%) were at current or future branching sites (30% of total hyphal length) and 31 (37%) were in the middle of hyphae (in interregion not near tip or branch sites, 59% of total hyphal length). Additionally, to assay mitotic frequency and position using an alternative method carried out by Amy Gladfelter, reference mycelia were grown in liquid medium, then processed for anti-tubulin immunofluorescence to visualize mitotic spindles. In this case, branchpoints were similarly enriched for mitoses with 45% of mitotic nuclei at these sites while tips hosted 30% of the dividing nuclei and 25% were present in the interregion (Figure I.10C, N>200 nuclei). Notably, we observed that when mitoses occurred in the absence of branching in the interregion that in many cases a branch later emerged from that spot suggesting that certain regions of a hypha are "marked" to promote mitosis (18% of mitoses, Figure I.11). Hyphal septin rings, formed earlier than the branching sites, are a possibility how these regions are marked. We tried to directly observe the influence of septin structures on the frequency and position of mitoses by doing time-lapse studies of a strain in which both, nuclei and Sep7p were tagged with GFP (AgHPH009). In order to reduce background fluorescence, we were forced to grow the mycelium on synthetic minimal medium (ASD) during time-lapse acquisition, which partially triggered the starvation response and greatly reduced the number of mitotic events. Therefore it was not possible to get any conclusive results from this experiment (Movie 2). In another attempt performed by Amy Gladfelter, AgCdc11p and tubulin were visualized in fixed mycelia by immunofluorescence. 71% of nuclei with mitotic spindles were adjacent to either a tip, main hyphal or branch septin ring and 52% of nuclei with duplicated SPBs were adjacent to septin rings (Figure I.10D, N=230 nuclei).

If septins are required for this spatial pattern of mitotic progression then mycelia lacking septins would be predicted to have a random spatial distribution of mitoses and potentially an altered frequency of mitoses. Amy Gladfelter observed that in mutant mycelia lacking the septin AgCdc12p both mitotic nuclei and nuclei with duplicated SPBs were no longer commonly observed at branch points as seen in the reference strain and instead appeared to be randomly distributed in hyphae. In reference mycelia grown in liquid, 45% of nuclei were near a branch whereas in Ag*cdc12*Δ only 13% were at branches (N>200 nuclei). In contrast, similar proportions of dividing nuclei in Ag*cdc12*Δ mutants (32%) were observed in growing tip regions compared to the reference (30%) suggesting that the septin ring at branch points wields greater influence over the nuclear cycle than the diffuse structures at the tips of hyphae. Thus at least certain septin rings seem to provide spatial directions to the mitotic machinery and potentially help to establish a sub-cellular region that favors nuclear progression.

Table 1. Homologues of the yeast MC components in *A. gossypii*

Protein	Size (aa) *A.g.*	*S.c.*	Identity	Syntenic homolog	Key Domains* *A.g.*	*S.c.*
Cdc28p	295	298	86 %	yes	Protein kinase	Protein kinase
Swe1p	727	819	52 %	yes	Protein kinase	Protein kinase
Mih1p	468	554	34 %	yes	Phosphatase, Rhodanese like	Phosphatase, Rhodanese like
Cdc5	708	705	73 %	Yes	Protein kinase, Polo box	Protein kinase, Polo box
Hsl1p	1425	1518	43 %	yes	Protein kinase	Protein kinase
Hsl7p	787	827	45 %	yes	Methyltransferase domain	Methyltransferase domain
Cdc3p	507	520	58 %	yes	GTP binding protein	GTP binding protein
Cdc10p	328	322	75 %	yes	GTP binding protein	GTP binding protein
Cdc11Ap	411	415	74 %	yes	GTP binding protein	GTP binding protein
Cdc11Bp	408		74 %	yes	GTP binding protein	
Cdc12p	390	407	78 %	yes	GTP binding protein	GTP binding protein
Sep7p	580	551	60 %	yes	GTP binding protein	GTP binding protein

*Domains identified using InterPro from the UniProtKB/Swiss-Prot database

A

```
                    10        20        30        40
                ....|....|....|....|....|....|....|....|
AgCdc28         MS-DLTNYKRLEKVGEGTYGVVYKAVDLR--HGQRIVALK  Ashbya gossypii
ScCdc28         MSGELANYKRLEKVGEGTYGVVYKALDLRPGQGQRVVALK  Saccharomyces cerevisiae
SpCdc2          ----MENYQKVEKIGEGTYGVVYKARHKL---SGRIVAMK  Schizosaccharomyces pombe
KLLA0B0979      MS-ELTNYKRLEKVGEGTYGVVYKAVDLR--HQNRVVAMK  Kluyveromyces lactis
CaCdc28         MV-ELSDYQRQEKVGEGTYGVVYKALDTK--HNNRVVALK  Candida albicans
AnnimX          ----MENYQKIEKIGEGTYGVVYKARELT--HPNRIVALK  Aspergillus nidulans
NCU09778.1      ----MENYQKLEKIGEGTYGVVYKARDLA--NSGRIVALK  Neurospora crassa
BrCdk2          ----MESFQKVEKIGEGTYGVVYKAKNKV---TGETVALK  Brachydanio rerio
BrCdc2          ----MDDYLKIEKIGEGTYGVVYKGRNKT---TGQVVAMK  Brachydanio rerio
GgCdc2          ----MEDYTKIEKIGEGTYGVVYKGRHKT---TGQVVAMK  Gallus gallus
XlCdk2          ----MENFQKVEKIGEGTYGVVYKARNRE---TGEIVALK  Xenopus laevis
MmCdk2          ----MENFQKVEKIGEGTYGVVYKAKNKL---TGEVVALK  Mus musculus
HsCdk2          ----MENFQKVEKIGEGTYGVVYKARNKL---TGEVVALK  Homo sapiens
HsCdc2          ----MEDYTKIEKIGEGTYGVVYKGRHKT---TGQVVAMK  Homo sapiens
HsCdk3          ----MDMFQKVEKIGEGTYGVVYKAKNRE---TGQLVALK  Homo sapiens
```

B

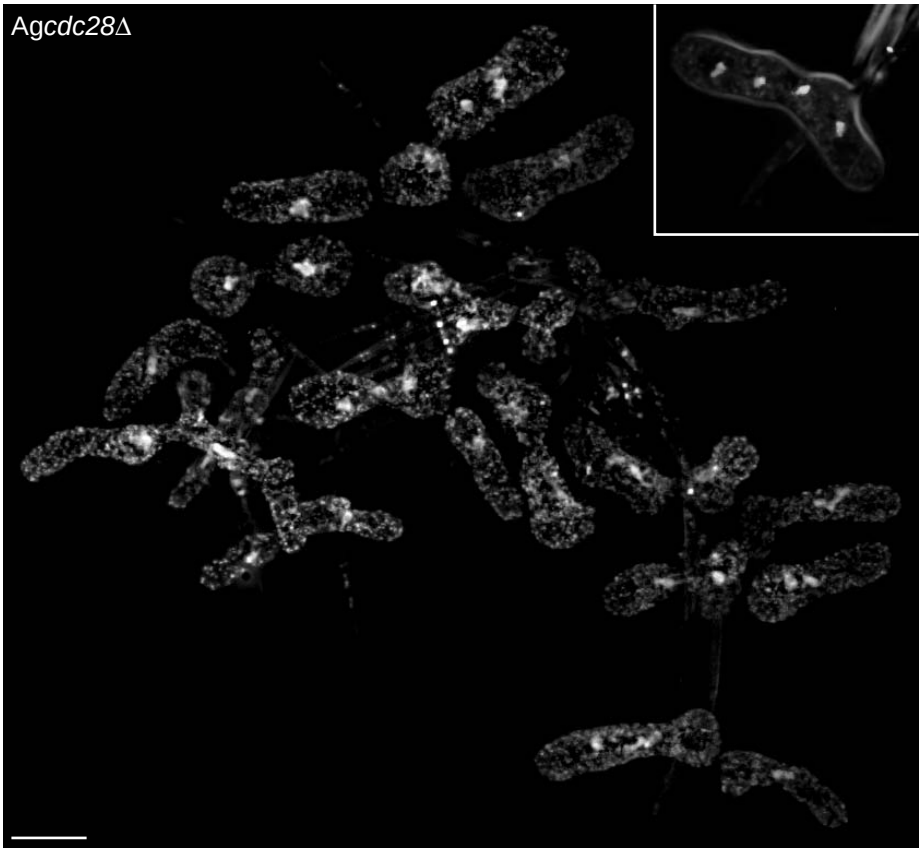

Figure I.2. Conserved tyrosine phosphorylation of the CDK. (A) Alignment of N-terminal sequences of cyclin dependant kinases among a selection of eukaryotes. The arrow indicates the phosphorylatable, conserved tyrosine residue (Tyr18 in AgCdc28p). **(B)** Hoechst staining of Ag*cdc28*Δ mutants (AgHPH35), grown for 10 h in liquid AFM at 30 °C.

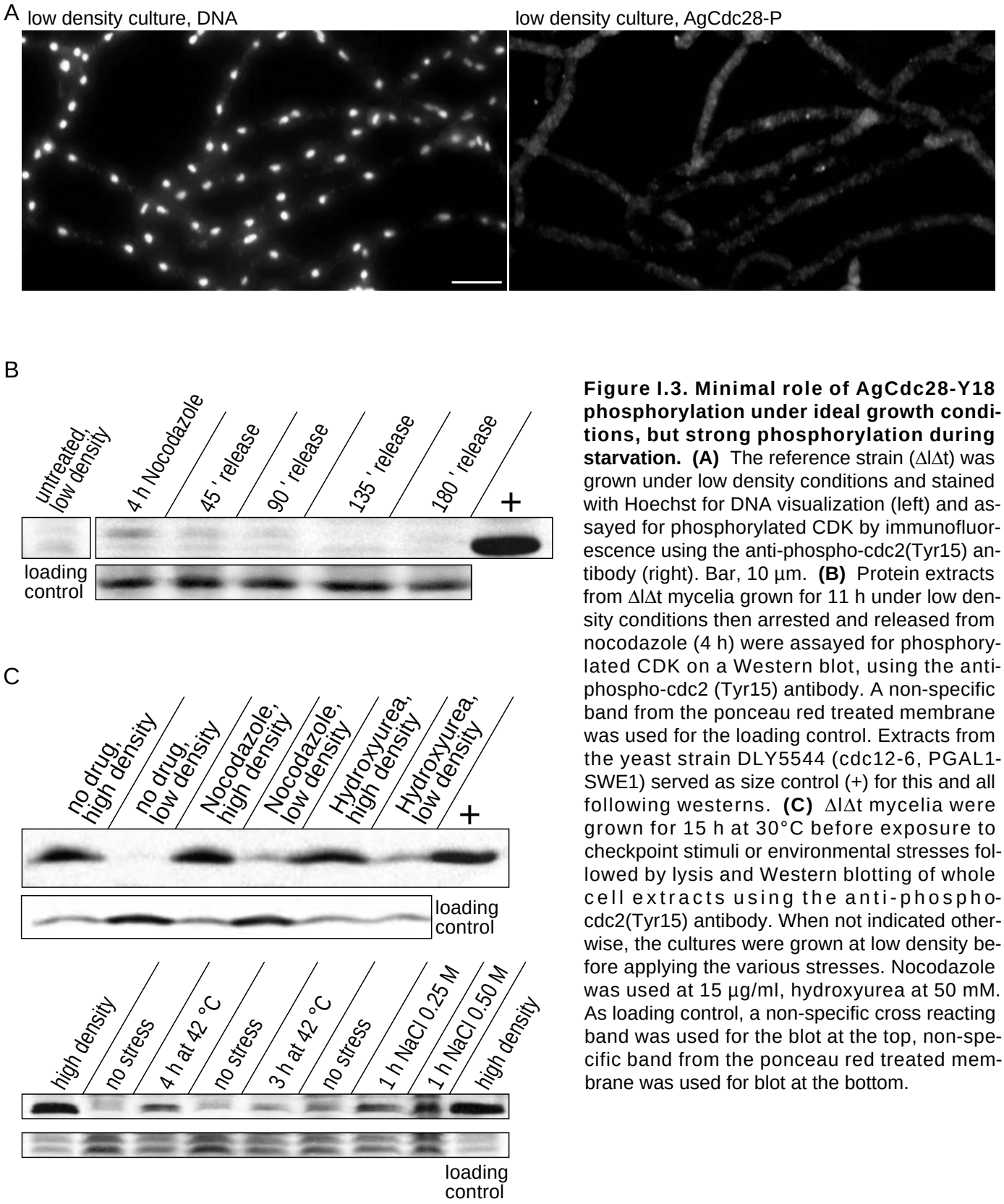

Figure I.3. Minimal role of AgCdc28-Y18 phosphorylation under ideal growth conditions, but strong phosphorylation during starvation. (A) The reference strain (ΔlΔt) was grown under low density conditions and stained with Hoechst for DNA visualization (left) and assayed for phosphorylated CDK by immunofluorescence using the anti-phospho-cdc2(Tyr15) antibody (right). Bar, 10 µm. **(B)** Protein extracts from ΔlΔt mycelia grown for 11 h under low density conditions then arrested and released from nocodazole (4 h) were assayed for phosphorylated CDK on a Western blot, using the anti-phospho-cdc2 (Tyr15) antibody. A non-specific band from the ponceau red treated membrane was used for the loading control. Extracts from the yeast strain DLY5544 (cdc12-6, PGAL1-SWE1) served as size control (+) for this and all following westerns. **(C)** ΔlΔt mycelia were grown for 15 h at 30°C before exposure to checkpoint stimuli or environmental stresses followed by lysis and Western blotting of whole cell extracts using the anti-phospho-cdc2(Tyr15) antibody. When not indicated otherwise, the cultures were grown at low density before applying the various stresses. Nocodazole was used at 15 µg/ml, hydroxyurea at 50 mM. As loading control, a non-specific cross reacting band was used for the blot at the top, non-specific band from the ponceau red treated membrane was used for blot at the bottom.

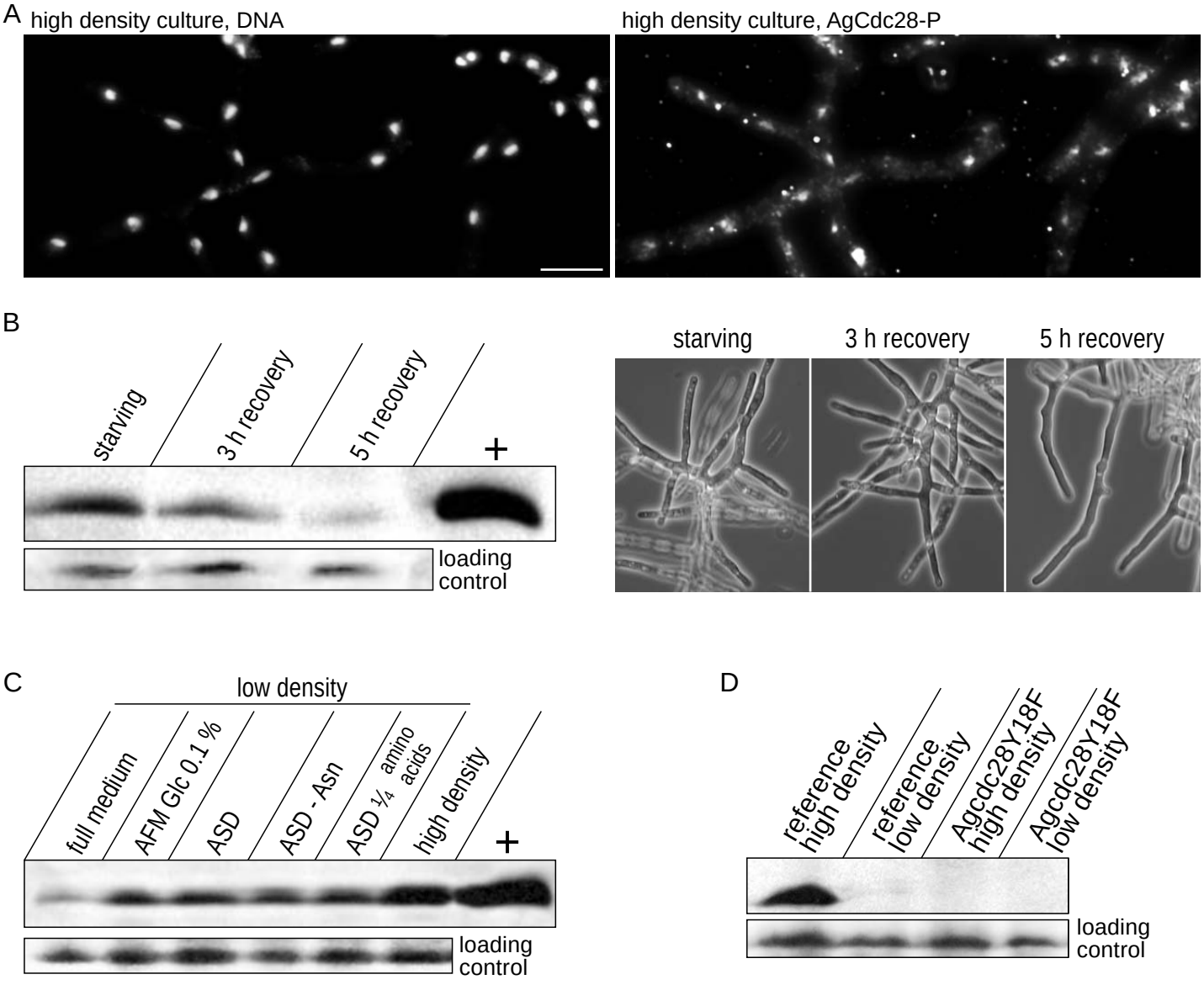

Figure I.4. Starvation induced AgCdc28-Y18 phosphorylation is reversible, independent of the type of restricted nutrient and not the result of quorum sensing. (A) The reference strain (ΔlΔt) was grown for 16 h under high density conditions, stained with Hoechst for DNA visualization (left) and assayed for phosphorylated CDK by immunofluorescence using the anti-phospho-cdc2(Tyr15) antibody (right). Bar, 10 µm. **(B)** ΔlΔt mycelia were grown under high density conditions in 20 ml of AFM until prominent vacuole formation was observed (18 h). The mycelia were washed and resuspended in 200 ml of fresh AFM to recover. Samples were taken after 3 h and 5 h, cells were lysed and the levels of CDK phosphorylation in whole cell extracts were detected by Western blotting using the anti-phospho-cdc2(Tyr15) antibody (left). A non-specific cross-reacting band was used as loading control. The degree of vacuolization was observed by phasecontrast microscopy (right). **(C)** Low density ΔlΔt mycelia were grown in full medium (AFM) for 12 h before shifting them into media limited for different resources: AFM Glc 0.1% (20 times less glucose than standard grwoth media), ASD(synthetic media without yeast extract), ASD-Asn (synthetic media lacking asparagine), and ASD with 0.25 normal amino acid concentration. Samples were taken 5 h after the media shift and assayed for CDK phosphorylation as described above. **(D)** ΔlΔt and Agcdc28Y18F(AgHPH36) mycelia were grown to the indicated densitites, lysed and processed by Western blot using the anti-phospho-cdc2(Tyr15) antibody. A non-specific cross-reacting band was used as loading control. **(E)** The reference strain was grown for 15 h under low density conditions before adding 200 nm Rapamycin or transferring the cells to MOPS/KCl (40 mM MOPS [pH 7.0], 137 mM KCl) except for the left lane where the culture was grown to high density for a positive control. CDK phosphorylation was detected by Western blotting as described above.

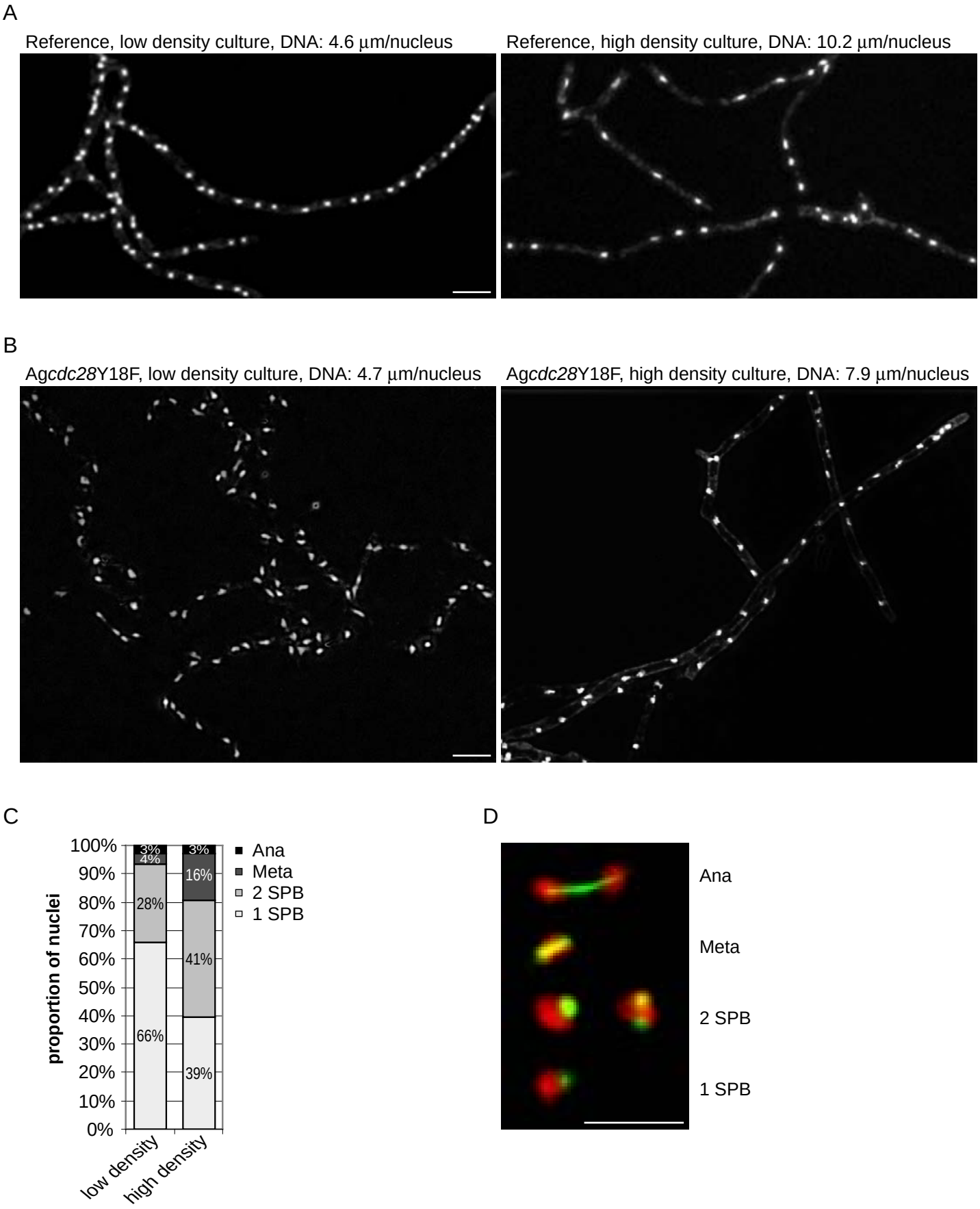

Figure I.5. The nuclear cycle is delayed in specific stages of division during starvation. (A) Reference (ΔlΔt) and **(B)** Ag*cdc28*Y18F (AgHPH36) mycelia grown under high and low density conditions were grown to low and high densities, fixed and stained with Hoechst to visualize nuclei. Bars, 10 µm. **(C)** ΔlΔt mycelia were grown for 16 h at 30°C to high/low density and then fixed and processed for anti-tubulin immunofluorescence to evaluate the percentage of nuclei in different nuclear division cycle stages (Ana: Anaphase, Meta: Metaphase, 2 SPB = 2 spindle pole bodies, 1 SPB = 1 spindle pole body). **(D)** Example of scoring method used in C (red: nuclei stained with Hoechst, green: anti-tubulin). Bar, 5 µm.

A

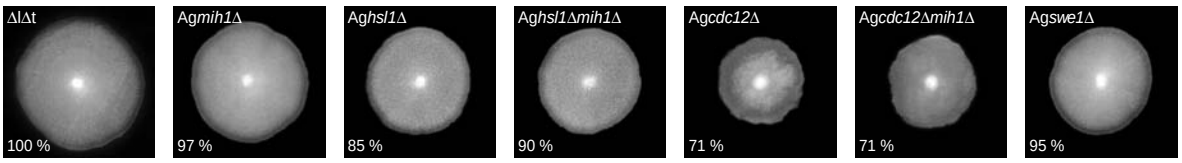

B

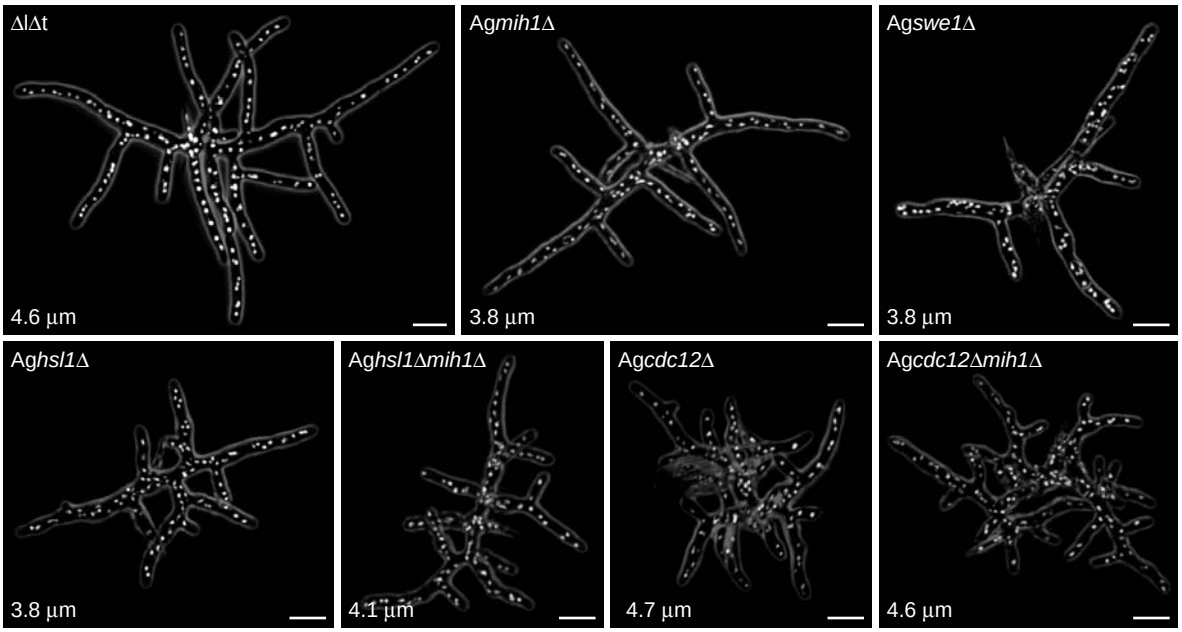

C

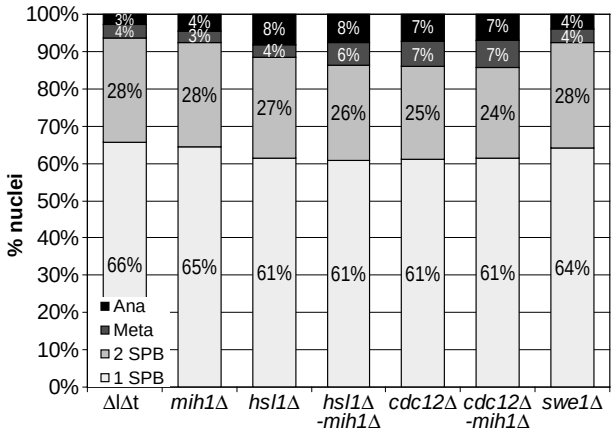

Figure I.6. Minimal role of homologues of the *S.c.* morphogenesis checkpoint components. **(A)** Radial growth on solid medium of the reference strain (ΔlΔt) and deletion mutants Ag*mih1*Δ (AgHPH23), Ag*hsl1*Δ (hsl1ΔNAT1), Ag*hsl1*Δ*mih1*Δ (AgHPH28), Ag*cdc12*Δ (AgHPH15), Ag*cdc12*Δ*mih1*Δ (AgHPH27), Ag*swe1*Δ (ASG35) compared to ΔlΔt (100 %). A small piece of homokaryotic mycelium (~1 mm^3) from each mutant was spotted on full medium plates and grown for 4 days. **(B)** Nuclei visualized in different strains. Mycelia (same strains as above) were grown overnight at 30°C in selective, liquid medium, fixed and processed for Hoechst dye staining. Numbers indicate average distance between two nuclei, which was determined by dividing variable lengths of hyphae by the number of nuclei observed in such a segment. **(C)** Percentage of nuclei (N>400) in different nuclear division cycle stages evaluated by Hoechst and anti-tubulin staining (Ana: anaphase; Meta: metaphase; 2 SPB: 2 spindle pole bodies; 1 SPB: 1 spindle pole body).

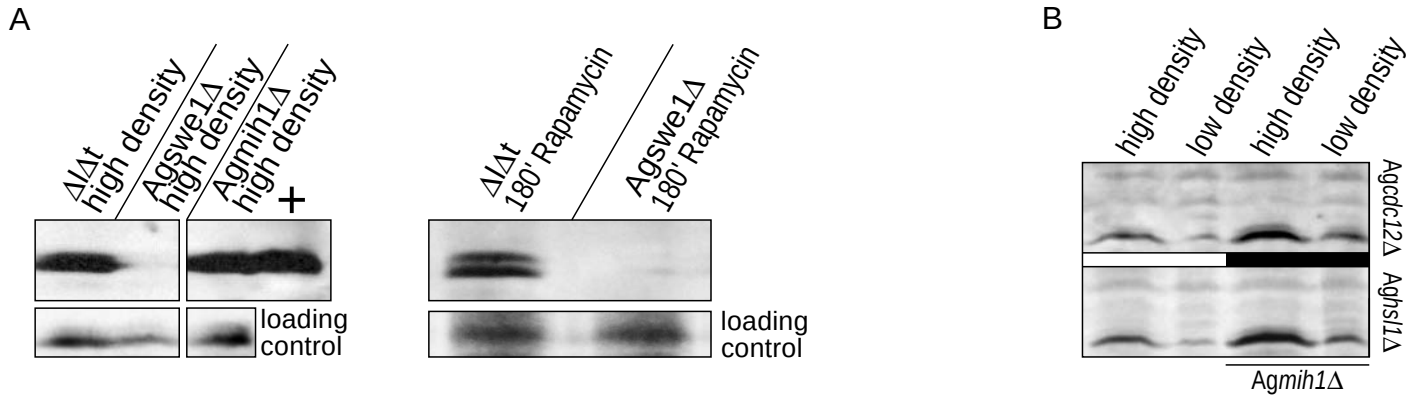

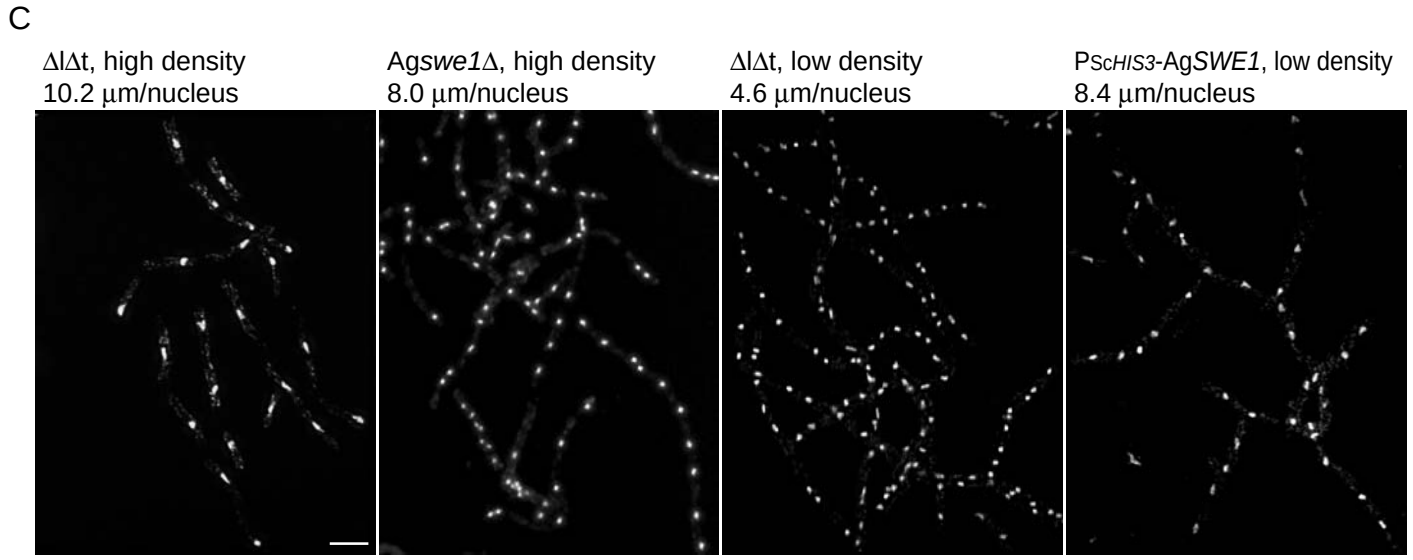

Figure I.7. AgSwe1p is responsible for AgCdc28Y18 phosphorylation and mitotic inhibition in starving hyphae. (A) ΔlΔt (reference), Ags*we1*Δ (AgHPH24) and Ag*mih1*Δ (AgHPH23) mycelia were grown to high density and whole cell extracts were assayed for CDK phosphorylation as described above (left). ΔlΔt and Ags*we1*Δ (AgHPH24) cells were grown 15 h to low density and then incubated with Rapamycin (200 nM). A non-specific cross-reacting band was used as loading control. **(B)** Ag*cdc12*Δ (AgHPH15), Ag*cdc12*Δ-Ag*mih1*Δ (AgHPH27), Ag*hsl1*Δ (hsl1ΔNAT1) and Ag*hsl1*Δ-Ag*mih1*Δ (AgHPH29) cultures were grown 19 h to high and low density and assayed for CDK phosphorylation. **(C)** Nuclei of mycelia grown for 16 h at 30 °C visualized by Hoechst staining. Bar, 10 µm.

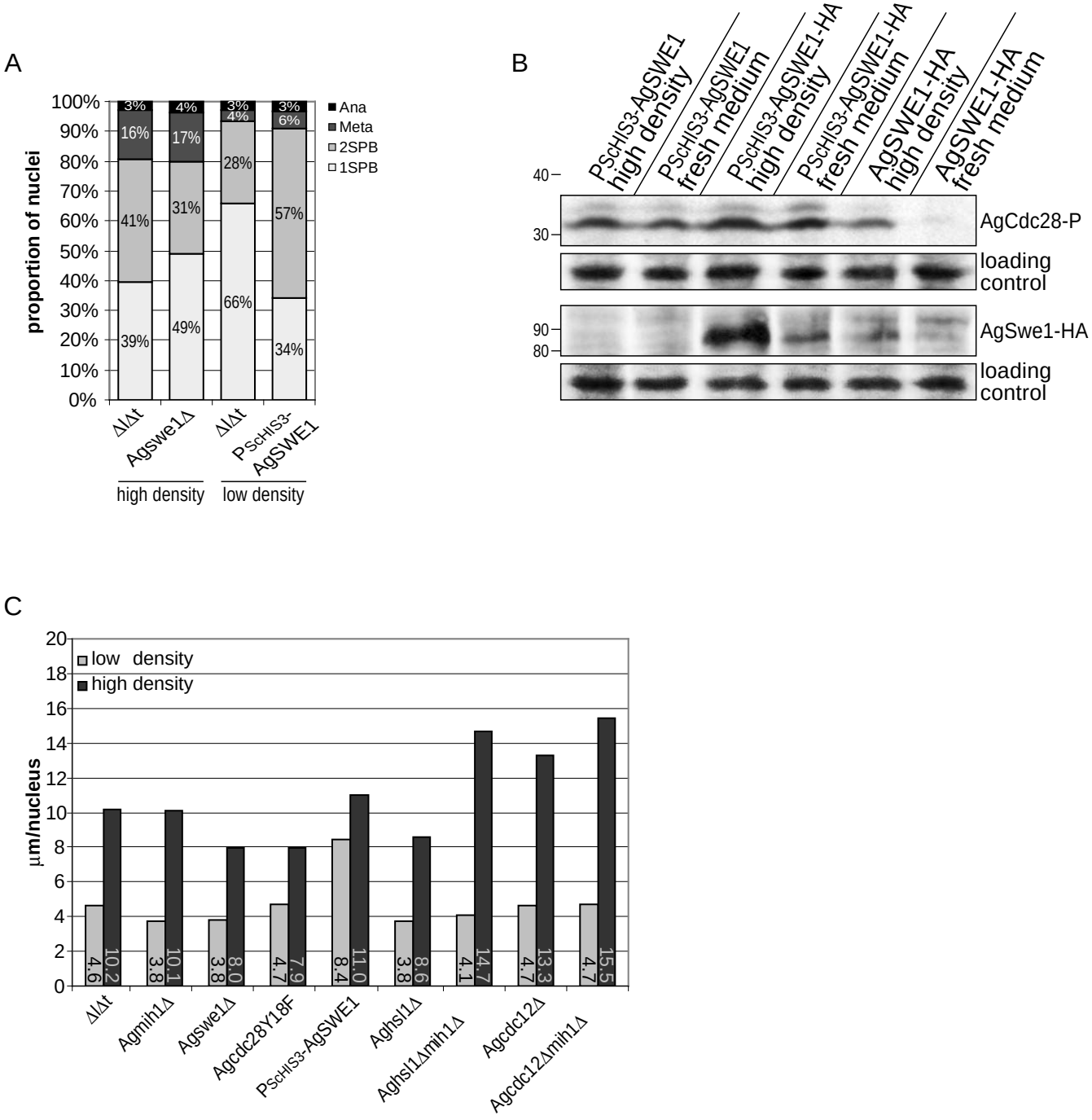

Figure I.8. AgSwe1p is responsible for AgCdc28Y18 phosphorylation and mitotic inhibition in starving cells. (A) ΔlΔt (reference), Ags*we1*Δ (AgHPH24) and PSc*HIS3*-Ag*SWE1* (AgHPH37) mycelia were grown at 30°C to high/low density and then fixed and processed for anti-tubulin immunofluorescence to evaluate the percentage of nuclei in different nuclear division cycle stages. **(B)** Whole cell extracts from PSc*HIS3*-Ag*SWE1* (AgHPH37, lanes 1-2), PSc*HIS3*-Ag*SWE1-6HA* (AgHPH38, lanes 3-4), Ag*SWE1-6HA* (AgHPH39, lanes 5-6) were generated from cultures grown for 16 h at 30°C to either high or low density. Extracts were then probed by Western blot using either the anti-phospho-cdc2 or anti-HA antibody. A non-specific cross-reacting band was used as loading control. **(C)** ΔlΔt (reference), Ag*mih1*Δ (AgHPH23), Ags*we1*Δ (AgHPH24), Ag*cdc28Y18F* (AgHPH36), PSc*HIS3*-Ag*SWE1* (AgHPH37), Ag*hsl1*Δ (hsl1ΔNAT1), Ag*hsl1*Δ*mih1*Δ (AgHPH28), Ag*cdc12*Δ (AgHPH15), and Ag*cdc12*Δ*mih1*Δ (AgHPH27) mycelia were grown to either high or low density, fixed and nuclei were visualized by Hoechst stainin to calculate the average distance between two nuclei for each strain and condition (N>200). The average distance was determined by dividing variable lengths of hyphae by the number of nuclei observed per measured segment.

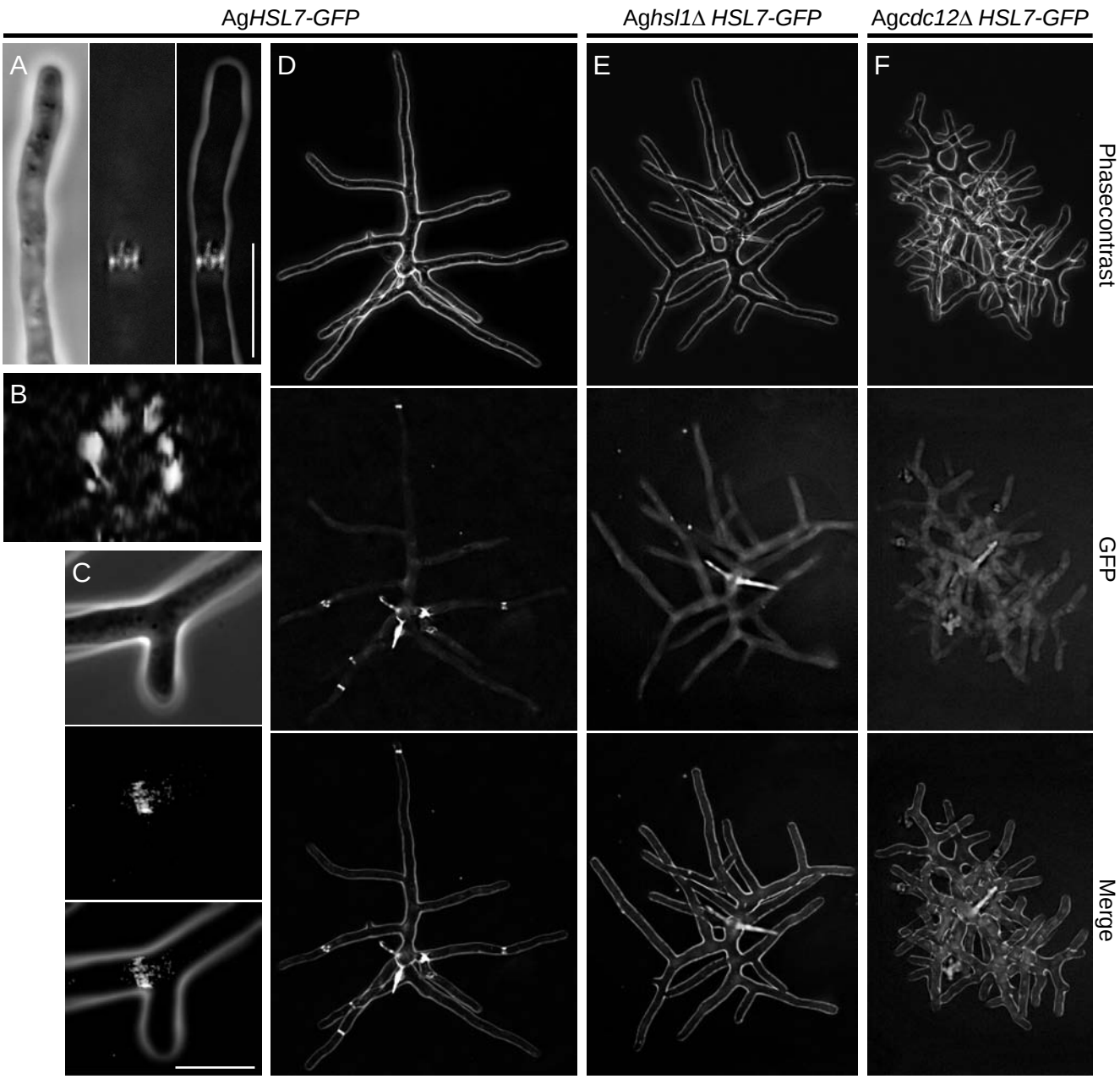

Figure I.9. AgHsl7p localizes to septin-dependent cortical rings. (A-D) Ag*HSL7-GFP* (ASG41) mycelia were grown for 12 hours at 30°C and then imaged live. **(B)** 90° 3D reconstruction of the discontinuous ring shown in **(A)**. **(E, F)** Ag*hsl1*Δ, Ag*HSL7-GFP* (AgHPH20) and Ag*cdc12*Δ, Ag*HSL7-GFP* (AgHPH19) were grown for 12 hours at 30°C and then imaged live. Phasecontrast, fluorescence and merged images are ordered from left to right **(A)** or from top to bottom **(C-F)**. Bars, 10 µm.

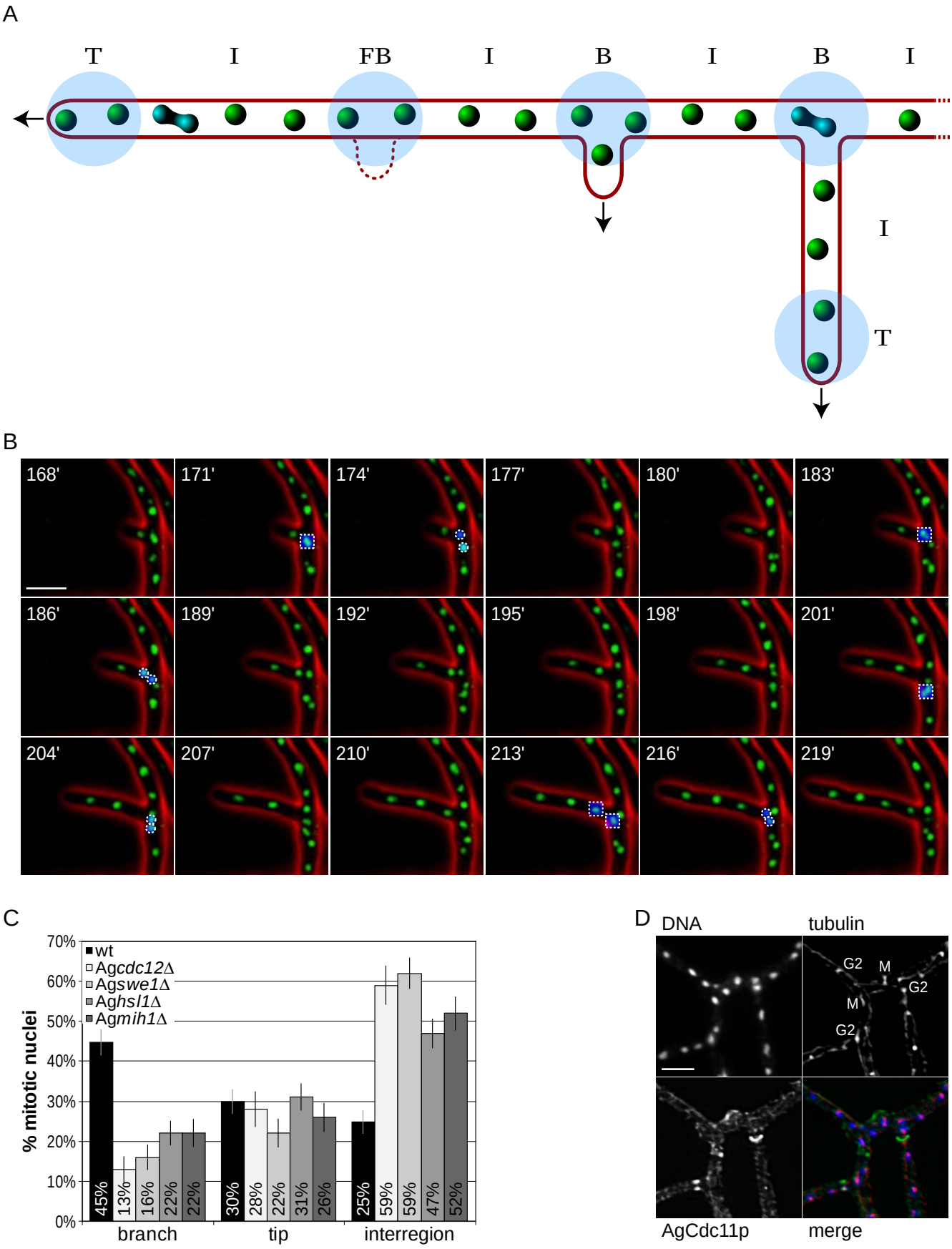

Figure I.10. Mitoses are enriched at branching points. (A) Scheme (designed by Peter Philippsen) showing the different regions of a developing mycelium that were considered for determining the spatial mitotic index: tip (T), interregion (I), future branch site (FB) and branch site (B). Tip nuclei were the 2 nuclei closest to the growing tip, branch/future branch nuclei were within 5 µm of a branch site (10 µm zone) and nuclei that were not within the tip or branches were scored as in the inter-region. **(B)** Myelia expressing GFP-labeled Histone H4 (AgH4-GFP) as nuclear marker were grown at 25°C on diluted medium containing agar and images were collected at 3 min intervals. Hyphal outlines are in red and nuclei are in green, mitoses are labeled with a box just prior to division and new daughter nuclei are outlined with circles. **(C)** Percentage of mitoses found at sites of branch formation, at tips and in the inter-region of hyphae evaluated by Amy Gladfelter by scoring Hoechst and anti-tubulin stainings (N>200 nuclei). **(D)** Reference strain mycelia (ΔlΔt) were grown overnight for 16 hours at 30°C and processed for anti-tubulin and anti-Cdc11p immunofluorescence (Amy Gladfelter). In overlay, DNA is blue, tubulin is red and septins are green. Bars, 10 µm.

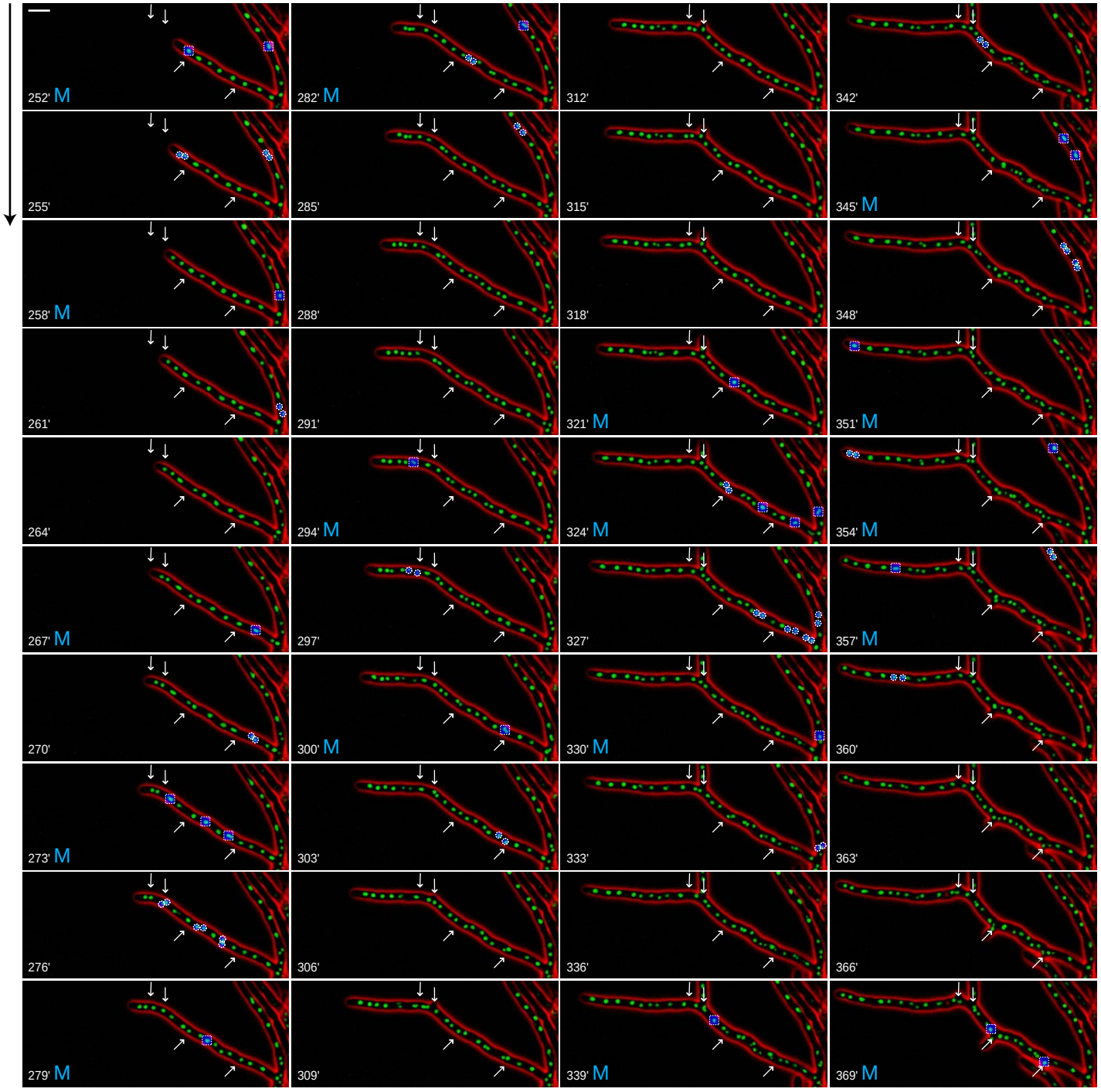

Figure I.11. Localization of mitoses at future branch sites. Mitoses in AgH4-GFP mycelium were monitored by *in vivo* time-lapse microscopy (Movie 1) as described for Figure I.10. Panels that contain a mitotic event are highlighted by a blue "M". Bars, 10 µm.

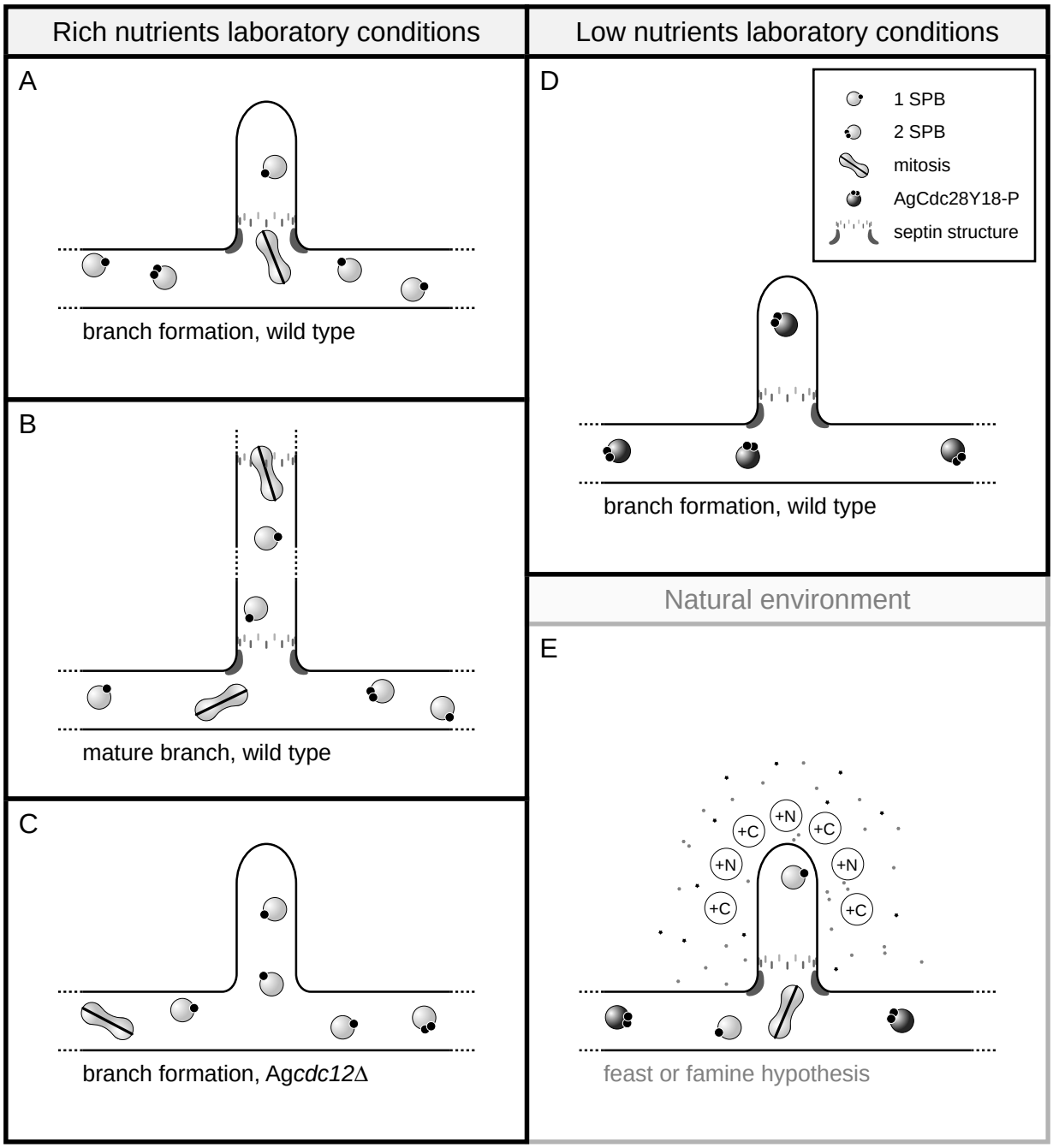

Figure I.12. Model of spatial control of mitosis by septins and nutrient availability. (A) Wild-type mycelia grown in the laboratory have mitoses enriched at branch sites near assembled septin rings. **(B)** As branch sites mature, new septin rings acquire mitosis promoting capacity, leading to mitotic events in interregions. **(C)** Mitoses are no longer localized preferentially to branch sites in mycelia lacking septins. **(D)** In low nutrient conditions, nuclei are arrested or delayed with duplicated SPBs and high CDK-Tyr18 phosphorylation levels. **(E)** Hypothesis for how mitoses may be spatially controlled in response to heterogeneous nutrient supplies in the natural world, where a single mycelium may simultaneously experience "feast and famine" conditions. Local pools of nutrients may trigger clustering of receptors/signaling factors for sensing nutrient status which promote local mitosis through the down-regulation of AgSwe1p, enabling the cell to exploit nutrients without duplicating nuclei distant to nutrient source.

Discussion

In this work, we have sought to identify mechanisms for how nuclear density may be regulated in multinucleated hyphal cells. We have shown that mitosis is limited in response to nutrient deprivation, and that this is achieved through inhibitory AgCdc28Y18 phosphorylation, promoted by the protein kinase AgSwe1p. We have shown further that mitoses are concentrated in the vicinity of branching sites, where they may be promoted by the septins. Here we discuss these data and propose a hypothetical model in which local regulation of AgSwe1p activity may enable the multinucleated mycelium to react to a spatially limited pool of nutrients and restrict mitoses to the area of the nutrient source (Figure I.12).

AgCdc28p is the only cyclin dependent kinase in *A. gossypii*. Although the CDK is essential for the nuclear division cycle, heterokaryotic deletion mutants are able to grow normally under selective pressure, which is only possible if the resistance marker used for the deletion is spread over the entire mycelium. This indicates that transformed nuclei are able to divide in heterokaryotic mycelium, despite the lack of the gene encoding the crucial kinase. This can either be explained by AgCdc28p being able to travel from wild-type nuclei into transformed nuclei, or by cytoplasmic localization being sufficient to perform the essential functions.

We observed that AgCdc28p is phosphorylated on the Y18 residue in high-density growth or conditions that mimic starvation and this is correlated with an accumulation of nuclei with duplicated SPBs and metaphase spindles and a decreased nuclear density (Figure I.12D). Overexpression of AgSwe1p is sufficient to induce some changes to the nuclear division cycle, the delay in G2, even without nutrient deprivation.

How might AgSwe1p activity be enhanced by nutrient limitation? In budding yeast cells, ScSwe1p participates in the filamentous differentiation response to nutrient limitation through inhibiting CDK/Clb2 complexes which extends G2 and promotes hyperpolarized bud growth (Edgington *et al.*, 1999; La Valle and Wittenberg, 2001). It is not clear how the status of environmental conditions is transmitted to ScSwe1p and its regulators that are partially responsible for sustaining this differentiation program. Both the STE MAPK and the RAS/cAMP pathways have known “anchors” at the plasma membrane sensor level and the nuclear transcriptional response level, however ScSwe1p can act independently of these pathways in filamentation (Ahn *et al.*, 1999). How ScSwe1p senses nutrient status in budding yeast has not been published so far, but there is strong data suggesting that the inactivating kinase of ScSwe1p, ScCdc5p, is under control of TORC1 (Nakashima *et al.*, unpublished). In fission yeast, nutrient limitation signals through a MAP kinase called Spc1 and triggers a SpWee1-mediated G2 delay potentially through the regulation of SpNim1 (Shiozaki and Russell, 1995; Belenguer *et al.*, 1997). *A. gossypii* is constitutively filamentous and unlike in *S. cerevisiae* strains, filamentous morphology changes are not observed under nutrient deprivation. Nevertheless, AgSwe1p activity makes dramatic contributions to the nuclear division cycle kinetics in starving *A. gossypii* mycelium. It was remarkable that inhibition of the Tor1/2p by rapamycin could activate Swe1p similarly to nutrient deprivation suggesting that Swe1p activity in response to starvation may be regulated downstream of this master-regulator of cell growth. This Tor1/2p path and/or a MAPK/RAS/cAMP path could communicate nutrient status and influence AgSwe1p in a variety of ways either by influencing its stability, its localization, its transcription, its intrinsic kinase activity, or affinity for AgCdc28p. Future work will be aimed at understanding how this conserved kinase senses and responds to nutrient fluctuations.

We have studied the distribution of mitoses in fixed and living mycelium. Both methods revealed a preference of mitosis to occur at branching sites. This could simply be due to cytoplasmic increases that trigger a cell-size cue that promotes mitosis. However, this would not explain why nuclei do not have a similarly pronounced preference for division near growing tips, nor would it explain why branching sites already have a mitosis promoting effect even before the branch emerges. It has been shown previously (Knechtle *et al.*, 2003) that polarization sites, such as branching points, do not occur randomly but at preformed landmarks in *A. gossypii.* It could be the same landmarks that locally promote mitosis to provide nuclei which will be required when the branch emerges. Throughout eukaryotes, septins are among the first proteins that localize to polarization sites where they serve as a scaffold for a vast number of proteins. Recent studies have shown that *A. gossypii* septins are no exception (Andreas Kaufmann, personal communication). Together with the localization pattern of the septins in *A.*

gossypii (see Chapter II), this makes them good candidates to establish landmarks for branch formation. In agreement with this view, septin deletion mutants, which are missing organized septin rings, have a random spatial distribution of mitoses. However, septin rings are not only found near existent and future branching sites but also at growing tips. Why do these structures not promote mitosis? Septin proteins have different appearing organizations depending upon their location in hyphae and potentially these morphologically different structures are also functionally distinct. Rings composed of elongated bands form at the tips, more compact rings of short septin bars appear more distant from the growing tip along the main hyphae and asymmetric bar structures are featured at most branchpoints. Conceivably, these different varieties of septin rings could recruit different pools of proteins, attract the same proteins with different affinities, or function to delineate different plasma or organelle membrane domains. Support for functional difference in the structures comes from the observation that only mitosis frequency near branches, not at tips, is diminished in septin deletion mutants. Thus, the rings of the main hyphae near branches and potentially the asymmetric structure that decorates the bases of branches may be directing mitoses in this area. Notably, this influence over the nuclear division cycle is transient and is most pronounced as the branch tip emerges, as seen in Movie 1. As the branch matures, while the ring persists there are fewer mitoses in this area suggesting a decay of the local mitotic inducing potential with time. This coincides with subtle changes in the structure of the asymmetric ring (greater distance between the two halves of the ring, see Chapter II, Figure II.3A) however it is unclear if this change is relevant for mitosis regulation.

How might the septins locally promote mitosis at branching sites? Based on the morphogenesis checkpoint in *S. cerevisae* and conservation of these factors, it is easy to hypothesize that septins direct mitosis through the recruitment and local inactivation of Swe1p. Potentially in unbranched areas of mycelia, some nuclei are delayed in division by active AgSwe1p. This delay then is relieved upon septin ring formation at branchpoints which leads to a local depletion/ inhibition of AgSwe1p and then nuclear division at such sites. The observation that deletions of Ag*SWE1,* Ag*HSL1,* Ag*MIH1,* or Ag*CDC12* similarly shift mitoses away from branches to random positions supports the possibility that the balance of AgSwe1p activity controls the spatial pattern of mitosis. Mycelia lacking Swe1p would no longer have the means to limit mitoses in unbranched areas and Mycelia lacking septins would not be able to promote mitoses at branches, both of which result in random division phenotypes. Furthermore, the localization of AgHsl7p, which functions in *S. cerevisae* as an adaptor that helps bring ScSwe1p to the septins where it is targeted for degradation, is suggestive that the links in this regulatory system may be preserved in *A. gossypii*. Thus, in response to some cell intrinsic patterning signals that direct branching in rich nutrient conditions, there is evidence that the septins may direct mitosis spatially through AgSwe1p activity.

There are some problems, however, in overlaying the details of the yeast checkpoint system onto the *A. gossypii* spatial control system that functions in response to cell intrinsic cues. AgHsl7p is not observed at all branch septin sites and rather seems to be more common at septin rings on the main hyphae although this could just be due to detection problems. Additionally, the AgHsl7p has a key residue differences in its sequence compared to the ScHsl7p at phenylalanine 242. When Sc*HSL7*F242 is mutated to leucine, the same substitution observed in the *A. gossypii* sequence (Appendix 3.6, arrow), ScHsl7p no longer can interact with ScHsl1p, and Swe1p is no longer targeted for degradation in yeast cells (Cid *et al.*, 2001b). This raises the question as to whether AgHsl1p and AgHsl7p are able to form a stable complex that could promote AgSwe1p recruitment. More notably, when mycelia are grown in high nutrient conditions, no phosphorylated AgCdc28Y18 is detectable by immunofluorescence and only a faint band is seen on Western blots. This implies that strong Cdc28Y18 phosphorylation does not occur under high nutrient conditions, leaving only little room for changes in phosphorylation levels caused by spatial control of mitosis. It is amazing that this control system is based on very subtle changes of Cdc28Y18 phosphorylation, although AgSwe1p is capable of much stronger phosphorylation of its substrate, as we have seen in starving mycelia. It is conceivable that such a system is fragile and therefore cannot be of great importance for the fitness of *A. gossypii* mycelium, at least not under laboratory conditions. This is endorsed by none of the analyzed single or double deletion mutants having any noticeable effect on nuclear density or distribution under rich nutrient conditions. With that, *A. gossypii* is in clear contrast to budding yeast, where the double deletion of the phosphatase ScMih1p and the ScSwe1 inhibitor ScHsl1p in leads to a lethal block at the G2-M transition. However, even if *A. gossypii* does not depend on spatial control of mitosis, we would expect to see at least some influence on the distribution and/or density of nuclei when this control mechanism is

eliminated. The fact that this is not the case suggests the existence of redundant, yet unidentified mechanisms to regulate nuclear division and distribution. If local control of mitosis is abolished, this could be compensated by other "global" ways to decrease AgSwe1p activity, coupled with more efficient distribution along microtubuli. Another possibility of compensation is offered by controlling where and how often branch formation occurs. Evidence for interdependence of branch formation and mitosis has already been provided in other filamentous fungi (Müller *et al.*, 2000; Westfall and Momany, 2002; Dynesen and Nielsen, 2003). Notably, these mechanisms can be bypassed or overstrained by overexpressing Ag*SWE1* from to Sc*HIS3* promoter, which results in decreased nuclear density even under non-starving conditions. AgSwe1p activity could globally be restricted on a transcriptional level in addition to locally controlling protein inhibition/degradation. This transcriptional control would no longer be functional when AgSwe1p is expressed from an exogenous promoter. Alternatively or additionally, the septins may interact more directly with nuclei at branches by capturing the ends of astral microtubules. Such associations have been observed by tubulin immunofluorescence of *A. gossypii* mycelia (Amy Gladfelter, personal communication) and potentially such physical connections which may generate tension on the astrals could be a trigger for mitosis. Swe1p may itself have other targets than AgCdc28 that are relevant for nuclear cycle progression and potentially Swe1p-dependent phosphorylation impacts their activity and in turn progression. Or AgSwe1p may be able to directly inhibit AgCdc28p independent of Y18 phosphorylation and there is actually precedent for this alternative inhibition of the CDK in the morphogenesis checkpoint in budding yeast (McMillan *et al.*, 1999b).

Whereas spatially controlled mitoses do not seem to be an important feature for *A. gossypii* grown in laboratory conditions, this may be different in its natural environment. Filamentous fungi inhabit heterogeneous environments in the natural world. There is spatial and temporal irregularity in many factors such as water, temperature, minerals, pH in addition to carbon and nitrogen sources. *A. gossypii* is found outside the laboratory as a tropical plant pathogen where it is transmitted by sucking insects and can infect cotton and citrus fruits leading to dry rot (Ashby and Nowell, 1926; Batra, 1973). Given the large potential size of a filamentous fungal mycelium in which many interconnected hyphae share a common cytoplasm, a single mycelium may simultaneously experience "feast and famine" conditions. In many fungi, branching is induced by exposure to pockets of nutrients allowing the mycelium to forage and exploit that presumably limited source. A mycelium would ideally target these resources locally, producing more nuclei to support the exploring hyphae while the rest of the nuclei and mycelium remain quiescent. In a syncytium, however, it is unclear how a mycelium may delineate the active and inactive regions. Our current laboratory culturing conditions of *A. gossypii* make it difficult to simulate the nutrient heterogeneity such mycelia would encounter in the natural world. However, we have attempted to integrate the data we have generated on Swe1p spatially directing mitosis in the presence of abundant nutrients and Swe1p inhibiting mitosis during starvation into a model. In this model, sudden increases in the pools of nutrients would lead to branch initiation and a promotion of mitoses in the limited area. Interestingly, the Swe1p-dependent response to low nutrients was exacerbated in mycelia lacking septins. Thus, the septins which reside close to and at the branching sites might regulate the Swe1p-dependent response to nutrient status. However, considering the problems we were facing when growing the septin mutants, this data has to be handled with care. The involvement of the TOR complex in starvation triggered phosphorylation of AgCdc28Y18 makes it more likely that this response is spatially controlled by clustering of receptors/signaling factors for sensing nutrient status on the cell surface, which then inactivate a pool of AgSwe1p to generate mitoses locally (Figure I.12E).

Chapter II

Septins – cytokinesis factors in the absence of cell division in *A. gossypii*

Introduction

A characteristic feature of filamentous fungi is their multifaceted morphology. Some are able to choose between yeast-like growth, pseudohyphal growth or true hyphal growth. Others, like *A. gossypii,* are restricted to the hyphal form, which is most different from unicellular growth and propagation. It is of high interest to study factors that are involved in morphogenesis of these organisms. A protein family of such morphogenesis factors are the septins. They were discovered in 1970 by Hartwell and colleagues in a screen for ts mutants affecting cell division (cdc mutants). The screen revealed four mutants which prevented cytokinesis at restrictive temperature. The corresponding genes represent the four original septins, Sc*CDC3,* Sc*CDC10,* Sc*CDC11,* and Sc*CDC12*. Despite disrupted cytokinesis, the cells continued budding, DNA synthesis, and nuclear division, which resulted in large multinucleated cells with multiple, elongated buds (Hartwell *et al.*, 1970; Hartwell, 1971a; Hartwell *et al.*, 1974). By analyzing electron micrographs in 1976, Byers and Goetsch discovered ~20 evenly spaced striations of 10-nm filaments around the mother-bud neck in wild-type but not septin-mutant cells. Immunofluorescence studies revealed that the septin proteins colocalize into a ring at the neck (Byers and Goetsch, 1976; Haarer and Pringle, 1987; Kim *et al.*, 1991; Longtine *et al.*, 1996; Field and Kellogg, 1999). The localization of all four septins is disrupted in conditional Sc*cdc3* and Sc*cdc12* mutants, indicating interdependence of the septin proteins. Strong support for this finding was provided by biochemical studies: The four original septins co-purified on affinity columns, together with a fifth septin protein, ScSep7p or ScShs1p (Carroll *et al.*, 1998; Frazier *et al.*, 1998). Purified septins from budding yeast, Drosophila, Xenopus, and mammalian cells are able to self associate in vitro to form highly ordered, filamentous structures (Frazier *et al.*, 1998; Kinoshita *et al.*, 2002; Casamayor and Snyder, 2003; Caviston *et al.*, 2003; Dobbelaere *et al.*, 2003; Versele *et al.*, 2004). How the septins interact *in vitr*o to form heteropentamers that assemble into filaments was studied in detail in *S. cerevisiae* (Versele *et al.*, 2004). Based on these and former studies, the septins are composed of a variable N-terminus with a basic phosphoinositide binding motif, a conserved core comprising a GTP-binding domain, a septin-unique element and a C-terminal extension including a predicted coiled coil (Saraste *et al.*, 1990; Field and Kellogg, 1999; Zhang *et al.*, 1999; Casamayor and Snyder, 2003; Versele *et al.*, 2004).

Micrographs of purified filaments raised the possibility that the septins are organized in parallel to the mother-bud axis. The 10-nm striations seen on electron micrographs may be the result of lateral interaction between the filaments (Frazier *et al.*, 1998; Longtine *et al.*, 1998; Gladfelter *et al.*, 2001b). Mutant strains lacking factors important for septin organization support this view. Instead of continuous rings, the septins form bars oriented along the mother-bud axis in deletion mutants of Sc*GIN4*, Sc*NAP1* and Sc*CLA4* (reviewed in Longtine *et al.*, 2000; Gladfelter *et al.*, 2001b).

The septins act as a scaffold, recruiting a plethora of proteins (reviewed by Longtine *et al.*, 1996). These protein complexes are involved in cytokinesis, chitin deposition, cell polarity (reviewed by Faty *et al.*, 2002), spore formation (Fares *et al.*, 1996), in the morphogenesis checkpoint (see Chapter I), spindle alignment checkpoint and bud site selection (Hartwell, 1971a; Byers and Goetsch, 1976; Fares *et al.*, 1996; Kartmann and Roth, 2001; Faty *et al.*, 2002; Dobbelaere and Barral, 2004; Douglas *et al.*, 2005; Gladfelter *et al.*, 2005).

Cytokinesis is driven through two septin dependent, redundant processes: recruitment and contraction of the actomyosin ring and formation of the septum by vesicle fusion with the plasma membrane (Epp and Chant, 1997; Bi *et al.*, 1998; Lippincott and Li, 1998b, 1998a; Vallen *et al.*, 2000). In contrast to septin mutants, disruption of one single pathway only leads to a delay in cytokinesis, not complete failure of cell division. Hence, the septins are predicted to act at the most upstream level of cytokinesis.

The role of septins in cell polarity is reviewed in detail by Faty *et al.*, 2002 . After the apical-isotropic switch in budding yeast, cortical

components, supposedly of the exocyst and polarisome, are delocalized from the apical pole to the entire plasma membrane of the bud, but not the mother cell. The septin ring at the neck serves as a cortical barrier that prevents membrane diffusion of these factors between the two compartments. This asymmetric distribution is abolished in septin mutants (Barral *et al.*, 2000; Takizawa *et al.*, 2000; Faty *et al.*, 2002).

Some conditional septin mutants do not form buds at their normal axial location. Moreover, the typical localization of some bud-site-selection factors in a double ring at the neck is lost or disturbed in these mutants. This indicates that the septins may serve as anchoring site for such factors in axially budding cells (Flescher *et al.*, 1993; Chant *et al.*, 1995; Cabib *et al.*, 1998).

It seems that one single septin organization should not be sufficient to fulfill such a variety of tasks. Accordingly, the septin cortex undergoes several changes throughout the cell cycle (reviewed by Gladfelter *et al.*, 2001b): The first visible septin structure is a distinct ring which appears ~15 min before bud emergence. After bud emergence, the ring broadens to assume the shape of an hourglass around the mother-bud neck. During cytokinesis, the septin cortex splits into a double ring which eventually disappears. How can the septin cortex undergo so dramatic changes, although some of its functions may require it to be a stable structure? FRAP analysis has revealed that the turnover of septins at the neck undergoes multiple changes during the cell cycle. The predominant, functional conformation is characterized by a low turnover rate (frozen state), during which the septins are phosphorylated. Structural changes require a destabilization of the septin cortex (fluid state) induced by dephosphorylation prior to bud emergence, ring splitting and cell separation (Dobbelaere *et al.*, 2003).

The composition of the septin cortex does not only vary throughout the cell cycle but also along the mother-bud axis. This inherent polarity of septin filaments allows concentration of some proteins primarily to the mother side of the neck, some to the center and others to the bud site (DeMarini *et al.*, 1997; Gladfelter *et al.*, 2001b).

Since their discovery in *S. cerevisiae,* septin homologues have been found throughout the eukaryotes, with the exception of plants. The variety of different shapes that septins can assume within a single cell is especially apparent in filamentous fungi (reviewed by Gladfelter, 2006). The genome of *C. albicans* encodes homologues to all *S. cerevisiae* septins (CaCdc3p, CaCdc10p, CaCdc11p, CaCdc12p, CaSep7p). They form a diffuse band at the base of emerging hyphae, a bright double ring at septation sites, an extended diffuse cap at hyphal tips and elongated filaments stretching around the spherical chlamydospores (Sudbery, 2001; Kaneko *et al.*, 2004; Martin and Konopka, 2004b; Wightman *et al.*, 2004; Martin *et al.*, 2005). Five septins are found in *A. nidulans* (AnAspAp, AnAspBp, AnAspCp, AnAspDp, AnAspEp). AnAspBp forms single rings at septation sites that eventually split into double rings. Additionally, AnAspBp forms a ring at sites of branch emergence which broadens into a band as the branch grows (Westfall and Momany, 2002). As a effect of maturation double rings reflect hyphal polarity by disassembling the tip proximal ring in *C. albicans* or the more basal ring in *A. nidulans* (Warenda and Konopka, 2002; Westfall and Momany, 2002). Bases for the various patterns of septin organization could be different modifications and/or localization of different septin interaction partners.

The septins in both, *A. nidulans* and *C. albicans* control aspects of filamentous cell shape. CaCdc3p and CaCdc12p are essential for proliferation in yeast or hyphal forms. Ca*cdc10*Δ and Ca*cdc11*Δ mutants are viable but show aberrant chitin localization and cannot properly maintain hyphal growth direction (Warenda and Konopka, 2002; Martin *et al.*, 2005). Conditional mutants of the essential AnAspBp display diffuse chitin deposition and a hyper-branching phenotype (Westfall and Momany, 2002).

Here, we add data on the function and localization of the septins in a fungus which grows exclusively in the hyphal form. Our studies have lead to the discovery of novel structures and revealed the astonishing fact that none of the analyzed septin genes in *A. gossypii* is essential, despite significant roles in morphogenesis.

Results

Septins are conserved in two organisms of most diverse morphology

Abscission (complete cytokinesis) is not observed in healthy, multinucleated *A. gossypii* hyphae, at least not until the sporulation program is initiated (Brachat, PhD thesis, 2003). Does this mean this *Ascomycete* does not require a full set of septin proteins as we find them in *S. cerevisiae*? Interestingly, not only were homologues to all budding yeast septins identified in *A. gossypii*, one of them even revealed two homologues, Ag*CDC11A* (AER445C) and Ag*CDC11B* (AFR436C), as a result of tandem duplication followed by chromosome break (Sophie Brachat, personal communication; Dietrich *et al.*, 2004). Pairwise alignment with the *S. cerevisiae* homologues was used to identify the domains described by Versele *et al.* (2004). With the exception of Cdc3p, all mitotic septins and their domain composition were found to be highly conserved between the two organisms (Figure II.1), despite their substantially different life cycles.

Continuous AgSep7p-GFP ring at the neck of budding yeast

To understand where the septins may be required in *A. gossypii,* we first studied their localization by using the AgSep7p-GFP construct. The GFP fusion was obtained by in vivo recombination in *S. cerevisiae* (see materials and methods). We used this opportunity to investigate whether AgSep7p was able to interact with the *S. cerevisiae* septin complex, despite the low conservation (38 % identity) between the C terminal extensions (CTEs) of AgSep7p and ScSep7p. Versele *et al.* (2004) had shown that the CTE of ScSep7p is required for proper interaction with ScCdc11p. Remarkably, a bright, continuous single or double ring structure at the neck was observed which did not look differently from septin formations in budding yeast (Figure II.2A) (Field and Kellogg, 1999; Yuzyuk and Amberg, 2003). This revealed that the Ag*SEP7* promoter is functional in budding yeast and the protein does properly localize and not disturb the assembly of the *S. cerevisiae* septins, despite the differences in the CTE.

Intermitted hyphal AgSep7p-GFP rings in *A. gossypii*

Surprisingly, very different structures were observed when we studied the localization of AgSep7p-GFP in *A. gossypii,* using strains carrying plasmids or integrated constructs. Most noticeably, ring-like structures were not continuous like in budding yeast, but rather made from 9 – 12 parallel bars (Figure II.2B). These bar rings changed their appearance depending on their position within the mycelium. They were long and diffuse close to the growing tips and got shorter and more compact the further away they were from the tip (Figure II.2C). In older parts of the mycelium we found double rings with various distances between the two rings, probably representing mature septa (Figure II.2B). At low magnification, these double rings and some compact single rings had a continuous appearance. To see whether the bars eventually fuse to form continuous rings, we investigated ambiguous structures at higher magnification and by using 3D reconstruction. Out of 28 single rings, bars were identified in 25 rings. In three cases, evaluation was not possible due to poor picture quality. The resolution of light microscopy was not high enough to resolve the structure of double rings. In some cases they appeared to be made from a large number of short bars, but this remains uncertain.

We had the possibility to study septin structures in giant hyphae of a strain expressing a constitutively active form of AgCdc42p created by (Köhli, Diploma thesis, 2003). We observed unusually long septin filaments at the tip and a double ring like structure composed of bars (Figure II.2D). It is not unlikely, however, that septin structures are influenced by mutations of AgCdc42p (Richman *et al.*, 1999; Cid *et al.*, 2001a; Gladfelter *et al.*, 2001a; Caviston *et al.*, 2003). Thus, we have to be careful when concluding from these “macro structures” to wild-type septin structures.

The bar and gap organization of hyphal rings was confirmed by immunofluorescence using an anti-Cdc11p antibody (Amy Gladfelter and Michael Köhli, personal communication). This made us wonder whether each bar consist of all mitotic septins, leaving real gaps in between, or whether there are various categories of filaments, made from different septin compositions. In the latter case it was conceivable that the septins actually form continuous rings which appear as bar-like when only one septin is labeled (Figure II.2E). To distinguish between the two possibilities, AgSep7p-GFP and AgCdc11A/Bp were co-immunostained using anti-GFP and anti-Cdc11p antibodies. Due to high background and low signal intensity we found only one ring were both stainings were useable. In this ring we could clearly observe co-localization of AgSep7p-GFP bars and AgCdc11A/Bp bars. This puts the first hypothesis (Figure II.2E, left) in favor, but is not sufficient to exclude the second hypothesis.

Variety of septin organizations

Septins in *A. gossypii* were not only found to localize as single and double rings at the hyphal cortex, they also formed a variety of asymmetric structures at the base of branches. Depending on the age/length of the branch, these structures had different appearances (Figure II.3A). Already at the base of branches that were just about to emerge, we observed septin localizations in the angles of the branch with the mother hyphae but not in between (Figure II.3A, first picture). It is not clear, whether this was an imaging artifact or whether the two localizations were actually not connected in most branches. In some cases it looked as if the two deposits were about to join each other to form a ring like organization. With proceeding growth of the branch, a diffuse ring appeared at the growing tip. In longer branches, the septin localization at the base of the branch was usually joined by a ring composed of bars on top of it, with various distances between the two formations. At the base of mature branches we could observe double rings which looked like those seen in other old parts of mycelium, distal from the base. Despite the different appearance of hyphal septin rings and the asymmetric septin organizations at the base of branches, both formations eventually lead to double rings of comparable appearance.

Another phenomenon, small rings or patches with a diameter of 0.5 µm, was only seen in mycelium expressing AgSEP7-GFP from plasmid and thus likely was an artifact due to local overexpression. These rings were of remarkable similarity with septin structures found in other organisms under some unnatural conditions (Figure II.3B) (Kinoshita *et al.*, 2002; Kozubowski *et al.*, 2003).

The commonly observed *A. gossypii* septin structures are summarized in Figure II.4A and put in relation to their position within the mycelium in Figure II.4B. Most of the structures seen with AgSep7p-GFP were confirmed by anti-Cdc11p immunofluorescence in fixed mycelium (Amy Gladfelter and Michael Köhli, personal communication).

Chronological order of septin localization

By analyzing time-lapse movies of Ag*SEP7-GFP* strains we aimed at gaining further insight in the temporal organization of septin structures. Unfortunately, the AgSep7-GFP signal was relatively week for the purpose of time-lapse analysis which – combined with the strong background of *A. gossypii* in the GFP channel – made it difficult to follow the formation of septin structures in detail. In Movie A, we were able to observe the transition from a hyphal single ring to a double ring (Figure II.5A). Remarkably, the single ring was fading around 100 min before the signal reappeared as a double ring. The best result was obtained with a movie of GFP labeled nuclei together with AgSep7-GFP (Movie B, Chapter I). Using minimal medium (2xASD) instead of full medium resulted in less background at the cost of reduced growth. Nevertheless we could follow the basic steps of septin deposition during hyphal growth: A broad septin signal appeared at sites of branch formation when the first bulging of a new branch was visible. When the bulge took hyphal shape, the septin deposit was split in two parts, one portion staying at the base of the branch, the other moving together with the growing tip. Eventually, a portion parted from the deposit at the tip to form a hyphal ring, whereas the other part remained at the tip (Figure II.5B). We tried to study these events in detail, by concentrating on two branching sites with acceptable quality. At each time point ($\Delta t = 2$ min), we analyzed each focal plane individually (5 planes covering 3 µm). The sketch shown in Figure II.6 was drawn based on these observations. In contrast to long exposure, high magnification picture stacks, signal strength and resolution in the movie were often too low to distinguish single septin bars and only a diffuse glow was visible, which is represented as such in the sketch. Analysis of both, fluorescence and phase contrast planes revealed that fainting of the structure and transition to a double ring occurred at about the same time as septum formation. This lead to a sandwich of two bright septin rings with the septum in between (indicated as red in Figure II.6). More movies will be required in order to confirm this data.

One ring to rule them all

The manifoldness of septin structures – many of them so far not described in wild-type budding yeast – made us wonder whether recruitment of other proteins is limited to only some of these conformations. Amy Gladfelter has observed that AgHsl7p-GFP co-localizes with some, but not all septin rings (personal communication). Here we wanted to know which of the septin structures are likely to be involved in the formation of actin rings. For that, we used mild fixation to stain the actin cytoskeleton while preserving the integrity of GFP. Actin rings were limited to mature, contracted septin structures and in no case was an actin ring observed in the absence of a septin ring (Figure II.7A).

Does this imply that the compact septin rings are essential for actin ring formation? To answer this and learn more about septin functions in a filamentous fungus in general, Ag*CDC3,* Ag*CDC10,* and Ag*CDC12* were deleted in an Ag*SEP7-GFP*

background. This allowed us to investigate the importance of single septins for the association into the structures we had observed. Each deletion resulted in delocalization of AgSep7p-GFP to the cytoplasm; no distinct septin structures were visible in these mutants. (Figure II.7B)

We have seen that actin rings are only found at compact septin rings. Further, septins have been found to permanently localize to growing tips. What is the effect of a total loss of septin structures on the actin cytoskeleton? Are they important for both, actin ring formation and polarization of actin patches? No actin rings were detectable in the mutants Ag*cdc3*Δ and Ag*cdc10*Δ (Figure II.7C). Though these strains exhibited a certain resistance to the staining procedure, actin patch polarization was still visible. Thus, while septin rings are essential for the formation of actin rings, the septin protein pool found at growing tips does not seem to be important for the polarization of the actin cytoskeleton.

It was shown previously that even in the absence of actin rings, malformed chitin rings, and aberrant septa can still be observed in Ag*myo1*Δ mutants, permitting low sporulation levels (Helfer, Diploma thesis, 2001). In Ag*cdc3*Δ and Ag*cdc10*Δ mutants neither chitin ring formation, nor septum formation, nor sporulation were observed (Figure II.8A). Ag*cdc12*Δ strains were not stained for actin or chitin, but AgSep7p-GFP localization, septum formation, and sporulation were abolished in this mutant. Thus, the septin structures in *A. gossypii* are recruiting more components than those required for actin ring formation. Unlike in Ag*myo1*Δ, there is no alternative way for septum formation that could substitute septin deletions.

When performing microscopy of septin deletion mutants, we could directly observe that damage induced leakage of the cytoplasm was not restricted to one compartment like in the reference strain but extended to the entire young mycelium (data not shown). As a result, liquid cultures of septin deletion strains were usually a mixture of living mycelia and thin “empty shells” (Figure II.8B). Similarly, cultures grown on solid medium had a high content of dead material. This strongly supports the idea of septa functioning as bulkheads to limit damage to the affected hyphae.

A. gossypii septins are not essential but required for efficient growth and proper morphogenesis

Can *A. gossypii* survive without such a protective mechanism, or will septin mutants inevitably lyse before mature colonies can be formed? Despite lethality of most septin null mutants in *S. cerevisiae,* Ag*cdc3*Δ, Ag*cdc10*Δ and Ag*cdc12*Δ deletion strains form colonies on solid medium at 30 °C and 37 °C with a moderate reduction of radial growth speed to roughly 70% – 80% of the reference strain (Figure II.9A).

We tried to get further insight in how the septins are required for growth by studying the morphology of small and mature mycelia in septin null mutants. Possible effects on the nuclear cycle, which could also lead to a decrease in radial growth, have already been discussed in Chapter I. Morphological defects in small mycelia grown in liquid (10 – 15 h) were already revealed when looking at the stainings described above. Mutant hyphae exhibit an erratic thickness with characteristic bulges in the area of branch points and especially around the spore (Figures II.7B, 7C, 8A and 8B).

Mature mycelia grown on plates (8 days) revealed invasive growth and a curly phenotype of hyphae, indicating reduced capability of maintaining growth direction. Lateral branching and apical branching occurred in septin null mutants, but the branching pattern appeared random. Long stretches free of branches or only with attempts of branch formation alternated with regions of unusually dense branching. Lateral branching was still ubiquitous close to growing tips, where in reference mycelia of the same age only apical branching was found (Figure II.9B). Apparently, septins in *A. gossypii* are involved in a variety of morphogenetic processes.

Cortical barrier?

In *S. cerevisiae,* the septins have been shown to form a cortical barrier around the mother bud neck which prevents membrane diffusion between mother and bud and maintains cortical polarity. Thus, components of the exocyst and the polarisome are restrained to the bud (Snyder, 1989; Barral *et al.*, 2000; Takizawa *et al.*, 2000; Faty *et al.*, 2002). We wondered whether the reduced growth rate and erratic thickness of hyphae in *A. gossypii* septin deletion mutants could be the result of absent diffusion barriers. The septins might be required to efficiently maintain a pool of growth components at the hyphal tips by preventing diffusion towards older parts of the hypha (Figure II.10A). We used Filipin to stain sterols as an indicator of membrane polarity (Wachtler *et al.*, 2003). Polarization of sterols at hyphal tips was clearly visible in reference hyphae and septin null mutants (Figure II.10B). Thus, the septin ring close to hyphal tips in *A. gossypii* apparently is not required to maintain sterol polarity. However,

it cannot be excluded that they serve as a barrier for certain membrane proteins.

Separating the "twins" *(AgCDC11A/B)*

The fact that the genome of *A. gossypii* encodes two homologues to Sc*CDC11* as a result of tandem duplication followed by chromosome break made Ag*CDC11A* and Ag*CDC11B* highly interesting candidates for functional analysis. Do both homologues occupy distinct roles, or are they redundant? The high degree of conservation between the two genes made it difficult to specifically delete and verify only one homologue at a time. With the exception of CDC11A/B-I1, Primers were designed to provide best possible diversity (Figure II.11). Verification PCRs for each strain were done with primer sets for both, AgCDC11A and AgCDC11B. Both ends of each replaced ORF were verified unambiguously, no unspecific binding to the wrong locus was detected (Figure Appendix 1.9B).

In terms of morphology, Ag*cdc11A*Δ isolates exhibited high similarity to other septin null mutants (Ag*cdc3*Δ, Ag*cdc10*Δ, Ag*cdc12*Δ). As in those strains, the actin cytoskeleton was difficult to stain in Ag*cdc11A*Δ mycelium, resulting in cloudy images with actin patches being barely visible. Amazingly, actin rings and chitin rings were both detectable in this strain (Figure II.12A). Fitting to these results, sporulation was not abolished entirely but only reduced to 30%. Whereas deletion of Ag*CDC11A* leads to a mild septin phenotype, we did not observe any mutant phenotype of Ag*cdc11B*Δ null mutants at all. Morphology, actin staining, chitin staining, and sporulation were as in reference mycelium (Figure II.12B). Apparently, the two homologues have diverged enough to be of different importance for the development of *A. gossypii* mycelium. More experiments are required to determine whether Ag*CDC11B* is expressed under laboratory conditions, whether the two homologues complement each other to exercise functions similar to the other septins, or whether they have partially adopted novel roles, tailored for the requirements in a filamentous fungus in natural environment.

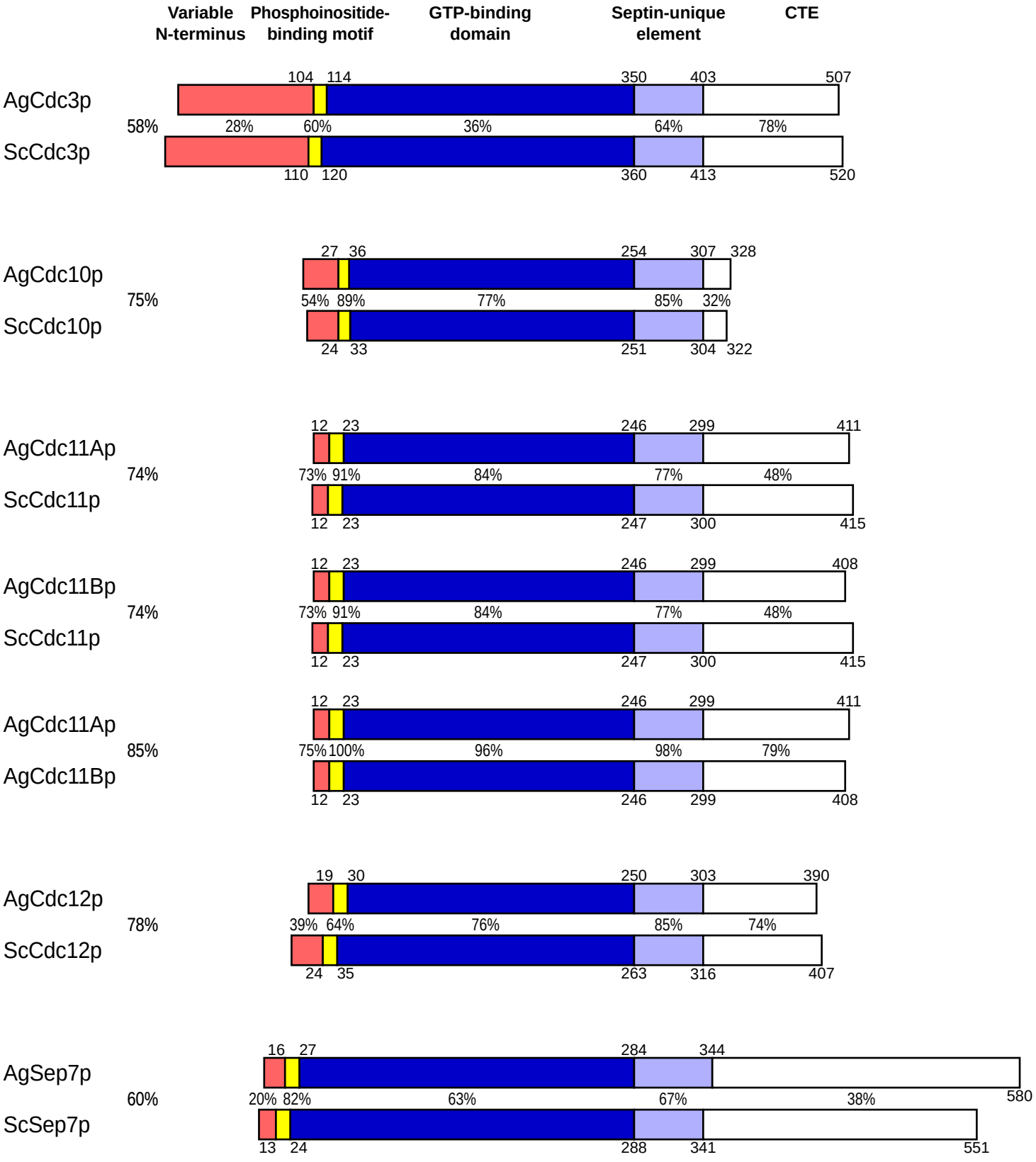

Figure II.1. Domain composition of *A. gossypii* and *S. cerevisiae* mitotic septins. The septins are composed of a variable N-terminus with a tract of basic and hydrophobic residues constituting a phosphoinositide-binding motif, a conserved core comprising a GTP-binding domain, a septin-unique element and a C-terminal extension (CTE) including a predicted coiled coil. The domains were identified by pairwise alignment with the *S. cerevisiae* homologues, using the boundaries defined by Versele *et al.,* 2004.

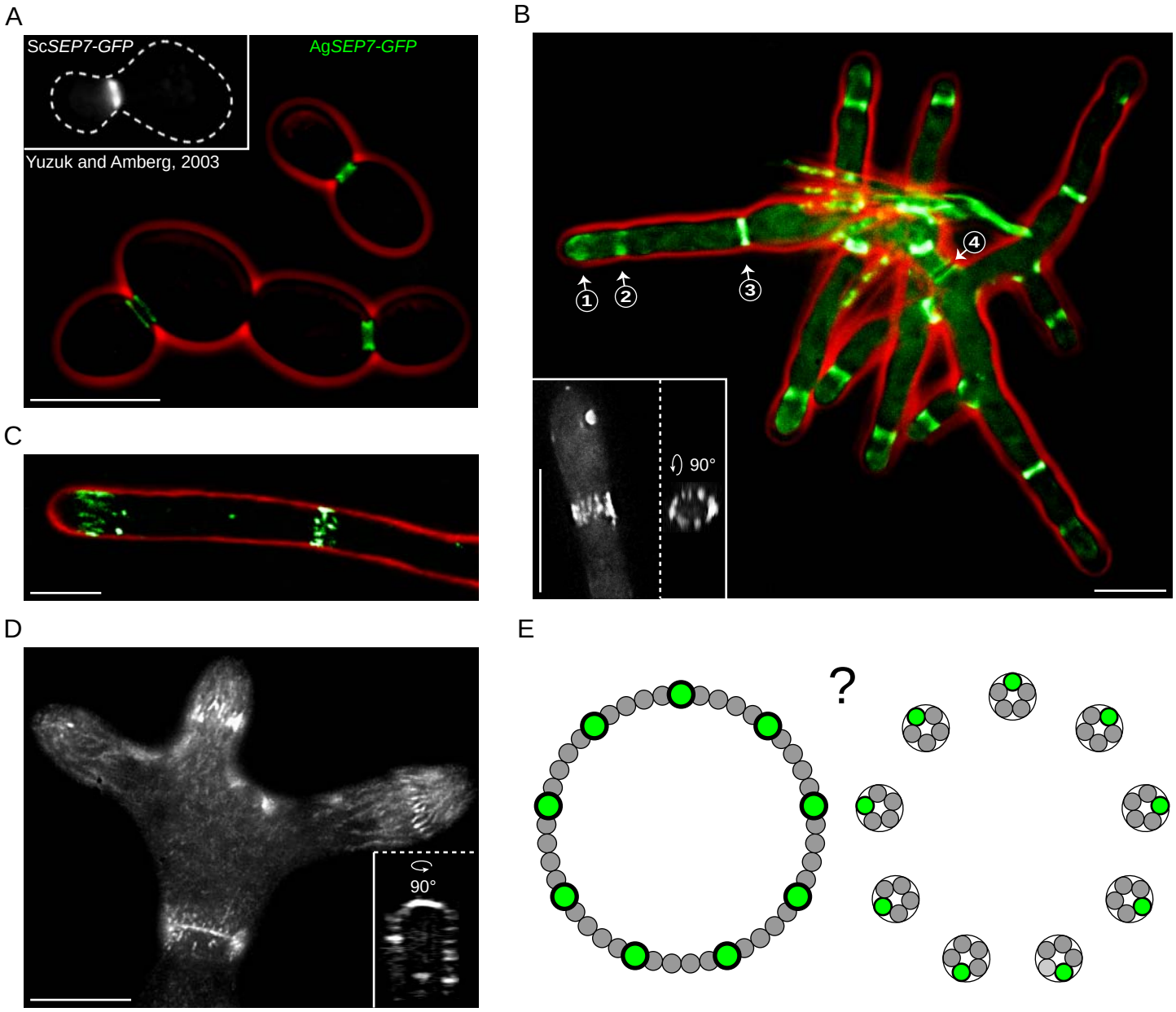

Figure II.2. Ag*SEP7-GPF* in *A. gossypii* and *S. cerevisiae.* (A) *S. cerevisiae* cells bearing Ag*SEP7-GFP* on the plasmid pagHPH002 were grown in liquid YPD with selection and imaged live. The inlay shows the localization of ScSep7p-GFP as reference (Yuzuk and Amberg, 2003). **(B, C)** *A. gossypii* mycelium with integrated Ag*SEP7-GFP* (AgHPH007) was grown for 12 h at 30°C, washed in minimal medium and subjected to *in vivo* fluorescence microcopy. The inlay in **(B)** shows a 90° 3D reconstruction of the discontinuous ring. The large picture shows how the septin rings contract the further away they are from the tip. 1: diffuse localization at the tip, 2: intermediate ring, 3: contracted ring, 4: double ring. **(C)** Diffuse tip localization consists of elongated septin filaments; rings distal from the tip are made from more contracted bars.**(D)** Ag*SEP7-GFP* in a background of constitutively active AgCdc42^{+}p (AgHPH016), grown as described above, 90° 3D reconstruction in the inlay. **(E)** Schematic representation of the two hypotheses according to which one bar represents one septin (left) or each bar is composed of all the septins (right). Bars, 10 µm.

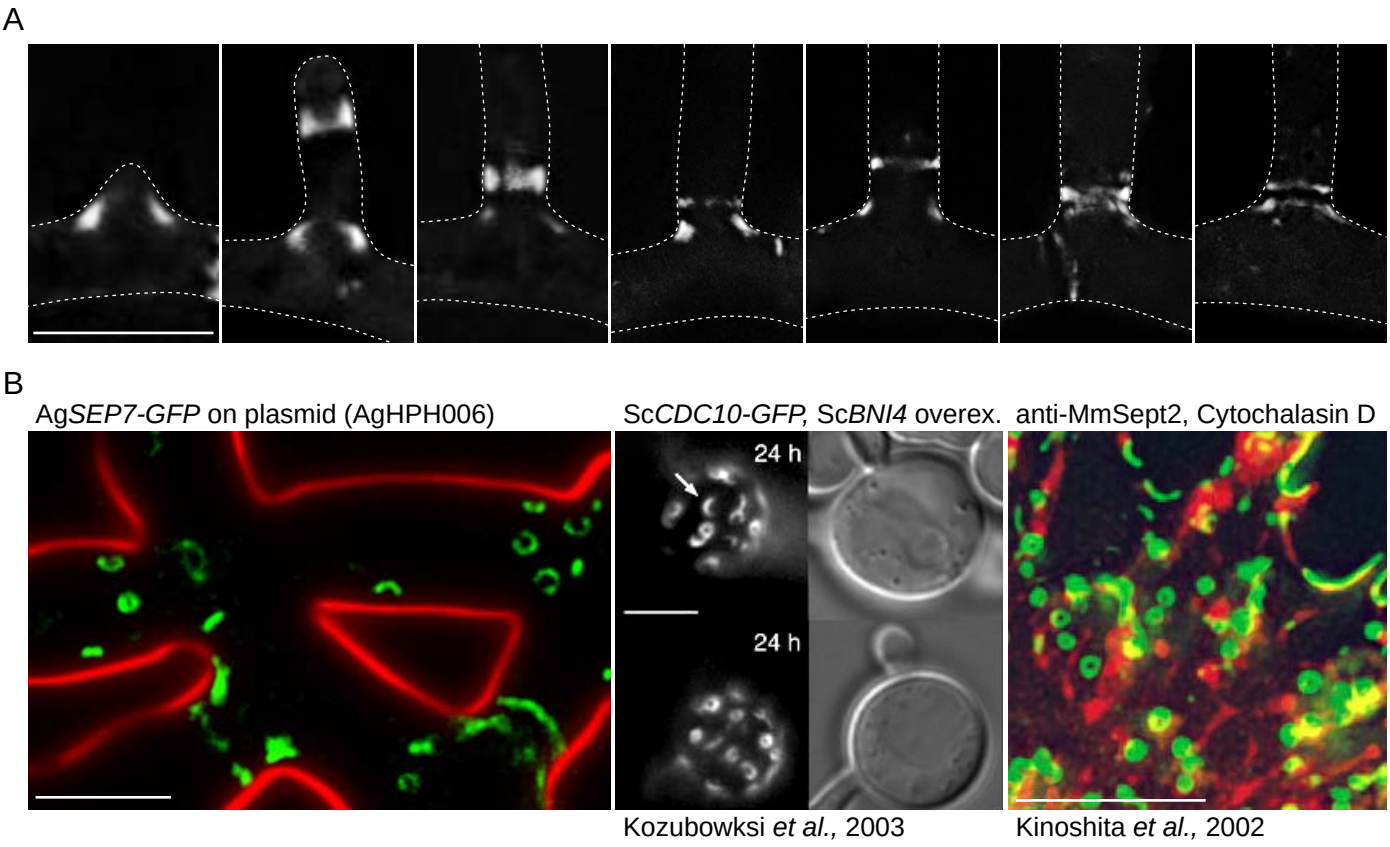

Figure II.3. Diversity of septin organizations. (A) *A. gossypii* mycelium with integrated Ag*SEP7-GFP* (AgHPH007, AgHPH008) was grown for 12 h - 15 h at 30°C, washed in minimal medium and imaged live. Pictures show septin structure at branching sites, with young branches at the left and old branches at the right. Outline of the mycelium is indicated by dotted lines. **(B)** Mycelium bearing Ag*SEP7-GFP* on plasmid (AgHPH006) (left) was grown as above. Small ~0.5 µm rings are only observed in plasmidic strains and have similarity with rings seen in *S. cerevisiae* cells with overexpressed Sc*BNI4* (middle) or in mammalian cells with disrupted actin cytoskeleton (right). Bars, (A) 10 µm, (B) 5 µm.

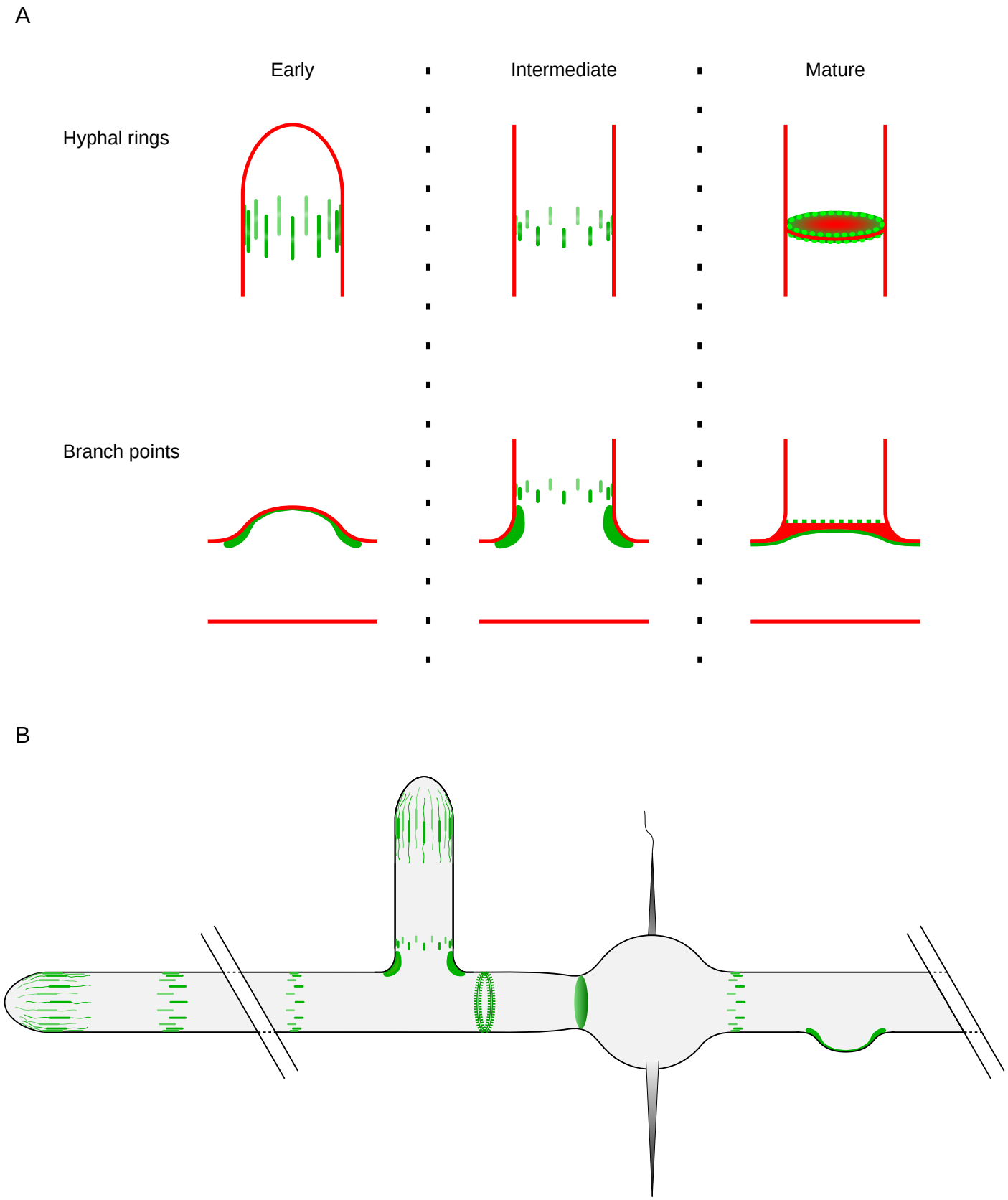

Figure II.4. Schematic overview of septin organizations seen in *A. gossypii*. (A) Early, intermediate and mature structures in hyphae (top) and at branching sites (bottom). **(B)** Septin structures put in relation with their positions within the mycelium. Schemes are based on microscopic observations of AgSep7-GFP.

A

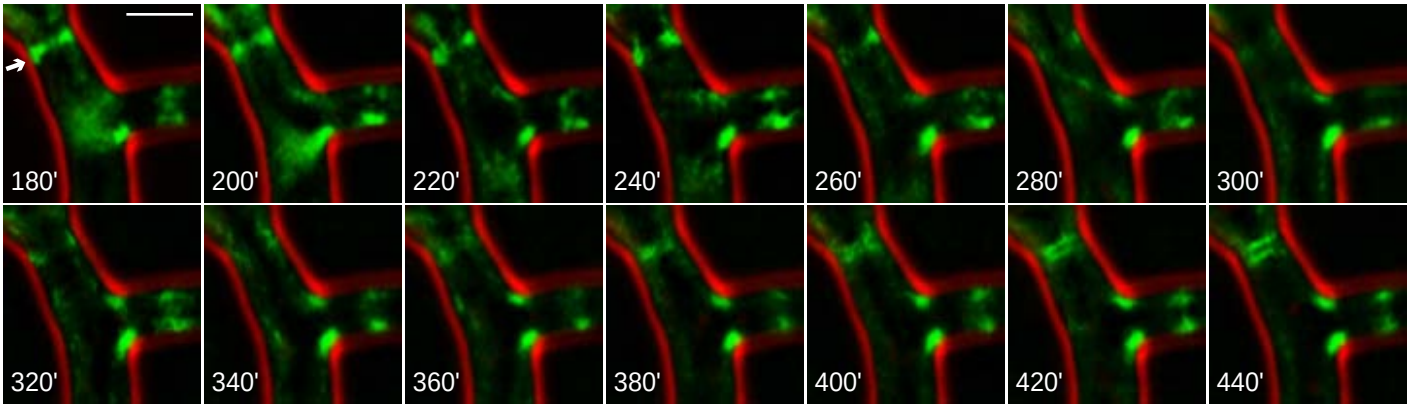

B

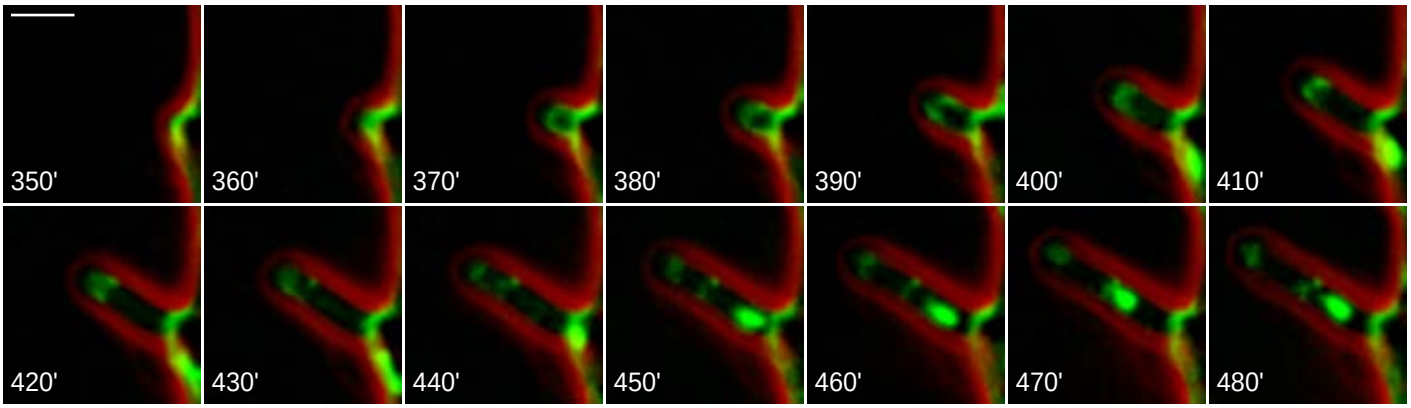

Figure II.5. Time-lapse analysis of septins in *A. gossypii.* (A) Ag*SEP7-GFP* mycelia (pagHPH02) were pregrown at 30°C in liquid AFM for 10 h and transferred to a time-lapse slide containing solid minimal medium (2xASD) at 25°C. Every 2 min, a Z-series of 7 frames was taken at 10% intensity and 150 ms exposure (Movie A). The figure was assembled from a selection of frames with a 20 min interval. The arrow indicates a single ring which splits into a double ring. **(B)** Ag*SEP7-GFP,* Ag*H4-GFP* mycelium (pagHPH09) was pregrown in selective liquid AFM for 14 h at 30°C and transferred to time-lapse slide containing solid 2xASD at 25°C. Every 2 min, a Z-series of 5 frames was taken at 10% intensity and 100 ms exposure (Movie B). The figure shows a selection of pictures with 10 min intervals, on which one can observe the division of the original septin organization at the emerging branch into three distinct parts: a structure staying at the branching site, a hyphal ring and a faint tip localization staying at the growing tip. Bars, 5 µm.

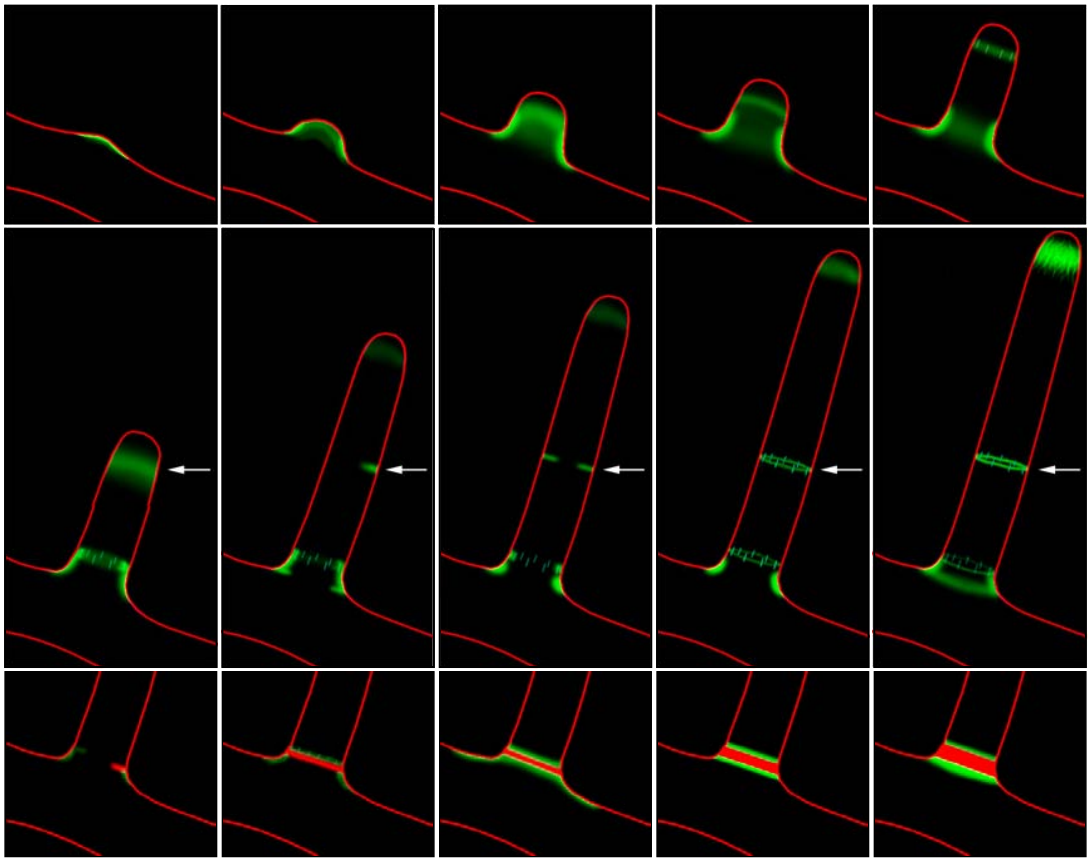

Figure II.6. Scheme of development of septin structures. The drawings are based on individual Z-plane analysis of Movie B. Green: AgSep7p-GFP, red: cell wall and septum. The arrow indicates that the hyphal rings are stationary, whereas the diffuse apical localization moves together with the tip. Maturation of hyphal double rings is not illustrated, but follows a similar pattern as double ring formation at branching sites. Due to technical limitations, bars were not always resolvable in the movie, which is drawn as diffuse signal.

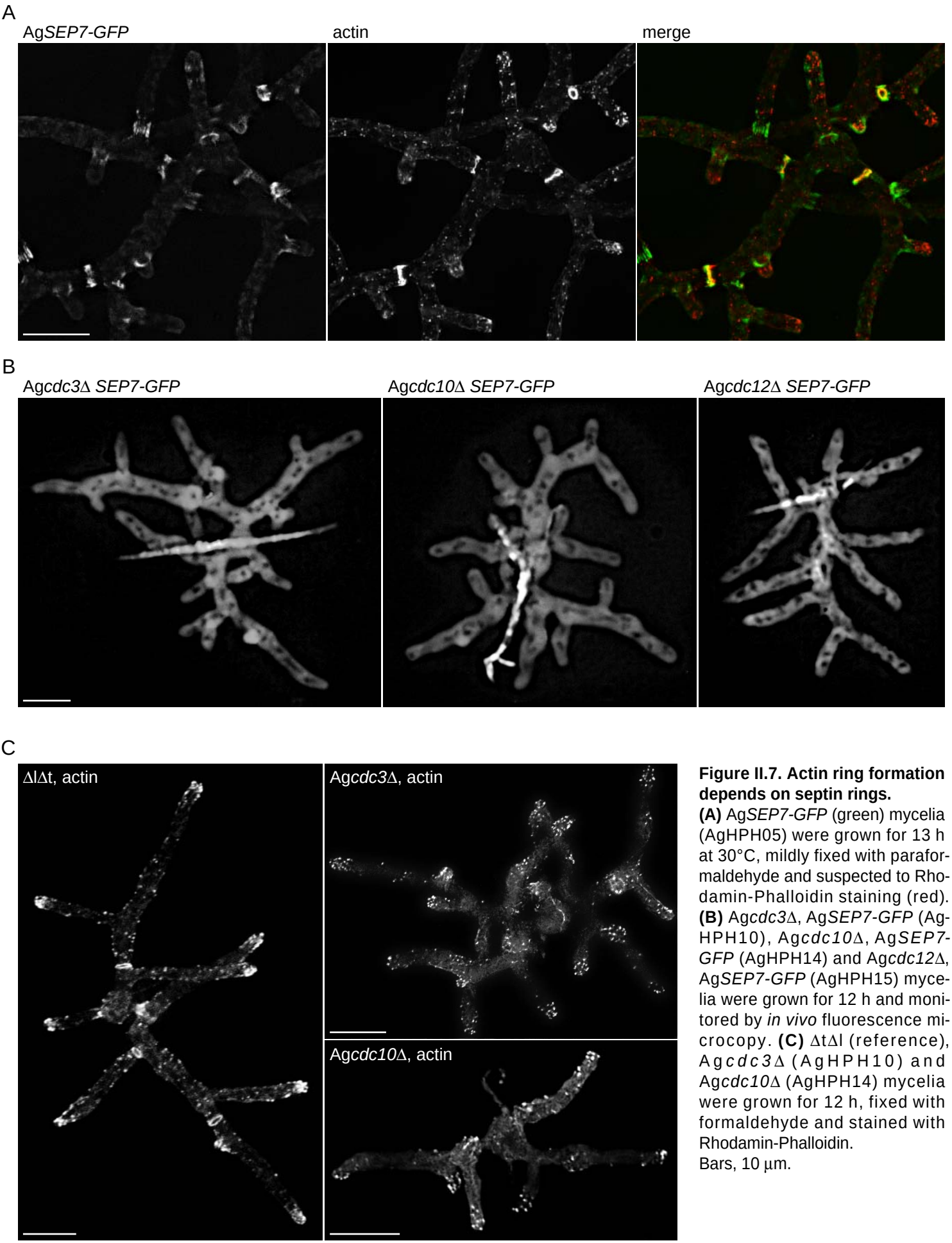

Figure II.7. Actin ring formation depends on septin rings.
(A) Ag*SEP7-GFP* (green) mycelia (AgHPH05) were grown for 13 h at 30°C, mildly fixed with paraformaldehyde and suspected to Rhodamin-Phalloidin staining (red). **(B)** Ag*cdc3*Δ, Ag*SEP7-GFP* (AgHPH10), Ag*cdc10*Δ, Ag*SEP7-GFP* (AgHPH14) and Ag*cdc12*Δ, Ag*SEP7-GFP* (AgHPH15) mycelia were grown for 12 h and monitored by *in vivo* fluorescence microcopy. **(C)** ΔtΔl (reference), Ag*cdc3*Δ (AgHPH10) and Ag*cdc10*Δ (AgHPH14) mycelia were grown for 12 h, fixed with formaldehyde and stained with Rhodamin-Phalloidin.
Bars, 10 µm.

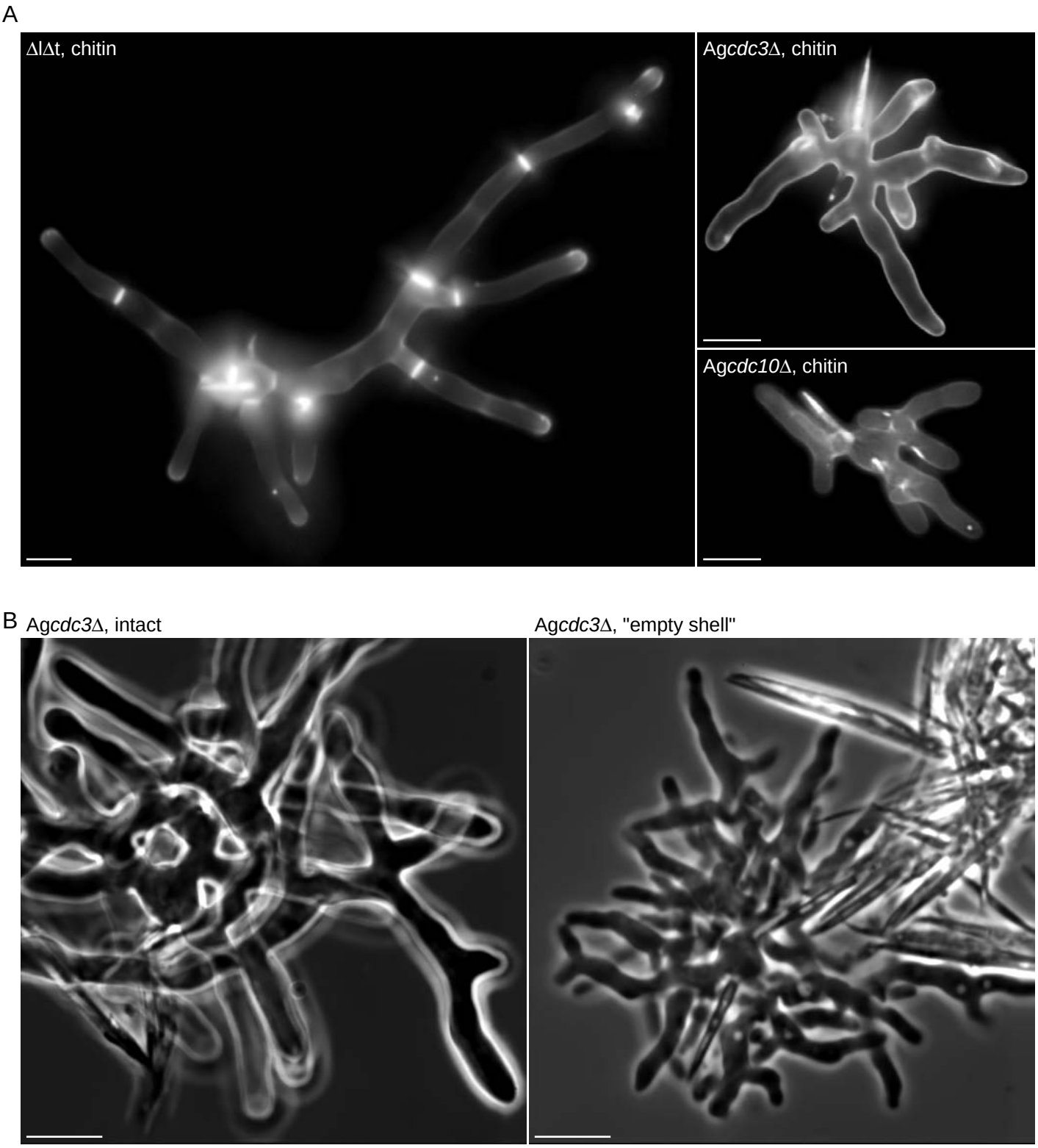

Figure II.8. Septins are required for chitin ring and septum formation. (A) ΔtΔl (reference), Ag*cdc3*Δ (AgHPH10) and Ag*cdc10*Δ (AgHPH14) mycelia were grown for 12 h in liquid AFM at 30°C, fixed with ethanol and stained with Calcofluor. (B) Brightfield pictures of an intact (left) and empty (right) Ag*cdc3*Δ mycelium (AgHPH10). Bars, 10 μm.

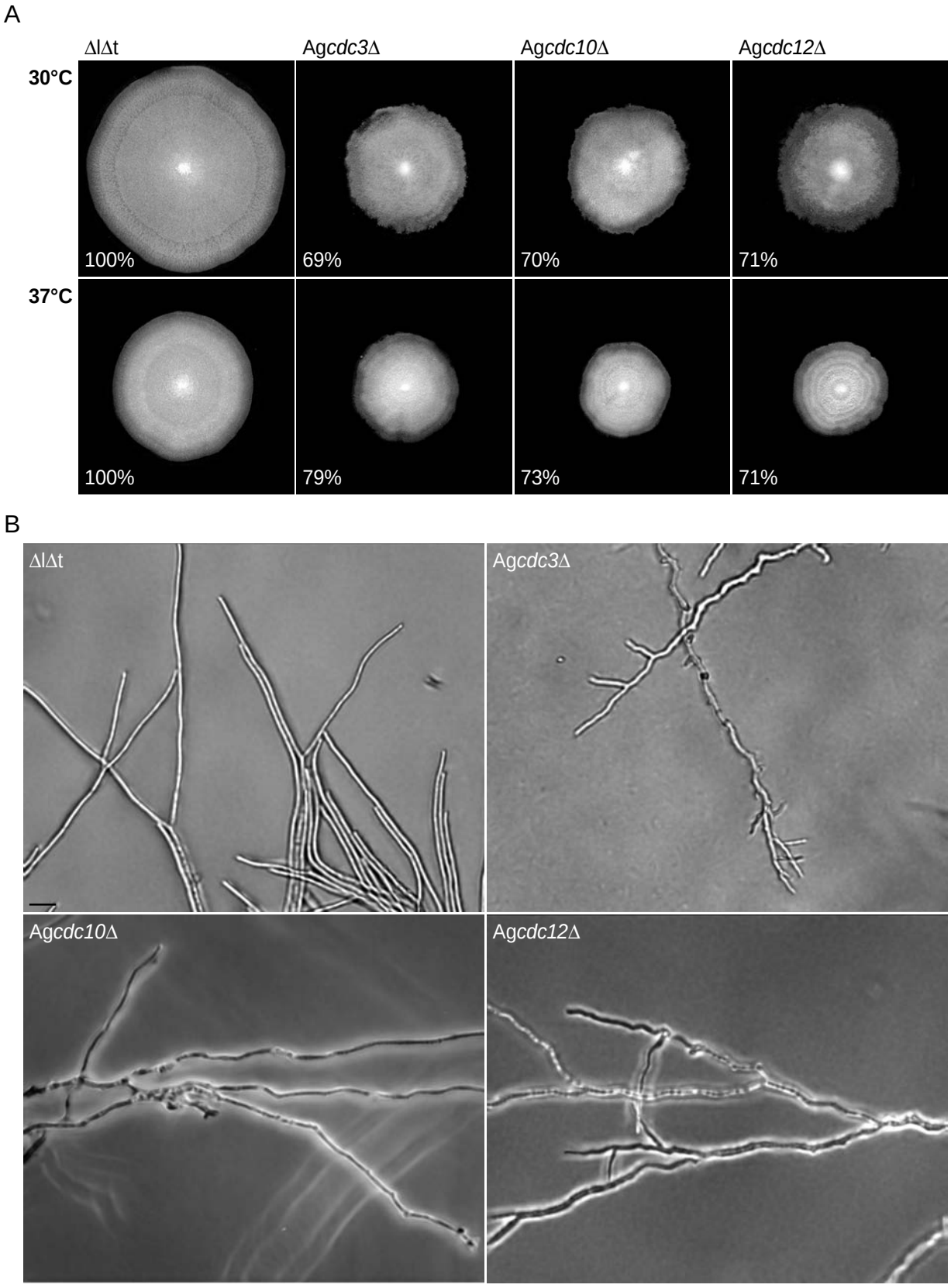

Figure II.9. Morphological defects of mature septin deletion mycelia (A) Radial growth on solid medium of the reference strain (ΔlΔt) and deletion mutants Ag*cdc3*Δ (AgHPH10), Ag*cdc10*Δ (AgHPH14) and Ag*cdc12*Δ (AgHPH15) compared to ΔlΔt (100%) at 30°C and 37°C. A small piece of homokaryotic mycelium (~1 mm^3) from each mutant was spotted on full medium plates and grown for 4 days. **(B)** Micrographs of ΔlΔt, Ag*cdc3*Δ (AgHPH10), Ag*cdc10*Δ (AgHPH14) and Ag*cdc12*Δ (AgHPH15) mycelia grown on full medium plates at 30°C for 8 days, illustrating the disordered branching pattern and wavy phenotype. Bar, 20 μm.

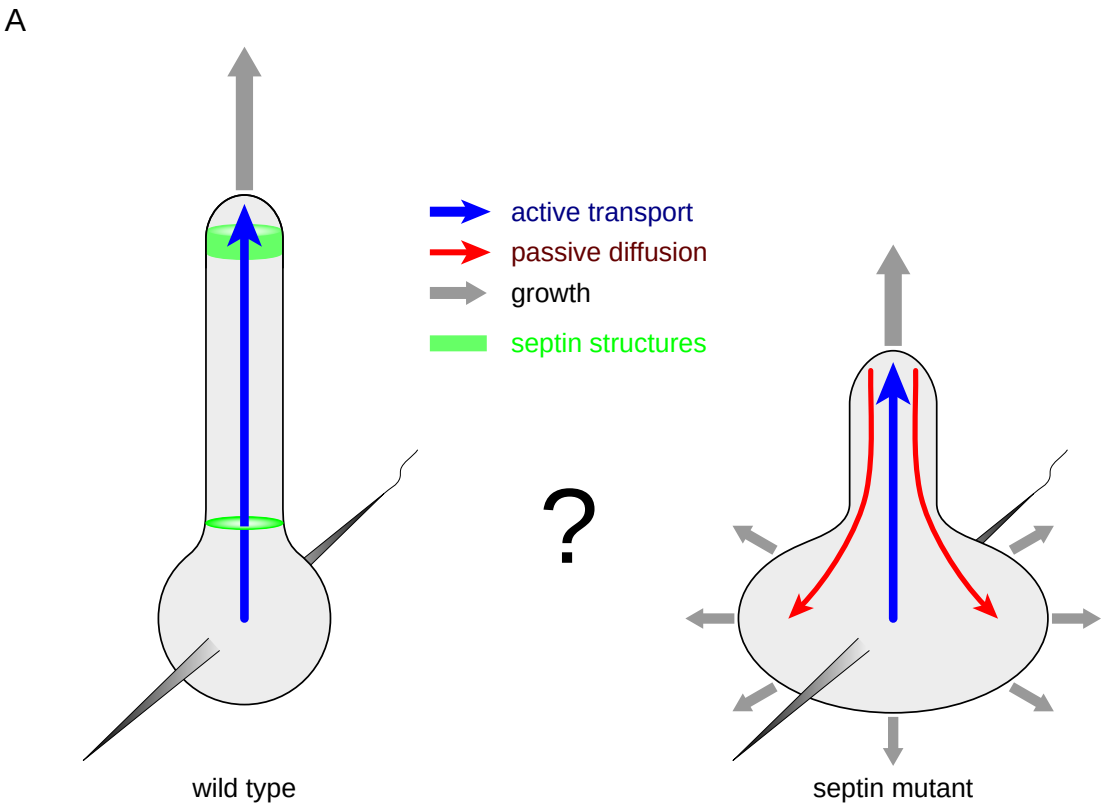

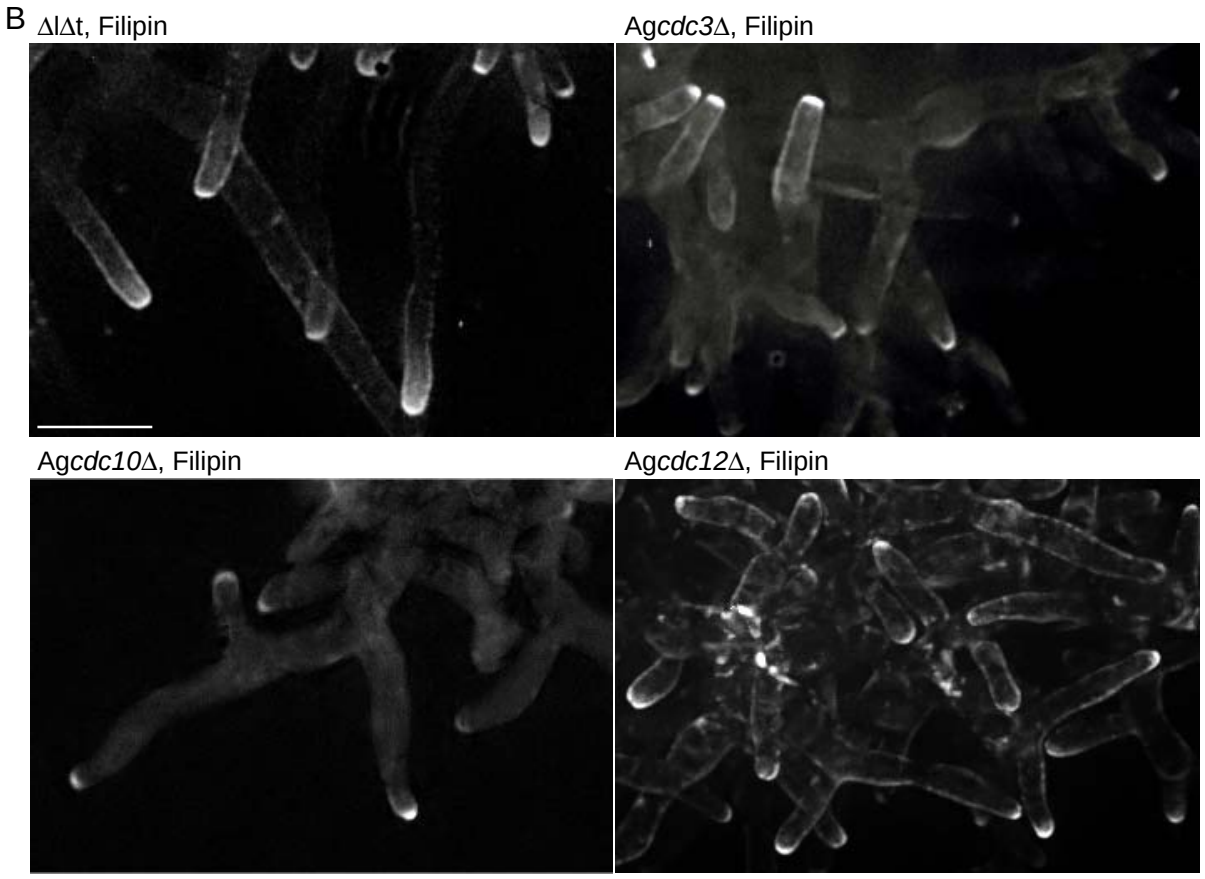

Figure II.10. Septins are not required for sterol polarity. (A) Scheme illustrating how the septins might be required for cortical polarity in *A. gossypii.* Lack of septin barriers would lead to diffusion of membrane associated material away from the tip, resulting in reduced tip extension and swollen hyphae. **(B)** The reference strain (ΔlΔt) and deletion mutants Ag*cdc3*Δ (AgHPH10), Ag*cdc10*Δ (AgHPH14) and Ag*cdc12*Δ (AgHPH15) were grown for 12 h at 30°C in full medium, stained with low concentrations of Filipin (2-4 µg/ml) and monitored after 2 min. Polarization of sterols is not affected in *A. gossypii* septin mutants. Bar, 10 µm.

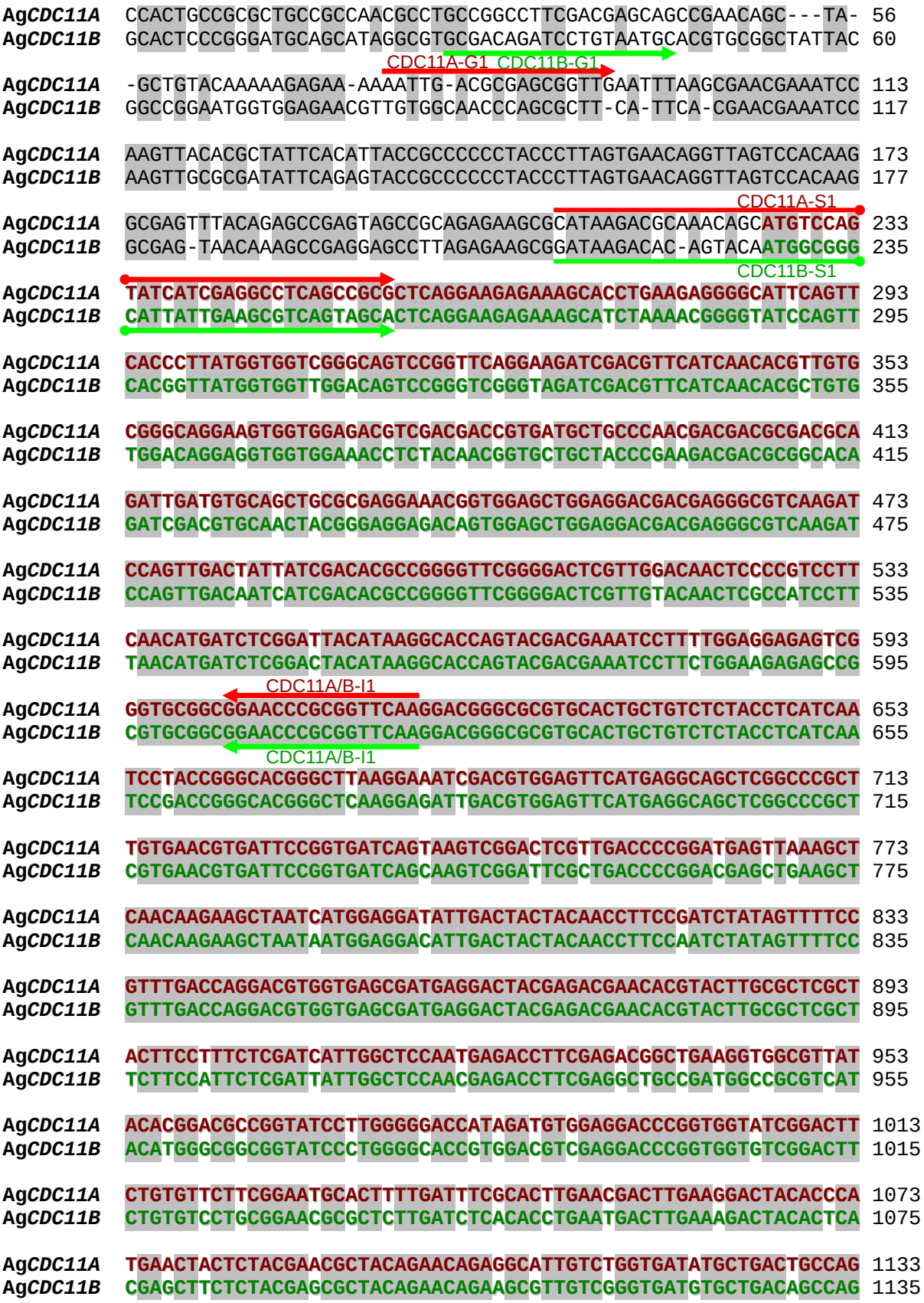
AgCDC11A CCACTGCCGCGCTGCCGCCAACGCCTGCCGGCCTTCGACGAGCAGCCGAACAGC---TA- 56
AgCDC11B GCACTCCCGGGATGCAGCATAGGCGTGCGACAGATCCTGTAATGCACGTGCGGCTATTAC 60
CDC11A-G1
CDC11B-G1
AgCDC11A -GCTGTACAAAAAGAGAA-AAAATTG-ACGCGAGCGGTTGAATTTAAGCGAACGAAATCC 113
AgCDC11B GGCCGGAATGGTGGAGAACGTTGTGGCAACCCAGCGCTT-CA-TTCA-CGAACGAAATCC 117
AgCDC11A AAGTTACACGCTATTCACATTACCGCCCCCCTACCCTTAGTGAACAGGTTAGTCCACAAG 173
AgCDC11B AAGTTGCGCGATATTCAGAGTACCGCCCCCCTACCCTTAGTGAACAGGTTAGTCCACAAG 177
CDC11A-S1
AgCDC11A GCGAGTTTACAGAGCCGAGTAGCCGCAGAGAAGCGCATAAGACGCAAACAGCATGTCCAG 233
AgCDC11B GCGAG-TAACAAAGCCGAGGAGCCTTAGAGAAGCGGATAAGACAC-AGTACAATGGCGGG 235
CDC11B-S1
AgCDC11A TATCATCGAGGCCTCAGCCGCGCTCAGGAAGAGAAAGCACCTGAAGAGGGGCATTCAGTT 293
AgCDC11B CATTATTGAAGCGTCAGTAGCACTCAGGAAGAGAAAGCATCTAAAACGGGGTATCCAGTT 295
AgCDC11A CACCCTTATGGTGGTCGGGCAGTCCGGTTCAGGAAGATCGACGTTCATCAACACGTTGTG 353
AgCDC11B CACGGTTATGGTGGTTGGACAGTCCGGGTCGGGTAGATCGACGTTCATCAACACGCTGTG 355
AgCDC11A CGGGCAGGAAGTGGTGGAGACGTCGACGACCGTGATGCTGCCCAACGACGACGCGACGCA 413
AgCDC11B TGGACAGGAGGTGGTGGAAACCTCTACAACGGTGCTGCTACCCGAAGACGACGCGGCACA 415
AgCDC11A GATTGATGTGCAGCTGCGCGAGGAAACGGTGGAGCTGGAGGACGACGAGGGCGTCAAGAT 473
AgCDC11B GATCGACGTGCAACTACGGGAGGAGACAGTGGAGCTGGAGGACGACGAGGGCGTCAAGAT 475
AgCDC11A CCAGTTGACTATTATCGACACGCCGGGGTTCGGGGACTCGTTGGACAACTCCCCGTCCTT 533
AgCDC11B CCAGTTGACAATCATCGACACGCCGGGGTTCGGGGACTCGTTGTACAACTCGCCATCCTT 535
AgCDC11A CAACATGATCTCGGATTACATAAGGCACCAGTACGACGAAATCCTTTTGGAGGAGAGTCG 593
AgCDC11B TAACATGATCTCGGACTACATAAGGCACCAGTACGACGAAATCCTTCTGGAAGAGAGCCG 595
CDC11A/B-I1
AgCDC11A GGTGCGGCGGAACCCGCGGTTCAAGGACGGGCGCGTGCACTGCTGTCTCTACCTCATCAA 653
AgCDC11B CGTGCGGCGGAACCCGCGGTTCAAGGACGGGCGCGTGCACTGCTGTCTCTACCTCATCAA 655
CDC11A/B-I1
AgCDC11A TCCTACCGGGCACGGGCTTAAGGAAATCGACGTGGAGTTCATGAGGCAGCTCGGCCCGCT 713
AgCDC11B TCCGACCGGGCACGGGCTCAAGGAGATTGACGTGGAGTTCATGAGGCAGCTCGGCCCGCT 715
AgCDC11A TGTGAACGTGATTCCGGTGATCAGTAAGTCGGACTCGTTGACCCCGGATGAGTTAAAGCT 773
AgCDC11B CGTGAACGTGATTCCGGTGATCAGCAAGTCGGATTCGCTGACCCCGGACGAGCTGAAGCT 775
AgCDC11A CAACAAGAAGCTAATCATGGAGGATATTGACTACTACAACCTTCCGATCTATAGTTTTCC 833
AgCDC11B CAACAAGAAGCTAATAATGGAGGACATTGACTACTACAACCTTCCAATCTATAGTTTTCC 835
AgCDC11A GTTTGACCAGGACGTGGTGAGCGATGAGGACTACGAGACGAACACGTACTTGCGCTCGCT 893
AgCDC11B GTTTGACCAGGACGTGGTGAGCGATGAGGACTACGAGACGAACACGTACTTGCGCTCGCT 895
AgCDC11A ACTTCCTTTCTCGATCATTGGCTCCAATGAGACCTTCGAGACGGCTGAAGGTGGCGTTAT 953
AgCDC11B TCTTCCATTCTCGATTATTGGCTCCAACGAGACCTTCGAGGCTGCCGATGGCCGCGTCAT 955
AgCDC11A ACACGGACGCCGGTATCCTTGGGGGACCATAGATGTGGAGGACCCGGTGGTATCGGACTT 1013
AgCDC11B ACATGGGCGGCGGTATCCCTGGGGCACCGTGGACGTCGAGGACCCGGTGGTGTCGGACTT 1015
AgCDC11A CTGTGTTCTTCGGAATGCACTTTTGATTTCGCACTTGAACGACTTGAAGGACTACACCCA 1073
AgCDC11B CTGTGTCCTGCGGAACGCGCTCTTGATCTCACACCTGAATGACTTGAAAGACTACACTCA 1075
AgCDC11A TGAACTACTCTACGAACGCTACAGAACAGAGGCATTGTCTGGTGATATGCTGACTGCCAG 1133
AgCDC11B CGAGCTTCTCTACGAGCGCTACAGAACAGAAGCGTTGTCGGGTGATGTGCTGACAGCCAG 1135

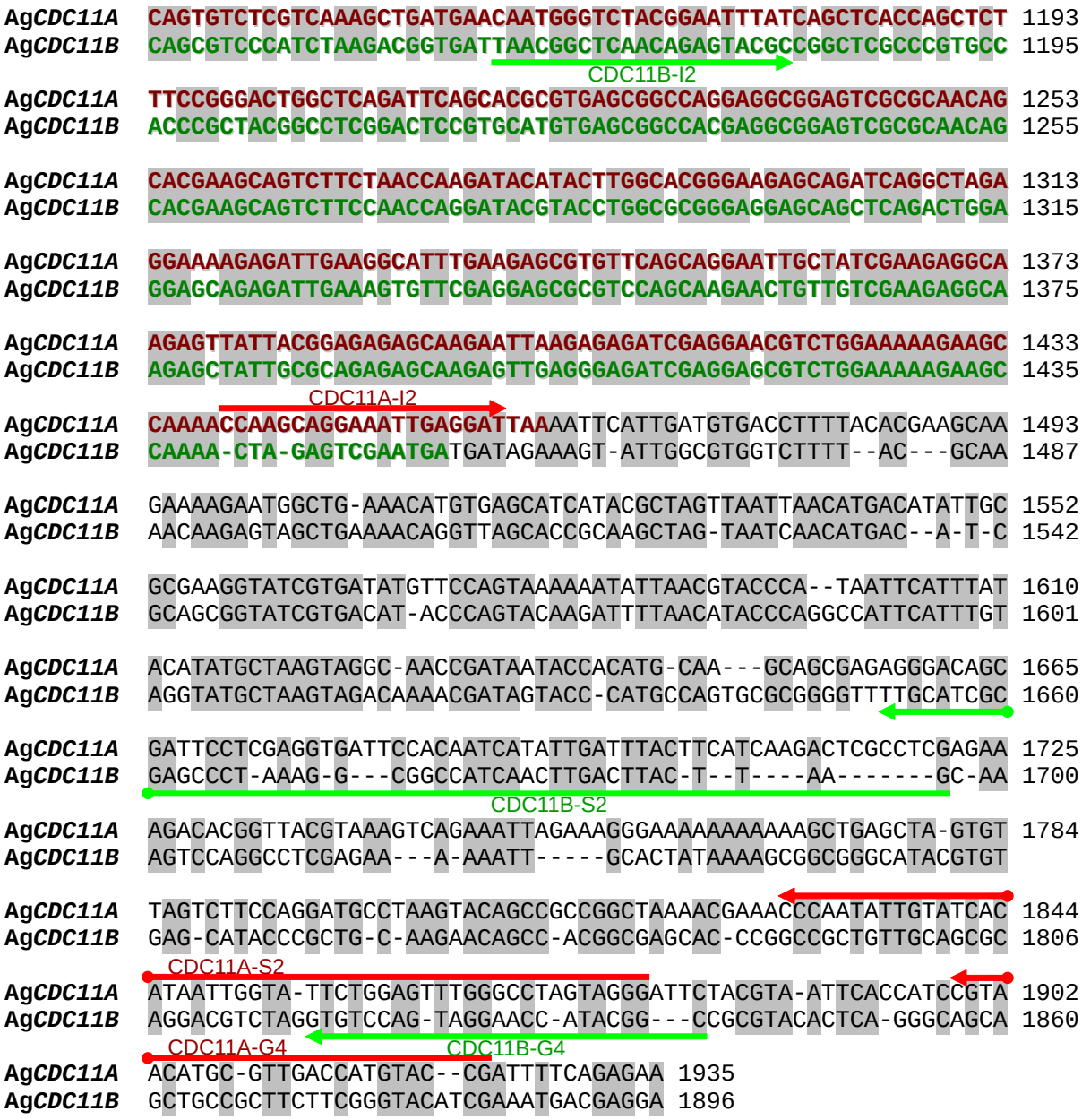

Figure II.11. Pairwise alignment of the highly conserved Ag*CDC11A* and Ag*CDC11B* genes. Oligos are designed to bind in places with highest possible diversity. The open reading frames are marked with bold, colored letters (red: Ag*CDC11A,* green: Ag*CDC11B*).

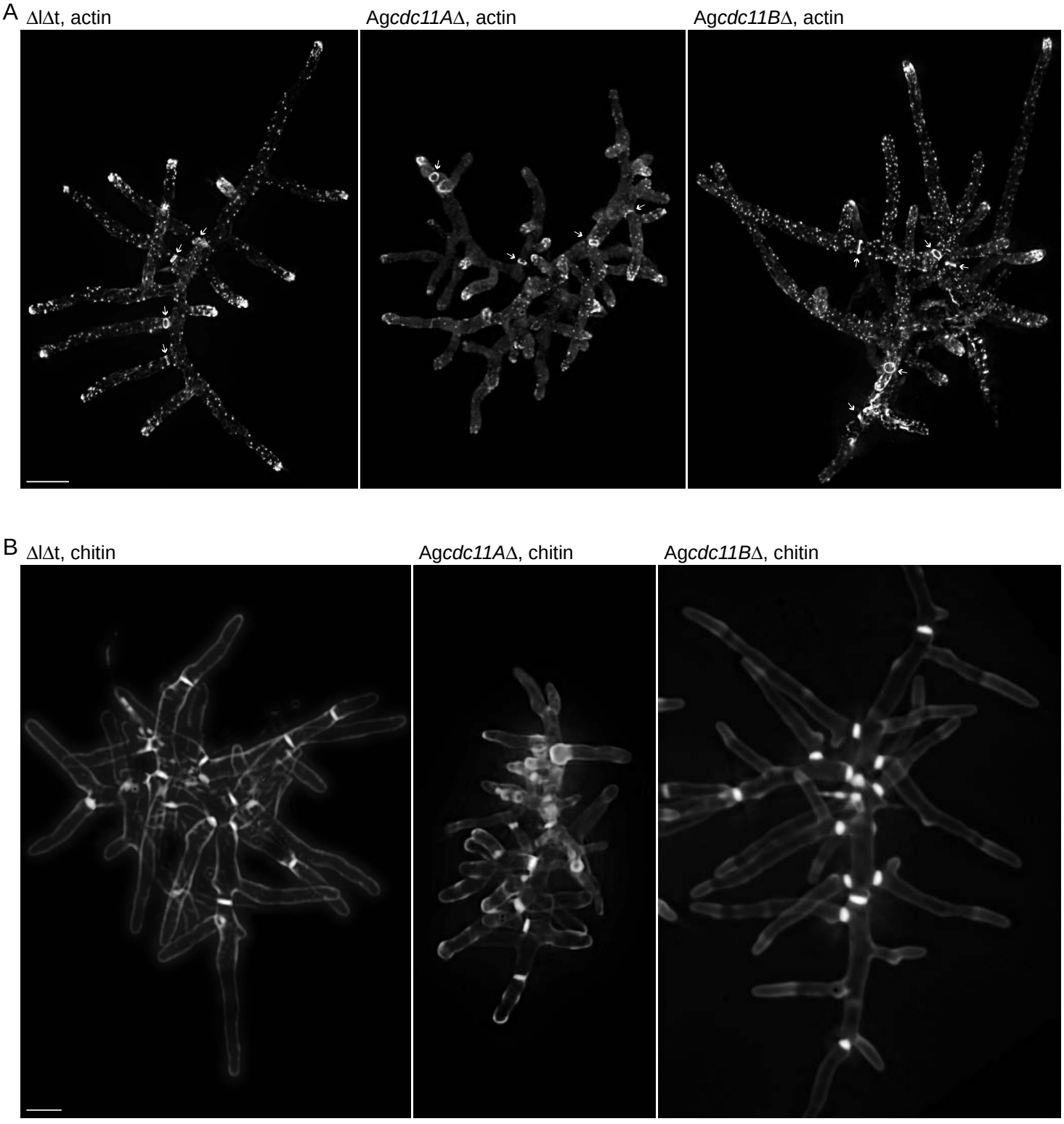

Figure II.12. Deletion of Ag*CDC11A* or Ag*CDC11B* results in a partial or no septin phenotype. ΔlΔt (reference), Ag*cdc11A*Δ (AgHPH17) and Ag*cdc11B*Δ (AgHPH18) mycelia were grown for 12 h in liquid AFM at 30°C, fixed with formaldehyde and stained with Alexa-Phalloidin **(A)** or fixed with ethanol and stained with Calcofluor **(B)**. Ag*cdc11A*Δ mutants display morphological defects similar to the other septin null mutants, but neither actin nor chitin rings are missing. No phenotype of Ag*cdc11B*Δ mutants has been found. Bars, 10 μm.

Discussion

The filamentous ascomycete *Ashbya gossypii* carries a *Saccharomyces*-like genome but its morphogenesis differs markedly from budding yeast. Large areas of nutrients are quickly covered by *A. gossypii* mycelium through permanently polarized hyphal growth and branch formation. Except during germination and in some mutants, isotropic growth is not observed. In stark contrast to budding yeast where nuclear division is obligatory followed by cytokinesis and cell separation (abscission), cytokinesis is not observed during vegetative growth of *A. gossypii.* It never propagates by yeast-like or pseudohyphal growth like other filamentous fungi. Nonetheless, *A. gossypii* is not only equipped with homologues to all *S. cerevisiae* septins – the key players in cytokinesis, one is even duplicated (Ag*CDC11A,* Ag*CDC11B).*

Cytokinesis is likely to be a crucial part of the sporulation program. Thus the *A. gossypii* septins could be required only late in the life cycle. However, our localization studies with AgSep7-GFP have revealed a complex set of structures that is already established in young mycelium, which makes it unlikely that the septins are only responsible for sporulation. A striking difference between AgSep7-GFP rings seen in *A. gossypii* and budding yeast is in their structural organization: whereas in *S. cerevisiae* they are continuous, they are intermittent in *A. gossypii,* made from parallel bars. How can the very same protein, expressed from the same promoter, lead to such different structures in different organisms? We must keep in mind that we are not looking at all septins at the same time, but only at one single component of the ring, AgSep7-GFP. In budding yeast, the septins form heteropentamers with ScSep7p (ScShs1p) being the most peripheral component of this structure (Versele *et al.*, 2004). Presumably, the role of Sep7 lies in recruiting other proteins to the septin ring, and not in defining the structural organization of the ring itself. To investigate whether and which septins are crucial for the observed structural differences, one could replace different subsets of septins in *S. cerevisiae* with their *A. gossypii* homologues and see which combinations lead to bar formation. There is also the possibility that the septin structure is not determined by the septins themselves. Discontinuous rings are known from mating *S. cerevisiae* cells at the neck of shmoos (Ford and Pringle, 1991; Kim *et al.*, 1991; Longtine *et al.*, 1998; Cid *et al.*, 2001a) or at the mother-bud-neck of budding yeast cells bearing mutations of septin regulators (reviewed in (Gladfelter *et al.*, 2001b). It has further been shown that the septin ring at the neck undergoes changes in protein dynamics to allow structural changes like single ring to double ring transition, and that this is regulated through the phosphorylation state of the septins (Dobbelaere *et al.*, 2003). In *C. albicans*, it has been speculated that sumolyation of the septins could be the bases for the different patterns of septin structures (Martin and Konopka, 2004b). Thus, modification of the septins could be a key element in determining their organizational structure. The fact that we see a great variety of different septin organizations in *A. gossypii* itself also makes it unlikely that having bar-like rings in *A. gossypii* and continuous rings in *S. cerevisiae* is solely the results of different septin proteins. The transient state of signal fading seen during single ring to double ring transition in *A. gossypii* is evidence for profound structural rearrangements which likely comes along with changes in protein dynamics. Mutants of potential septin modification proteins could help to understand how such transitions are regulated and whether different structures are related to different modifications. FRAP analysis could be used to analyze protein dynamics of individual structures.

What is the nature of the septin bars we see in *A. gossypii?* Do they represent filaments made from individual septins? If so, it was possible that the gaps between the bars are in fact filled by the other septins. All the septins together would then form a continuous ring. Our colocalization analysis of AgCdc11p and AgSep7-GFP and *in vitro* interaction studies in budding yeast (Versele *et al.*, 2004) rather support the hypothesis that each filament incorporates all the septins, though. There is still the possibility that AgSep7-GFP bars and AgCdc11p bars just appear to co-localize because they are very close together. Ideally, we would tag all the septins and observe whether they together form continuous rings or still bar-like rings.

How does this potential discontinuity of the rings influence the recruitment of other proteins to these structures? AgHsl7-GFP colocalized with some but not all septin rings and actin rings were limited to mature, contracted septin structures. We have shown that even contracted septin rings consist of bars. Thus, the bar-like organization of septin rings in *A. gossypii* does not prevent recruitment of other proteins or even formation of continuous structures like actin rings. Nevertheless, localization of actin rings or AgHsl7-GFP to the asymmetric septin structures

at young branching sites or colocalization with young, diffuse hyphal rings has never been observed. Possibly, hyphal septin rings need to mature before they can recruit other proteins. Alternatively, septin structures of different localization and age may recruit different sets of protein.

Interestingly, we have seen that a diffuse portion of AgSep7-GFP always stays at the growing tips. Do these faint, elongated filaments only serve as precursor for hyphal ring formation, or are they also involved in recruiting and/or maintaining actin patches at the tips? Deletion of single septin proteins (Ag*cdc3*Δ, Ag*cdc10*Δ and Ag*cdc12*Δ) leads to complete delocalization of AgSep7-GFP: neither distinct structures nor polarization at the tips is seen in these mutants. Although the actin cytoskeleton is difficult to stain in septin deletion mutants and actin patches are less clearly visible than in the reference strain or even reduced in number, actin patch polarization does not seem to be affected. Even if the septins are not crucial for actin patch polarity, they are essential for the formation of actin rings, which are no longer observed in Ag*cdc3*Δ and Ag*cdc10*Δ, nicely fitting to the colocalization data. Ag*myo1*Δ mutants, which likewise have no actin rings, are still able to form aberrant septa which allows limited sporulation. The nature of this complementing mechanism in *A. gossypii* has not yet been identified, but could be similar to *S. cerevisiae,* where strains lacking a contractile actomyosin ring can still undergo cytokinesis through formation of a septum by vesicle fusion with the plasma membrane (Bi *et al.*, 1998; Lippincott and Li, 1998b; Vallen *et al.*, 2000; Faty *et al.*, 2002). Unlike in these Ag*myo1*Δ mutants, we have neither seen chitin rings nor septa in the above septin mutants. Coming along with this is a total loss of sporulation capability. Thus, all pathways that can lead to septum formation and sporulation depend on the septins, be it actin ring formation or potential localized vesicle fusion.

Notably, the severe or lethal phenotype of septin mutants in *S. cerevisiae* is largely due to the inability to complete cytokinesis in the absence of a proper septin ring at the bud neck (Hartwell, 1971a). Contrasting budding yeast, cytokinesis does not occur in *A. gossypii* mycelium before sporulation and hence disruption of cytokinesis should not affect vegetative growth of this fungus. Although septin deletion mutants in *A. gossypii* are not lethal, they exhibit reduced radial growth speed and aberrant morphology. Together with the complex localization pattern which is already established in young mycelium, this clearly indicates significant roles of *A. gossypii* septins during vegetative growth. We have seen that the lack of septa in septin mutants causes the mycelium to be very susceptible to hyphal damage. Whereas in wild type, damage induced lysis is restricted to the affected hypha, it spreads over the entire mycelium in septin mutants grown in liquid. Considering this, it is surprising that these mutants are able to form large colonies on solid medium at all. One can imagine that even without mechanical stress from shaking, lysis-inducing events should occur at some point during several days of growth. Nonetheless, complete lysis of mature colonies has never been observed. Mere size of the mycelium could prevent leakage of the entire cytoplasm. Especially when immobilized on solid medium, sites of leakage should eventually be clogged by escaping cytoplasm. Even so, the amount of cytoplasm lost during such incidents could be enough to notably reduce growth efficiency.

Reduced radial growth rate is also likely linked to the morphological defects we have observed: *A. gossypii* septin deletion mutants exhibit erratic thickness of the hyphae, show difficulties in maintaining growth direction and have a disordered branching pattern. Regulation of hyphal thickness may be required for optimal tip extension speed, whereas adjusting direction of growth and the branching pattern should be critical to efficiently grow towards and exploit regions rich in nutrients. How are the septins involved in these processes? It has been shown that the branching pattern of *A. gossypii* is largely determined by AgRax1p and AgRax2p. AgBud10p is required for stable localization of AgRax2p at growing tips (Boudier, PhD thesis, 2005). Septin mutants in *S. cerevisiae* display mislocalisation of ScBud3p, ScBud4p and ScBud10p and disruption of the axial budding pattern (Flescher *et al.*, 1993; Chant *et al.*, 1995). It is likely that the homologues of these proteins are similarly localized by the septins in *A. gossypii,* which would explain why the branching pattern is disturbed in septin mutants. Strikingly, the septins at the branching site do not disappear after branch emergence but rather stay there to form an asymmetric structure of yet unknown function. AgHsl7p has never been found to localize to these places. Does this imply that the septins at the base of branches recruit a different set of proteins than the hyphal rings? Are they required for stabilization of the angle between the branch and the mother hyphae, thus helping to maintain direction of growth? Another unanswered question is proposed by the faint but permanent localization of septins to the growing tips. This localization is not required for actin patch polarity, nevertheless maintenance of the

axis of polarity and hyphal diameter seems to be affected in septin mutants. How may the septins contribute to polarity in *A. gossypii?* It has been shown that during isotropic bud growth, cortical components of the polarisome and the exocyst in *S. cerevisiae* are restricted to the bud membrane by a septin mediated membrane diffusion barrier (Barral *et al.*, 2000; Takizawa and Morgan, 2000). Likewise there is evidence that the septins might colocalize with sterols in *C. albicans* and might establish or maintain membrane polarity (Martin and Konopka, 2004a). In S. pombe, sterol localization correlates with sites of active cell growth and cytokinesis, as it was revealed by Filipin staining (Wachtler *et al.*, 2003). Are the septins in *A. gossypii* involved in maintaining cortical polarity at the growing tips? Lack of such a membrane barrier could result in partial delocalization of polarity factors over the entire hypha. This would explain reduced growth and the swollen appearance of the hyphae in septin mutants. On the other hand, it is hard to imagine how the septins in *A. gossypii* could serve as barrier, considering the diffuse and bar-like appearance of septins at growing tips. Additionally, Filipin does not only localize to growing tips in the reference strain but also in septin deletion mutants. Alternatively, the septins could directly recruit and maintain polarity factors at the tip. All the same, we cannot completely abandon the hypothesis of cortical polarity. The space between the AgSep7-GFP or AgCdc11p bars could be filled by other proteins that support the barrier function. Further, Filipin staining is prone to artifacts and does not reliably indicate the distribution of sterols in *S. cerevisiae* live cells (Valdez-Taubas and Pelham, 2003). Localizing cortical exocytosis or polarity components in the *A. gossypii* reference strain and septin mutants could shed light on the question of whether cortical polarity is also a relevant feature of apical growth.

A very interesting aspect of the septins in *A. gossypii* is the duplication of *CDC11*. Despite 85 % identity between the two proteins, deletion of each results in some different phenotypes. Whereas Ag*cdc11B*Δ cannot be distinguished from the reference, Ag*cdc11A*Δ strains display morphological defects that are typical for septin mutants. Strikingly, actin and chitin rings are still formed in Ag*cdc11A*Δ mycelia and sporulation is not completely abolished but occurs at 30 % efficiency. This indicates that altered morphology of small mutant mycelium is not the result of absent septa. It would be highly interesting to delete Ag*CDC11A* in the AgSEP7-GFP background to see which of the septin structures are affected by this deletion. This has the potential to answer many of the above questions by yielding insight into which structures are required for which morphogenetic process. So far we could not resolve the function of AgCdc11Bp. The two proteins may be partially redundant, allowing actin and chitin ring formation even if one of them is disrupted. This could be tested by analyzing double deletion mutants. Alternatively, AgCdc11Bp could have adopted a function which is of advantage in the natural environment of *A. gossypii*, but has so far escaped our observations under laboratory conditions. We have just begun to study these twins. More detailed examination may reveal the processes in which the two proteins are involved and why it was worthwhile for *A. gossypii* to preserve two copies of *CDC11*.

Thanks to the peculiar morphogenetic processes coming along with filamentous growth, future studies of the septins in *A. gossypii* and other filamentous fungi may draw secrets from these versatile proteins, which uninucleated cells would have kept forever.

Materials and Methods

A. gossypii methods, media and growth conditions

A. gossypii media, culturing, and transformation protocols are described in (Wendland *et al.*, 2000) and (Ayad-Durieux *et al.*, 2000). *A. gossypii* strains used here are listed in Table 2. To test the influence of high culture density, 10 – 20 ml of full medium were densely inoculated with spores and the cultures were grown until vacuoles were clearly observable by phase contrast microscopy. For all other conditions, 50 – 100 ml of full medium were inoculated at low density, regularly controlled for the absence of visible vacuoles and fresh medium was added 1 – 2 hours before taking samples or exposing the cultures to conditions of potential stress. Nocodazole stocks for the arrest and release experiment were 3 mg/ml in DMSO and used at a final concentration of 15 μg/ml (Sigma). Hydroxyurea was directly added to the cultures to a final concentration of 50 mM. Rapamycin stocks (LC Laboratories, Woburn, MA) were 1 mg/ml in 90 % EtOH, 10% Tween-20 and used at a final concentration of 200 nM (Loewith *et al.*, 2002). To simulate the starvation response, low density cultures were washed twice and resuspended in 40 mM MOPS [pH 7.0], 137 mM KCl. To test the lack of certain nutrients, different media based on Ashbya Synthetic Dextrose (ASD) medium were used: 1.70 g/l YNB w/o amino acids and w/o ammoniumsulfate (Difco), 0.69 g/l CSM-LEU (Bio 101), 1.00 g/l Asn, 0.01 g/l adenine, 1.00 g/l myo-inositol, 20 g/l glucose, 50 mM MOPS [pH 6.5].

Plasmid and strain construction

All DNA manipulations were carried out according to (Sambrook, 2001) with DH5αF' as host (Hanahan, 1983). Plasmids used here are listed in Table 3. PCR was performed using standard methods with different polymerases from Roche (Basel, Switzerland), Amersham Biosciences (Little Chalfont, Buckinghamshire, United Kingdom), or GenScript (Piscataway, NJ). Oligos were synthesized at MWG (Ebersberg, Germany) or Microsynth (Switzerland) and all restriction enzymes came from New England Biolabs or Roche. Oligonucleotide primers are listed in Table 4. Plasmid isolation from yeast and sequencing were performed as described in (Schmitz *et al.*, 2006).

A. gossypii deletion mutants were generated using the PCR based one-step gene targeting approach with non-homologous selection markers (McElver and Weber, 1992; Baudin *et al.*, 1993; Wach *et al.*, 1994; Wendland *et al.*, 2000). For G418 resistance, the deletion cassettes were amplified off the pGEN3 template using "gene name"-S1/S2 primer pairs. ClonNAT® resistance was obtained using pUC19NATPS as template. N*S1/N*S2 primer pairs were used for expression of the NAT1 resistance module under the control of the promoter and terminator of the targeted gene. NS1/NS2 primer pairs lead to NAT1 expression under the control of the ScPDC1 promoter and terminator. Correct integration was verified by analytical PCR with oligonucleotides "gene name"-(N)G1, -(N)G4, -I1/I2 (genomic) and G2.1, G3, V2PDC1P, V3PDC1T, V2*NAT1, V3*NAT1 (marker). To exclude phenotypes by random mutations, at least two independent transformants were characterized for each deletion. Transformation of multinucleate mycelium leads to heterokaryotic cells, which contain a mixture of transformed and wild-type nuclei, and usually do not display an apparent phenotype. For subsequent analysis, homokaryotic mycelium was obtained by isolating and growing single spores. To evaluate phenotypes of lethal mutants or mutants with sporulation deficiency, spores from heterokaryotic mycelium were germinated and analyzed under selective conditions.

For the creation of the double deletion strains AgHPH29 and AgHPH31, at least three homokaryotic isolates bearing the first deletion that were phenotypically not distinguishable were tested for correct integration of both ends of the deletion cassette and absence of the wild-type gene using verification PCR. One of these isolates was grown and transformed with the deletion cassette for the second gene, using a different selection marker. If no homokaryotic mycelium of the first deletion mutant was available yet (for creation of AgHPH27 and AgHPH28), spores from heterokaryotic mycelium were grown under selection and transformed with the second deletion cassette. In both cases, three primary transformants resulting from the second transformation were isolated. Verification PCR was used to test correct integration of both deletion markers. To test absence of both wild-type genes, homokaryotic mycelium was isolated from the double deletion mutants and verified using PCR.

To construct a strain with integrated histone-H4-GFP (AgHPH004), the plasmid pAG-H4-GFP-

KanMX6 (Alberti-Segui *et al.*, 2001) was digested with *Bgl*II and *Sac*I. Blunt ends were generated using the 5'–3' exonuclease activity of Vent polymerase. The 1,747-bp fragment was subcloned into pAIC (kindly provided by Philipp Knechtle) opened at the *Sca*I site (Knechtle, PhD thesis, 2002). The new plasmid pHPH001 carried a COOH-terminal fusion of GFP (S65T) to the ORF of histone H4 *(*Ag*HHF1)* with flanking homologies to the Ag*ADE2* locus. HHF1-GFP was under the control of the Ag*HHF1* promoter and was terminated by Sc*ADH1-T*. 5 μg pHPH001 were isolated from *Escherichia coli,* digested with *EcoR*I–*HindI*II, and transformed into the partially deleted Ag*ADE2* locus of the Ag*ade2Δ1* strain (Knechtle, PhD thesis, 2002). Transformants were obtained on minimal medium lacking adenine (ASD -ADE).

A C-terminal fusion of GFP to Ag*SEP7* was obtained by amplifying pGUG and pGUC with S7-G-S1 and S7-G-S2 or S7-G-S1 and S7-G-CS2, respectively. To generate Ag*SEP7-GFP-NAT1*, the pGUC cassette was first constructed by digesting pGUG with *Bgl*II and *Bam*HI and ligating the gel purified 1026 bp fragment into the dephosphorylated pUC19NATPS vector which was linearized with *Bam*HI. The S7-G–S1 primer was designed with homology to the C-terminal region of Ag*SEP7* before the stop codon. The PCR products were each transformed together with pAG4401, containing Ag*SEP7,* into the yeast strain CEN.PK2 for *in vivo* recombination. The resulting plasmids pAGHPH002 and pAGHPH003 were purified and transformed into *A. gossypii* ΔlΔt cells, leading to the strains AgHPH05 and AgHPH06. For integration into the genome, the two constructs were first subcloned into pUC19 to eliminate ARS activity. pUC19 was opened with *Sal*I and *Xba*I, Ag*SEP7-GFP-GEN3* was excised from pAGHPH002 with *Eco*RI and *Sph*I and pAGHPH003 was cut with *Xho*I and *Spe*I to extract Ag*SEP7-GFP-NAT1.* The fragments were gel purified and separately ligated into the dephosphorylated pUC19 fragment to produce pUCHPH002 and pUCHPH003. The cassettes were excised with *Eco*RI and transformed into *A. gossypii* ΔlΔt cells, giving rise to AgHPH07 and AgHPH08.

To generate ASG41 (Ag*HSL7-GFP-GEN3,* constructed by Amy Gladfelter), the oligos Hsl7-S1 and Hsl7-S2 (with homology to the C-terminus of Ag*HSL7*) were used with the template pGUG to generate PCR product which was used to directly transform *A. gossypii* cells.

To make the nonphosphorylatable Y18F mutation of Ag*CDC28,* the plasmid pAGHPH007 was created using *in vivo* gap repair in *S. cerevisiae.* First, the plasmid pRS416CDC28GEN3 was created by Amy Gladfelter: Ag*CDC28* was amplified from genomic DNA using oligos Cdc28aIEcoR1 and Cdc28aIIBamH1, with homology upstream of Cdc28 including the promoter region and limited downstream sequence. This PCR fragment was purified and digested with *EcoR*I and *BamH*I, sites present in the oligos, to clone it into pRS316 that was opened with these same enzymes. The entire CDC28 ORF was sequenced to confirm that PCR did not introduce point mutations. pRS416CDC28GEN3 was cut with *Xho*I at two sites, one being 23 bp upstream of Y18, the other being located in the pRS416 backbone. The resulting fragments were cotransformed into the yeast strain DHD5 (Arvanitidis and Heinisch, 1994) together with the annealed oligonucleotides CDC28-Y18F-A / CDC28-Y18F-B and CDC28-glue-A / CDC28-glue-B for *in vivo* recombination. The pair CDC28-Y18F-A / CDC28-Y18F-B overlapped the first *Xho*I site and contained the Y18F replacement flanked by a total of 15 silent mutations to improve the fidelity of subsequent genomic integration into *A. gossypii.* The second *Xho*I site was overlapped by the pair CDC28-glue-A / CDC28-glue-B, which contained no mutations. The gap-repaired plasmid (pAGHPH007) was isolated and verified by sequencing of the altered regions. pAGHPH007 was digested with *Eco*RI, *Bam*HI and *Pst*I and transformed into *A. gossypii* ΔlΔt cells, resulting in AgHPH36. Correct integration and presence of the altered region was verified by analytical PCR with the oligonucleotides CDC28-IB / CDC28-Y18F-IA (binds to altered sequence, only), G3 / CDC28-G4.2 and CDC28-IB / CDC28-IA-Y18 (binds to wild-type sequence, only). For additional verification, a fragment containing the altered sequence was amplified using CDC28-G1.2 / CDC28-IB and digested with *Kpn*I, which cuts the mutated fragment at two places and the wild-type fragment and one site, only (Appendix 1.8).

The plasmid carrying Ag*SWE1* (pAGHPH004) was generated by amplification of the gene from genomic *A. gossypii* DNA using the primers SWE1-B1 and SWE1-B2, which contain *EcoR*I and *BamH*I restriction sites. The fragments were purified, cut and ligatet into pRS416. The resulting plasmid was verified by sequencing.

To C-terminally tag SWE1 with GFP or 13-myc, the pGUC or pAG13-myc cassette was amplified with SWE1-G-S1 and SWE1-G-NS2 or SWE1-MS1 and SWE1-MS2, respectively. The resulting PCR products were cotransformed into the yeast strain DHD5 together with pAGHPH004 for *in vivo* recombination, giving rise to pAGHPH005

and pAGHPH006. Correct fusion was verified by sequencing. Transformation of the plasmid pAGHPH006 into *A. gossypii* ΔlΔt cells produced the strain AgHPH34. To obtain AgHPH32, pAGHPH005 was digested with *Bmg*BI and *Bss*HII before transforming it into *A. gossypii* ΔlΔt cells, leading to genomic integration.

For overexpression of Ag*SWE1,* the plasmid pAGHPH008 was constructed: the *ScHIS3* promoter was amplified off pAGrPXC (kindly provided by Dominic Hœpfner) using the primer pair MH1 and SWE1-SH2. The *GEN3* cassette was amplified using the oligonucleotides MH2 and SWE1-SH2 with pGEN3 as template. MH1 and MH2 contained homology to both, the *GEN3* cassette and the *ScHIS3* promoter, generating an overlap between the two PCR products. SWE1-SH1 and SWE1-SH2 added 45 bp homology to a region upstream of Ag*SWE1* START and 54 bp homology to the very START of Ag*SWE1.* The two PCR products were used together as template in a subsequent PCR reaction with the primers SWE1-SH1 and SWE1-SH2. The resulting *GEN3-ScHIS3* cassette was fused in front of Ag*SWE1* by *in vivo* recombination with pAGHPH004 in the yeast strain DHD5, leading to pAGHPH008. The plasmid was purified and verified by sequencing and transformed into *A. gossypii* ΔlΔt cells to produce AgHPH37. To C-terminally tag *GEN3*-PSc*HIS3*-Ag*SWE1* with HA, a 980 bp fragment carrying the carboxy end of Ag*SWE1* fused to 6HA was cut out of pAgSWE1-HA-NAT1 using *Msc*I and *Sca*I. pAGHPH008 was opened with *Msc*I and *Xba*I. T4 DNA polymerase was used to fill the 5´ protruding end generated by *Xba*I. The dephosphorylated 8910 bp vector fragment was gel purified and ligated with the 980 bp insert to produce pAGHPH009. In frame fusion of the tag was verified by sequencing. Transformation of the plasmid pAGHPH009 into *A. gossypii* ΔlΔt cells produced the strain AgHPH38. To generate pAgSWE1-HA-NAT1 (done by Amy Gladfelter), the Swe1F1 and Swe1F2 oligos, which have homology to the C-terminus of Ag*SWE1* and the universal tagging cassette, were used in a PCR reaction with the pN1-6HA (pAGT105-kindly provided by Andreas Kaufman) template and the resulting product was cotransformed into yeast cells with the plasmid pAGHPH004. Recombination of the plasmid with the linear PCR fragment resulted in yeast cells resistant to CloNAT. Plasmids were rescued from these resistant yeast strains and correct fusion of 6HA to Ag*SWE1* was verified by restriction digest.

Protein extraction and Western blotting

Cells grown under the desired conditions were collected, washed once with ice-cold PBS containing 1 mM Na_3VO_4 and 1 mM β-glyerolphosphate and suspended in ice-cold lysis buffer (50 mM Tris-HCl [pH 7.5], 150 mM NaCl, 5 mM EDTA, 1% NP-40, 2 mM sodium pyrophosphate, 1 mM Na_3VO_4, 1 mM β-glyerolphosphate and Roche complete protease inhibitor cocktail). An equal volume of 0.5 mm glass beads was added to this suspension, and cells were broken by vigorous vortexing during 6 x 30 sec intervals in a bead beater at 4 °C. Total cellular proteins were separated by SDS-PAGE (12%) and transferred to nitrocellulose membranes (Amersham Biosciences), using standard conditions. Blocking was performed with 5% milk in TBS-Tween-20 (0.1%). For detection of phosphorylated Cdc28p, rabbit anti-phospho-cdc2(Tyr15) (Cell Signaling, #9111) was used at 1:1000 in TBS, 5% BSA, 0.1% Tween-20, and HRP-anti-rabbit (Cell Signaling, #7074) was used at 1:2000 in TBS, 5% milk, 0.1% Tween-20. As positive control for phosphorylated CDK, total cellular proteins were extracted from the yeast strain DLY5544 *(cdc12-6, GAL/SWE1)*, grown in YP 2 % sucrose and induced by adding 2 % galactose. For detection of HA tagged proteins, mouse anti-HA was used at 1:1000 in TBS, 5% BSA, 0.1% Tween-20, and HRP-anti-mouse (Jackson Immunoresearch) was used at 1:1000 in TBS, 5% milk, 0.1% Tween-20. Detection of labeled proteins was performed by using the enhanced chemiluminescence (ECL) detection system (Amersham Biosciences). Either non-specific cross reacting bands or bands from ponceau red staining of the membrane were used as loading controls.

Fluorescence stainings, image acquisition and processing

DNA stainings (Hoechst 33342) and anti-tubulin immunofluorescence stainings were performed as described previously (Gladfelter *et al.*, 2006). Rabbit anti-ScCdc11p (Santa Cruz Biotechnology) was diluted in PBS and used at a 1/10 dilution. Rabbit anti-phospho-cdc2(Tyr15) was used at 1/50 for immunofluorescence. For *in vivo* observation of mycelium containing GFP tagged proteins, the cells were grown for 10 - 12 hours in full medium and then washed and resuspended in ASD or MOPS/KCl for observation under the microscope.

Visualization of the actin cytoskeleton by Alexa Fluor Phalloidin 488 was done as described in (Knechtle *et al.*, 2003) with slight modifications: to improve the yield when staining young mycelia, 9 ml of culture were mixed with 1 ml of 37 % formaldehyde and 10 µl of 10 % Triton-X and fixed for 10 min. Mycelia were collected in 15 ml Falcon tubes by 1 min centrifugation in a Heraeus Minifuge at 1000 rpm and resuspended

in 900 µl PBS containing 4 % formaldehyde and processed as described previously. For staining of the actin cytoskeleton while preserving the GFP signal mild fixation was used: The mycelia were fixed 20 min in 2 – 4 % p-formaldehyde, washed twice with PBS and resuspended in 100 µl PBS containing 0.6 µM Rhodamine-Phalloidin. After incubating the cells for one hour on ice, they were washed five times with PBS, resuspended in 50 – 200 µl mounting medium and mounted on slide (Sambrook, 2001; Knechtle, PhD thesis, 2002; Laissue, PhD thesis, 2004 , Andreas Kaufmann, personal communication).

Calcofluor white was used to stain chitin rings. 20 µl of a 1 mg/ml Calcofluor solution were added to 100 µl of liquid culture, incubated for 5 min, washed twice with dH_2O and mounted on a glass slide for microscopic inspections.

To visualize the distribution of sterols, a fresh stock of 2 mg/ml Filipin in DMSO was prepared. 2 - 4 µl of this solution were added to 2 ml liquid culture (2 µg/ml final concentration) and incubated for 2 min. During the incubation time, the mycelia were washed twice with dH_2O, once with AFM and resuspended in 500 µl AFM. The toxic effect of Filipin resulted in rapid death of the mycelia, necessitating immediate microscopic inspection.

The microscopy setup used was the same as described in (Hoepfner *et al.*, 2000; Knechtle *et al.*, 2003; Gladfelter *et al.*, 2006). The following filter sets were used for the different fluorophores: #02 for Hoechst, Calcofluor and Filipin, #10 for Alexa 488, #15 for rhodamine 568 (Carl Zeiss) and #4108 for GFP (Chroma Technology).

Multiple planes (20 – 50 for still pictures and 3 – 7 for time-lapse pictures) with a distance between 0.3 and 0.5 µm in the Z-axis were taken. MetaMorph 4.6r9 software (Universal Imaging Corp) was used for “no-neighbors” 2D-deconvolution. The stacks were flattened into a single plane using stack arithmetic “maximize” command. Outlines of the cells were obtained by doing phase-contrast Z-series. The stacks were passed through the Metamorph filter “detect edges: Laplace 2” and flattened into a single plane using the stack arithmetic “sum” command. Fluorescent and phase-contrast images were scaled and overlayed using “color align”.

Time-lapse series were taken as described in (Gladfelter *et al.*, 2006) and assembled into movies using QuickTimePro 6.5. Mitotic events in Movie 1 were labeled manually using Adobe Photoshop CS.

Table 2. *A. gossypii* strains used in this study

Strain	Relevant Genotype	Source
Reference (ΔlΔt)	*leu2Δ thr4Δ*	Altmann-Johl and Philippsen, 1996; Mohr 1997
Agade2Δ1	Agade2(310-566)Δ::GEN3, *leu2Δ thr4Δ*	Knechtle, thesis, 2002
AgH4-GFP	pAG-H4-GFP-KanMX6*[*Ag*HHF1-GFP-GEN3], leu2Δ thr4Δ*	Alberti-Segui *et al.*, 2001
AgHPH04	Ag*HHF1,* Ag*ADE2*_Ag*HHF1-GFP, leu2Δ thr4Δ,* G418^S	this study
AgHPH05	pAGHPH002*[*Ag*SEP7-GFP-GEN3], leu2Δ thr4Δ*	this study
AgHPH06	pAGHPH003*[*Ag*SEP7-GFP-NAT1], leu2Δ thr4Δ*	this study
AgHPH07	Ag*SEP7-GFP-GEN3, leu2Δ thr4Δ*	this study
AgHPH08	Ag*SEP7-GFP-NAT1, leu2Δ thr4Δ*	this study
AgHPH09	pAG-H4-GFP-KanMX6*[*Ag*HHF1-GFP-GEN3],* Ag*SEP7-GFP-NAT1, leu2Δ thr4Δ*	this study
AgHPH10	Ag*cdc3Δ::GEN3,* Ag*SEP7-GFP-NAT1, leu2Δ thr4Δ*	this study
AgHPH14	Ag*cdc10Δ::GEN3,* Ag *SEP7-GFP-NAT1, leu2Δ thr4Δ*	this study
AgHPH15	Ag*cdc12Δ::GEN3,* Ag*SEP7-GFP-NAT1, leu2Δ thr4Δ*	this study
Cdc42Q61H	Ag*CDC42,* Ag*cdc42G183C, thr4Δ*	Köhli, diploma thesis, 2003
AgHPH16	Ag*SEP7-GFP-NAT1,* Ag*CDC42,* Ag*cdc42G183C, thr4Δ*	this study
hsl1ΔNAT1	Ag*hsl1Δ::NAT1, leu2Δ thr4Δ*	this study, A Gladfelter
AgHPH17	Ag*cdc11AΔ::GEN3, leu2Δ thr4Δ*	this study
AgHPH18	Ag*cdc11BΔ::GEN3, leu2Δ thr4Δ*	this study
ASG41	Ag*HSL7-GFP-GEN3, leu2Δ thr4Δ*	this study, A Gladfelter
AgHPH19	Ag*cdc12Δ::NAT1,* Ag*HSL7-GFP-GEN3, leu2Δ thr4Δ*	this study
AgHPH20	Ag*hsl1Δ::NAT1,* Ag*HSL7-GFP-GEN3, leu2Δ thr4Δ*	this study
AgHPH21	Ag*hsl7Δ::GEN3, leu2Δ thr4Δ*	this study
AgHPH22	Ag*mih1Δ::NAT1, leu2Δ thr4Δ*	this study
AgHPH23	Ag*mih1Δ::GEN3, leu2Δ thr4Δ*	this study
ASG35	Ags*we1Δ::NAT1, leu2Δ thr4Δ*	this study, A Gladfelter
AgHPH24	Ags*we1Δ::GEN3, leu2Δ thr4Δ*	this study
AgHPH25	Ag*cdc3Δ::GEN3,* Ag*mih1Δ::NAT1, leu2Δ thr4Δ*	this study
AgHPH26	Ag*cdc10Δ::GEN3,* Ag*mih1Δ::NAT1, leu2Δ thr4Δ*	this study
AgHPH27	Ag*cdc12Δ::GEN3,* Ag*mih1Δ::NAT1, leu2Δ thr4Δ*	this study
AgHPH28	Ag*hsl1Δ::NAT1,* Ag*mih1Δ::GEN3, leu2Δ thr4Δ*	this study
AgHPH29	Ag*hsl1Δ::GEN3,* Ag*mih1Δ::NAT1, leu2Δ thr4Δ*	this study
AgHPH30	Ag*hsl7Δ::GEN3,* Ag*mih1Δ::NAT1, leu2Δ thr4Δ*	this study
AgHPH31	Ags*we1Δ::GEN3,* Ag*mih1Δ::NAT1, leu2Δ thr4Δ*	this study
AgHPH32	Ag*SWE1-13myc-GEN3, leu2Δ thr4Δ*	this study
AgHPH34	pAGHPH006*[*Ag*SWE1-GFP-NAT1], leu2Δ thr4Δ*	this study
AgHPH35	Ag*cdc28Δ::NAT1, leu2Δ thr4Δ*	this study
AgHPH36	Ag*cdc28Y18F-GEN3, leu2Δ thr4Δ*	this study
AgHPH37	pAGHPH008*[GEN3-*P$_{ScHIS3}$-Ag*SWE1], leu2Δ thr4Δ*	this study
AgHPH38	pAGHPH009*[GEN3-*P$_{ScHIS3}$-Ag*SWE1-6HA], leu2Δ thr4Δ*	this study
AgHPH39	pAGSWE1HANAT1*[*Ag*SWE1-6HA-NAT1], leu2Δ thr4Δ*	this study

With the exception of plasmidic strains (square brackets), all analyzed mycelia were homokaryotic (all nuclei have same genotype). This was obtained either by sporulating homokaryotic strains or by applying selective pressure during germination.

Table 3. Plasmids used in this study

Plasmid	Vector	Relevant insert	Source
pUC19	—	—	
pRS416	—	—	Sikorski and Hieter, 1989
pGEN3	pAF100	*GEN3*	Wendland *et al.*, 2000
pAg13-myc	pGEN3	*13myc-GEN3*	Gladfelter *et al.*, 2006
pGUG	pGEN3	*GFP-GEN3*	Knechtle *et al.*, 2003
pUC19NATPS	pUC19	*NAT1*	Hœpfner, personal communication
pGUC	pGUG	*GFP-NAT1*	this study
pAIC	pBSIISK(+)$^{Sca-}$	*AIC* (partial Ag*ADE2)*	Knechtle, Thesis, 2002
pAG-H4-GFP-KanMX6	pAG1552	Ag*HHF1-GFP-GEN3*	Alberti-Segui *et al.*, 2001
pHPH001	pAIC	Ag*HHF1-GFP-GEN3*	this study
pAG4401	pRS416	Ag*SEP7*	Mohr, Thesis, 1995; Dietrich *et al.,* 2004
pAGHPH002	pAG4401	Ag*SEP7-GFP-GEN3*	this study
pAGHPH003	pAG4401	Ag*SEP7-GFP-NAT1*	this study
pUCHPH002	pUC19	Ag*SEP7-GFP-GEN3*	this study
pUCHPH003	pUC19	Ag*SEP7-GFP-NAT1*	this study
pAGHPH004	pRS416	Ag*SWE1*	this study
pAGHPH005	pAGHPH004	Ag*SWE1-13myc-GEN3*	this study
pAGHPH006	pAGHPH004	Ag*SWE1-GFP-NAT1*	this study
pRS416CDC28GEN3	pRS416	Ag*CDC28-GEN3*	this study, A Gladfelter
pAGHPH007	pRS416Cdc28GEN3	Ag*cdc28Y18F-GEN3*	this study
pAGrPXC	YCplac111	P$_{ScHIS3}$-*CFP*	Hœpfner, personal communication
pAGHPH008	pAGHPH004	*GEN3*-P$_{ScHIS3}$-Ag*SWE1*	this study
pAGSWE1HANAT1	pAGHPH004	Ag*SWE1-6HA-NAT1*	this study, A Gladfelter
pAGHPH009	pAGHPH008	*GEN3*-P$_{ScHIS3}$-Ag*SWE1-6HA*	this study

pAG plasmids are based on the pRS416 vector Sikorski and Hieter, 1989.

Table 4. Oligonucleotide primers used in this study

Primer	Sequence 5'-3'
S7-G-S1	CAATTTGCTAGTGATGGATATGCTTCCCGCGCAACAGGCCAGGTACAAggtgcaggcgctggagctg
S7-G-S2	GCATTGACCCTCGGGCAAAGGATAAGATATATAGTTAGAAGATGTTagggacctggcacggagc
S7-G-CS2	GCATTGACCCTCGGGCAAAGGATAAGATATATAGTTAGAAGATGTTgattacgccaagcttgcatgcc
S7-G-G1	GCCAAACAACAAAAGCTGGAG
S7-G-G4	GTGCCCAGCATTTCATGGAAC
S7-G-CG4	GCCGTACGCGATCTGGCAATAGATGCGACATCC
Hsl7-S1	GACAAATACCACTGAGTTACACAATATTGGCGGTCATGCCTACATGATTAAATTGggtgcaggcgctggagctg
Hsl7-S2	GTATGCGGAAGCATAAATAGAAATGTTGCTTTTATGTTAGCATAGCGCGAagggacctggcacggagc
C3-S1	GCGTTATACAGGACCTACACACGTACAGGACTACCAAATCAGAACAAGCgctagggataacagggtaat
C3-S2	GTGACAATAATCAAGACAAATAGACTGTTTTTTTCGATTGCGGGTAGCaggcatgcaagcttagatct
C3-G1	AAACAGCGGACCACCACAAC
C3-G4	GACTTCTGCTGGCGGATACC
C3-I1	CCCACGCAGAGCAAATTGAG
C10-S1	GTTCACTCAAAGGAGCGCAAACAGCACTACTCATCCGAAACACGTTTACACCAGTTCCgctagggataacagggtaat
C10-S2	GTTTGAGTACCCTCAATATTGGTAGATCTGGTGACTTTTAAAAAGTTAGGGGTTATTCaggcatgcaagcttagatct
C10-G1	CTCCGCCTCCTTAGGAACTG
C10-G4	TGTCGCTTACTGCAGGCCATC
C10-I1	GTGTCCACGATGTGCTTCTC
CDC11A-S1	CATAAGACGCAAACAGCATGTCCAGTATCATCGAGGCCTCAGCCGCGgctagggataacagggtaat
CDC11A-S2	CCCTACTAGGCCCAAACTCCAGAATACCAATTATGTGATACAATATTGGGaggcatgcaagcttagatct
CDC11A-G1	TTCGACGAGCAGCCGAACAG
CDC11A-G4	CGGTACATGGTCAACGCATGTTACG
CDC11A/B-I1	TTGAACCGCGGGTTCC
CDC11A-I2	CCAAGCAGGAAATTGAGGAT
CDC11B-S1	GATAAGACACAGTACAATGGCGGGCATTATTGAAGCGTCAGTAGCAgctagggataacagggtaat
CDC11B-S2	CTTAAGTAAGTCAAGTTGATGGCCGCCTTTAGGGCTCGCGATGCAAaggcatgcaagcttagatct
CDC11B-G1	GCGACAGATCCTGTAATGC
CDC11B-G4	GCCGTATGGTTCCTACTGGACAC
CDC11B-I2	TAACGGCTCAACAGAGTACGC
C12-S1	CCTCAGACGCAAGGGCAACAGTGCAATAGGTGTGTTTGGTAACTTCgctagggataacagggtaat
C12-S2	GCTGATCTGTCATTTCTAGTTGGTTCCACTACTGAAGATGATACGGaggcatgcaagcttagatct
C12-NS1	CCTCAGACGCAAGGGCAACAGTGCAATAGGTGTGTTTGGTAACTTCccagtgaattcgagctcgg
C12-NS2	GCTGATCTGTCATTTCTAGTTGGTTCCACTACTGAAGATGATACGGtacgccaagcttgcatgcct
C12-G1	GATTATGTCCGCGTCGCAC
C12-G1.2	GCGGCTTCCAAAGGACAAC
C12-G4	TGGCACGGCTGCATCTTTAC
C12-I1	GCTGCCTCCGATTCTGATTC
HSL1-NS1	GCAGCACAGAGTGTAAGAAACCACAGAGGAGGATGACCGCAGGGCAccagtgaattcgagctcgg
HSL1-NS2	CATTTGCAGCATTCTCCTTTGCTTTAATGAGTGCCTCAATGTCTGtacgccaagcttgcatgcct
HSL1-NG1	GCTACTATTGAAGGTTGCAGC
HSL1-NG4	CTTCTTATGTCGGCGTACCTAGTG
HSL1-I2	CGCAGCAACCAAGGTGTCTG
HSL1-S1.2	GTGTAAGAAACCACAGAGGAGGATGACCGCAGGGCACCGAGACGAGAGgctagggataacagggtaat
HSL1-S2.2	CTCATCACTTCTTCCCTTTTGCTTGACAGACACCTTGGTTGCTGCGCTATaggcatgcaagcttagatct
HSL1-G1.2	TGCAGCCCGTTTCCAACTAC
HSL1-S4.2	GAGTGCCTCAATGTCTGTG
HSL1-IA	TTGCGAGGGCCTCTAACAAC
HSL1-IB	TCTCCGCCATGTGAATCAGC
HSL7-S1.2	GTATCAAGGGCCACGGGGTGCTAGAAGGCGCTGCGTACCGGGAGAAGTACgctagggataacagggtaat
HSL7-S2.2	CGGTCGGAAGTGATCATGAGAAGTGAAATTCAGTTGCCACAGTGCTAGCCaggcatgcaagcttagatct
HSL7-G1.2	GTTTGTTTACTGCGGTGGTC
HSL7-G4.2	GTTAGCATAGCGCGAACA
HSL7-I2.2	ACCAGGTCGAAGAAACAC
MIH1-S1	CAAAAAAAAGCCTACTTTCTCTACTTAATAGTGTTTACTCGAGCACgctagggataacagggtaat
MIH1-S2	CTTAAGAGTCGTTGTCCTCCTCCTTGACGATCTCTGGGAAAAGCCaggcatgcaagcttagatct
MIH1-NS1	CAAAAAAAAGCCTACTTTCTCTACTTAATAGTGTTTACTCGAGCACccagtgaattcgagctcgg
MIH1-NS2	CTTAAGAGTCGTTGTCCTCCTCCTTGACGATCTCTGGGAAAAGCCtacgccaagcttgcatgcct
MIH1-G1	CAGGCGCAGAAGTCGTTAC
MIH1-G4	GACGCGCAGTTGTTGCTTC
MIH1-I1	CCTCTGTCTCGCTCTTTCG
SWE1-NS1	CAAGGTACCAGCGGCAAGCGCGCAGAGAAGACACAGACTAAGAATGccagtgaattcgagctcgg
SWE1-NS2	CCTTATGGTGGCCGGGGAGCGCGATATGCGCCGAACATGCATTCTGtacgccaagcttgcatgcct
SWE1-S1	CAAGGTACCAGCGGCAAGCGCGCAGAGAAGACACAGACTAAGAATGgctagggataacagggtaat
SWE1-S2	CCTTATGGTGGCCGGGGAGCGCGATATGCGCCGAACATGCATTCTGaggcatgcaagcttagatct
SWE1-B1	gcgaattcCGCCTCAGCTTGATCATCGTCAC
SWE1-B2	cgggatccATCGGTATCTGCCGAACACAATGC
SWE1-G-S1	CCATCATCCAAGAAGACGACTTTGGTCCCAAGCCGGAGTTCTTCAGCggtgcaggcgctggagctg
SWE1-G-NS2	CGCACGTTCACTTGTAGCCGAGAAGCCCCTTATGGTGGCCGGGGAGgattacgccaagcttgcatgcc
SWE1-MS1	CCATCATCCAAGAAGACGACTTTGGTCCCAAGCCGGAGTTCTTCAGCcggatccccgggttaattaacggtgaa
SWE1-MS2	CGCACGTTCACTTGTAGCCGAGAAGCCCCTTATGGTGGCCGGGGAGcactagtggatctgatatcagatctgg
AgSWE1 G1	CTCACCTCGAGGCCACTCCGTGTGAGG

SWE1-G-G1	CATCGCGCCGGAAATCATC
AgSWE1 G4	GCAGAGACGCTCAGAGAGATTCCCATTG
AgSWE1 I	GCGACTGAGAGCGATCCGATATTAAGG
SWE1-SH1	AGGAGAAGGGCATACAGTTCCCCACGAATTTCGGCATAGAAAGGCgaattcaggcatgcaagcttagatct
SWE1-SH2	GTTCAGAAACGGCGACTCGCGCAGCGCTGCCATGCTGTCGTGCCGGAGCGTCATggatccccgggtaccgagctctttg
MH1	GTATTACCCTGTTATCCCTAGCATTCTATTACTCTTGGCCTCC
MH2	GGAGGCCAAGAGTAATAGAATGCTAGGGATAACAGGGTAATAC
HISP-HG2	TTTCCACCTAGCGGATGAC
SWE1-HG1	ATGGACGCCACAGGTTATCTC
CDC28-N*S1	ACTCCCTATGTACCCCACGGGCACGGGCCCATAAACCGGCAAAAAACGCGCCTGCGACAGA AAATTTTGTGTACCTCTACCACCAGCACCCTCatgggtaccactcttgacgac
CDC28-N*S2	AGCAGCGCAATCTACATGCAAACGCGGTACAGCACCAGCGCTACTATTTATACCACCTACG TAGCTGCCTGTTCTGGCAGCGAGCGGGCCCTAggggcagggcatgctcatgtag
CDC28-N*G1	TGCTGACGATGGGCTCCTTC
CDC28-N*G4	TGTGGACCCTCCCAGTTACC
CDC28-IB	TGCACATTTCGGCGAAGATG
CDC28-G1.2	AGGAGTGACCTCCTCTACAG
CDC28-IA-Y18	GAACGTATGGTGTCGTCTAC
CDC28-Y18F-A	CCCTCATGAGCGATCTCACCAACTACAAGCGCTTGGAAAAAGTCGGTGAAGGTACCTTCGG GGTTGTTTATAAAGCGGTTG
CDC28-Y18F-B	CGCCACGATGCGCTGCCCATGCCGCAGGTCAACCGCTTTATAAACAACCCCGAAGGTACCT TCACCGACTTTTTCCAAGC
CDC28-glue-A	GGGCGAATTGGGTACCGGGCCCCCCCTCGAGGTCGACGGTATCGATAAGC
CDC28-glue-B	GCTTATCGATACCGTCGACCTCGAGGGGGGGCCCGGTACCCAATTCGCCC
CDC28-Y18F-IA	GGTACCTTCGGGGTTGTTTA
CDC28-G4.2	ATGTGCGCGAGGCTCTTTC
Cdc28alEcoR1	CATAGAATTCACTTCCGTGCCTGGGTGCAGCAGCATCGGCTTC
Cdc28alIBamH1	GTTCGGATCCTGACGATGGGCTCCTTCGACGGCCTGTTG
Swe1F1	CCATCATCCAAGAAGACGACTTTGGTCCCAAGCCGGAGTTCTTCAGCAAAACGACGGCCAGTGAATTCG
Swe1F2	CGCACGTTCACTTGTAGCCGAGAAGCCCCTTATGGTGGCCGGGGAGACCATGATTACGCCAAGCTTGC
G2.1	tgcctccagcatagtcgaag
G3	tcgcagaccgataccaggatc
V2PDC1P	gaacaaacccaaatctgattgcaaggagagtgaaagagcctt
V3PDC1T	gaccagacaagaagttgccgacagtctgttgaattggcctg
V2*NAT1	gtgtcgtcaagagtggtacc
V3*NAT1	acatgagcatgccctgcccc
GG2	catcaccttcaccctctccac
MYCI	cgagtccgttcaagtcttcttctgag

Lower case letters are regions of homology to the cassette containing a selectable marker. Underlined letters represent intragenic replacements (alternative codons, point mutations).

Appendix

I. Verification PCRs

II. Plasmid maps

III. Sequence alignments

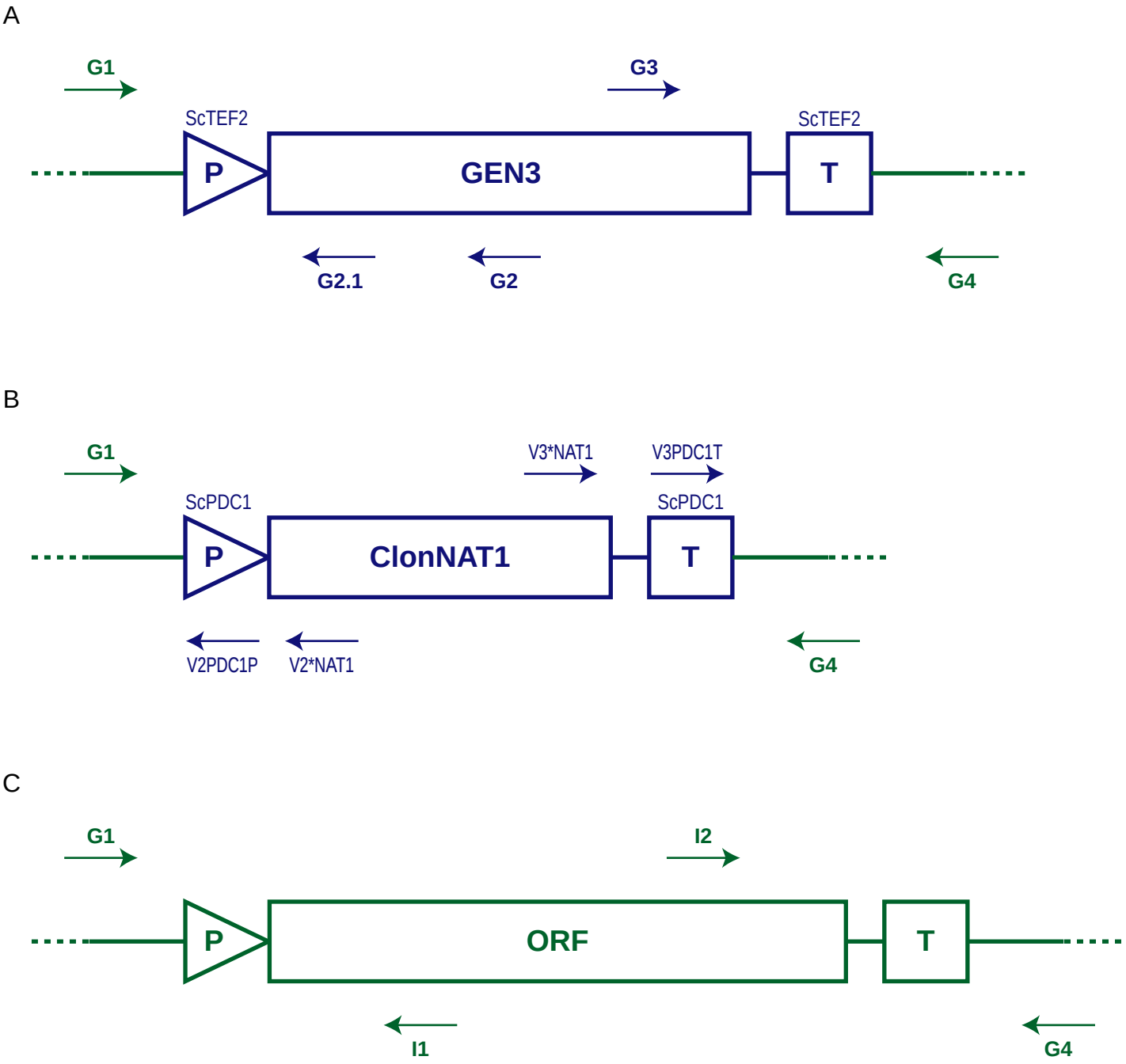

Appendix 1.1. Oligos used for verification of deletion strains. (A) Verification of correct integration of the GEN3 deletion cassette. **(B)** Verification of correct integration of the ClonNAT deletion cassette. **(C)** Verification of absence of the targeted ORF in homokaryons. PCR products are obtained in wild type and heterokaryons, only.

A

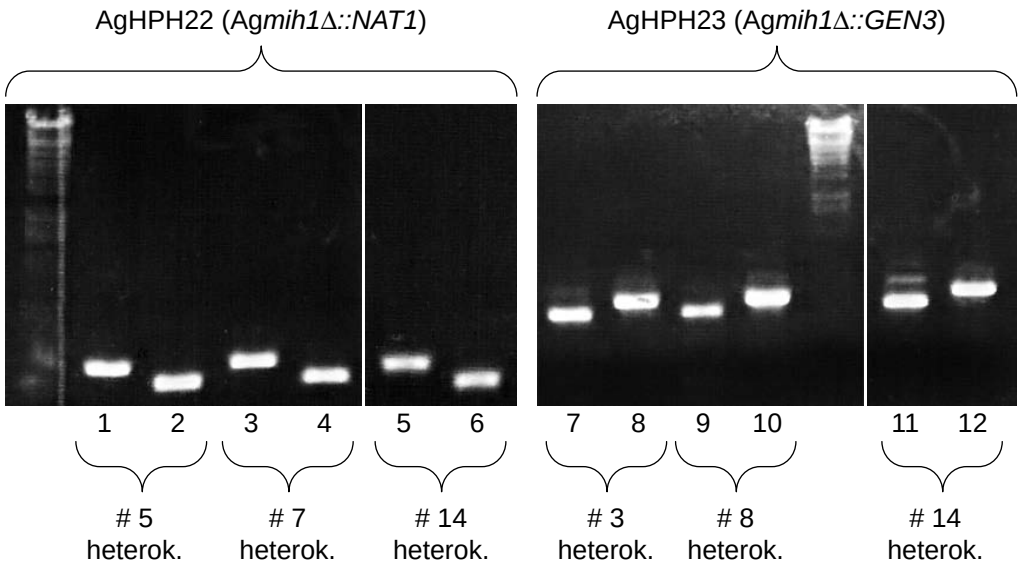

1, 3, 5:	MIH1-G1 + V2PDC1P	→	506 bp
2, 4, 6:	MIH1-G4 + V3PDC1T	→	401 bp
7, 9, 11:	MIH1-G1 + G2.1	→	508 bp
8, 10, 12:	MIH1-G4 + G3	→	618 bp

B

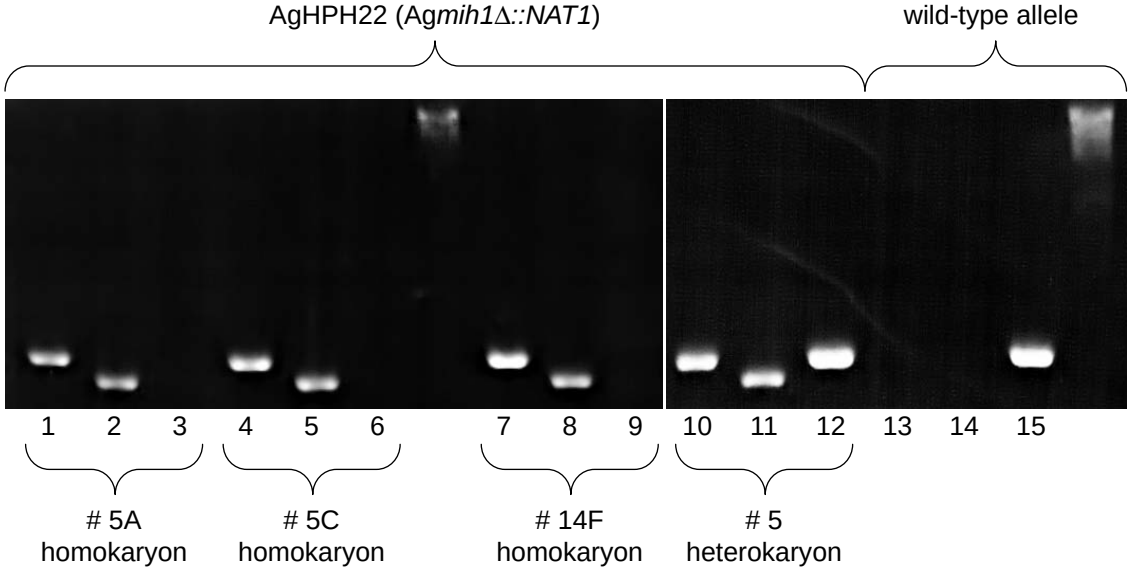

1, 4, 7, 10, 13:	MIH1-G1 + V2PDC1P	→	506 bp
2, 5, 8, 11, 14:	MIH1-G4 + V3PDC1T	→	401 bp
3, 6, 9, 12, 15:	MIH1-G1 + MIH1-I1	→	503 bp (wt)

Appendix 1.2. Verfification of Ag*mih1*Δ strains. (A) heterokaryons **(B)** homokaryons

A

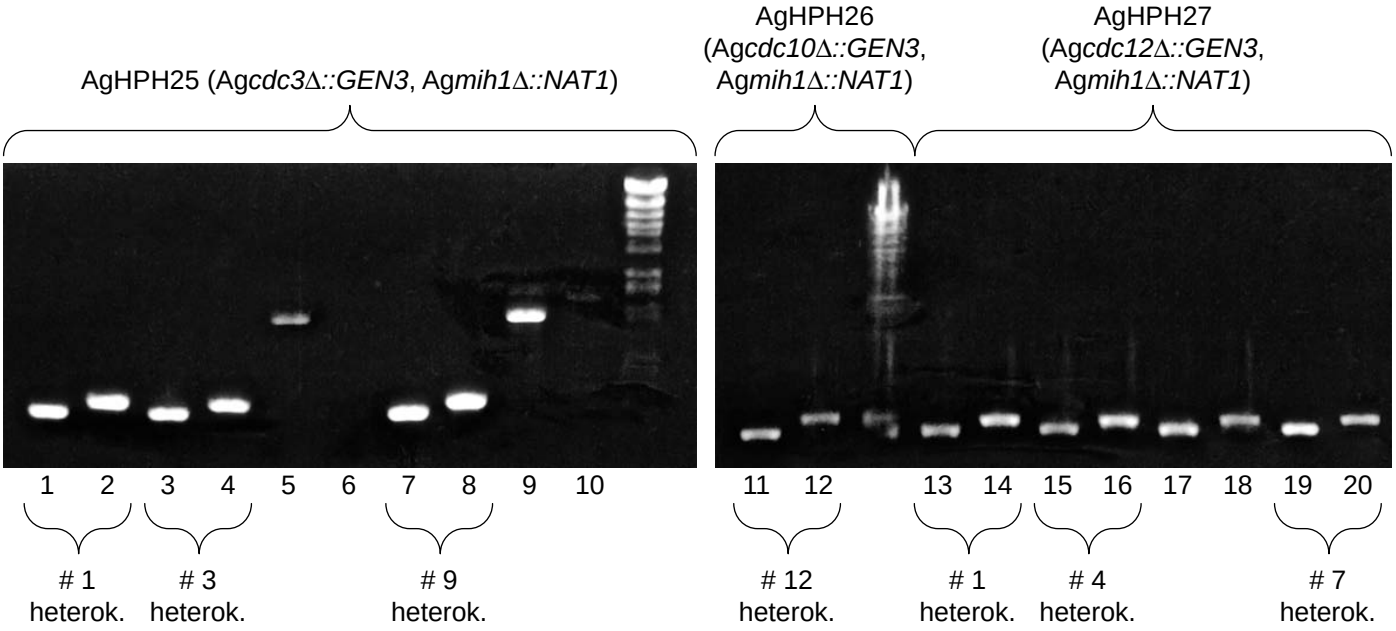

1, 3, 5, 7, 9:	C3-G1 + G2.1	→	530 bp
2, 4, 6, 8, 10:	C3-G4 + G3	→	615 bp
11:	C10-G1 + G2.1	→	511 bp
12:	C10-G4 + G3	→	621 bp
13, 15, 17, 19:	C12-G1.2 + G2.1	→	512 bp
14, 16, 18, 20:	C12-G4 + G3	→	587 bp

B

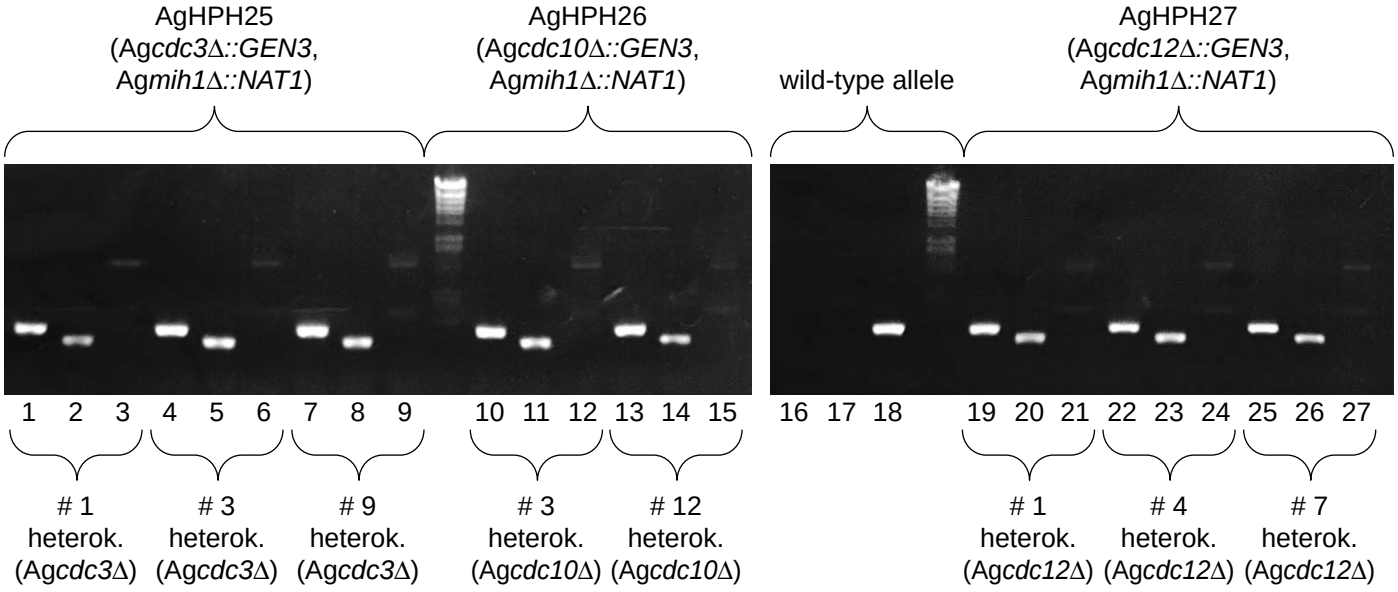

1, 4, 7, 10, 13, 16, 19, 22, 25:	MIH1-G1 + V2PDC1P	→	506 bp
2, 5, 8, 11, 14, 17, 20, 23, 26:	MIH1-G4 + V3PDC1T	→	401 bp
3, 6, 9, 12, 15, 18, 21, 24, 27:	MIH1-G1 + MIH1-I1	→	503 bp (wt)

Appendix 1.3. Verfification of Ag*septin*Δ*mih1*Δ strains. (A) Verification of the heterokaryotic septin knock-outs. **(B)** Verfification of the homokaryotic Ag*mih1*Δ background.

A

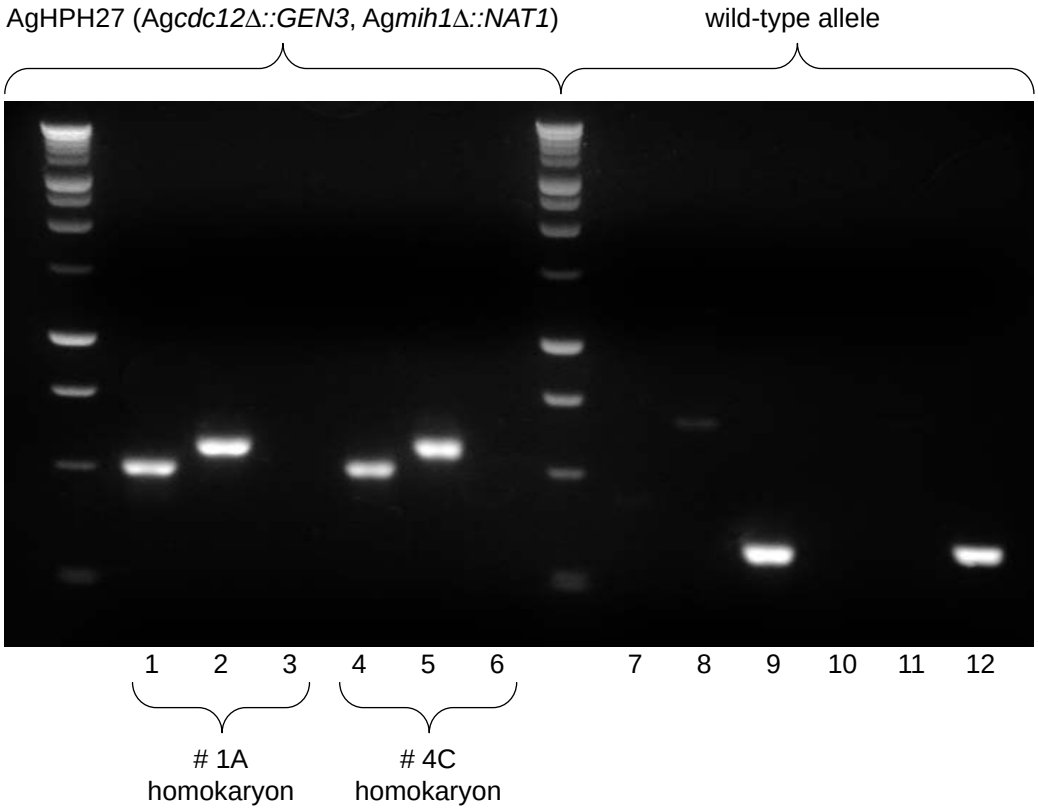

1, 4, 7, 10:	C12-G1.2 + G2.1	→	512 bp
2, 5, 8, 11:	C12-G4 + G3	→	587 bp
3, 6, 9, 12:	C12-G1.2 + C12-I1	→	336 bp (wt)

B

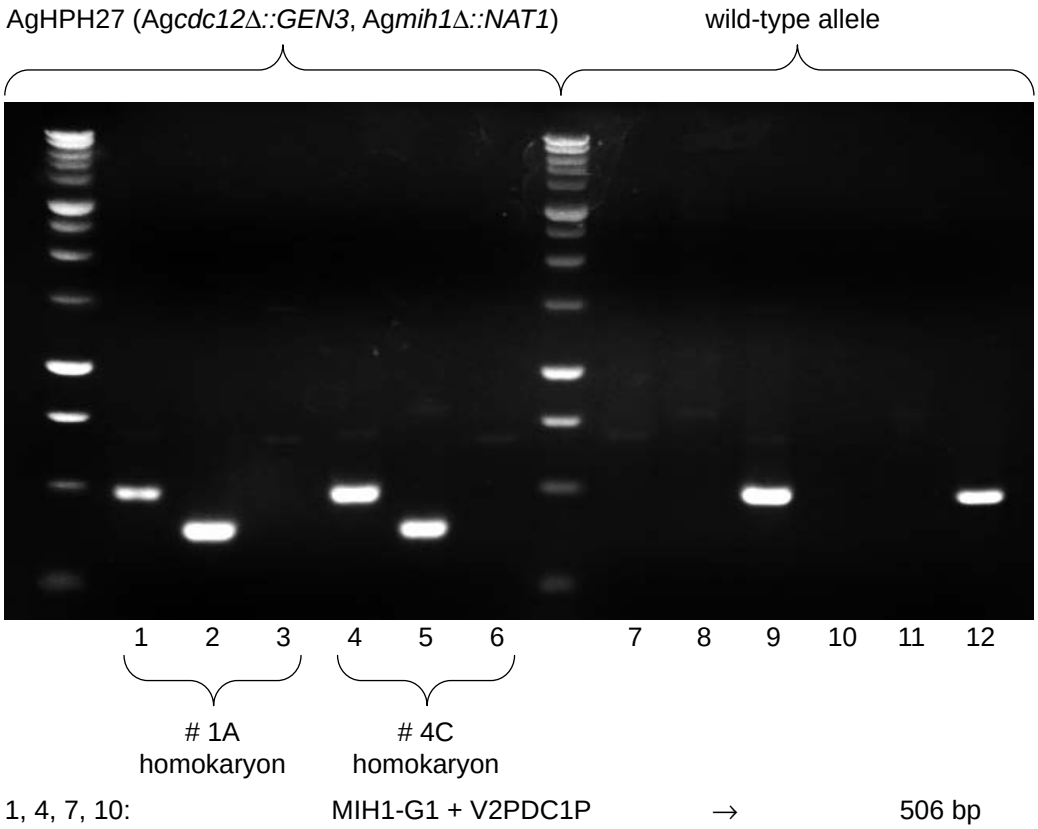

1, 4, 7, 10:	MIH1-G1 + V2PDC1P	→	506 bp
2, 5, 8, 11:	MIH1-G4 + V3PDC1T	→	401 bp
3, 6, 9, 12:	MIH1-G1 + MIH1-I1	→	503 bp (wt)

Appendix 1.4. PCR verfification of Ag*cdc12*Δ*mih1*Δ (AgHPH27) homokaryons.
(A) Verification of correct integration of the *GEN3* cassette at the Ag*CDC12* locus and absence of the wt allele **(B)** Verification of the homokaryotic Ag*mih1*Δ background. The Promega 1 kb DNA ladder was used as marker (lowest three bands: 750, 500 and 250 bp).

A

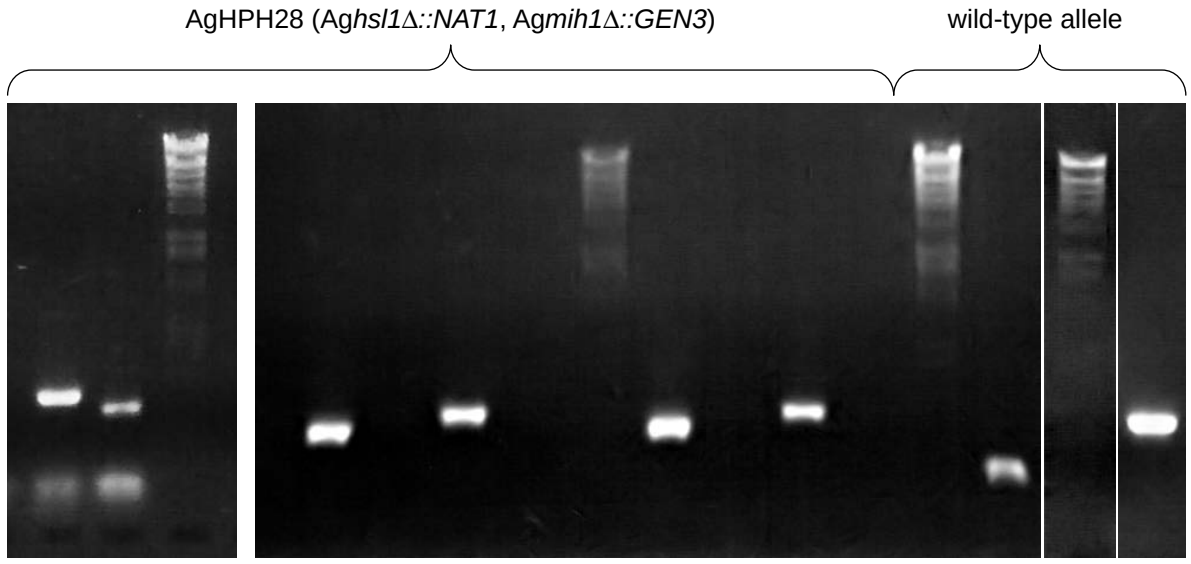

# 7 heterokaryon			
1:	HSL1-NG1 + V2PDC1P	→	501 bp
2:	HSL1-NG4 + V3PDC1T	→	426 bp
# 7B homokaryon			
3, 7:	HSL1-NG4 + V3PDC1T	→	426 bp
4, 8, 11:	HSL1-I2 + HSL1NG4	→	264 bp (wt)
5, 9:	MIH1-G1 + G2.1	→	508 bp
# 7F homokaryon			
6, 10, 12:	MIH1-G1 + I1	→	503 bp (wt)

B

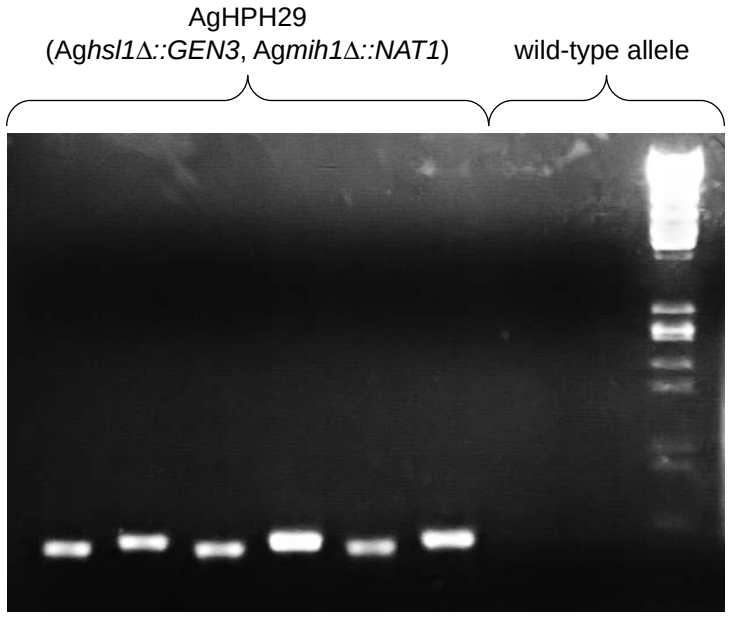

# 1 heterok. (Ag*hsl1*Δ)			
# 2 heterok. (Ag*hsl1*Δ)			
# 3 heterok. (Ag*hsl1*Δ)			
1, 3, 5, 7:	HSL1-NG1.2 + G2.1	→	500 bp
2, 4, 6, 8:	HSL1-NG4.2 + G3	→	536 bp

Appendix 1.5. Verfification of Ag*hsl1*Δ*mih1*Δ strains. (A) For the construction of AgHPH28, spores from heterokaryotic AgHPH23 (Ag*mih1*Δ*::GEN3*) were grown under selection and transformed with the Ag*hsl1*Δ*::NAT1* cassette. The Ag*mih1*Δ background was verified by one end only, since both ends were already verified in AgHPH23. **(B)** For AgHPH29, spores from homokaryotic AgHPH22 (Ag*mih1*Δ*::NAT1*) were used. Verification of the homokaryons including Ag*mih1*Δ background is shown in Appendix 1.6.

A

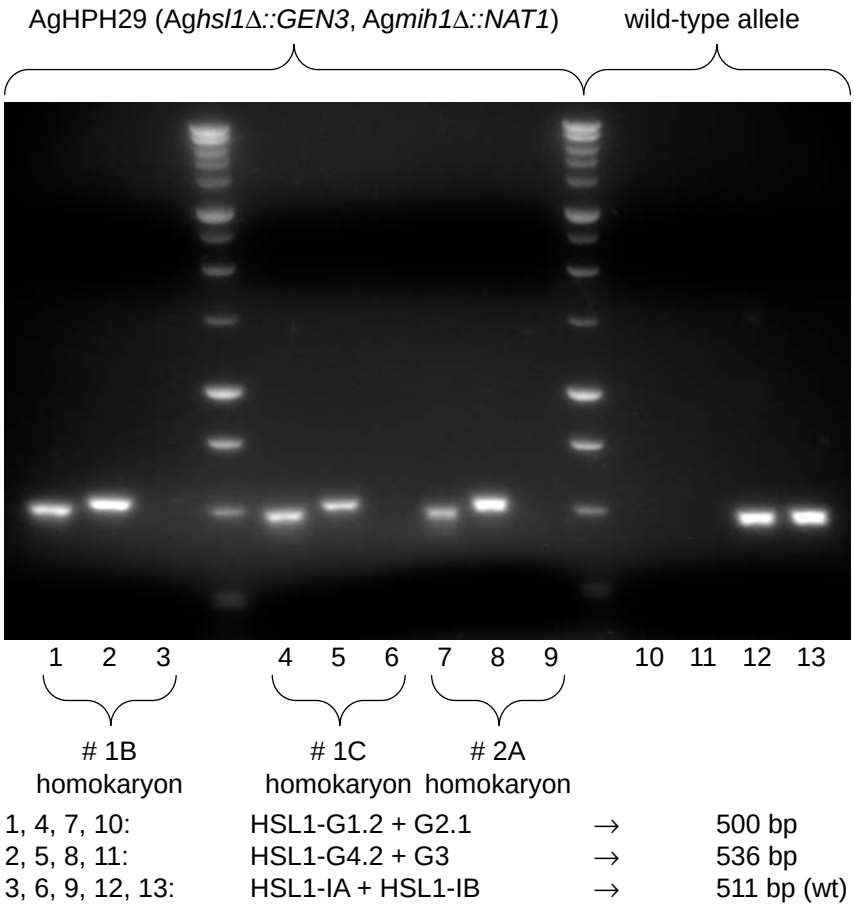

B

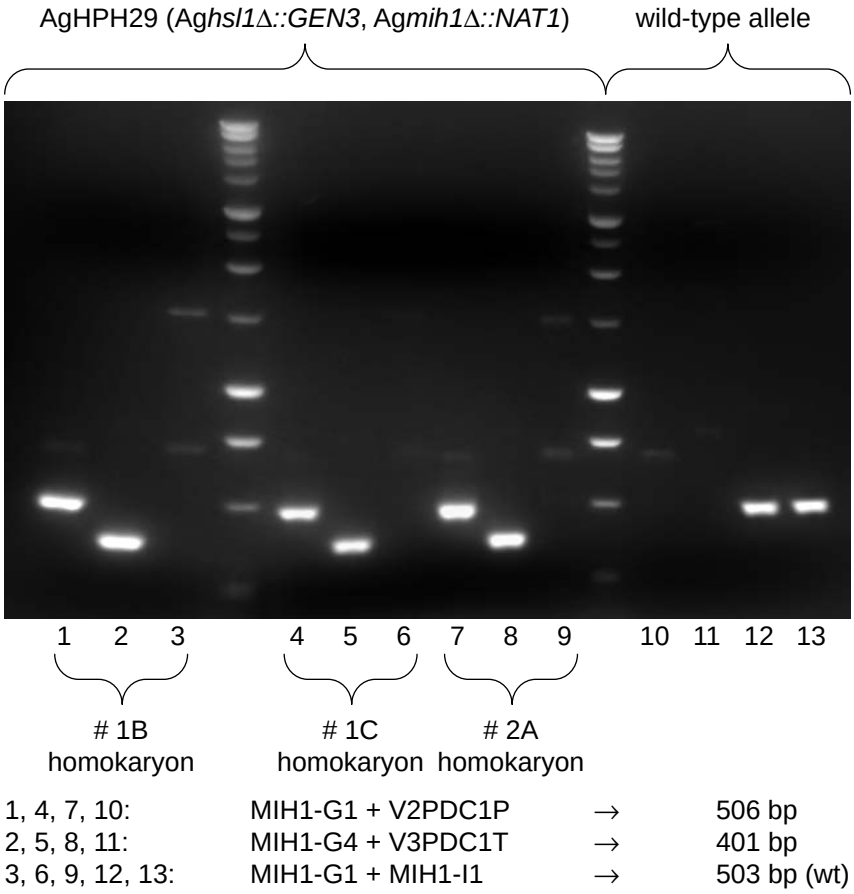

Appendix 1.6. PCR verfification of Ag*hsl1*Δ*mih1*Δ (AgHPH29) homokaryons. (A) Verification of correct integration of the *GEN3* cassette at the Ag*HSL1* locus and absence of the wt allele. **(B)** Verification of the homokaryotic Ag*mih1*Δ background. The Promega 1 kb DNA ladder was used as marker (lowest three bands: 750, 500 and 250 bp).

A

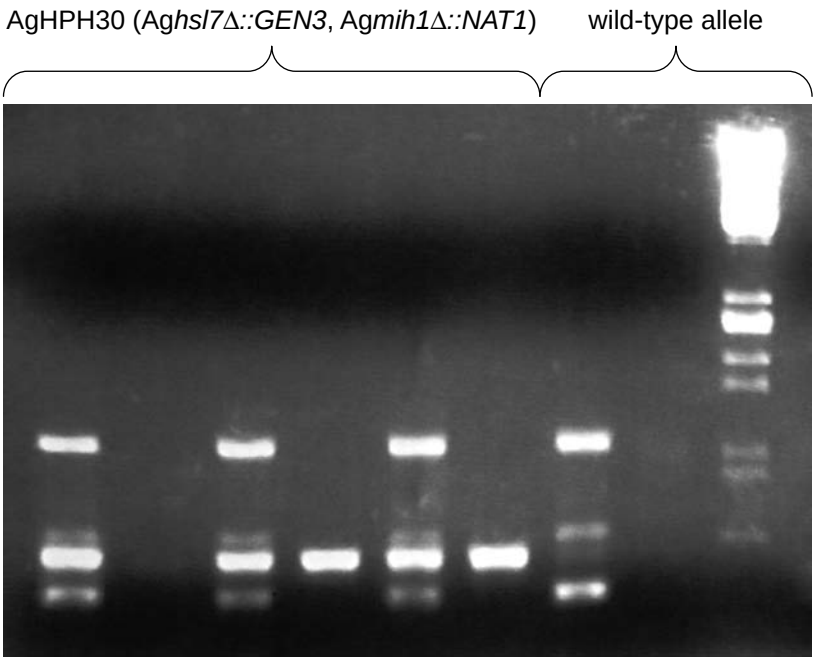

1, 3, 5, 7:	HSL7-G1.2 + G2.1	→	533 bp
2, 4, 6, 8:	HSL7-G4.2 + G3	→	541 bp

B

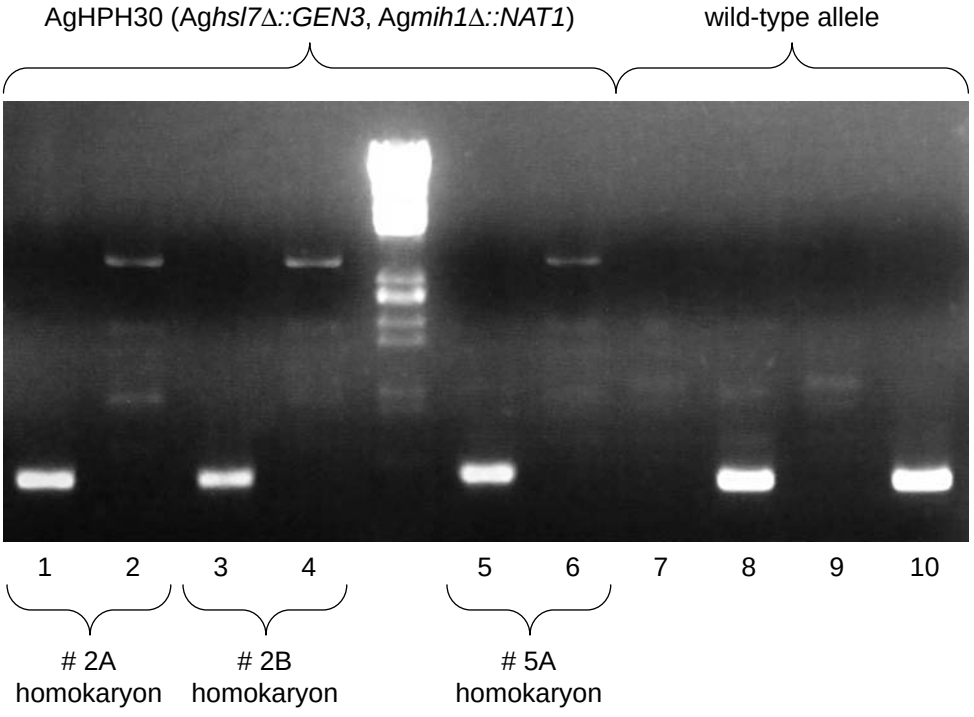

1, 3, 5, 7, 9:	HSL7-G4.2 + G3	→	541 bp
2, 4, 6, 8, 10:	HSL7-G4.2 + HSL7-I2.2	→	495 bp (wt)

Appendix 1.7. Verfification of Ag*hsl7*Δ*mih1*Δ strains. (A) Verification of heterokaryons. Unspecific bands are the result of low annealing temperature. The pattern of true transformants can clearly be distinguished from false positives or the reference strain. **(B)** Verfification of homokaryons. Ag*mih1*Δ background. Spores from homokaryotic AgHPH22 (Ag*mih1*Δ*::NAT1*) were used for transformation.

A

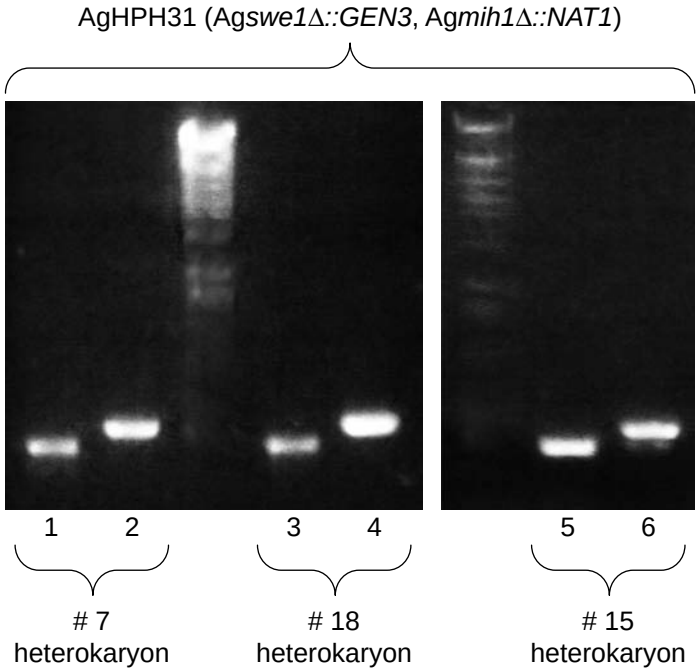

1, 3, 5:	SWE1-G1 + G2.1	→	721 bp
2, 4, 6:	SWE1-G4 + G3	→	824 bp

B

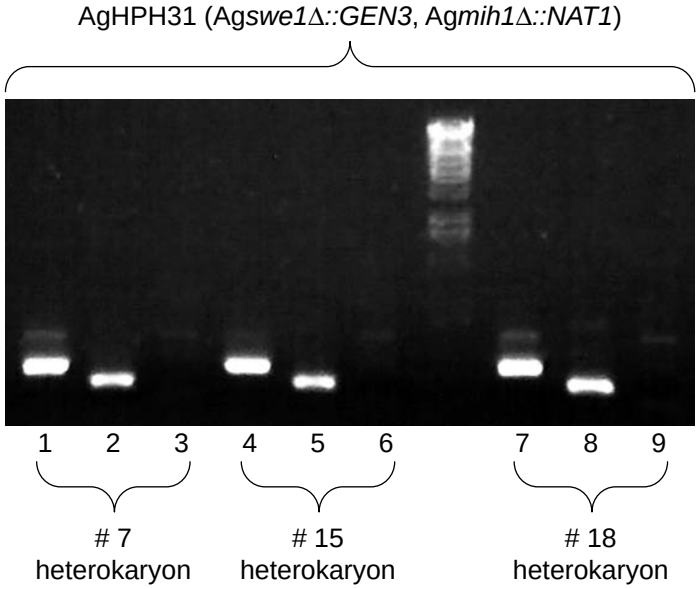

1, 4, 7:	MIH1-G1 + V2PDC1P	→	506 bp
2, 5, 8:	MIH1-G4 + V3PDC1T	→	401 bp
3, 6, 9:	MIH1-G1 + MIH1-I1	→	503 bp (wt)

C

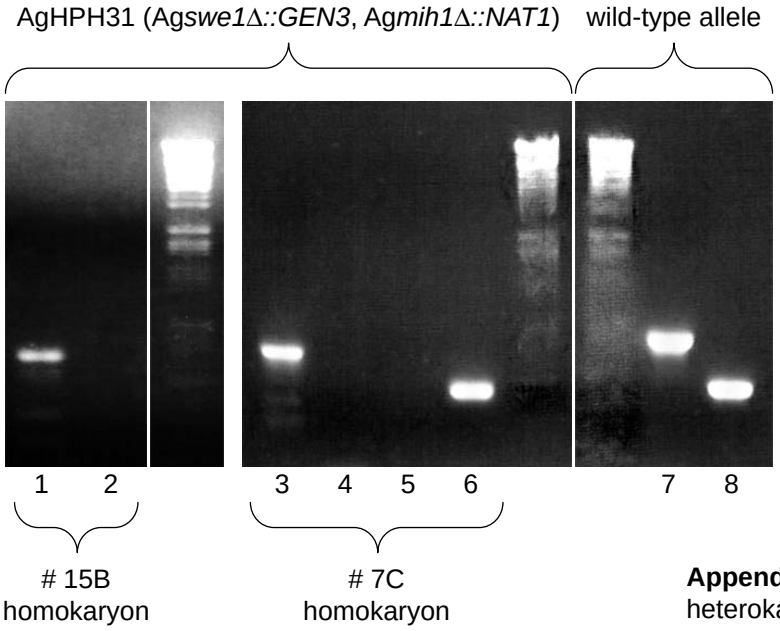

1, 3:	SWE1-G1 + G2.1	→	721 bp
2, 4, 7:	SWE1-G1+ SWE1-I1	→	839 bp
5, 8:	MIH1-G1 + MIH1-I1	→	503 bp (wt)
6:	MIH1-G1 + V2PDC1P	→	506 bp

Appendix 1.8. Verfification of Ags*we1*Δ*mih1*Δ strains. (A) heterokaryons, **(B)** Ag*mih1*Δ background, **(C)** homokaryons

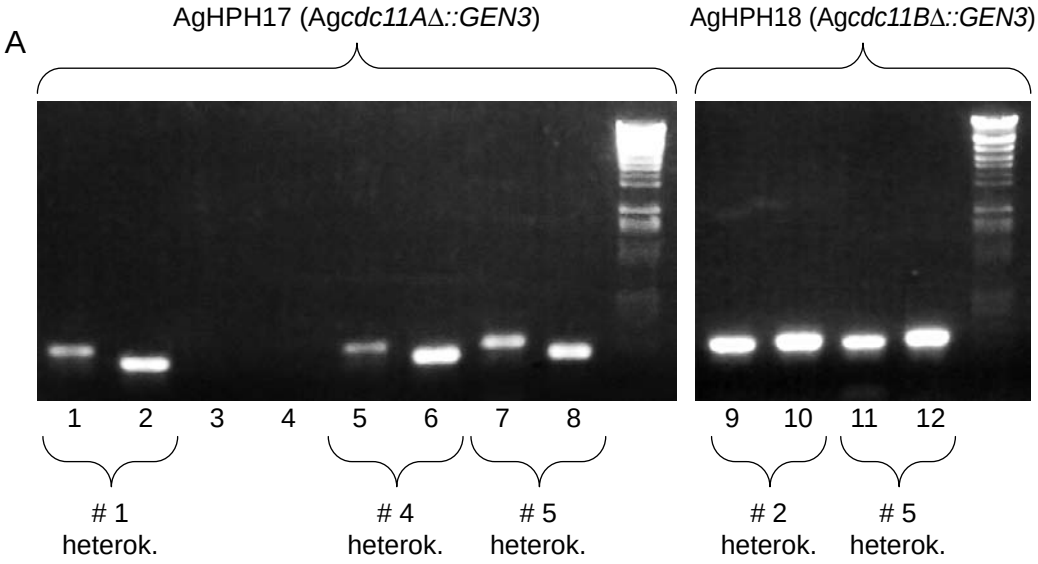

1, 3, 5, 7: CDC11A-G1 + G2.1 → 603 bp
2, 4, 6, 8: CDC11A-G4 + G3 → 542 bp
9, 11: CDC11B-G1 + G2.1 → 612 bp
10, 12: CDC11B-G4 + G3 → 636 bp

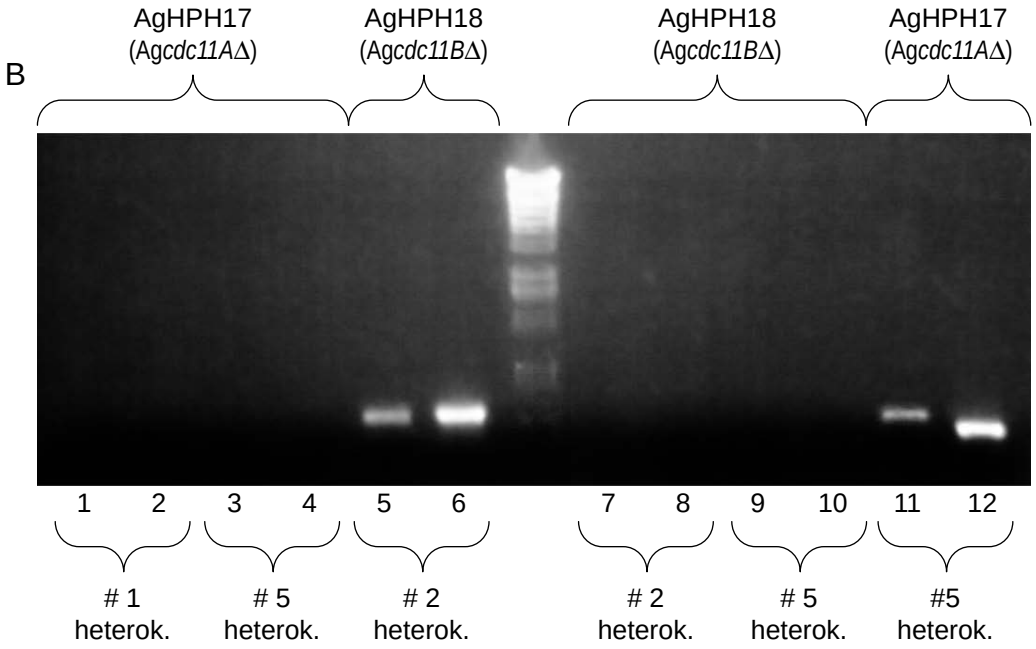

1, 3, 5: CDC11B-G1 + G2.1 → 612 bp
2, 4, 6: CDC11B-G4 + G3 → 636 bp
7, 9, 11: CDC11A-G1 + G2.1 → 603 bp
8, 10, 12: CDC11A-G4 + G3 → 542 bp

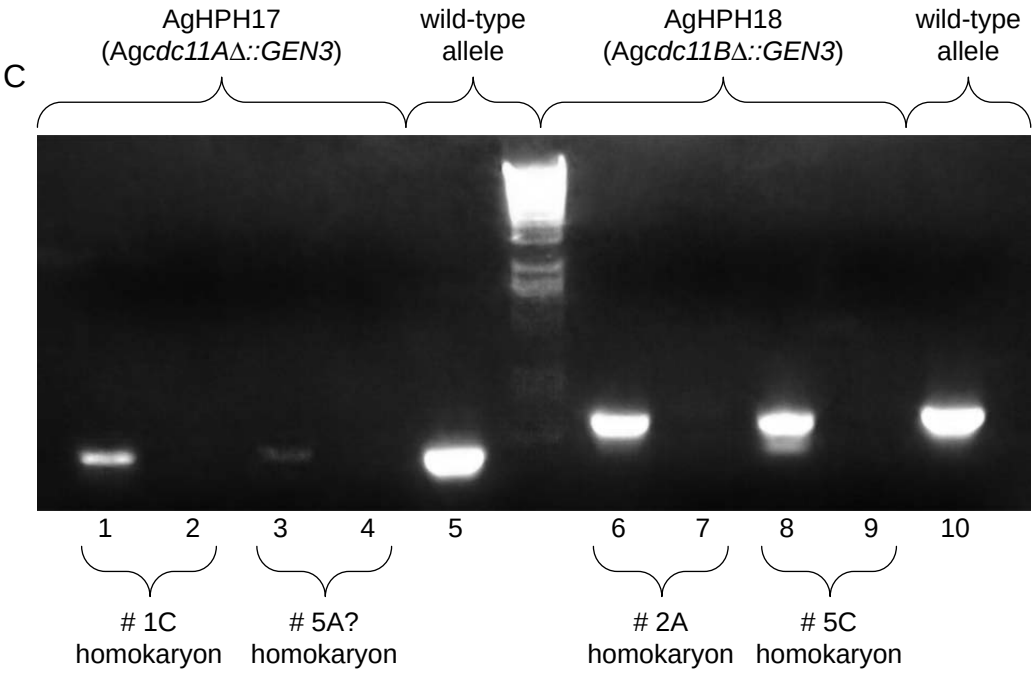

1, 3: CDC11A-G4 + G3 → 542 bp
2, 4, 5: CDC11A-G4 + CDC11A-I2 → 485 bp (wt)
6, 8: CDC11B-G4 + G3 → 636 bp
7, 9, 10: CDC11B-G4 + CDC11B-I2 → 681 bp (wt)

Appendix 1.9. Verfification of Ag*cdc11A*Δ and Ag*cdc11B*Δ strains.
(A) heterokaryons, **(B)** *CDC11A* verification oligos G1 and G4 were tested for unspecific binding to the Ag*CDC11B* promotor and terminator region in Ag*cdc11B*Δ strains and *vice versa.* No crossreaction was detected. **(C)** Verification of homokaryons.

A

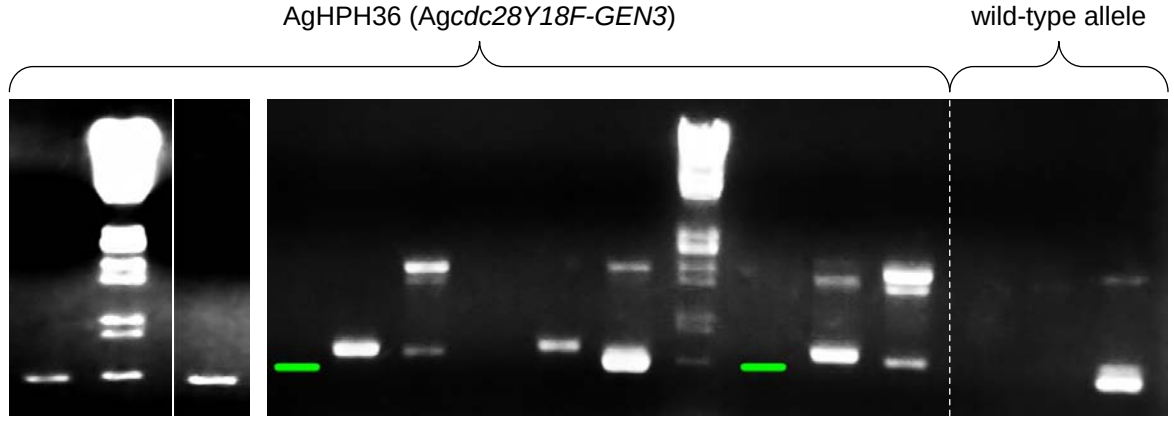

1, 2, 3, 6, 9, 12:	CDC28-Y18F-IA + CDC28-IB	→	565 bp (Y18F-IA binds mutated seq.)
4, 7, 10, 13:	CDC28-G4.2 + G3	→	704 bp
5, 8, 11, 14:	CDC28-IA-Y18 + CDC28-IB	→	564 bp (IA-Y18 binds wt seq.)

B

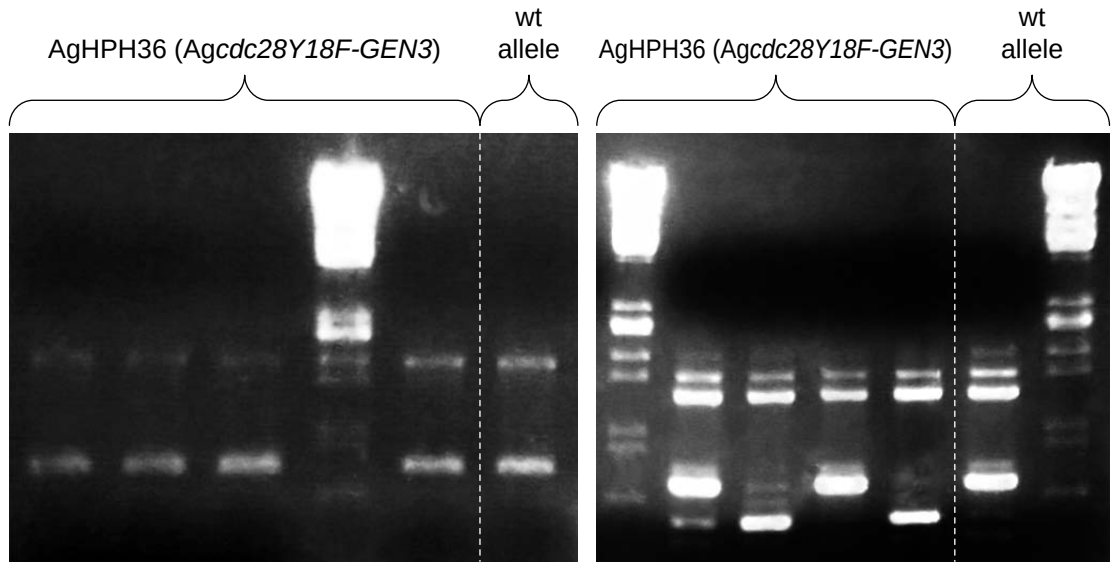

CDC28-G1.2 + CDC28-IB uncleaved		→	732 bp
*Kpn*I	AgHPH36	→	472, 172, 88 bp
*Kpn*I	reference	→	644, 88 bp

Appendix 1.10. Verification of Ag*cdc28Y18F* strains. (A) Verification by PCR. CDC28-Y18F-IA binds specifically to the mutated sequence (incl. Phe18), but binding is weak. Bands that were seen by eye on a UV table but were to weak for printing using the gel imager are painted in green. CDC28-G4.2 + G3 was used to confirm correct integration of the *GEN3* module. CDC28-IA-Y18 was designed to bind to the wild-type sequence, only (incl. Tyr 18), but results in unspecific, weaker bands in the mutant strains. The pattern is clearly distinguishable between true mutants and false positives or the wild-type allele. A band of correct size (564 pb) is only observed for false positives or the wild-type allele, not for true positives. The lowest band in true positives corresponds to the second lowest (false) band in wild type. **(B)** A 732 bp fragment including Tyr 18 / Phe 18 was amplified and digested with *Kpn*I, which cuts the mutant fragment three times and the wild-type fragment twice. Additional bands are likely to be the result of the 1.5 kb unspecific PCR product.

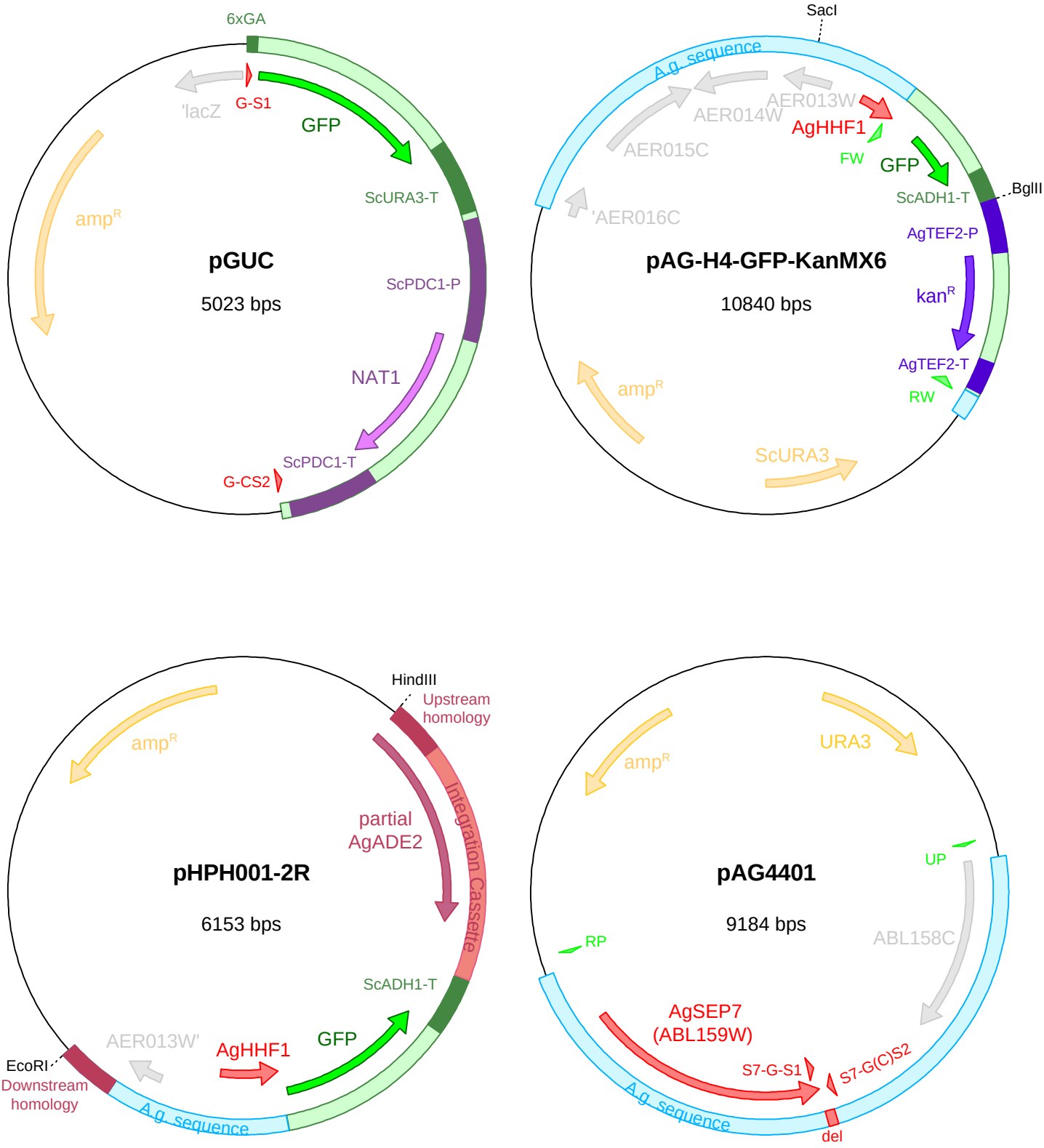

Appendix 2.1. pAG-H4-GFP-KanMX6 was constructed by C. Alberti-Segui, but no map or sequence was provided. We reconstructed the map based on information gathered from Alberti-Segui *et al.*, 2001 and Alberti-Segui, Thesis, 2001. pAG4401 is part of the pAG collection created by C. Mohr (C. Mohr, Thesis, 1995; Dietrich *et al.*, 2004). The map is shown to illustrate the construction of pAGHPH002 and pAGHPH003 (see Appendix 2.2).

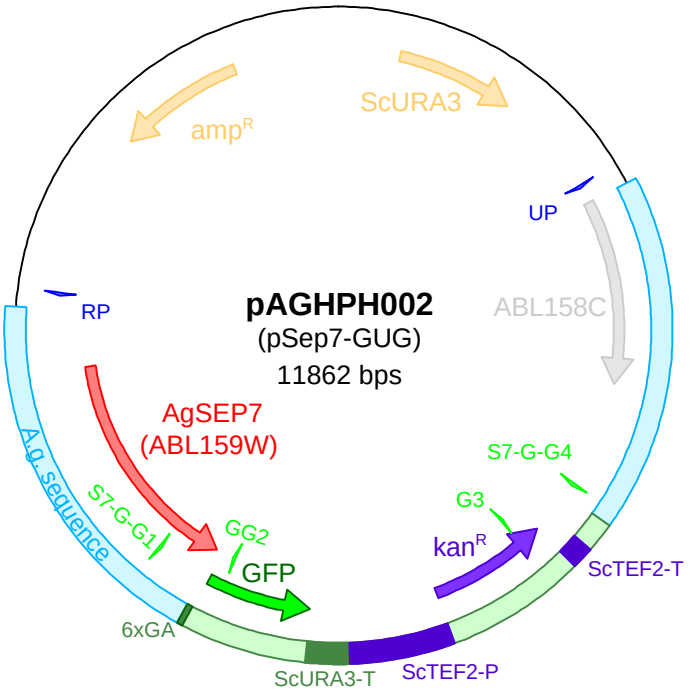
ampR
ScURA3
UP
ABL158C
RP
pAGHPH002
(pSep7-GUG)
11862 bps
AgSEP7
(ABL159W)
A.g. sequence
S7-G-G1
GG2
GFP
S7-G-G4
G3
kanR
ScTEF2-T
6xGA
ScURA3-T
ScTEF2-P

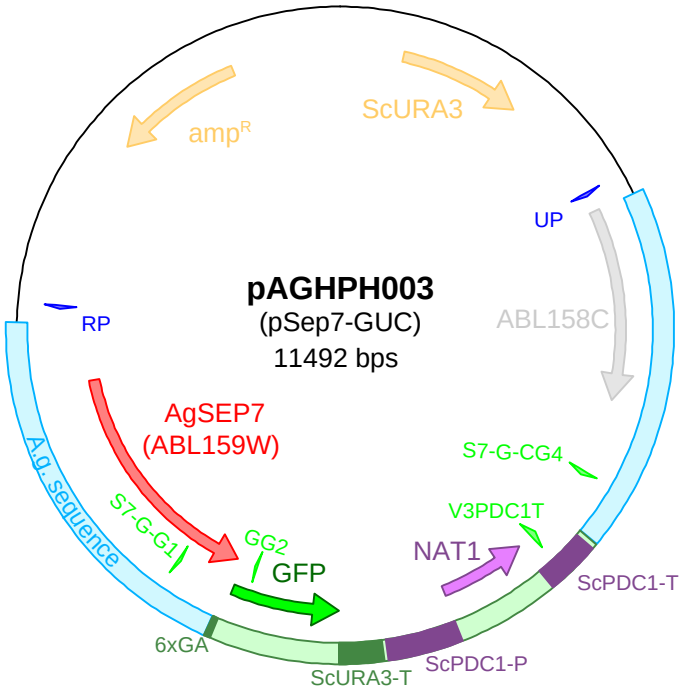
ampR
ScURA3
UP
ABL158C
RP
pAGHPH003
(pSep7-GUC)
11492 bps
AgSEP7
(ABL159W)
A.g. sequence
S7-G-G1
GG2
GFP
S7-G-CG4
V3PDC1T
NAT1
ScPDC1-T
6xGA
ScURA3-T
ScPDC1-P

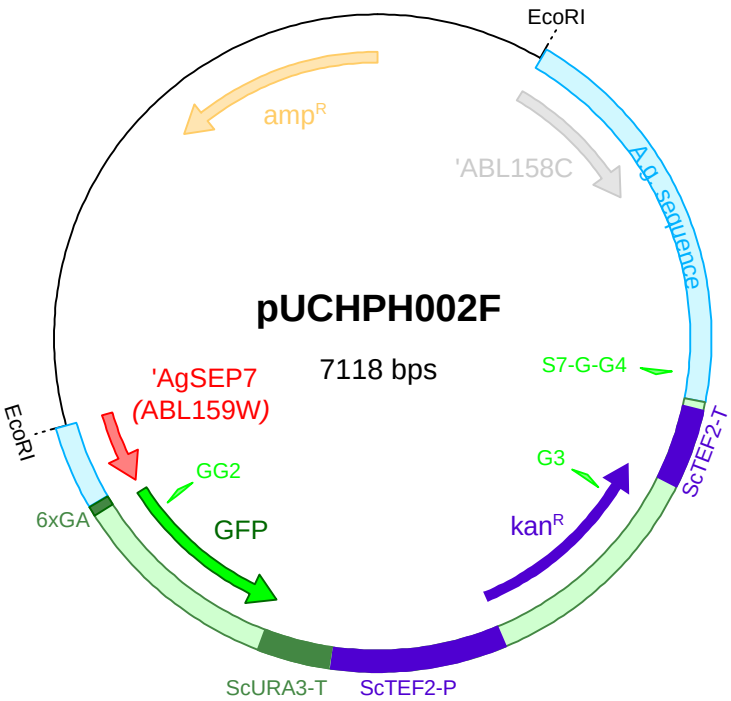
EcoRI
ampR
'ABL158C
A.g. sequence
pUCHPH002F
7118 bps
'AgSEP7
(ABL159W)
S7-G-G4
EcoRI
GG2
G3
ScTEF2-T
6xGA
GFP
kanR
ScURA3-T
ScTEF2-P

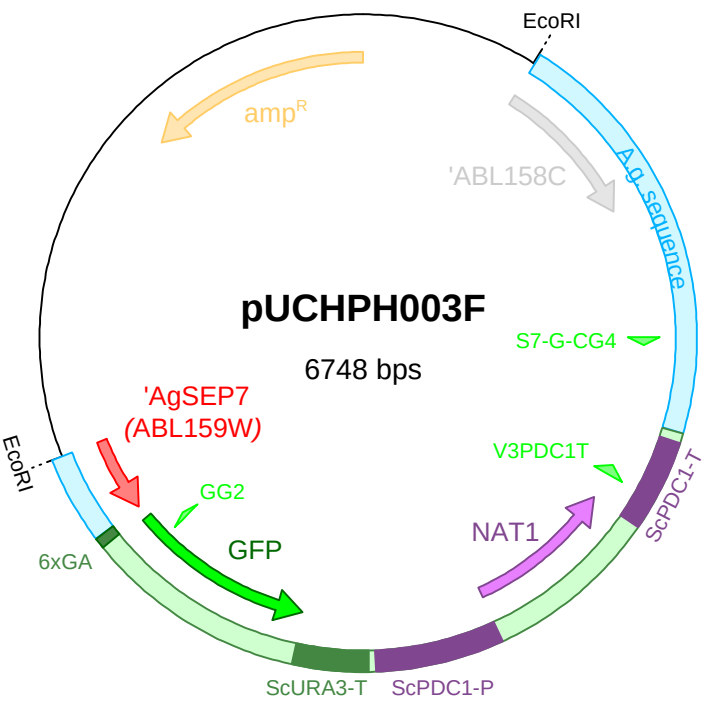
EcoRI
ampR
'ABL158C
A.g. sequence
pUCHPH003F
6748 bps
S7-G-CG4
'AgSEP7
(ABL159W)
EcoRI
V3PDC1T
GG2
NAT1
ScPDC1-T
6xGA
GFP
ScURA3-T
ScPDC1-P

Appendix 2.2.

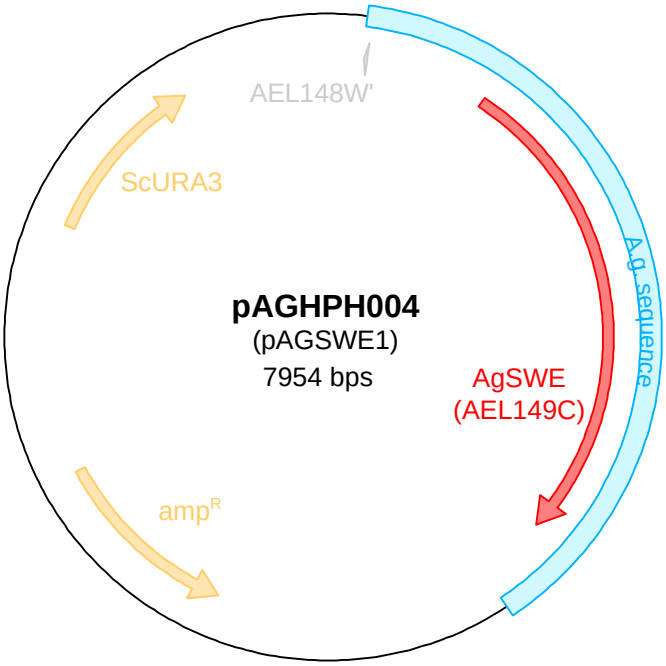

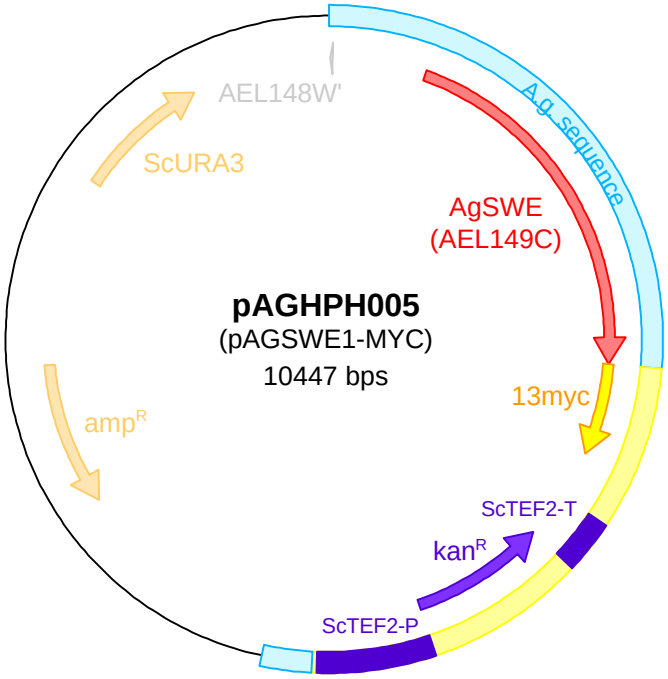

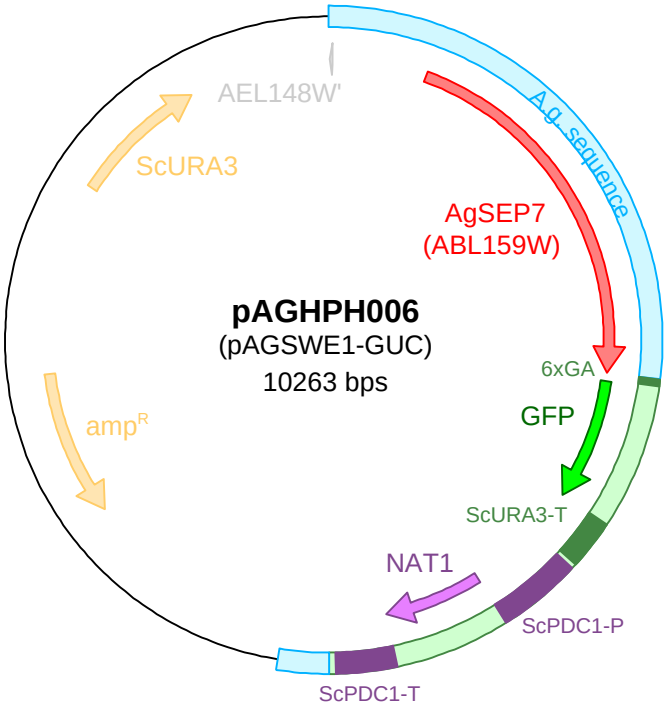

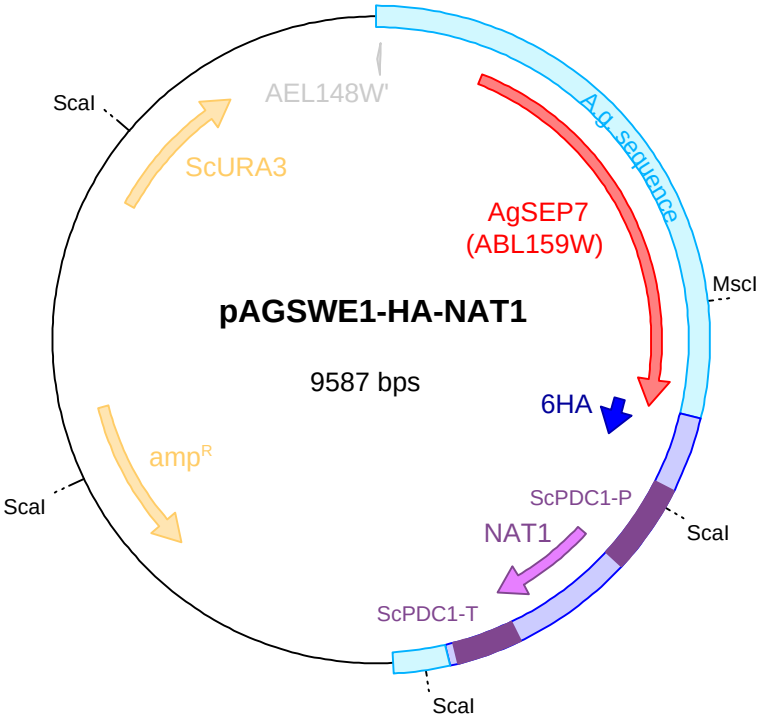

Appendix 2.3. pAGSWE1-HA-NAT1 was created by A. Gladfelter.

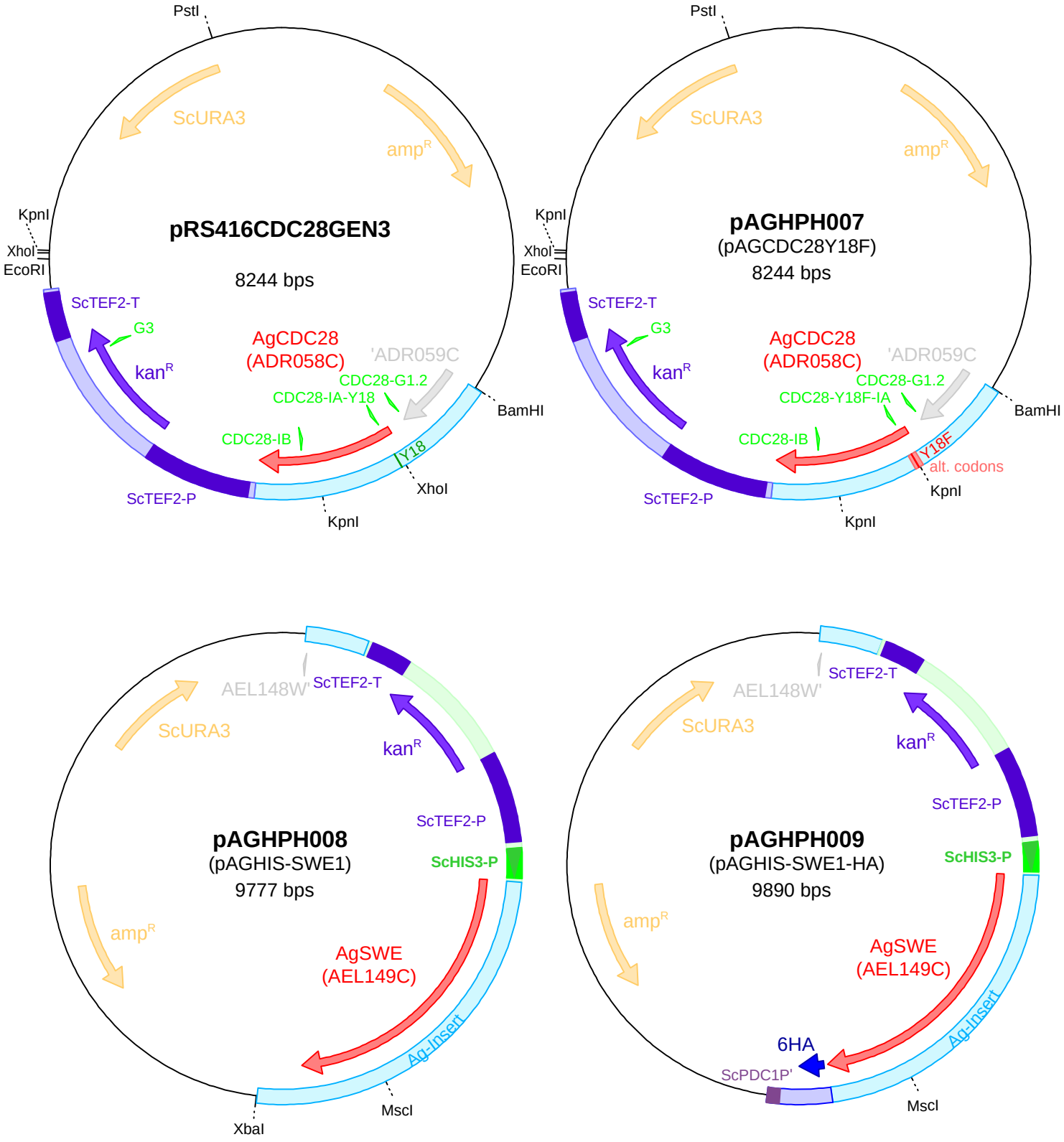

Appendix 2.4. pRS416CDC228GEN3 was constructed by A. Gladfelter and is shown here to illustrate the methods used to distinguish mutant from reference strains (see Appendix 1.7).

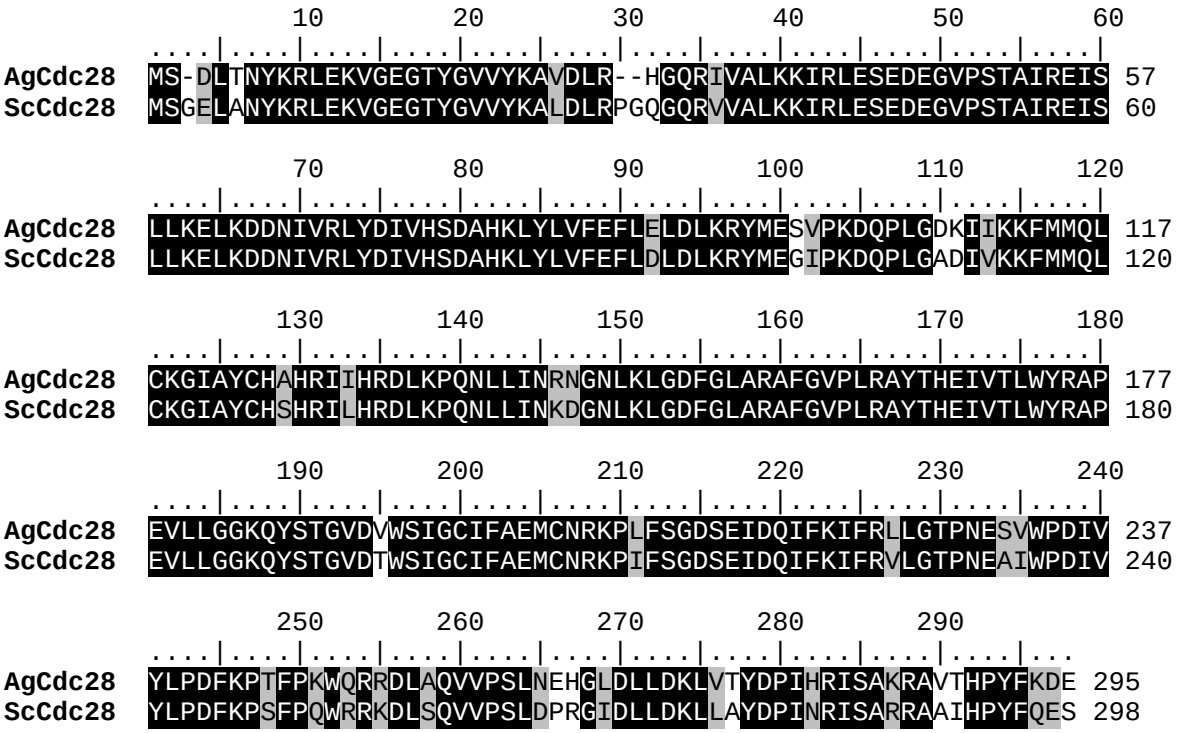

Appendix 3.1. Alignment of AgCdc28p and ScCdc28p (1/1)

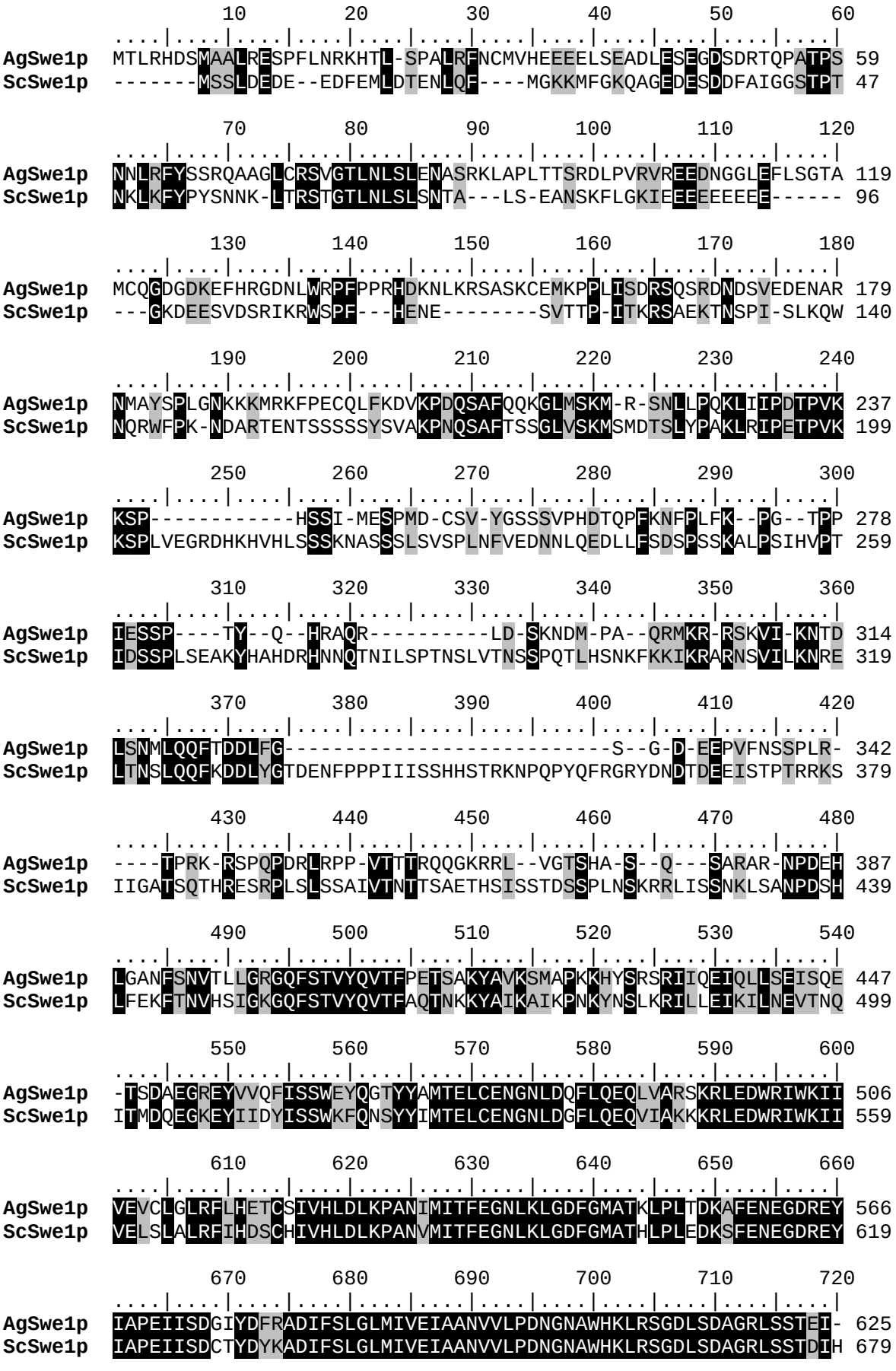

Appendix 3.2. Alignment of AgSwe1p and ScSwe1p (1/2)

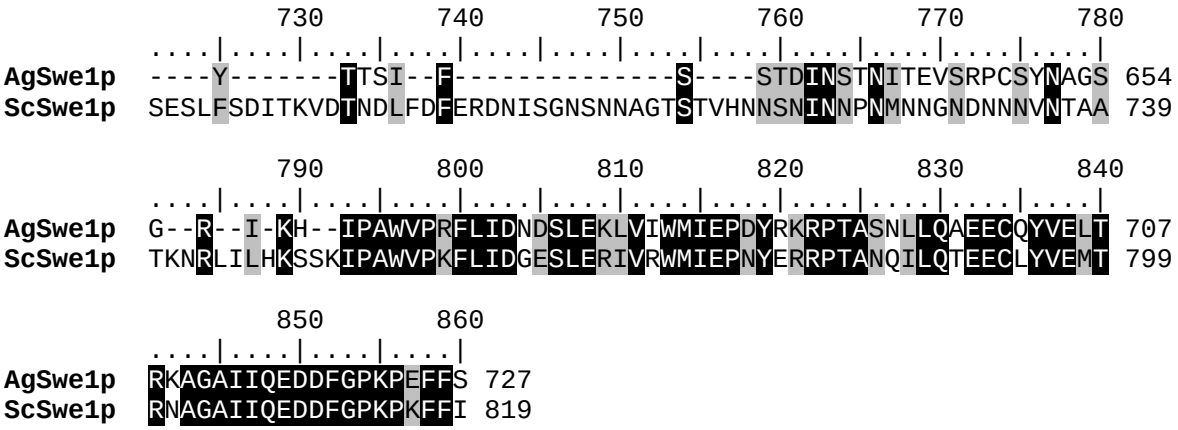
730 740 750 760 770 780
AgSwe1p ----Y-------TTSI--F----------S----STDINSTNITEVSRPCSYNAGS 654
ScSwe1p SESLFSDITKVDTNDLFDFERDNISGNSNNAGTSTVHNNSNINNPNMNNGNDNNNVNTAA 739
790 800 810 820 830 840
AgSwe1p G--R--I-KH--IPAWVPRFLIDNDSLEKLVIWMIEPDYRKRPTASNLLQAEECQYVELT 707
ScSwe1p TKNRLILHKSSKIPAWVPKFLIDGESLERIVRWMIEPNYERRPTANQILQTEECLYVEMT 799
850 860
AgSwe1p RKAGAIIQEDDFGPKPEFFS 727
ScSwe1p RNAGAIIQEDDFGPKPKFFI 819

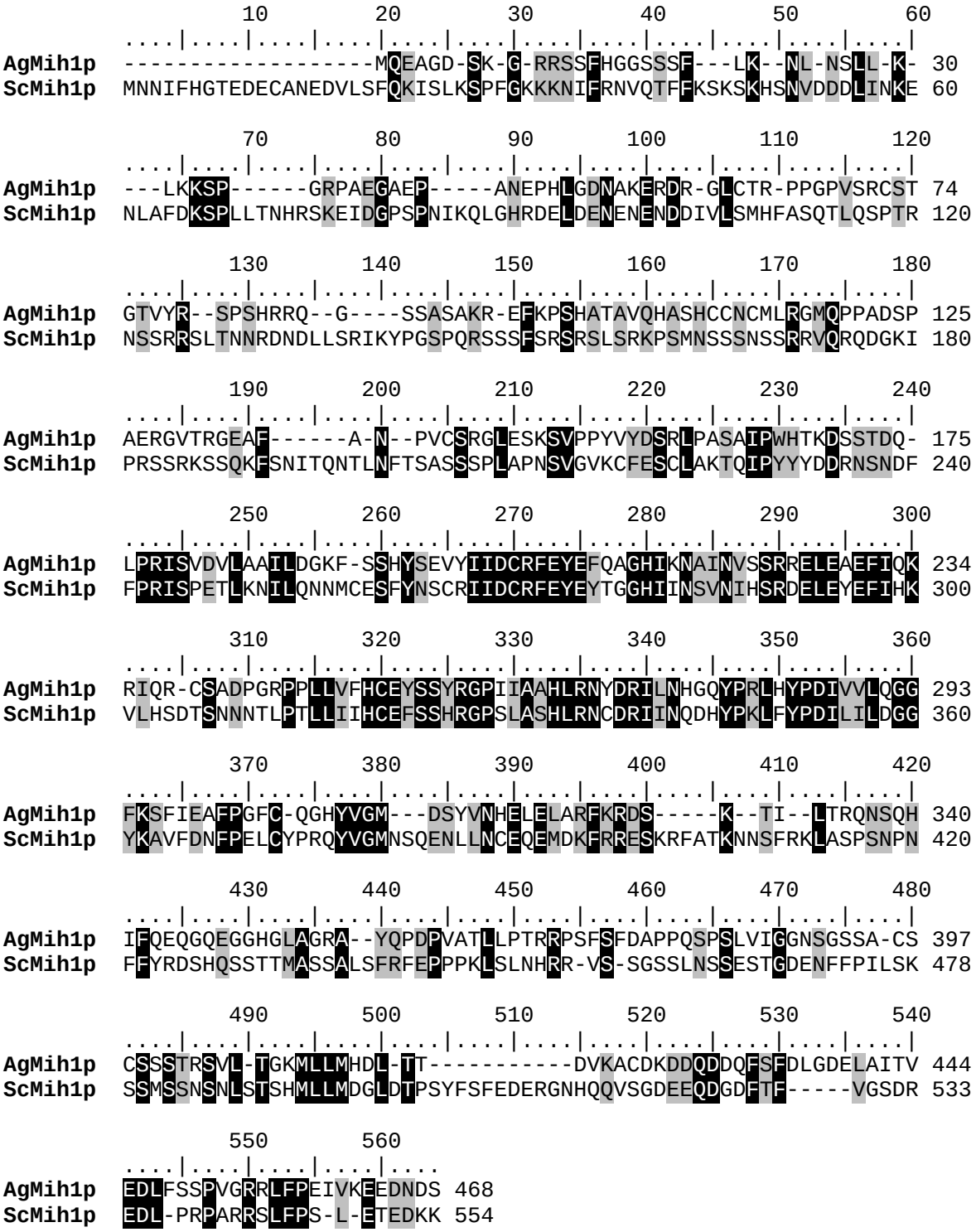

Appendix 3.3. Alignment of AgMih1p and ScMih1p (1/1)

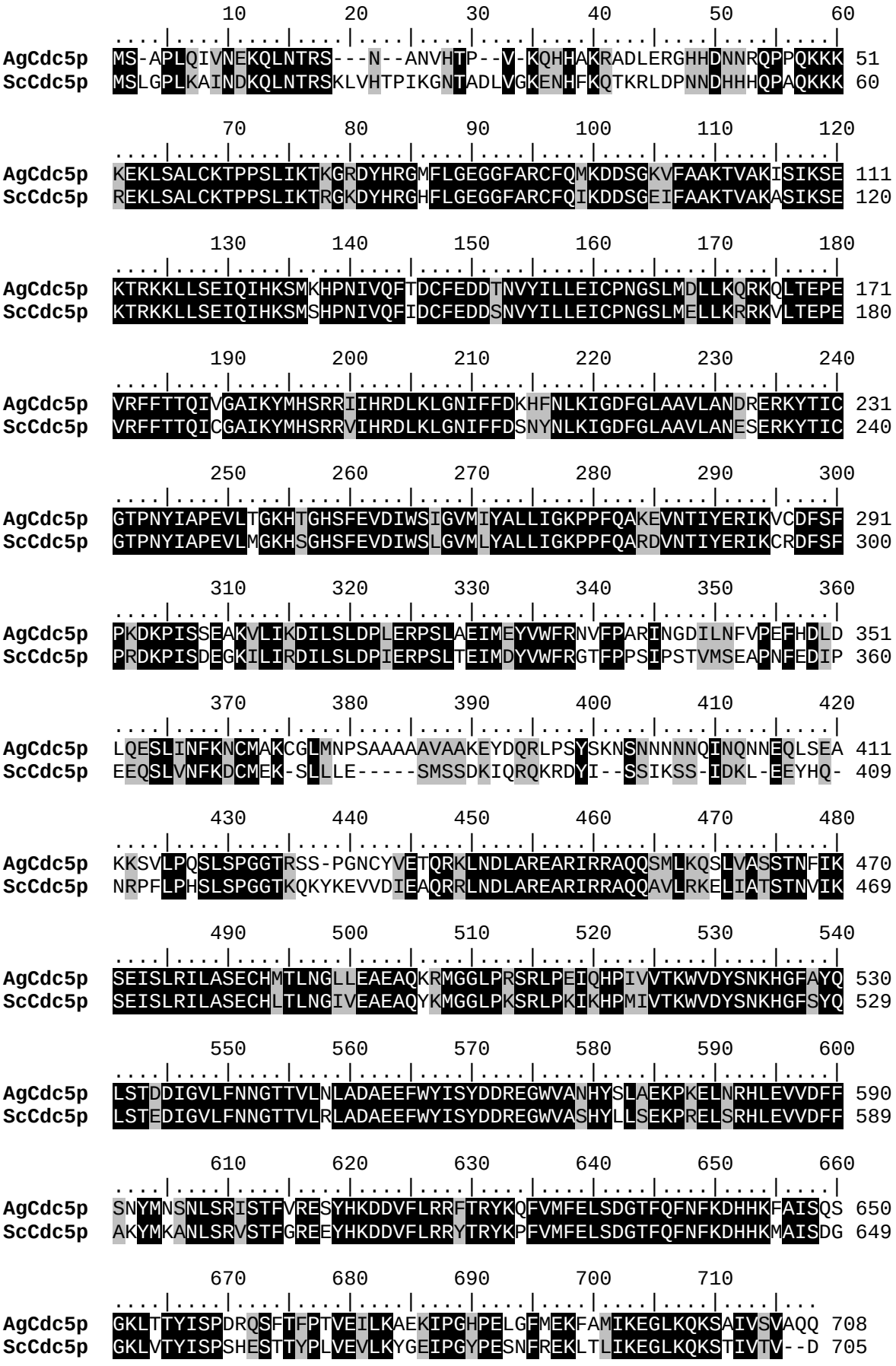

Appendix 3.4. Alignment of AgCdc5p and ScCdc5p (1/1)

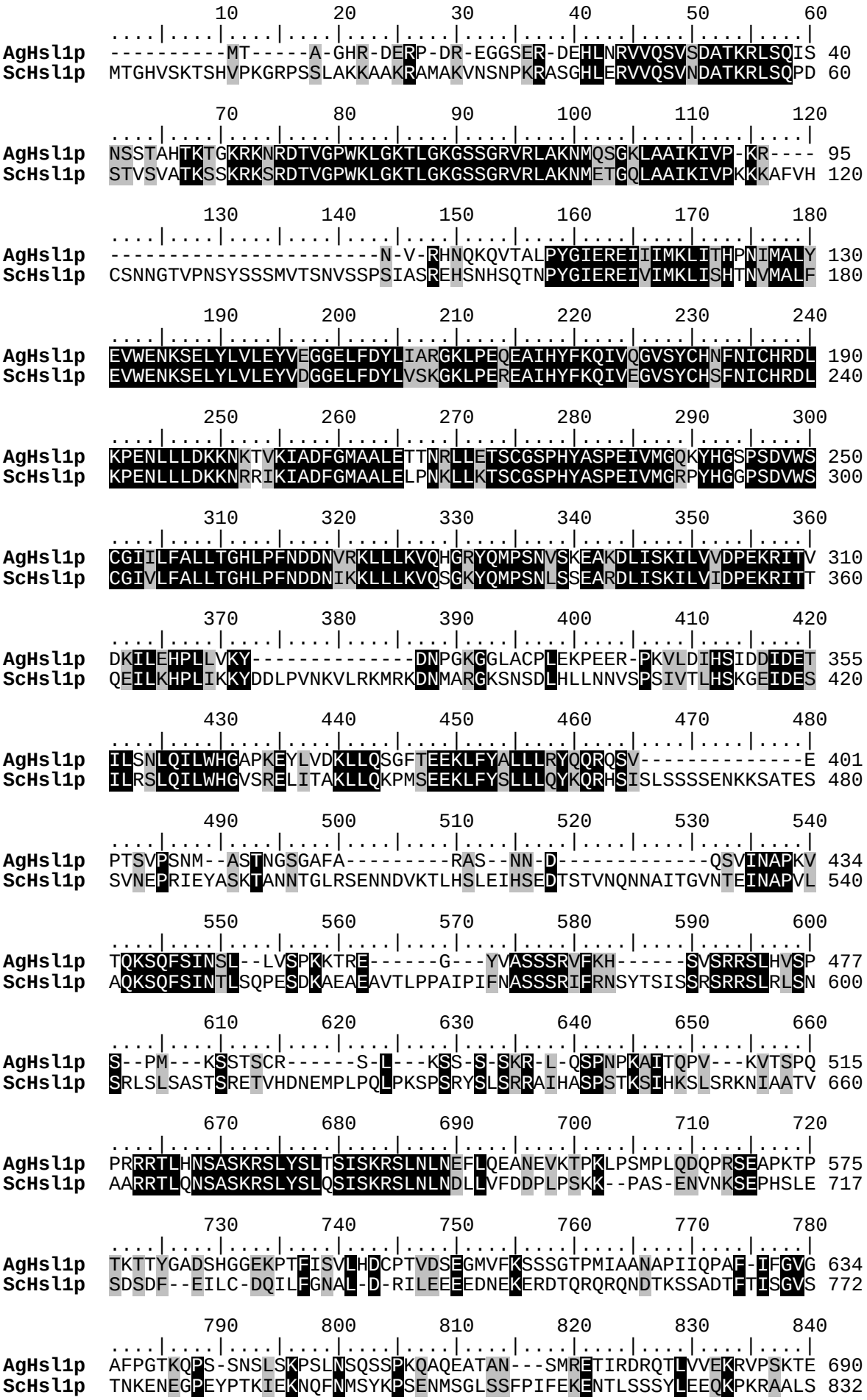

Appendix 3.5. Alignment of AgHsl1p and ScHsl1p (1/2)

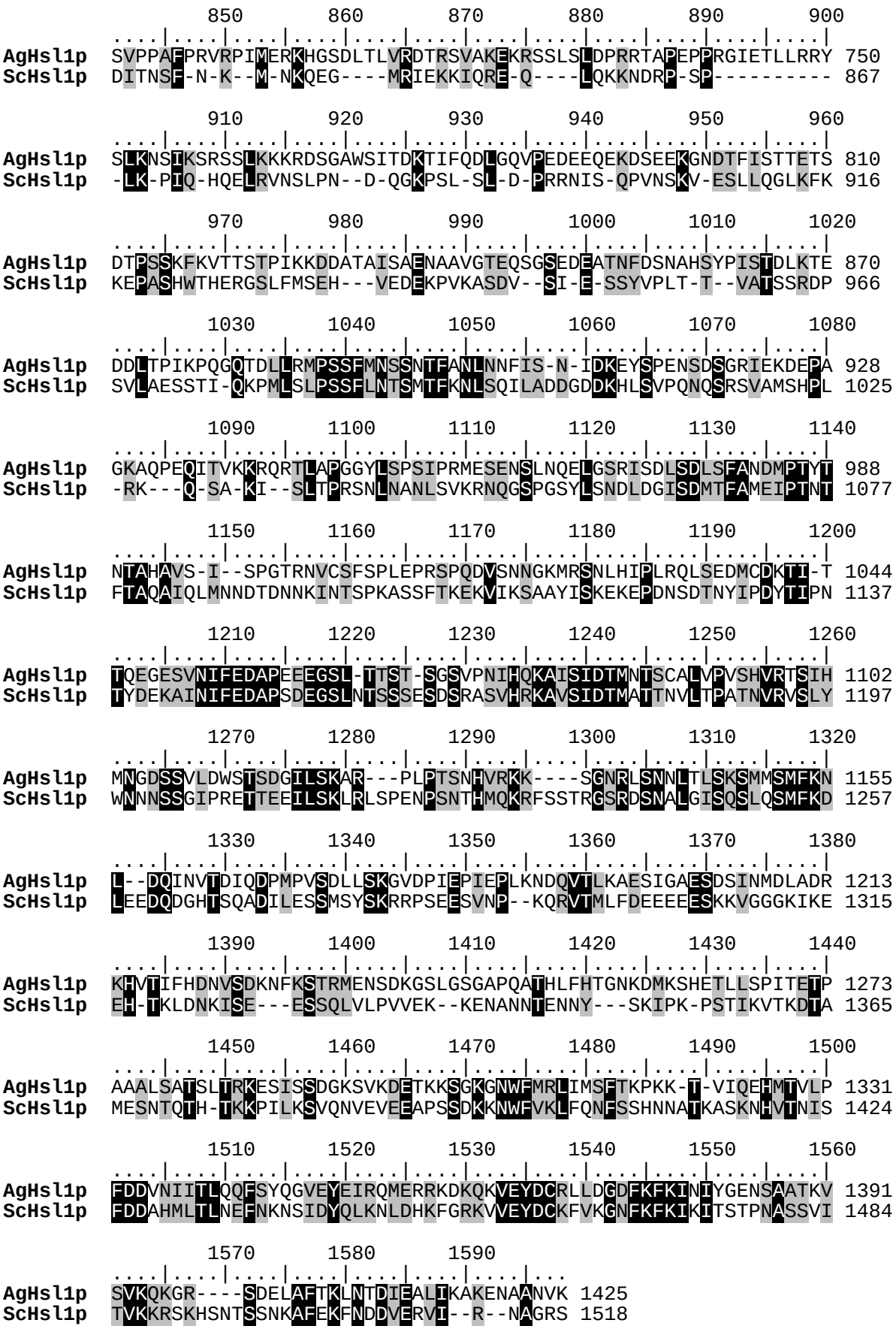

Appendix 3.5. Alignment of AgHsl1p and ScHsl1p (2/2)

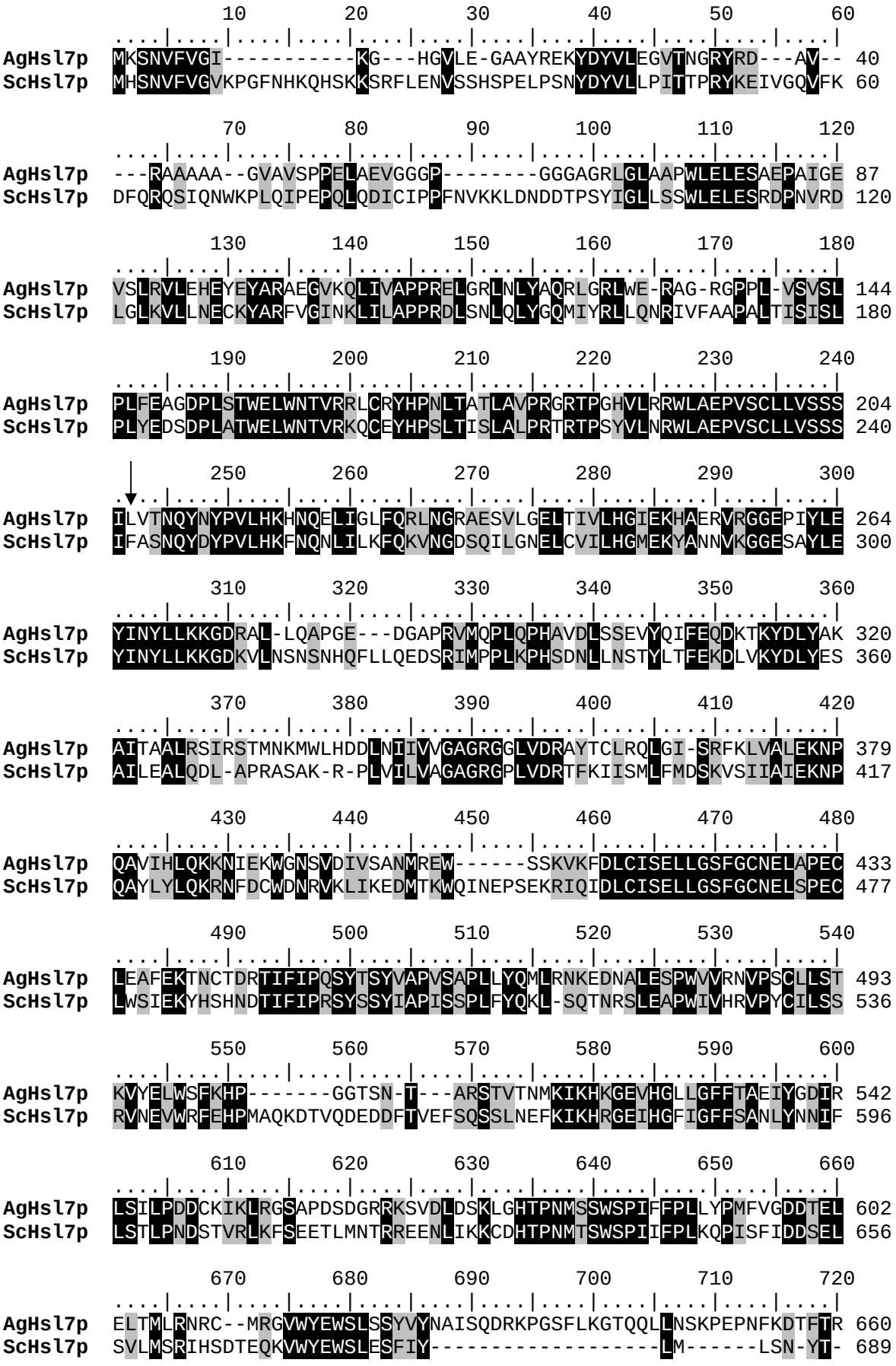

Appendix 3.6. Alignment of AgHsl7p and ScHsl7p (1/2)

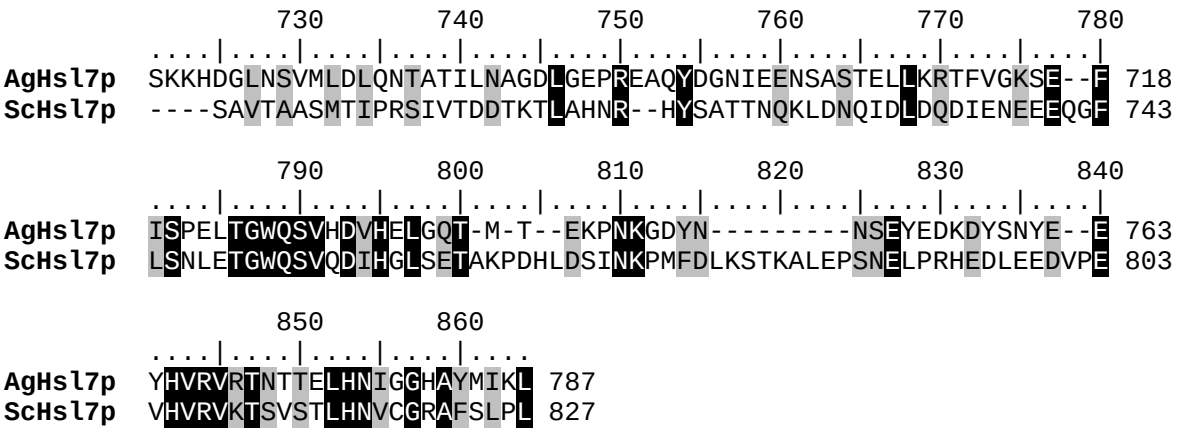
730 740 750 760 770 780
AgHsl7p SKKHDGLNSVMLDLQNTATILNAGDLGEPREAQYDGNIEENSASTELLKRTFVGKSE--F 718
ScHsl7p ----SAVTAASMTIPRSIVTDDTKTLAHNR--HYSATTNQKLDNQIDLDQDIENEEEQGF 743
790 800 810 820 830 840
AgHsl7p ISPELTGWQSVHDVHELGQT-M-T--EKPNKGDYN---------NSEYEDKDYSNYE--E 763
ScHsl7p LSNLETGWQSVQDIHGLSETAKPDHLDSINKPMFDLKSTKALEPSNELPRHEDLEEDVPE 803
850 860
AgHsl7p YHVRVRTNTTELHNIGGHAYMIKL 787
ScHsl7p VHVRVKTSVSTLHNVCGRAFSLPL 827

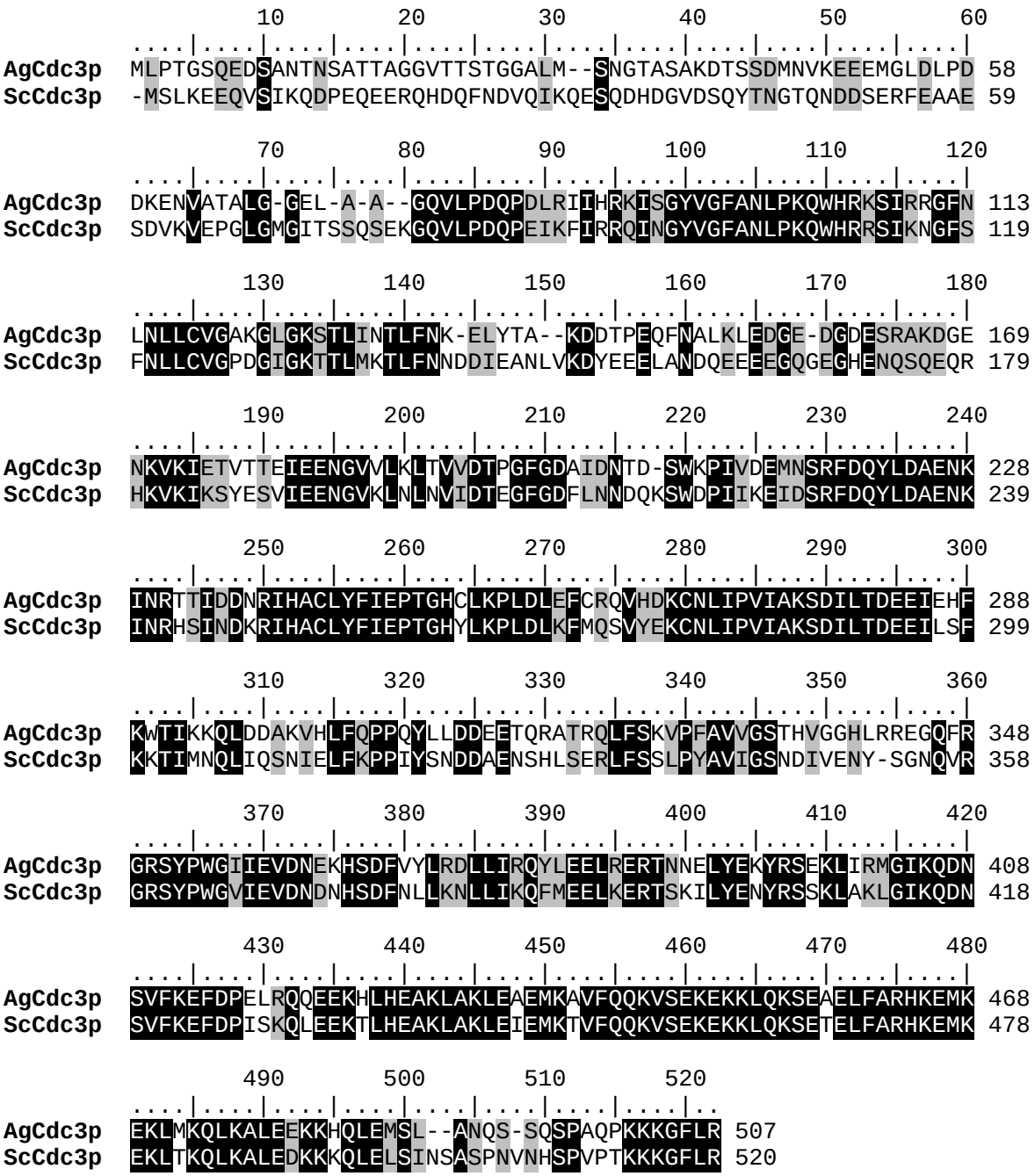

Appendix 3.7. Alignment of AgCdc3p and ScCdc3p (1/1)

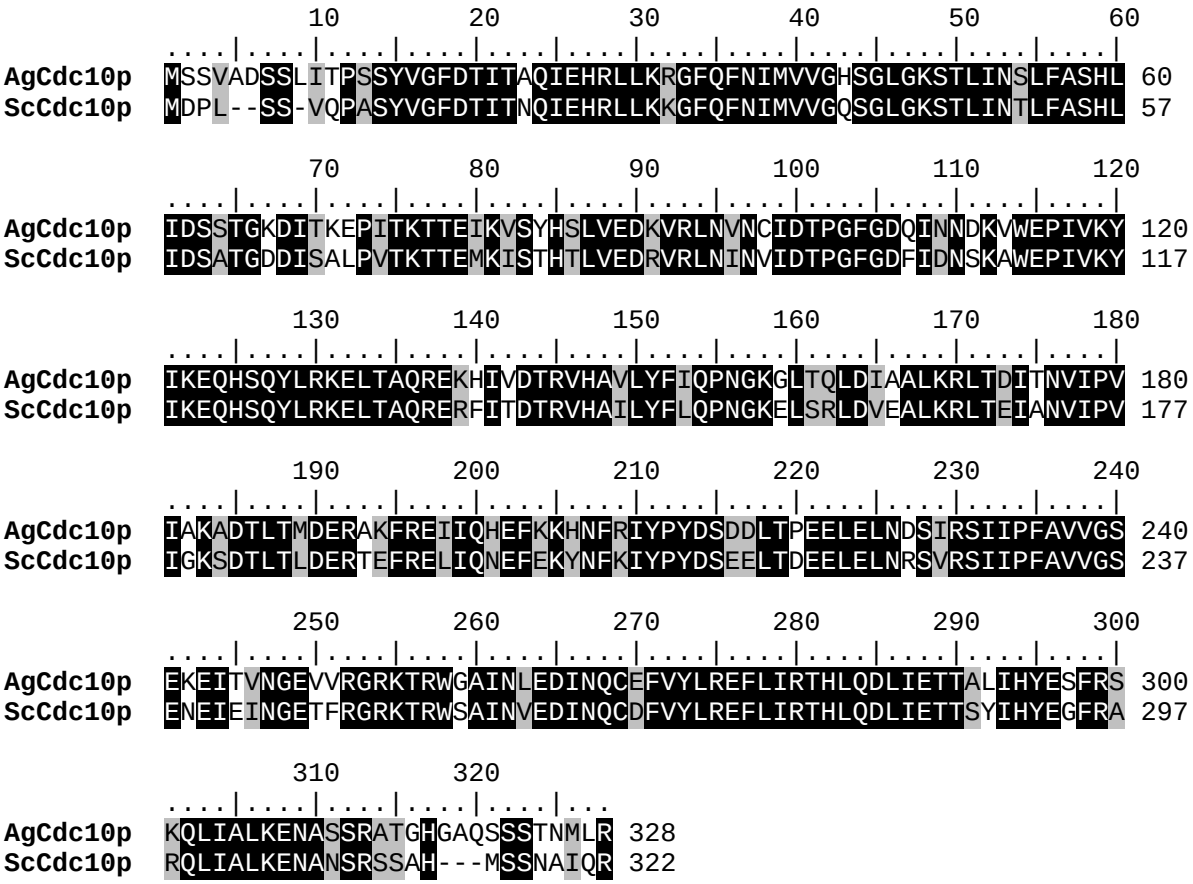

Appendix 3.8. Alignment of AgCdc10p and ScCdc10p (1/1)

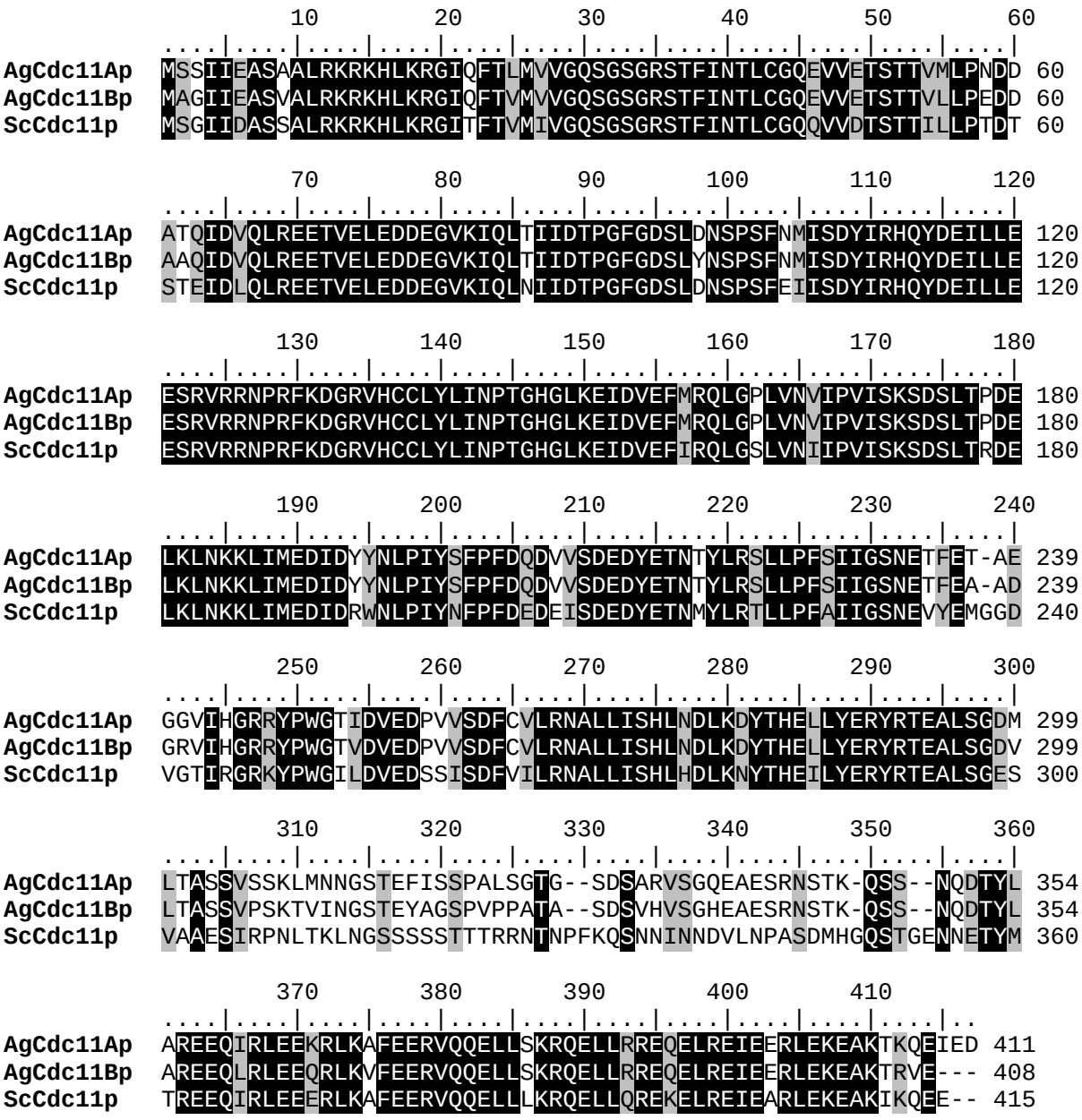

Appendix 3.9. Alignment of AgCdc11Ap, AgCdc11Bp and ScCdc11p (1/1)

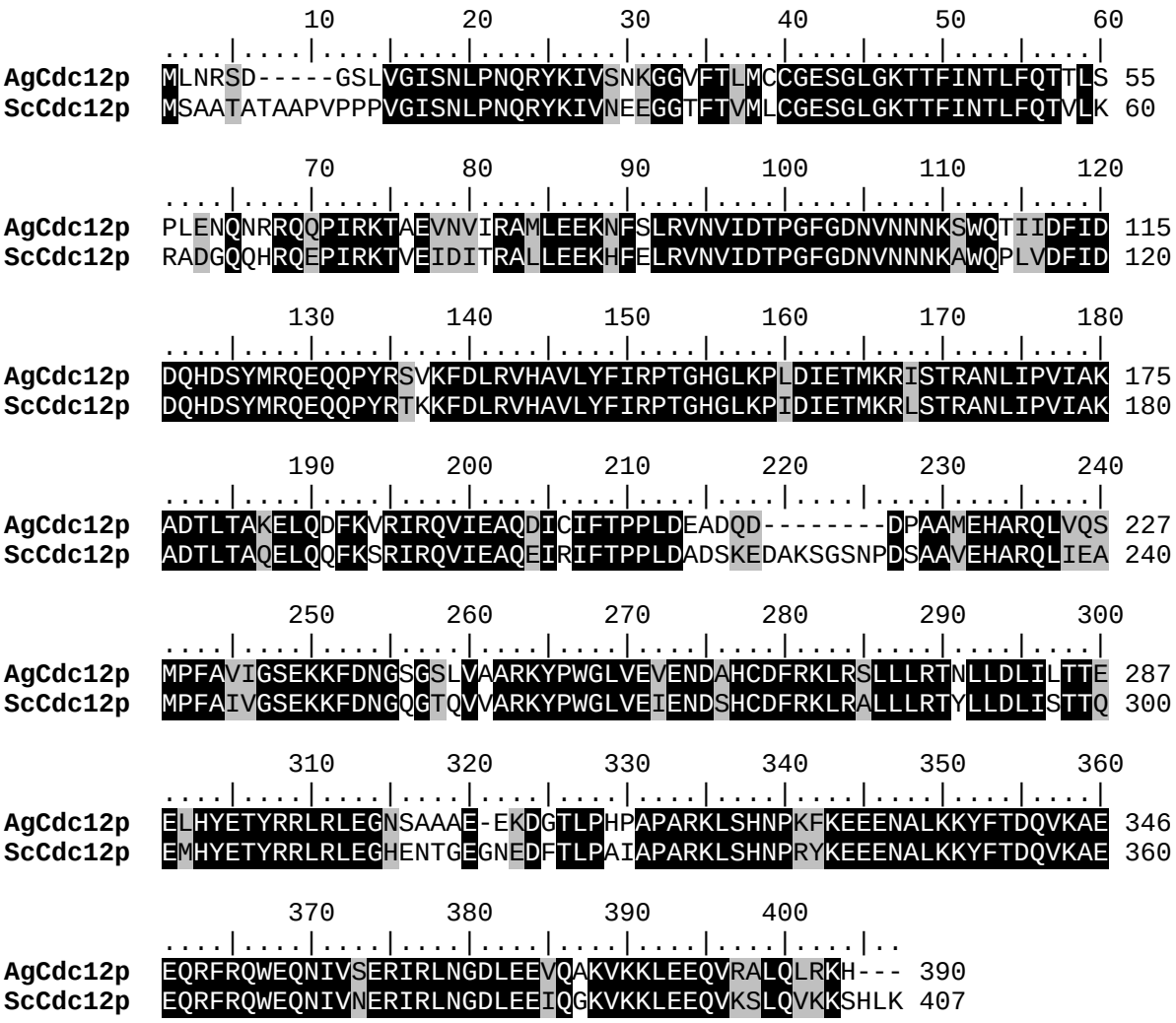

Appendix 3.10. Alignment of AgCdc12p and ScCdc12p (1/1)

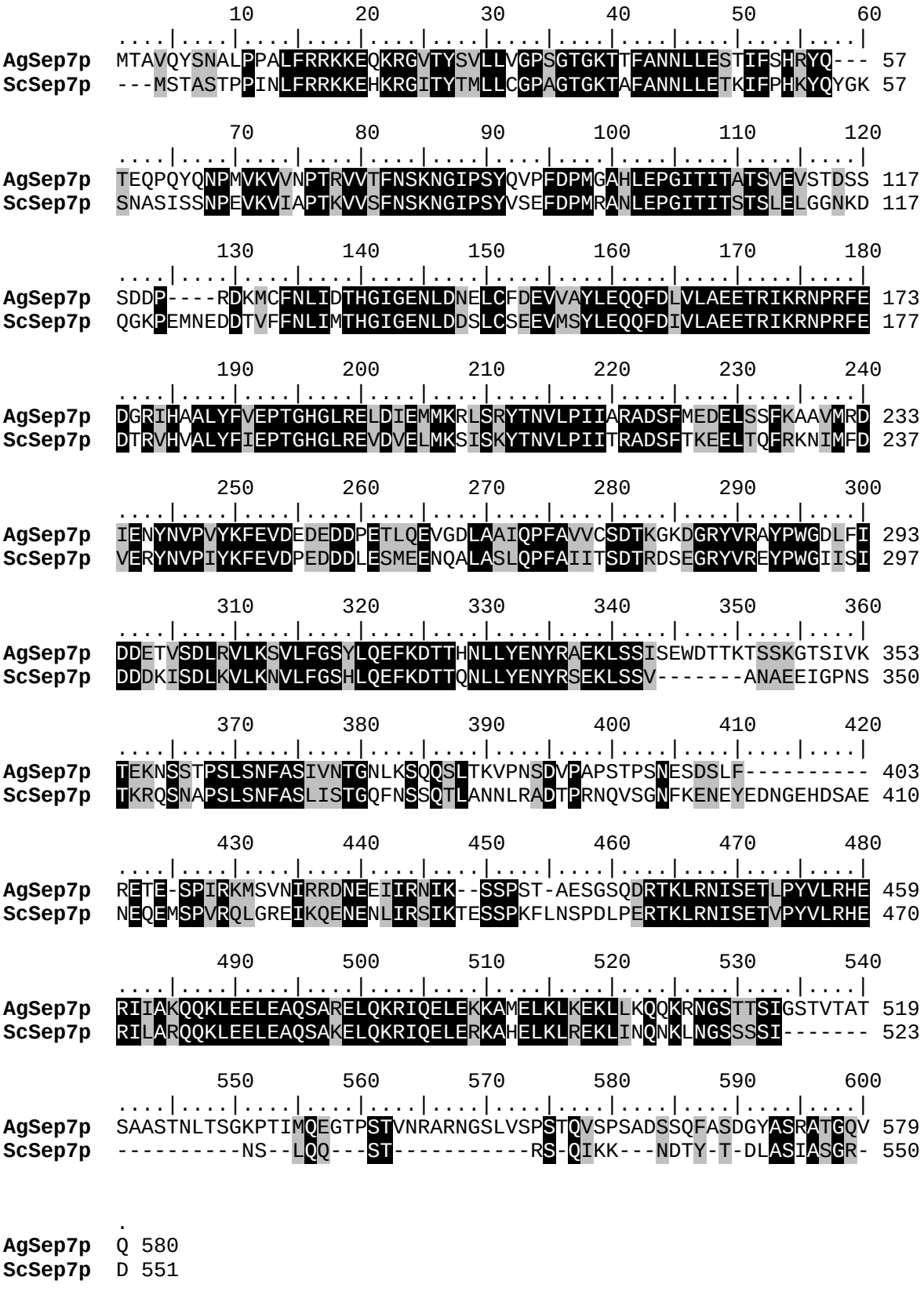

Appendix 3.11. Alignment of AgSep7p and ScSep7p (1/1)

References

Ahn, S.H., Acurio, A., and Kron, S.J. (1999). Regulation of G2/M Progression by the STE Mitogen-activated Protein Kinase Pathway in Budding Yeast Filamentous Growth. *Mol Biol Cell 10,* 3301-3316.

Alberti-Segui, C. (2001). Control of nuclear dynamics by microtubule-based motors in the fi lamentous fungus *Ashbya gossypii. PhD thesis,* Biozentrum, Universität Basel, Switzerland.

Alberti-Segui, C., Dietrich, F., Altmann-Johl, R., Hoepfner, D., and Philippsen, P. (2001). Cytoplasmic dynein is required to oppose the force that moves nuclei towards the hyphal tip in the filamentous ascomycete Ashbya gossypii.PG. *J Cell Sci 114*.

Altmann-Johl, R., and Philippsen, P. (1996). AgTHR4, a new selection marker for transformation of the filamentous fungus Ashbya gossypii, maps in a four-gene cluster that is conserved between A. gossypii and Saccharomyces cerevisiae. *Mol Gen Genet 250,* 69-80.

Amon, A. (1999). The spindle checkpoint. *Curr Opin Genet Dev 9,* 69-75.

Arvanitidis, A., and Heinisch, J.J. (1994). Studies on the function of yeast phosphofructokinase subunits by in vitro mutagenesis. *J Biol Chem 269,* 8911-8918.

Asano, S., Park, J.E., Sakchaisri, K., Yu, L.R., Song, S., Supavilai, P., Veenstra, T.D., and Lee, K.S. (2005). Concerted mechanism of Swe1/Wee1 regulation by multiple kinases in budding yeast. *Embo J 24,* 2194-2204.

Ashby, S., and Nowell, W. (1926). The fungi of stigmatomycosis. *Ann. Botany 40,* 69-84.

Atkins, G.J., Bouralexis, S., Haynes, D.R., Graves, S.E., Geary, S.M., Evdokiou, A., Zannettino, A.C., Hay, S., and Findlay, D.M. (2001). Osteoprotegerin inhibits osteoclast formation and bone resorbing activity in giant cell tumors of bone.PG - 370-7. *Bone 28*.

Ayad-Durieux, Y., Knechtle, P., Goff, S., Dietrich, F., and Philippsen, P. (2000). A PAK-like protein kinase is required for maturation of young hyphae and septation in the filamentous ascomycete Ashbya gossypii. *J Cell Sci 113 Pt 24,* 4563-4575.

Barbet, N.C., Schneider, U., Helliwell, S.B., Stansfield, I., Tuite, M.F., and Hall, M.N. (1996). TOR controls translation initiation and early G1 progression in yeast. *Mol Biol Cell 7,* 25-42.

Bardin, A.J., Visintin, R., and Amon, A. (2000). A mechanism for coupling exit from mitosis to partitioning of the nucleus. *Cell 102,* 21-31.

Barral, Y., Mermall, V., Mooseker, M.S., and Snyder, M. (2000). Compartmentalization of the cell cortex by septins is required for maintenance of cell polarity in yeast. *Mol Cell 5,* 841-851.

Barral, Y., Parra, M., Bidlingmaier, S., and Snyder, M. (1999). Nim1-related kinases coordinate cell cycle progression with the organization of the peripheral cytoskeleton in yeast. *Genes Dev. 13,* 176-187.

Bartholomew, C.R., Woo, S.H., Chung, Y.S., Jones, C., and Hardy, C.F. (2001). Cdc5 interacts with the Wee1 kinase in budding yeast. *Mol Cell Biol 21,* 4949-4959.

Batra, L.R. (1973). Nematosporaceae (Hemiascomycetidae): Taxonomy, pathogenicity, distribution, and vector relations. *USDA Technical Bulletin 1469,* 1–71.

Baudin, A., Ozier-Kalogeropoulos, O., Denouel, A., Lacroute, F., and Cullin, C. (1993). A simple and efficient method for direct gene deletion in *Saccharomyces cerevisiae*. *Nucleic Acids Res. 21,* 3329-3330.

Belenguer, P., Pelloquin, L., Oustrin, M.L., and Ducommun, B. (1997). Role of the fission yeast nim 1 protein kinase in the cell cycle response to nutritional signals. *Biochem Biophys Res Commun 232,* 204-208.

Bi, E., Maddox, P., Lew, D.J., Salmon, E.D., McMillan, J.N., Yeh, E., and Pringle, J.R. (1998). Involvement of an actomyosin contractile ring in *Saccharomyces cerevisiae* cytokinesis. *J. Cell Biol. 142,* 1301-1312.

Bloecher, A., Venturi, G.M., and Tatchell, K. (2000). Anaphase spindle position is monitored by the BUB2 checkpoint. *Nat Cell Biol 2,* 556-558.

Boudier, K. (2005). The role of AgRax1p, AgRax2p, AgBud7p and AgBud10p in mycelial development of the filamentous fungus *Ashbya gossypii*. *PhD thesis,* Biozentrum, Universität Basel, Switzerland.

Brachat, S. (2003). Exploring the potential of complete sequence information and synteny: Comparative genome annotation and analysis of *Ashbya gossypii* and *Saccharomyces cerevisiae*. *PhD thesis,* Biozentrum, Universität Basel, Switzerland.

Byers, B., and Goetsch, L. (1975). Behaviour of spindles and spindle plaques in the cell cycle and conjugation of Saccharomyces cerevisiae. *J. Bacteriol. 124,* 511-523.

Byers, B., and Goetsch, L. (1976). A highly ordered ring of membrane-associated filaments in budding yeast. *J. Cell Biol. 69,* 717-721.

Cabib, E., Drgonova, J., and Drgon, T. (1998). Role of small G proteins in yeast cell polarization and wall biosynthesis. *Annu Rev Biochem 67,* 307-333.

Carminati, J., and Stearns, T. (1997). Microtubules orient the mitotic spindle in yeast through dynein-dependent interactions with the cell cortex. *J. Cell Biol. 138,* 629-641.

Carroll, C.W., Altman, R., Schieltz, D., Yates III, J.R., and Kellogg, D. (1998). The septins are required for the mitosis-specific activation of the Gin4 kinase. *J. Cell Biol. 143,* 709-717.

Casamayor, A., and Snyder, M. (2003). Molecular dissection of a yeast septin: distinct domains are required for septin interaction, localization, and function. *Mol Cell Biol 23,* 2762-2777.

Caviston, J.P., Longtine, M., Pringle, J.R., and Bi, E. (2003). The role of Cdc42p GTPase-activating proteins in assembly of the septin ring in yeast. *Mol Biol Cell 14,* 4051-4066.

Chant, J., Mischke, M., Mitchell, E., Herskowitz, I., and Pringle, J.R. (1995). Role of Bud3p in producing the axial budding pattern of yeast. *J. Cell Biol. 129,* 767-778.

Cid, V.J., Adamikova, L., Sanchez, M., Molina, M., and Nombela, C. (2001a). Cell cycle control of septin ring dynamics in the budding yeast. *Microbiology 147,* 1437-1450.

Cid, V.J., Shulewitz, M.J., McDonald, K.L., and Thorner, J. (2001b). Dynamic localization of the Swe1 regulator Hsl7 during the Saccharomyces cerevisiae cell cycle. *Mol Biol Cell 12,* 1645-1669.

Ciliberto, A., Novak, B., and Tyson, J.J. (2003). Mathematical model of the morphogenesis checkpoint in budding yeast. *J Cell Biol 163,* 1243-1254.

Clotet, J., Escote, X., Adrover, M.A., Yaakov, G., Gari, E., Aldea, M., de Nadal, E., and Posas, F. (2006). Phosphorylation of Hsl1 by Hog1 leads to a G(2) arrest essential for cell survival at high osmolarity. *Embo J*.

Clutterbuck, A.J. (1970). Synchronous nuclear division and septation in Aspergillus nidulans. *J Gen Microbiol 60,* 133-135.

Cooper, J.A., and Kiehart, D.P. (1996). Septins may form a ubiquitous family of cytoskeletal filaments. *J Cell Biol 134,* 1345-1348.

DeMarini, D.J., Adams, A.E., Fares, H., De Virgilio, C., Valle, G., Chuang, J.S., and Pringle, J.R. (1997). A septin-based hierarchy of proteins required for localized deposition of chitin in the Saccharomyces cerevisiae cell wall. *J Cell Biol 139,* 75-93.

Dietrich, F.S., Voegeli, S., Brachat, S., Lerch, A., Gates, K., Steiner, S., Mohr, C., Pohlmann, R., Luedi, P., Choi, S., Wing, R.A., Flavier, A., Gaffney, T.D., and Philippsen, P. (2004). The Ashbya gossypii genome as a tool for mapping the ancient Saccharomyces cerevisiae genome. *Science 304,* 304-307.

Dobbelaere, J., and Barral, Y. (2004). Spatial coordination of cytokinetic events by compartmentalization of the cell cortex. *Science 305,* 393-396.

Dobbelaere, J., Gentry, M.S., Hallberg, R.L., and Barral, Y. (2003). Phosphorylation-dependent regulation of septin dynamics during the cell cycle. *Dev Cell 4,* 345-357.

Donaldson, A.D., and Kilmartin, J.V. (1996). Spc42p: a phosphorylated component of the S. cerevisiae spindle pole body (SPD) with an essential function during SPB duplication. *J Cell Biol 132,* 887-901.

Douglas, L.M., Alvarez, F.J., McCreary, C., and Konopka, J.B. (2005). Septin function in yeast model systems and pathogenic fungi. *Eukaryot Cell 4,* 1503-1512.

Dynesen, J., and Nielsen, J. (2003). Branching is coordinated with mitosis in growing hyphae of Aspergillus nidulans. *Fungal Genet Biol 40,* 15-24.

Edgington, N.P., Blacketer, M.J., Bierwagen, T.A., and Myers, A.M. (1999). Control of *Saccharomyces cerevisiae* filamentous growth by cyclin- dependent kinase Cdc28. *Mol Cell Biol 19,* 1369-1380.

Epp, J.A., and Chant, J. (1997). An IQGAP-related protein controls actin-ring formation and cytokinesis in yeast. *Curr. Biol. 7,* 921-929.

Fares, H., Goetsch, L., and Pringle, J.R. (1996). Identification of a developmentally regulated septin and involvement of the septins in spore formation in Saccharomyces cerevisiae. *J Cell Biol 132,* 399-411.

Faty, M., Fink, M., and Barral, Y. (2002). Septins: a ring to part mother and daughter. *Curr Genet 41,* 123-131.

Field, C.M., and Kellogg, D. (1999). Septins: cytoskeletal polymers or signalling GTPases? [In Process Citation]. *Trends Cell Biol 9,* 387-394.

Fitch, I., Dahmann, C., Surana, U., Amon, A., Nasmyth, K., Goetsch, L., Byers, B., and Futcher, B. (1992). Characterization of four B-type cyclin genes of the budding yeast Saccharomyces cerevisiae. *Mol Biol Cell 3,* 805-818.

Flescher, E.G., Madden, K., and Snyder, M. (1993). Components required for cytokinesis are important for bud site selection in yeast. *J Cell Biol 122,* 373-386.

Ford, S.K., and Pringle, J.R. (1991). Cellular morphogenesis in the *Saccharomyces cerevisiae* cell cycle: localization of the *CDC11* gene product and the timing of events at the budding site. *Dev. Genet. 12,* 281-292.

Frazier, J.A., Wong, M.L., Longtine, M.S., Pringle, J.R., Mann, M., Mitchison, T.J., and Field, C. (1998). Polymerization of purified yeast septins: evidence that organized filament arrays may not be required for septin function. *J. Cell Biol. 143,* 737-749.

Freitag, M., Hickey, P.C., Raju, N.B., Selker, E.U., and Read, N.D. (2004). GFP as a tool to analyze the organization, dynamics and function of nuclei and microtubules in Neurospora crassa. *Fungal Genet Biol 41,* 897-910.

Gallego, C., Gari, E., Colomina, N., Herrero, E., and Aldea, M. (1997). The Cln3 cyclin is down-regulated by translational repression and degradation during the G1 arrest caused by nitrogen deprivation in budding yeast. *Embo J 16,* 7196-7206.

Gladfelter, A.S. (2006). Control of filamentous fungal cell shape by septins and formins. *Nat Rev Microbiol 4,* 223-229.

Gladfelter, A.S., Hungerbuehler, A.K., and Philippsen, P. (2006). Asynchronous nuclear division cycles in multinucleated cells. *J Cell Biol 172,* 347-362.

Gladfelter, A.S., Kozubowski, L., Zyla, T.R., and Lew, D.J. (2005). Interplay between septin organization, cell cycle and cell shape in yeast. *J Cell Sci 118,* 1617-1628.

Gladfelter, A.S., Moskow, J.J., Zyla, T.R., and Lew, D.J. (2001a). Isolation and characterization of effector-loop mutants of CDC42 in yeast. *Mol Biol Cell 12,* 1239-1255.

Gladfelter, A.S., Pringle, J.R., and Lew, D.J. (2001b). The septin cortex at the yeast mother-bud neck. *Curr Opin Microbiol 4,* 681-689.

Haarer, B.K., and Pringle, J.R. (1987). Immunofluorescence localization of the *Saccharomyces cerevisiae CDC12* gene product to the vicinity of the 10-nm filaments in the mother-bud neck. *Mol. Cell. Biol. 7,* 3678-3687.

Hanahan, D. (1983). Studies on transformation of Escherichia coli with plasmids. *J Mol Biol 166,* 557-580.

Harris, T.E., and Lawrence, J.C., Jr. (2003). TOR signaling. *Sci STKE 2003,* re15.

Harrison, J.C., Bardes, E.S., Ohya, Y., and Lew, D.J. (2001). A role for the Pkc1p/Mpk1p kinase cascade in the morphogenesis checkpoint. *Nat Cell Biol 3,* 417-420.

Hartwell, L.H. (1971a). Genetic Control of the Cell Division Cycle in Yeast. *Experimental Cell Research 69,* 265-276.

Hartwell, L.H. (1971b). Genetic control of the cell division cycle in yeast. IV. Genes controlling bud emergence and cytokinesis. *Exp. Cell Res. 69,* 265-276.

Hartwell, L.H., Culotti, J., Pringle, J.R., and Reid, B.J. (1974). Genetic control of the cell division cycle in yeast. *Science 183,* 46-51.

Hartwell, L.H., Culotti, J., and Reid, B. (1970). Genetic control of the cell-division cycle in yeast. I. Detection of mutants. *Proc Natl Acad Sci U S A 66,* 352-359.

Hartwell, L.H., and Weinert, T.A. (1989). Checkpoints: Controls that ensure the order of cell cycle events. *Science 246,* 629-634.

Harvey, S.L., and Kellogg, D.R. (2003). Conservation of mechanisms controlling entry into mitosis: budding yeast wee1 delays entry into mitosis and is required for cell size control. *Curr Biol 13,* 264-275.

Helfer, H. (2001). Effects of myosin gene deletions on growth and development of the filamentous fungus *Ashbya gossypii*. *Diploma thesis,* Biozentrum, Universität Basel, Switzerland.

Helliwell, S.B., Schmidt, A., Ohya, Y., and Hall, M.N. (1998). The Rho1 effector Pkc1, but not Bni1, mediates signalling from Tor2 to the actin cytoskeleton. *Curr Biol 8,* 1211-1214.

Hoepfner, D., Brachat, A., and Philippsen, P. (2000). Time-lapse video microscopy analysis reveals astral microtubule detachment in the yeast spindle pole mutant cnm67. *Mol Biol Cell 11,* 1197-1211.

Hoyt, M.A., Totis, L., and Roberts, B.T. (1991). S. cerevisiae genes required for cell cycle arrest in response to loss of microtubule function. *Cell 66,* 507-517.

Izumi, T., Walker, D.H., and Maller, J.L. (1992). Periodic changes in phosphorylation of the Xenopus cdc25 phosphatase regulate its activity. *Mol Biol Cell 3,* 927-939.

Jacinto, E., and Hall, M.N. (2003). Tor signalling in bugs, brain and brawn. *Nat Rev Mol Cell Biol 4,* 117-126.

Jacobs, C.W., Adams, A.E.M., Szaniszlo, P.J., and Pringle, J.R. (1988). Functions of microtubules in the *Saccharomyces cerevisiae* cell cycle. *J. Cell Biol. 107,* 1409-1426.

Jimenez, J., Cid, V.J., Cenamor, R., Yuste, M., Molero, G., Nombela, C., and Sanchez, M. (1998). Morphogenesis beyond cytokinetic arrest in Saccharomyces cerevisiae. *J Cell Biol 143,* 1617-1634.

Kaneko, A., Umeyama, T., Hanaoka, N., Monk, B.C., Uehara, Y., and Niimi, M. (2004). Tandem affinity purification of the Candida albicans septin protein complex. *Yeast 21,* 1025-1033.

Kartmann, B., and Roth, D. (2001). Novel roles for mammalian septins: from vesicle trafficking to oncogenesis. *J Cell Sci 114,* 839-844.

Kilmartin, J.V., and Adams, A.E.M. (1984). Structural rearrangements of tubulin and actin during the cell cycle of the yeast *Saccharomyces*. *J. Cell Biol. 98,* 922-933.

Kim, H.B., Haarer, B.K., and Pringle, J.R. (1991). Cellular morphogenesis in the *Saccharomyces cerevisiae* cell cycle: localization of the *CDC3* gene product and the timing of events at the budding site. *J. Cell Biol. 112,* 535-544.

Kinoshita, M. (2003). The septins. *Genome Biol 4,* 236.

Kinoshita, M., Field, C.M., Coughlin, M.L., Straight, A.F., and Mitchison, T.J. (2002). Self- and actin-templated assembly of Mammalian septins. *Dev Cell 3,* 791-802.

Knechtle, P. (2002). AgSPA2 and AgBOI control landmarks of filamentous growth in the filamentous *Ascomycete Ashbya gossypii*. *PhD thesis,* Biozentrum, Universität Basel, Switzerland.

Knechtle, P., Dietrich, F., and Philippsen, P. (2003). Maximal polar growth potential depends on the polarisome component AgSpa2 in the filamentous fungus Ashbya gossypii. *Mol Biol Cell 14,* 4140-4154.

Köhli, M. (2003). Functional analysis of the Rho GTPases Cdc42, Rho1a, Rho1b and Rho3 in the filamentous fungus *Ashbya gossypii* by directed mutagenesis. *Diploma thesis,* Biozentrum, Universität Basel, Switzerland.

Kozubowski, L., Panek, H., Rosenthal, A., Bloecher, A., DeMarini, D.J., and Tatchell, K. (2003). A Bni4-Glc7 phosphatase complex that recruits chitin synthase to the site of bud emergence. *Mol Biol Cell 14,* 26-39.

Kusch, J., Meyer, A., Snyder, M.P., and Barral, Y. (2002). Microtubule capture by the cleavage apparatus is required for proper spindle positioning in yeast. *Genes Dev 16,* 1627-1639.

La Valle, R., and Wittenberg, C. (2001). A role for the Swe1 checkpoint kinase during filamentous growth of Saccharomyces cerevisiae. *Genetics 158,* 549-562.

Laissue, P.P. (2004). Morphogenesis of a filamentous fungus: Dynamics of the actin cytoskeleton and control of hyphal integrity in *Ashbya gossypii*. *PhD thesis,* Biozentrum, Universität Basel, Switzerland.

Lee, K.S., Asano, S., Park, J.E., Sakchaisri, K., and Erikson, R.L. (2005). Monitoring the cell cycle by multi-kinase-dependent regulation of Swe1/Wee1 in budding yeast. *Cell Cycle 4,* 1346-1349.

Lew, D.J., and Reed, S.I. (1995). A cell cycle checkpoint monitors cell morphogenesis in budding yeast. *J. Cell Biol. 129,* 739-749.

Li, R., and Murray, A.W. (1991). Feedback control of mitosis in budding yeast. *Cell 66,* 519-531.

Lippincott, J., and Li, R. (1998a). Dual function of Cyk2, a cdc15/PSTPIP family protein, in regulating actomyosin ring dynamics and septin distribution. *J Cell Biol 143,* 1947-1960.

Lippincott, J., and Li, R. (1998b). Sequential assembly of myosin II, an IQGAP-like protein, and filamentous actin to a ring structure involved in budding yeast cytokinesis. *J. Cell Biol. 140,* 355-366.

Lippincott, J., Shannon, K.B., Shou, W., Deshaies, R.J., and Li, R. (2001). The Tem1 small GTPase controls actomyosin and septin dynamics during cytokinesis. *J Cell Sci 114,* 1379-1386.

Loewith, R., Jacinto, E., Wullschleger, S., Lorberg, A., Crespo, J.L., Bonenfant, D., Oppliger, W., Jenoe, P., and Hall, M.N. (2002). Two TOR complexes, only one of which is rapamycin sensitive, have distinct roles in cell growth control. *Mol Cell 10,* 457-468.

Longtine, M.S., DeMarini, D.J., Valencik, M.L., Al-Awar, O.S., Fares, H., De Virgilio, C., and Pringle, J.R. (1996). The septins: roles in cytokinesis and other processes. *Curr. Opin. Cell Biol. 8,* 106-119.

Longtine, M.S., Fares, H., and Pringle, J.R. (1998). Role of the yeast Gin4p protein kinase in septin assembly and the relationship between septin assembly and septin function. *J. Cell Biol. 143,* 719-736.

Longtine, M.S., Theesfeld, C.L., McMillan, J.N., Weaver, E., Pringle, J.R., and Lew, D.J. (2000). Septin-dependent assembly of a cell-cycle-regulatory module in *Saccharomyces cerevisiae*. *Mol. Cell. Biol.,* in press.

Martin, D.E., and Hall, M.N. (2005). The expanding TOR signaling network. *Curr Opin Cell Biol 17,* 158-166.

Martin, S.W., Douglas, L.M., and Konopka, J.B. (2005). Cell cycle dynamics and quorum sensing in Candida albicans chlamydospores are distinct from budding and hyphal growth. *Eukaryot Cell 4,* 1191-1202.

Martin, S.W., and Konopka, J.B. (2004a). Lipid raft polarization contributes to hyphal growth in Candida albicans. *Eukaryot Cell 3,* 675-684.

Martin, S.W., and Konopka, J.B. (2004b). SUMO modification of septin-interacting proteins in Candida albicans. *J Biol Chem 279,* 40861-40867.

McElver, J., and Weber, S. (1992). Flag N-terminal epitope overexpression of bacterial alkaline phosphatase and Flag C-terminal epitope tagging by PCR one-step targeted integration. *Yeast 8 (special issue),* S627.

McMillan, J.N., Longtine, M.S., Sia, R.A., Theesfeld, C.L., Bardes, E.S., Pringle, J.R., and Lew, D.J. (1999a). The Morphogenesis Checkpoint in Saccharomyces cerevisiae: Cell Cycle Control of Swe1p Degradation by Hsl1p and Hsl7p. *Mol Cell Biol 19,* 6929-6939.

McMillan, J.N., Sia, R.A.L., Bardes, E.S.G., and Lew, D.J. (1999b). Phosphorylation-independent inhibition of Cdc28p by the tyrosine kinase Swe1p in the morphogenesis checkpoint. *Mol. Cell. Biol. 19,* 5981-5990.

McMillan, J.N., Sia, R.A.L., and Lew, D.J. (1998). A morphogenesis checkpoint monitors the actin cytoskeleton in yeast. *J. Cell Biol. 142,* 1487-1499.

McMillan, J.N., Theesfeld, C.L., Harrison, J.C., Bardes, E.S., and Lew, D.J. (2002). Determinants of Swe1p degradation in Saccharomyces cerevisiae. *Mol Biol Cell 13,* 3560-3575.

Mills, B.G., and Frausto, A. (1997). Cytokines expressed in multinucleated cells: Paget's disease and giant cell tumors versus normal bone.PG - 16-21. *Calcif Tissue Int 61*.

Minke, P.F., Lee, I.H., and Plamann, M. (1999). Microscopic analysis of Neurospora ropy mutants defective in nuclear distribution. *Fungal Genet Biol 28,* 55-67.

Mino, A., Tanaka, K., Kamei, T., Umikawa, M., Fujiwara, T., and Takai, Y. (1998). Shs1p: a novel member of septin that interacts with spa2p, involved in polarized growth in saccharomyces cerevisiae. *Biochem Biophys Res Commun 251,* 732-736.

Mitchell, D.A., and Sprague, G.F., Jr. (2001). The phosphotyrosyl phosphatase activator, Ncs1p (Rrd1p), functions with Cla4p to regulate the G(2)/M transition in Saccharomyces cerevisiae. *Mol Cell Biol 21,* 488-500.

Mohr, C. (1997). Genetic engineering of the filamentous fungus *Ashbya gossypii:* construction of a genomic library, isolation of genes for beta-isopropylmalate-dehydrogenase (LEU2) and a protein kinase (APK1) by heterologous complementation, and characterization of non-reverting mutants. *PhD Thesis,* Biozentrum, Universität Basel, Switzerland.

Müller, C., Spohr, A.B., and Nielsen, J. (2000). Role of substrate concentration in mitosis and hyphal extension of Aspergillus. *Biotechnol Bioeng 67,* 390-397.

Nakashima, A., Maruki, Y., Miyoshi, Y., Kondo, C., Ohsumi, Y., Takata, H., Matsuura, A., Lee, K.S., Yonezawa, K., and Kamada, Y. (2005). The Tor signaling pathway regulates mitotic entry via polo-kinase. *unpublished,* Division of Molecular Cell Biology, National Institute for Basic Biology, Okazaki, Japan.

Nakashima, A., Maruki, Y., Miyoshi, Y., Kondo, C., Ohsumi, Y., Takata, H., Matsuura, A., Lee, K.S., Yonezawa, K., and Kamada, Y. (2006). The Tor signaling pathway regulates mitotic entry via polo-kinase. *unpublished,* Division of Molecular Cell Biology, National Institute for Basic Biology, Okazaki, Japan.

Nasmyth, K.A., and Reed, S.I. (1980). Isolation of genes by complementation in yeast: molecular cloning of a cell-cycle gene. *Proc Natl Acad Sci U S A 77,* 2119-2123.

Nygaard, O.F., Guttes, S., and Rusch, H.P. (1960). Nucleic acid metabolism in a slime mold with synchronous mitosis. *Biochim Biophys Acta 38,* 298-306.

Park, C.J., Song, S., Lee, P.R., Shou, W., Deshaies, R.J., and Lee, K.S. (2003). Loss of CDC5 function in Saccharomyces cerevisiae leads to defects in Swe1p regulation and Bfa1p/Bub2p-independent cytokinesis. *Genetics 163,* 21-33.

Pereira, G., Hofken, T., Grindlay, J., Manson, C., and Schiebel, E. (2000). The Bub2p spindle checkpoint links nuclear migration with mitotic exit. *Mol Cell 6,* 1-10.

Petersen, J., and Hagan, I.M. (2005). Polo kinase links the stress pathway to cell cycle control and tip growth in fission yeast. *Nature 435,* 507-512.

Prillinger, H., Schweigkofler, W., Breitenbach, M., Briza, P., Staudacher, E., Lopandic, K., Molnar, O., Weigang, F., Ibl, M., and Ellinger, A. (1997). Phytopathogenic filamentous (Ashbya, Eremothecium) and dimorphic fungi (Holleya, Nematospora) with needle-shaped ascospores as new members within the Saccharomycetaceae. *Yeast 13,* 945-960.

Pringle, J.R., and Hartwell, L.H. (1981). The *Saccharomyces cerevisiae* cell cycle. In: The Molecular Biology of the Yeast *Saccharomyces*, eds. J.D. Strathern, E.W. Jones, and J.R. Broach, Cold Spring Harbor, N.Y.: Cold Spring Harbor Laboratory, 97-142.

Rhind, N., Furnari, B., and Russell, P. (1997). Cdc2 tyrosine phosphorylation is required for the DNA damage checkpoint in fission yeast. *Genes Dev. 11,* 504-511.

Rhind, N., and Russell, P. (1998). Tyrosine phosphorylation of cdc2 is required for the replication checkpoint in *Schizosaccharomyces pombe*. *Mol. Cell. Biol. 18,* 3782-3787.

Richardson, H., Lew, D.J., Henze, M., Sugimoto, K., and Reed, S.I. (1992). Cyclin-B homologs in Saccharomyces cerevisiae function in S phase and in G2. *Genes Dev 6,* 2021-2034.

Richardson, H.E., Wittenberg, C., Cross, F., and Reed, S.I. (1989). An essential G1 function for cyclin-like proteins in yeast. *Cell 59,* 1127-1133.

Richman, T.J., Sawyer, M.M., and Johnson, D.I. (1999). The Cdc42p GTPase is involved in a G2/M morphogenetic checkpoint regulating the apical-isotropic switch and nuclear division in yeast. *J Biol Chem 274,* 16861-16870.

Sakchaisri, K., Asano, S., Yu, L.R., Shulewitz, M.J., Park, C.J., Park, J.E., Cho, Y.W., Veenstra, T.D., Thorner, J., and Lee, K.S. (2004). Coupling morphogenesis to mitotic entry. *Proc Natl Acad Sci U S A 101,* 4124-4129.

Sambrook, J.a.D.R. (2001). Molecular Cloning: A Laboratory Manual. Cold Spring Harbor Laboratory Press: Cold Spring Harbor.

Sanders, S.L., and Herskowitz, I. (1996). The BUD4 protein of yeast, required for axial budding, is localized to the mother/BUD neck in a cell cycle-dependent manner. *J Cell Biol 134,* 413-427.

Saraste, M., Sibbald, P.R., and Wittinghofer, A. (1990). The P-loop--a common motif in ATP- and GTP-binding proteins. *Trends Biochem Sci 15,* 430-434.

Schmitz, H.P., Kaufmann, A., Kohli, M., Laissue, P.P., and Philippsen, P. (2006). From function to shape: a novel role of a formin in morphogenesis of the fungus Ashbya gossypii. *Mol Biol Cell 17,* 130-145.

Schwob, E., and Nasmyth, K. (1993). CLB5 and CLB6, a new pair of B cyclins involved in DNA replication in Saccharomyces cerevisiae. *Genes Dev 7,* 1160-1175.

Shaw, S.L., Yeh, E., Maddox, P., Salmon, E.D., and Bloom, K. (1997). Astral microtubule dynamics in yeast: a microtubule-based searching mechanism for spindle orientation and nuclear migration into the bud. *J. Cell Biol. 139,* 985-994.

Shiozaki, K., and Russell, P. (1995). Cell-cycle control linked to extracellular environment by MAP kinase pathway in fission yeast. *Nature 378,* 739-743.

Shulewitz, M.J., Inouye, C.J., and Thorner, J. (1999). Hsl7 localizes to a septin ring and serves as an adapter in a regulatory pathway that relieves tyrosine phosphorylation of Cdc28 protein kinase in *Saccharomyces cerevisiae*. *Mol. Cell. Biol. 19,* 7123-7137.

Sia, R.A., Herald, H.A., and Lew, D.J. (1996). Cdc28 tyrosine phosphorylation and the morphogenesis checkpoint in budding yeast. *Mol Biol Cell 7,* 1657-1666.

Sia, R.A.L., Bardes, E.S.G., and Lew, D.J. (1998). Control of Swe1p degradation by the morphogenesis checkpoint. *EMBO J. 17,* 6678-6688.

Sikorski, R.S., and Hieter, P. (1989). A system of shuttle vectors and yeast host strains designed for efficient manipulation of DNA in *Saccharomyces cerevisiae*. *Genetics 122,* 19-27.

Snyder, M. (1989). The SPA2 protein of yeast localizes to sites of cell growth. *J. Cell Biol. 108,* 1419-1429.

Snyder, M. (1994). The spindle pole body of yeast. *Chromosoma 103,* 369-380.

Steiner, S., Wendland, J., Wright, M.C., and Philippsen, P. (1995). Homologous recombination as the main mechanism for DNA integration and cause of rearrangements in the filamentous ascomycete Ashbya gossypii. *Genetics 140,* 973-987.

Su, T.T., Sprenger, F., DiGregorio, P.J., Campbell, S.D., and O'Farrell, P.H. (1998). Exit from mitosis in Drosophila syncytial embryos requires proteolysis and cyclin degradation, and is associated with localized dephosphorylation. *Genes Dev 12,* 1495-1503.

Sudbery, P.E. (2001). The germ tubes of Candida albicans hyphae and pseudohyphae show different patterns of septin ring localization. *Mol Microbiol 41,* 19-31.

Surana, U., Robitsch, H., Price, C., Shuster, T., Fitch, I., Futcher, A.B., and Nasmyth, K. (1991). The role of *CDC28* and cyclins during mitosis in the budding yeast *S. cerevisiae*. *Cell 65,* 145-161.

Takizawa, C.G., and Morgan, D.O. (2000). Control of mitosis by changes in the subcellular location of cyclin-B1-Cdk1 and Cdc25C.PG - 658-65. *Curr Opin Cell Biol 12*.

Takizawa, P.A., DeRisi, J.L., Wilhelm, J.E., and Vale, R.D. (2000). Plasma membrane compartmentalization in yeast by messenger RNA transport and a septin diffusion barrier. *Science 290,* 341-344.

Tyers, M., Tokiwa, G., Nash, R., and Futcher, B. (1992). The Cln3-Cdc28 kinase complex of *S. cerevisiae* is regulated by proteolysis and phosphorylation. *EMBO J. 11,* 1773-1784.

Valdez-Taubas, J., and Pelham, H.R. (2003). Slow diffusion of proteins in the yeast plasma membrane allows polarity to be maintained by endocytic cycling. *Curr Biol 13,* 1636-1640.

Vallen, E.A., Caviston, J., and Bi, E. (2000). Roles of Hof1p, Bni1p, Bnr1p, and myo1p in cytokinesis in Saccharomyces cerevisiae. *Mol Biol Cell 11,* 593-611.

Versele, M., Gullbrand, B., Shulewitz, M.J., Cid, V.J., Bahmanyar, S., Chen, R.E., Barth, P., Alber, T., and Thorner, J. (2004). Protein-protein interactions governing septin heteropentamer assembly and septin filament organization in Saccharomyces cerevisiae. *Mol Biol Cell 15,* 4568-4583.

Wach, A., Brachat, A., Pohlmann, R., and Philippsen, P. (1994). New heterologous modules for classical or PCR-based gene disruptions in Saccharomyces cerevisiae. *Yeast 10,* 1793-1808.

Wachtler, V., Rajagopalan, S., and Balasubramanian, M.K. (2003). Sterol-rich plasma membrane domains in the fission yeast Schizosaccharomyces pombe. *J Cell Sci 116,* 867-874.

Wakefield, J.G., Huang, J.Y., and Raff, J.W. (2000). Centrosomes have a role in regulating the destruction of cyclin B in early Drosophila embryos. *Curr Biol 10,* 1367-1370.

Warenda, A.J., and Konopka, J.B. (2002). Septin function in Candida albicans morphogenesis. *Mol Biol Cell 13,* 2732-2746.

Weiss, E., and Winey, M. (1996). The Saccharomyces cerevisiae spindle pole body duplication gene MPS1 is part of a mitotic checkpoint. *J Cell Biol 132,* 111-123.

Wendland, J., Ayad-Durieux, Y., Knechtle, P., Rebischung, C., and Philippsen, P. (2000). PCR-based gene targeting in the filamentous fungus Ashbya gossypii. *Gene 242,* 381-391.

Wendland, J., and Philippsen, P. (2000). Determination of cell polarity in germinated spores and hyphal tips of the filamentous ascomycete Ashbya gossypii requires a rhoGAP homolog. *J Cell Sci 113 (Pt 9),* 1611-1621.

Wendland, J., Pohlmann, R., Dietrich, F., Steiner, S., Mohr, C., and Philippsen, P. (1999). Compact organization of rRNA genes in the filamentous fungus Ashbya gossypii. *Curr Genet 35,* 618-625.

Westfall, P.J., and Momany, M. (2002). Aspergillus nidulans septin AspB plays pre- and postmitotic roles in septum, branch, and conidiophore development. *Mol Biol Cell 13,* 110-118.

Wightman, R., Bates, S., Amornrrattanapan, P., and Sudbery, P. (2004). In Candida albicans, the Nim1 kinases Gin4 and Hsl1 negatively regulate pseudohypha formation and Gin4 also controls septin organization. *J Cell Biol 164,* 581-591.

Winding, B., Misander, H., Sveigaard, C., Therkildsen, B., Jakobsen, M., Overgaard, T., Oursler, M.J., and Foged, N.T. (2000). Human breast cancer cells induced angiogenesis, recruitment, and activation of osteoclasts in osteolytic metastasis.PG - 631-40. *J Cancer Res Clin Oncol 126*.

Winey, M., and Byers, B. (1993). Assembly and functions of the spindle pole body in budding yeast. *Trends Genet 9,* 300-304.

Woodhouse, E.C., Chuaqui, R.F., and Liotta, L.A. (1997). General mechanisms of metastasis. *Cancer 80,* 1529-1537.

Wullschleger, S., Loewith, R., and Hall, M.N. (2006). TOR signaling in growth and metabolism. *Cell 124,* 471-484.

Yamada, A., Duffy, B., Perry, J.A., and Kornbluth, S. (2004). DNA replication checkpoint control of Wee1 stability by vertebrate Hsl7. *J Cell Biol 167,* 841-849.

Yuzyuk, T., and Amberg, D.C. (2003). Actin recovery and bud emergence in osmotically stressed cells requires the conserved actin interacting mitogen-activated protein kinase kinase kinase Ssk2p/MTK1 and the scaffold protein Spa2p. *Mol Biol Cell 14,* 3013-3026.

Zhang, J., Kong, C., Xie, H., McPherson, P.S., Grinstein, S., and Trimble, W.S. (1999). Phosphatidylinositol polyphosphate binding to the mammalian septin H5 is modulated by GTP. *Curr Biol 9,* 1458-1467.

Acknowledgements

I am very grateful to Prof. Peter Philippsen for having accepted me as a member of his team, for guiding me through all these years with valuable scientific and personal advises and for making this work possible through his generous support. His ability to keep up a warm and familial atmosphere in the team not only made this time rich in experience and education, but also made it a very enjoyable part of my life. “Thesis supervisor” does not describe Peter’s role adequately enough; I prefer “Doktorvater”.

Similarly, I would like to thank my “Doktormutter”, Dr. Amy Gladfelter for lending her time, her experience, ideas, and moral support. She always had an open ear for my thoughts – no matter how crazy they were, and got never tired to comfort and encourage me – in scientific and personal matters.

I also wish to acknowledge the other members of my thesis committee and participants of my exam, Prof. Yves Barral, Prof. Mike Hall, Prof. Anne Spang and Prof. Jean Pieters for lending their time and offering helpful suggestions on my project.

My warm thanks to all present and former members of the “lab family”, especially Philippe Laissue for his loyal friendship and for sharing my peculiar taste of humor, Michael Köhli for accompanying me through the odyssey in Copenhagen and for sharing adventures with “Bonny and Clyde”, Sylvia Vögeli, Virginie Galati for making lunch times and coffee breaks amusing events, Riccarda Rischatsch, Philipp Knechtle, Anita Lerch, Sophie Brachat and Daniele Cavicchioli for having been wonderful office mates, Kamila Boudier for encouraging discussions and memorable parties, Dominic Hœpfner, Hans-Peter Schmitz, Florian Schärer, Christine Alberti-Segui and Yasmina Bauer for teaching me first and advanced steps in lab techniques, Andreas Kaufmann for his unfailing engagement in keeping lab equipment running, Claudia Birrer, Nicoleta Sustreanu, Tineke van den Hoorn, Pilar Garcia, Kathrin Brogli, Ivan Schlatter, Nijas Alijoski, Jérôme Ailhas, Zaki Sellam, and the new diploma students for adding to the friendly atmosphere in the lab, Brigitte Berglas for constantly providing the lab with perfectly clean vessels, and Bettina Hersberger, Sandra Götz-Krebs, Doris Rossi and Esther Graf for their help concerning office and paperwork.

I additionally thank my colleagues and friends from the Biozentrum, Petr Broz, Thomas Rhomberg and Stefan Langheld, for sharing joy and sorrow over a drink or at the movies, and my trusty friend Cyrill Rémy for the inspiring and philosophical discussions about biology and other matters of life.

None of this would have possible without the unwavering support and love of my parents, Madeleine and Fritz Helfer. Especially, I would like to thank my dear Katrin for sweetening my life since the last year of my thesis work, for her unfailing support and patience, for buoying me up in desperate moments, and most of all: for her love.

Curriculum vitae

Hanspeter Helfer

Date of birth: 11.10.1976
Place of birth: Selzach, Switzerland
Nationality: Swiss

Education:

Primary school:	1983 – 1989	Primarschule Selzach, Switzerland
Secondary school:	1989 – 1992	Bezirksschule Selzach, Switzerland
Grammar school:	1992 – 1997	Kantonsschule Solothurn, Switzerland
University:	1997 – 2002	Diploma in Biology II (Molecular Biology), Universität Basel, Switzerland
Diploma Thesis:	2000 – 2002	In the lab of Prof. P. Philippsen, Biozentrum, Basel, Switzerland "Effects of myosin gene deletions on growth and development of the filamentous fungus *Ashbya gossypii*"
Ph.D.:	2002 – 2006	In the lab of Prof. P. Philippsen, Biozentrum, Basel, Switzerland "New aspects of septin assembly and cell cycle control in multinucleated *A. gossypii*"

Publications

H Helfer and AS Gladfelter. AgSwe1p regulates mitosis in response to morphogenesis and nutrients in multinucleated *A. gossypii* cells. *MBC,* **selected for InCytes,** Epub ahead of print August 9, 2006.

Y Bauer, P Knechtle, J Wendland, H Helfer and P Philippsen. A Ras-like GTPase is involved in hyphal growth guidance in the filamentous fungus *Ashbya gossypii. MBC,* Vol. 15, Issue 10, 4622-4632, October 2004

Meetings and Seminars

European Conference on Fungal Genetics, Pisa, Italy, April 2002. Poster presentation: Effects of myosin gene deletions on growth and development of the filamentous fungus *Ashbya gossypii.*

Swiss Yeast Meeting, Zürich, Switzerland. September 2002. Poster presentation: Effects of myosin gene deletions on growth and development of the filamentous fungus *Ashbya gossypii*.

European Conference on Fungal Genetics, Copenhagen, Denmark, April 2004. Oral presentation: In search of a link between morphogenesis and nuclear division in the filamentous fungus *Ashyba gossypii.*

Fungal Genetics Conference, Asilomar, CA, USA, March 2005. Poster presentation: Spatial and nutritional control of mitosis in *Ashyba gossypii.*

Erklärung

Ich erkläre, dass ich die Dissertation

“New aspects of septin assembly and cell cycle control in multinucleated *A. gossypii”*

nur mit der darin angegebenen Hilfe verfasst und bei keiner anderen Fakultät eingereicht habe.

Basel, Mai 2006

Hanspeter Helfer